Passive Acoustic Monitoring in the greater Cook Strait region with particular focus on Queen Charlotte Sound / Tōtaranui

Prepared for Marlborough District Council

June 2017

Prepared by:
Kimberly Goetz, NIWA
Krista Hupman, NIWA

For any information regarding this report please contact:

Kimberly Goetz
Marine Ecologist

+64-4-382 1623
kim.goetz@niwa.co.nz

National Institute of Water & Atmospheric Research Ltd
Private Bag 14901
Kilbirnie
Wellington 6241

Phone +64 4 386 0300

NIWA CLIENT REPORT No: 2017216WN
Report date: June 2017
NIWA Project: ELF17306

Quality Assurance Statement		
	Reviewed by:	Krista Hupman
	Formatting checked by:	Helen Neil
	Approved for release by:	Alison MacDiarmid

Front cover image: Bottlenose dolphin sighted after deployment of station 1 acoustic recorder.

Contents

Tables

Figures

Executive Summary

At the request of Marlborough District Council (MDC), the National Institute of Water and Atmospheric Research (NIWA) undertook data analysis, interpretation and reporting on the acoustic data collected as part of a monitoring project in the greater Cook Strait region. The purpose of this work is to provide MDC with information on the soundscape characteristics of the Cook Strait region with particular emphasis on Queen Charlotte Sound / Tōtaranui (QCS) over a six month period (July – December 2016).

As part of a collaboration between NIWA and JASCO Applied Sciences, the marine soundscape, including contributions from ambient and anthropogenic noise as well as marine mammal vocalizations and fish chorusing events, was quantified. When possible, automated detectors/classifiers were used to detect marine mammal species and manual verification was performed on 1% of the data to assess detector performance. In cases where automated detectors performed poorly, results from manual analysis are provided.

The soundscape of QCS was the most consistent and stable of all the stations deployed in the Cook Strait region and was largely dominated by noise levels in the 100-1000 Hz band which encompasses most of the vessel activity, weather, and fish chorusing events. The only notable disturbance in the overall soundscape was found in the 10-100 Hz band as a result of the 7.8 magnitude earthquake on 14 November 2016.

Unlike many of the other stations, noise from seismic activity was not detected in QCS. The sole anthropogenic contributor to the soundscape, more than any other station, was from vessel traffic – particularly from small vessels. Except during the 14 November 2016 earthquake and subsequent aftershocks, vessel associated noise drove the daily sound exposure level (SEL) throughout the entire recording period. On average, vessels were detected 12 hours per day.

The sound levels in QCS near station 1 are strongly influenced by noise from vessel traffic associated with recreational activities, ferries, fish farms and large vessels. Because of the narrow and shallow waterways that are typical within QCS, the majority of vessels passed near the acoustic recorder and were detected for a relatively short amount of time.

The acoustic presence of cetaceans, whales and dolphins, was identified at all stations and included: Cuvier's beaked (Ziphius cavirostris), unidentified beaked, pilot (*Globicephala sp.),* sperm (*Physeter macrocephalus*), Antarctic blue (*Balaenoptera musculus intermedia*), New Zealand blue (*B. musculus*), Humpback (*Megaptera novaeangliae*), Antarctic minke (*B. bonaerensis*), southern right (*Eubalaena australis*), and sei (*Balaenoptera borealis*) whales, as well as Hector's dolphins (*Cephalorhynchus hectori*) and unidentified dolphin whistles and delphinid clicks.

Hector's and unidentified dolphins were the only confirmed marine mammals detected in QCS. Hector's dolphins were not detected at any of the other six stations. Detections occurred on 38.5% of the recording days and peaked in mid-July, mid-August, and October with few detections between and after these periods. The restricted range of Hector's dolphins combined with the limited listening radius of the recorder suggests that the numbers of individuals in the area is probably less than 20.

Detections of whistles from unidentified dolphin species were detected in 69% of the recording days and occurred in higher densities in early August, the first three weeks of September, and December. Echolocation clicks from unidentified delphinid species were detected daily. However, the automated detector performed poorly and did not match results from the manual analysis. In addition, results from the automated detector did not show a diel pattern typically found in echolocation data. Further investigation revealed that impulsive signals associated with the outboard engines of small vessels falsely triggered the automated click detector, and explained why detections were prevalent more than expected during the day.

Because dusky dolphins (*Lagenorhynchus obscurus*) and are not known to produce whistles and common dolphins (*Delphinus delphis*) are typically found kilometres from shore, it is likely that that whistle detections from the unidentified dolphins can be attributed to bottlenose dolphins (*Tursiops truncatus*) that are known to frequent QCS.

Fish chorusing was prevalent at all stations and were typically associated with increased levels from 600-1000 Hz around dawn and dusk. Despite having the highest levels of vessel traffic, fish choruses were detected daily around dusk throughout the 6-month recording period in QCS.

Overall, the soundscape of the marine environment is complex. However, quantifying the contribution of different noise sources is essential to assess baseline noise levels, specifically for QCS where vessel traffic is high. This research highlights the potential of using fixed passive acoustic monitoring (PAM) to identify natural, biological and anthropogenic noise within the marine soundscape. The acoustic techniques used here were non-invasive and successfully identified sources of underwater noise and the presence of cetaceans. In addition, considering the marine environment is particularly difficult to access, the acoustic devices used here provide a way to measure the diversity of marine mammals in both shallow and deep water environments. While this project provides the first insight into the soundscape of the greater Cook Strait region, future monitoring over longer time scales is needed to further our knowledge on the seasonal variability and long terms trends in this area.

1 Background

The National Institute of Water and Atmospheric Research (NIWA) deployed six acoustic moorings as part of a large-scale project using fixed passive acoustic monitoring (PAM) to assess the soundscape of the greater-Cook Strait region, New Zealand. Following this, Marlborough District Council (MDC) requested the deployment of an additional mooring in Queen Charlotte Sound / Tōtaranui (QCS). The Cook Strait project provided a unique opportunity for MDC to monitor and characterize noise over a six month period. The full data set consisted of seven months of acoustic recordings obtained from six locations in and near the entrances of Cook Strait and six months of data collected in QCS. This report provides a synthesis of the data collected in QCS within the context of data collected at other moorings within the greater Cook Strait region for comparative purposes.

2 Introduction

Marine mammals have an extremely high public profile. These charismatic animals, perhaps more than any other group, define the character of New Zealand's diverse marine estate. Furthermore, New Zealand waters provide important habitat for nearly half of the world's cetacean species (whales and dolphins), a higher proportion of cetacean species than occurs in any other nation. Despite this, little is known about the spatial-temporal patterns of cetaceans within New Zealand's Exclusive Economic Zone and managers, decision makers and the public alike are often faced with a lack of detailed and robust information to gauge how particular threats could potentially impact these species. The deployment of a PAM system provides New Zealand with much-needed data on the seasonal use and distribution for many cetacean species traveling through Cook Strait.

The overall objectives of this project were to:

- Document baseline ambient noise conditions over a long period in an area known for its strong currents and that is heavily used by the fishing industry and ferry traffic.
- Characterise sounds produced by oil and gas exploration activities.
- Address knowledge gaps about spatial and temporal distributions, habitat use, calling behavior, and migration paths of marine mammal species based on acoustic detections of their vocalisations.

3 Methods

3.1 Deployment and Recovery Voyages

Before deploying acoustic moorings in coastal and offshore New Zealand waters, permits from the Wellington Regional Council and the Environmental Protection Authority were obtained.

On 3-5 June 2016, we deployed six acoustic moorings in the Cook Strait region (four in deep water (> 500 m) and two in shallow water (< 250 m)) (Table 3-1, Figure 3-1). Later, on 20 July 2016, an additional acoustic mooring was deployed in QCS (Table 3-1, Figure 3-2, Figure 3-3). Each mooring containing an Autonomous Multichannel Acoustic Recorder (AMAR) manufactured by JASCO Applied Sciences (hereafter referred to as JASCO) that was fitted with an M36-V35-100 omnidirectional hydrophone (GeoSpectrum Technologies Inc.; −164 dB re 1 V/µPa sensitivity). The duty cycle for each

AMAR (presented in Table 3-1) was chosen to maximize recording time while accounting for cetacean species likely to be present at each mooring station.

Mooring components were specifically selected to minimise all sources of acoustic noise in the mooring, and the influence of flow noise. Ensuring the mooring itself is as quiet as possible maximises the detection range for the target signals. The mooring designs were made to standard oceanographic practice, with the following adaptations to improve acoustic performance and reliability:

- Acoustic releases were placed at a distance from the hydrophone to minimise mooring motion from current drag.
- A tandem pair of acoustic releases was fitted to all moorings to provide redundancy for retrieval.
- Hydrophones were mounted away from surfaces that could cause unwanted reflected sound.
- A GPS positioning beacon with bi-directional Iridium communications was fitted as retrieval aids in case of premature release or difficulties visually spotting the equipment after it returns to the surface.

Due to bad weather, moorings were recovered during a series of trips which took place between 05 December 2016 and 25 February 2017. Data collected in the QCS spanned from 20 July 2016 to 15 December 2016 (Table 3-1).

Table 3-1: Summary of acoustic mooring deployments in the Cook Strait Region. Queen Charlotte Sound / Tōtaranui station highlighted in grey.

Station	Type of Station	Deployment	Last Recording	Latitude	Longitude	Depth (m)	Duty Cycle
1	Shallow	20/07/2016	15/12/2016	-41.200067	174.190317	48.5	630 s at 16 ksps 125 s at 375 ksps 145 s sleep
2	Shallow	04/06/2016	20/12/2016	-40.419567	174.5074	110	630 s at 16 ksps 125 s at 250 ksps 145 s sleep
3	Shallow	03/06/2016	19/12/2016	-41.0927	174.5469	252	
4	Deep	06/06/2016	20/12/2016	-41.61233	174.7353	711	
5	Deep	06/06/2016	21/12/2016	-42.3087	174.2145	1251	
6	Deep	06/06/2016	21/12/2016	-41.805017	175.081	1188	
7	Deep	05/06/2016	21/12/2016	-41.6098	175.9029	1481	

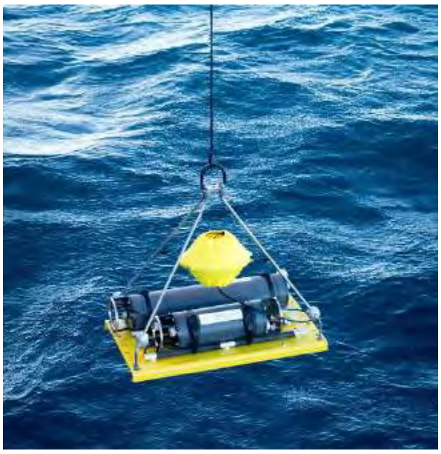

Figure 3-1: JASCO Acoustic Multichannel Acoustic Receivers (AMAR). On a bottom base plate for shallow water deployments at stations1-3 (left) and housed in a glass sphere for deep water deployments at stations 4-7 (right).

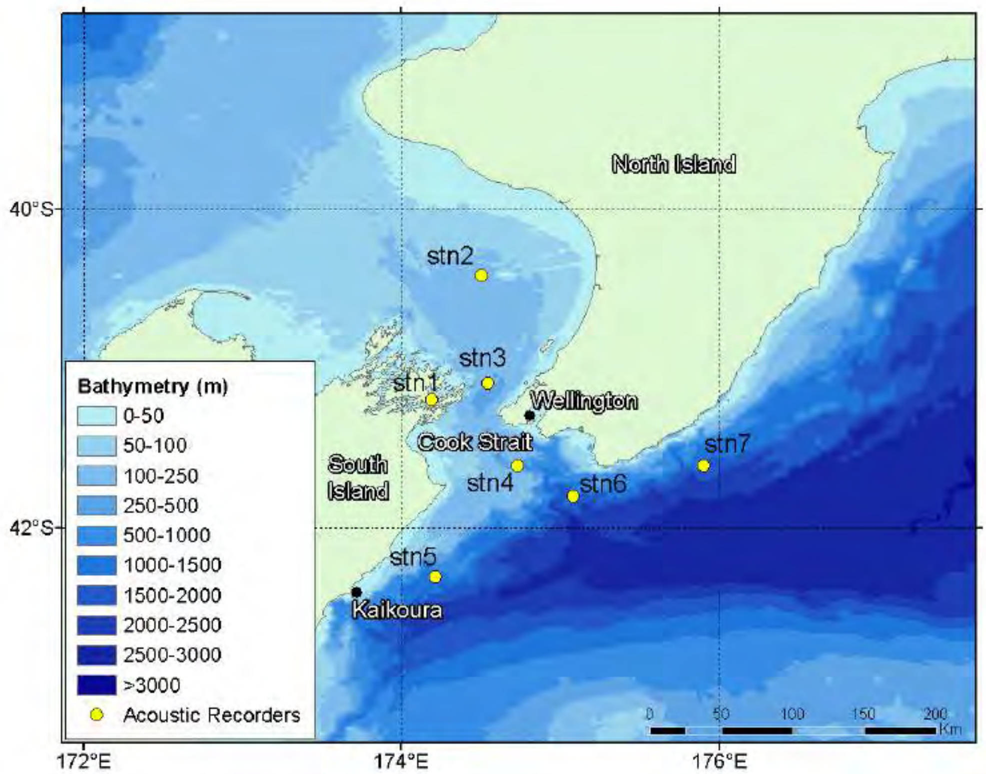

Figure 3-2: Overview map of the Cook Strait region showing all deployment locations. Yellow dots show stations 1-7.

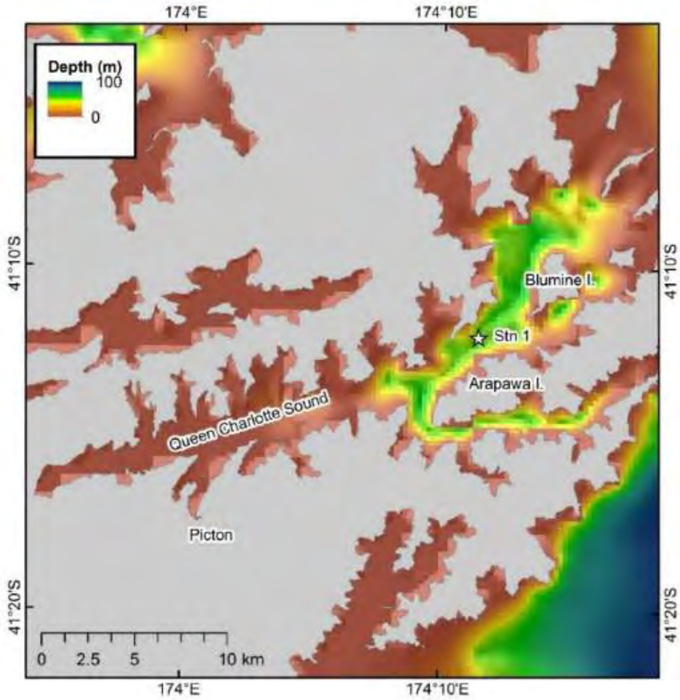

Figure 3-3: Overview map of the Marlborough Sound region showing deployment location. White star, station 1.

3.2 Summary of Data Analysis

The AMARs recorded over 11 TB of acoustic data (256,974 individual files). We collaborated with JASCO's expert acoustics team to analyse the data. JASCO has developed robust and accurate methods for transforming the raw data into information about the presence of marine mammals and quantifying the influence of anthropogenic activities on the marine soundscape. Automated analysis of ocean noise, vessel traffic, seismic surveys, and marine mammal detections was conducted on JASCO's specialised computer platform capable of processing acoustic files hundreds of times faster than real time. NIWA has access and ownership of all results. Full details on the analysis and summary results are presented in McPherson et al. (2017) (Appendix B). To provide context for this report, some of the methods from McPherson et al. (2017) are either copied or summarised below.

3.2.1 Ambient and Anthropogenic Noise

Automated analysis was used classify the dominant sound source in each minute of data as 'Vessel', 'Seismic', or 'Ambient'. Ambient, or background, noise levels were quantified to determine the local baseline underwater sound conditions.

The ambient sound levels that create the ocean soundscape are comprised of many natural and anthropogenic sources. The main environmental sources of sound are wind and precipitation. Wind-generated noise in the ocean is well-described (e.g., Wenz 1962; Ross 1976), and surf noise is known to be an important contributor to near-shore soundscapes (Deane 2000). Weather events and precipitation is a frequent noise source, with contributions typically concentrated at frequencies above 500 Hz. At low frequencies (<100 Hz), earthquakes and other geological activities contribute to the soundscape.

Sound level statistics quantify the observed distribution of recorded sound levels and are presented in terms of sound pressure level (SPL) and sound exposure level (SEL). Following standard acoustical practice, the *n*th percentile level (L_n) is the sound level exceeded by *n*% of the data. L_{max} is the maximum recorded sound level. L_{mean} is the equivalent continuous sound level that represents the level of a continuous constant sound that produces the same sound power as the time varying signal level being measured over the same time period. The median level (L_{50}) is considered most representative since it is less affected by high level outliers that can more strongly affect mean sound levels. The L_{50} is compared to the Wenz curves (Figure 3-4) for the upper and lower limits on prevailing ambient noise. L_5, the level exceeded by only 5% of the data, generally represents the highest typical sound levels measured. Sound levels between L_5 and L_{max} are due to close passes of vessels, intense weather, or other abnormal conditions. L_{95} represents the quietest typical conditions.

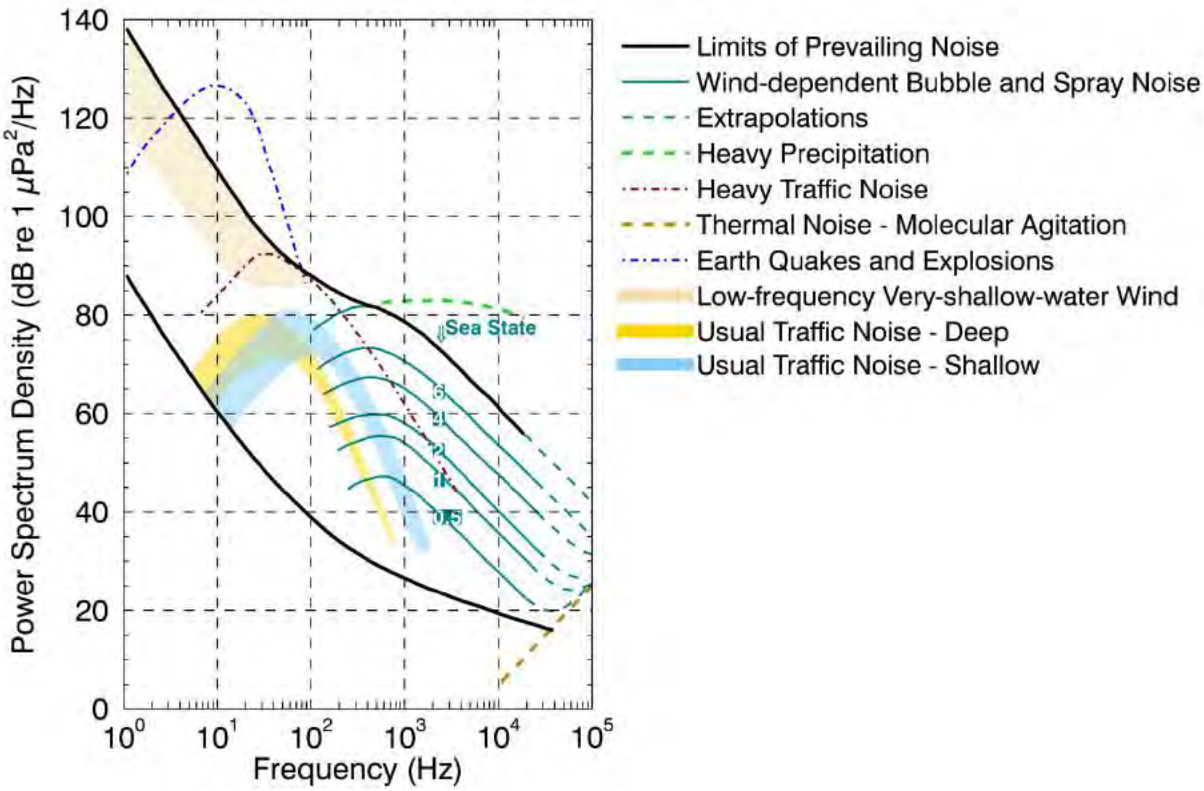

Figure 3-4: Wenz curves (NRC 2003). Adapted from (Wenz 1962),describes pressure spectral density levels (PSD) of marine ambient noise from weather, wind, geologic activity and commercial shipping.

One-third octave band analysis was conducted on the data to examine sound levels that represent the frequency filtering of the mammalian auditory system which has a bandwith of approximately 1/3-octave wide. The division of these bands indicates how noise will interfere with cetacean hearing in the same band.

Because vessels emit constant narrowband tones, algorithms can be used to detect vessel tonals in the acoustic data. For this analysis, three criteria were used for vessel detection: 1) The SPL in the shipping band is at least 3 dB above the median, 2) at least 5 shipping tonals (0.125 Hz bandwidth) are present, and 3) the sound pressure levels (SPL) in the shipping band is within 8 dB of the broadband SPL. We also examined the presence of seismic pulses using correlated spectrogram contours.

3.2.2 Marine Mammal Detections

Detections of marine mammal calls were based on automated detections and the manual validation of those results by experienced acoustic analysts. Odontocete (toothed whales) clicks and whistles were recorded and detected in the high-frequency (250 and 375 ksps) data and mysticete (baleen whale) calls were detected in the low-frequency (16 ksps) data.

An automated click detector/classifier was applied to the high-frequency data to detect clicks from sperm whales, beaked whales, and delphinids and a tonal call detector was used to identify marine mammal moans, songs, and whistles. The tonal detector identifies delphinid whistles in the high-frequency recordings and baleen whales in the low-frequency recordings. Details on species specific detectors and detector performance can be found in Appendix B. In addition to the automated analysis, 1% of the low and high frequency files per station were manually validated (2,600 files or about 260 hours of acoustic data). A goodness of fit of a sample of files was scored according to how well it conformed to the 'preferred' distribution of detections.

Due to the difficulty of identifying species in the family *Delphinidae* based on click characteristics, they were detected as a single class, 'unidentified delphinid click'. However, based on their known occurrence patterns in New Zealand, detections are most likely to be from common dolphins (*Delphinus sp.*) and bottlenose dolphins (*Tursiops truncatus*), but it is possible that other species are present.

4 Results

4.1 Ambient and Anthropogenic Noise Measurements

When possible, results for ambient and anthropogenic noise are presented for station 1 in QCS as well as for an additional shallow water station (station 2) and two deep water stations (stations 5 and 7) to provide context and for comparative purposes.

An overview of the sound variability in time and frequency, and the presence and level of contribution from different sources for two shallow water stations and two deep water stations is shown in Figure 4-1. Short-term events appear as vertical stripes on the spectrograms and spikes on the band level plots. Long-term events appear as horizontal bands of colour in the spectrograms. The soundscape at station 1 in the QCS is the most consistent and stable with only one irregularity due to the 7.8 magnitude earthquake on 14 November 2016, visible as a peak in the 10-100 Hz band (Figure 4-1).

Overall, median broadband SPL was lowest in QCS (98.1 dB re 1µPa) relative to the other stations (Figure 4-2). However, broadband SPL in QCS was largely driven by noise levels in the 100–1000 Hz band, which reflects most of the vessel activity as well as fish chorusing and weather events. The maximum in-band noise level value was highest in the 10–100 Hz band, as a result of the earthquake which reached the maximum SPL values (164.4 dB re 1µPa) recorded during the study (Figure 4-2). Seismic activity was not recorded in QCS but can be seen below 200 Hz at end of the recording period at stations 5 and 7.

The percentile power spectral density (PSD) levels were generally within the limits of the Wenz curves (Figure 4-3). The undulations in the percentile values between 20 and 100 Hz reveal the contribution of vessel noise to the soundscape. These undulations are most obvious at station 1 which had the most vessel traffic (Figure 4-3). The bump around 500 Hz, most pronounced at station 1 but present at all stations, is caused by fish chorusing. Finally, the smaller bump at ~4000 Hz in the 95^{th} and 75^{th} percentiles for station 1 is the result of chain noise from a nearby mooring or other underwater equipment.

The 14 November 2016 earthquake was recorded at all stations where it either approached or exceeded the maximum SPL values that can resolved by the hydrophone (165 dB re 1µPa). The recording of the earthquake at station 7 is shown on Figure 4-4. Despite the epicentre being ~190 km away from station 1, the earthquake and subsequent aftershocks generated the highest sound levels recorded in QCS during the recording period. At the time of the earthquake, the hourly levels in the 10–100 Hz reached 151.4 dB re 1µPa. Figure 4-5 shows that the highest increase in noise occurred between 10 and 50 Hz and that the power spectrum density levels generally increased by 15 dB over the course of the week from 12 to 19 Nov 2016.

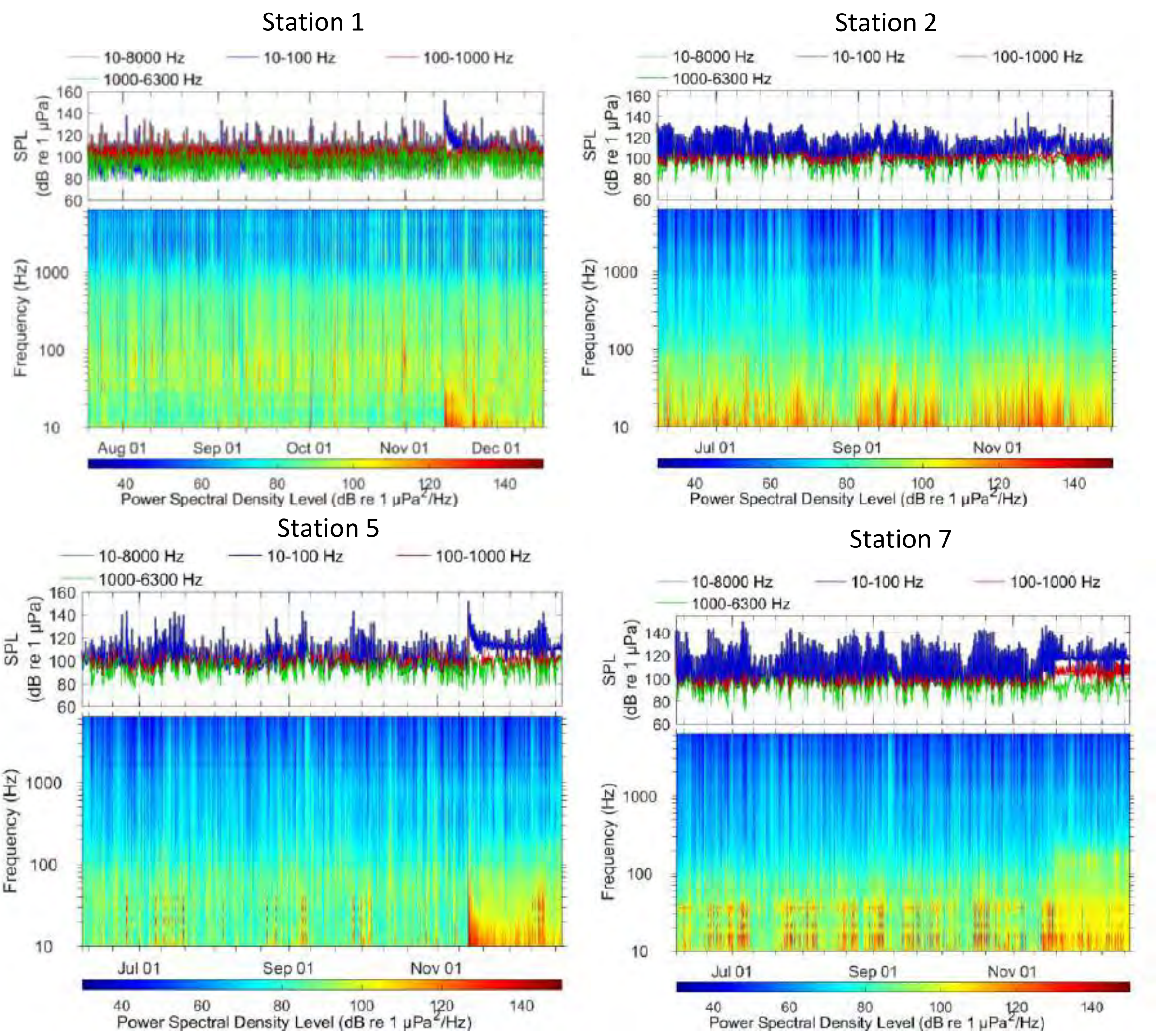

Figure 4-1: Sound level summary during the deployment period. In-band sound pressure level (SPL) (top) and spectrogram of underwater sound (bottom) for stations 1 and 2 (top row) and stations 5 and 7 (bottom row).

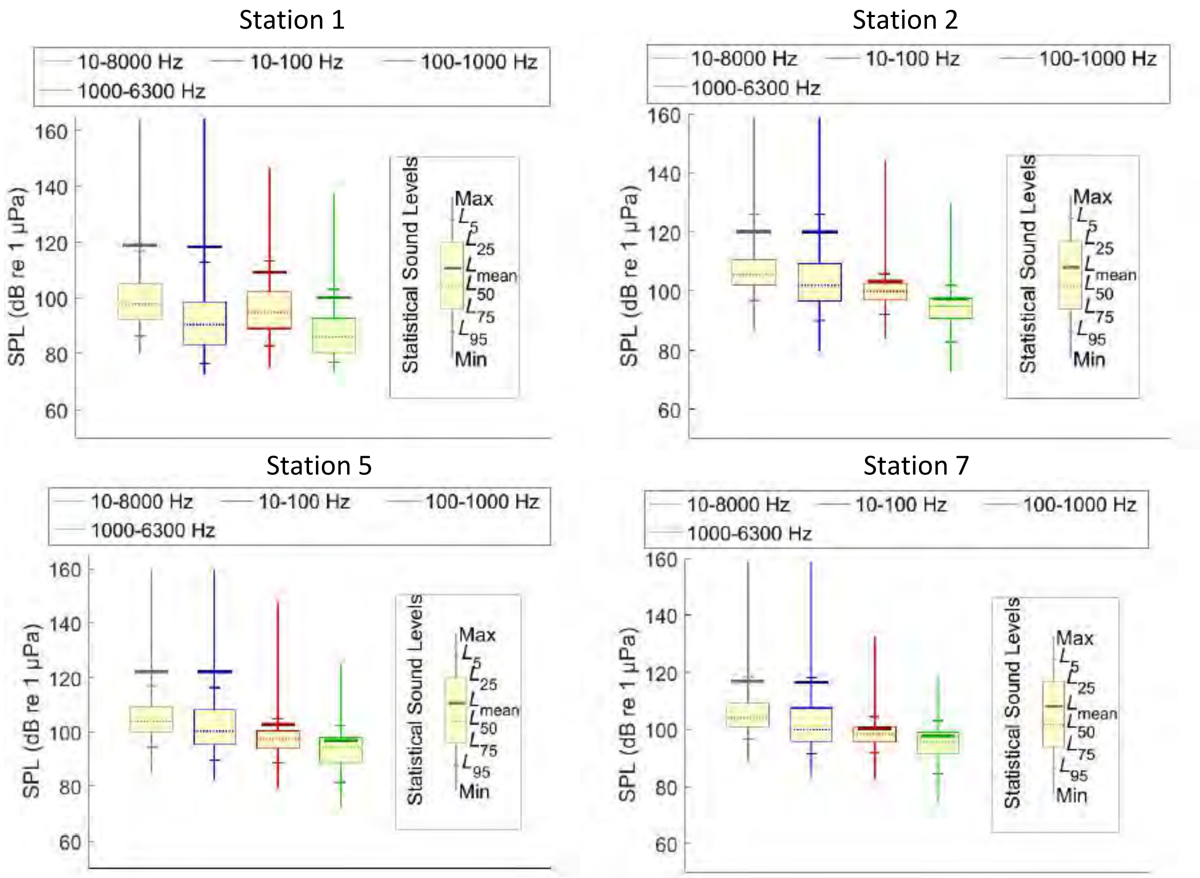

Figure 4-2: Broadband and in-band 1-min sound pressure level (SPL). Stations 1 and 2 (top row) and stations 5 and 7 (bottom row).

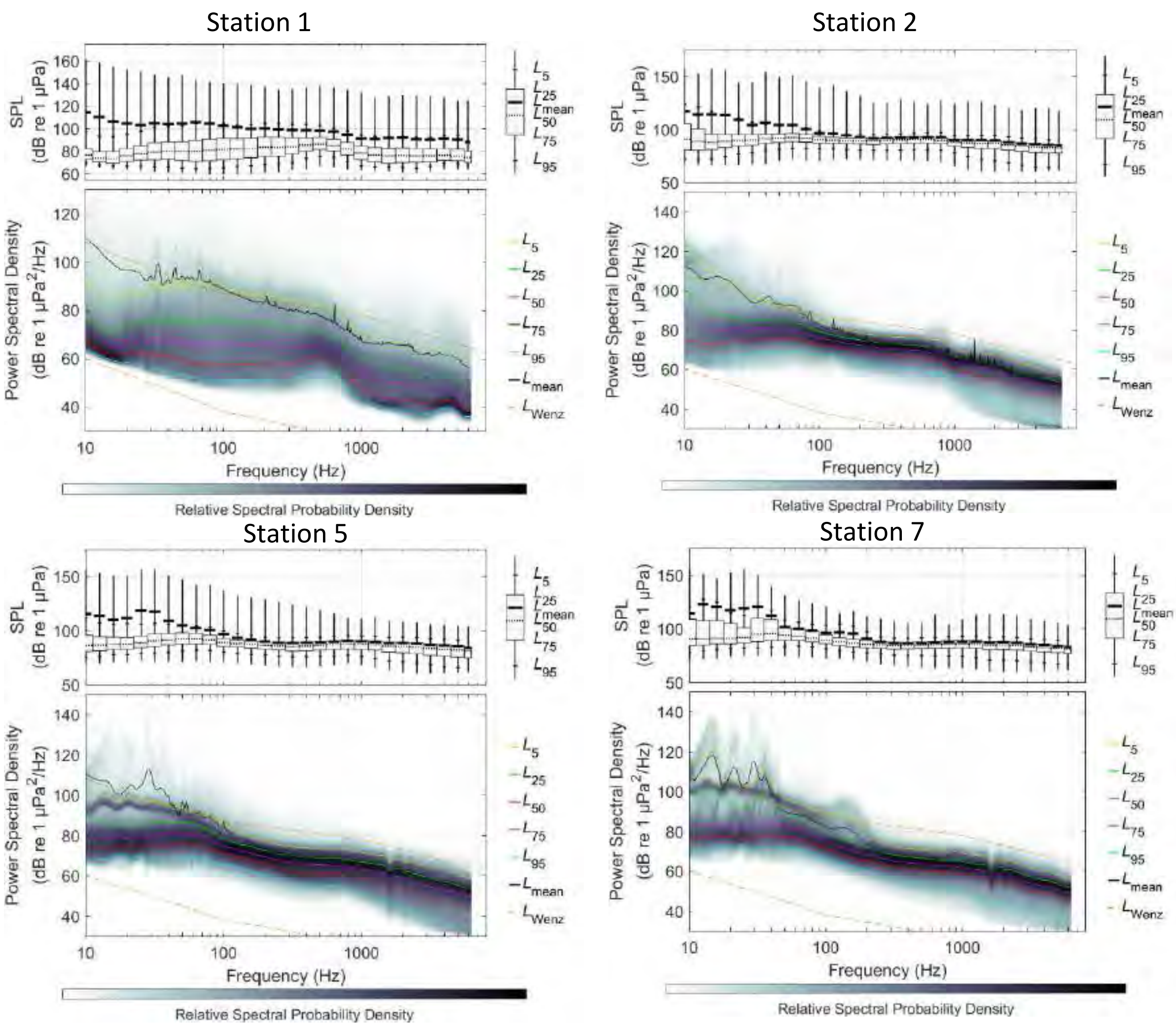

Figure 4-3: Stations 1 and 2 (top row) and stations 5 and 7 (bottom row) from 20 July to 15 December 2016. Exceedance percentiles and mean of 1/3 octave band sound pressure level (SPL) (top) and exceedance percentiles and probability density (grayscale) of 1-min power spectral density (PSD) levels Compared to the limits of prevailing noise (Wenz 1962).

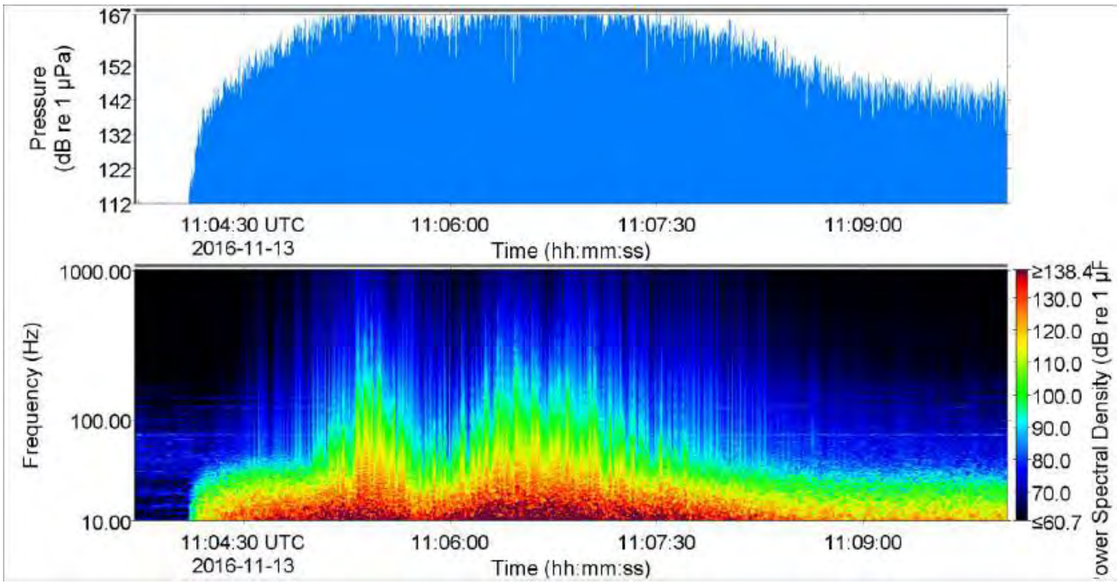

Figure 4-4: Spectrogram of the 7.8 magnitude earthquake on 14 November 2016 recorded at station 7.

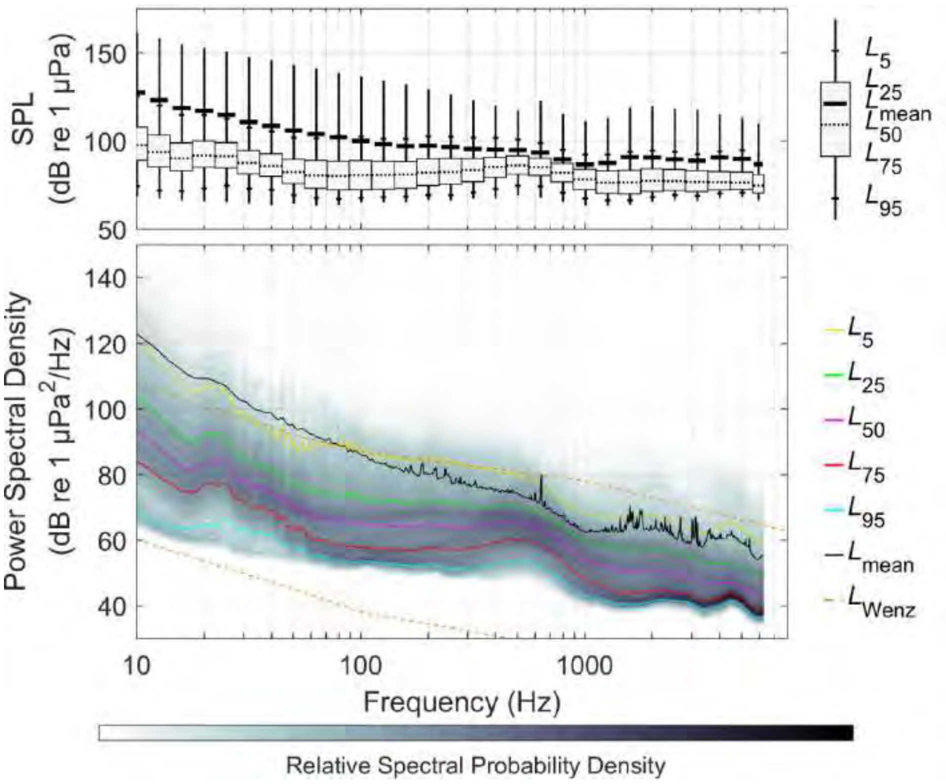

Figure 4-5: Station 1 from 12 to 19 November 2016. Exceedance percentiles and mean of 1/3 octave band sound pressure level sound pressure level (SPL) (top) and exceedance percentiles and probability density (grayscale) of 1-min power spectral density (PSD) levels compared to the limits of prevailing noise (bottom) (Wenz 1962).

4.2 Sources of Anthropogenic Noise

The contribution of noise from vessel traffic varied across the Cook Strait region, with bathymetry significantly affecting the received levels and the time period that individual vessels were detected. Vessels at station 1 were detected for a relatively short period of time due to the shallow water location (50 m) and narrow passageways characteristic of QCS. In contrast, vessels at stations 5 and 7 were detected for hours, due to the deep open water environment and the propagation of sound off the continental shelf. Vessels were detectable as tonals associated with machinery noise as shown in Figure 4-6, with the vessel transit at approximately 02:00 am shown in Figure 4-7.

With the exceptions of stations 5 and 6 where the contribution of seismic survey activity to the daily sound exposure limit was higher than vessel traffic, vessel noise was the dominant anthropogenic contributor to the soundscape. The soundscape at station 1 in QCS was dominated by vessel-associated noise which drove the daily SEL throughout the recording period, except during the 14 November earthquake and subsequent aftershocks (Figure 4-8). This result differs from stations 2, 5 and 7 where weather events and seismic activity also contributed to the soundscape.

Station 1 in QCS had the highest number of, and the most hours with, vessel detections but the daily SEL was similar to other stations (

Figure 4-9). On average, vessels were detected for 12 hours per day at station 1 as compared to less than 5 hours per day for stations 2, 5 and 7. Similarly, the average number of vessels detected per day was 9 at station 1, and less than 5 for each of the other three stations (Figure 4-9).

Daily and weekly rhythmic pattern analysis of the data showed that the elevated mid-day SPL levels at station 1 were attributed to traffic from ferries and small boats (Figure 4-10). Due to vessel noise, increased sound levels were a persistent feature of the soundscape and were highest in the 100-10000 Hz band. Elevated levels around dusk (6-8 p.m.) in the 100-1000 Hz band is due to fish chorusing events.

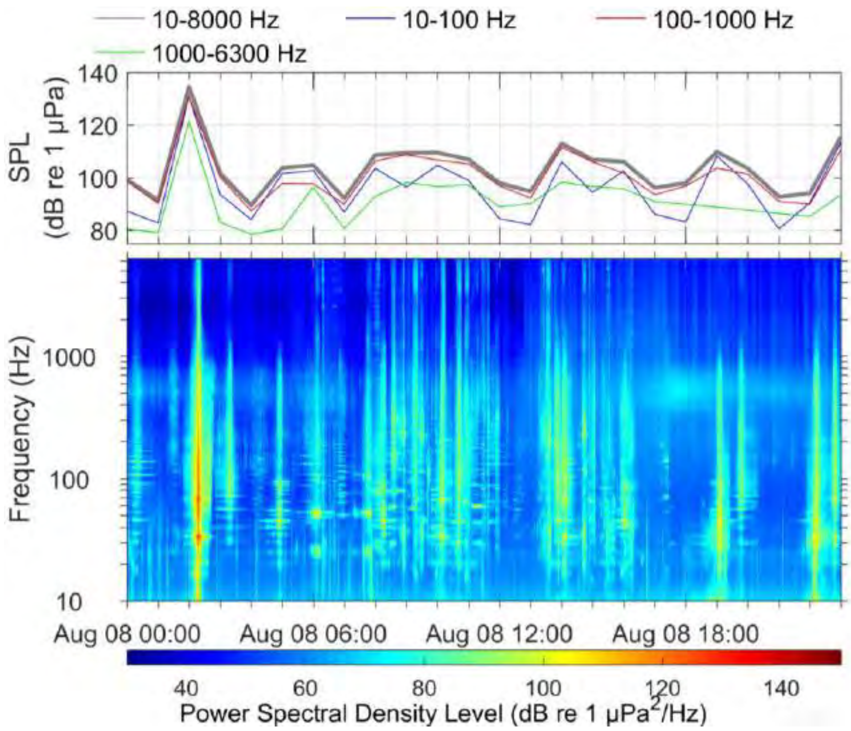

Figure 4-6: Sound level summary for station 1 from 8 August 2016. In-band sound pressure level (SPL) (top) and spectrogram of underwater sound showing tonals associated with vessel machinery (bottom).

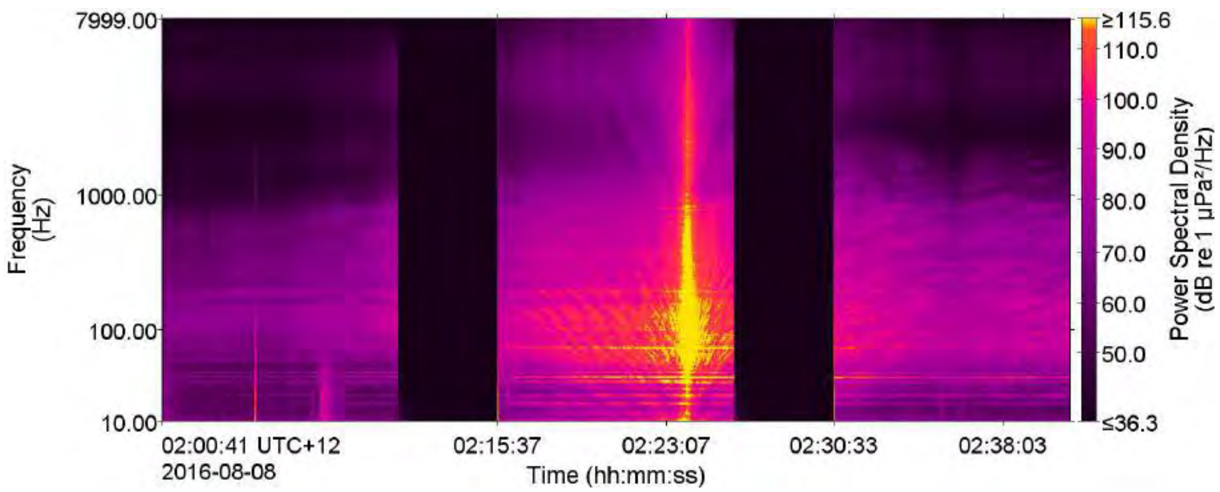

Figure 4-7: Spectrogram of a vessel recorded at station 1 on 8 August 2016. Black sections indicates when the instrument was recording at a different frequency or asleep.

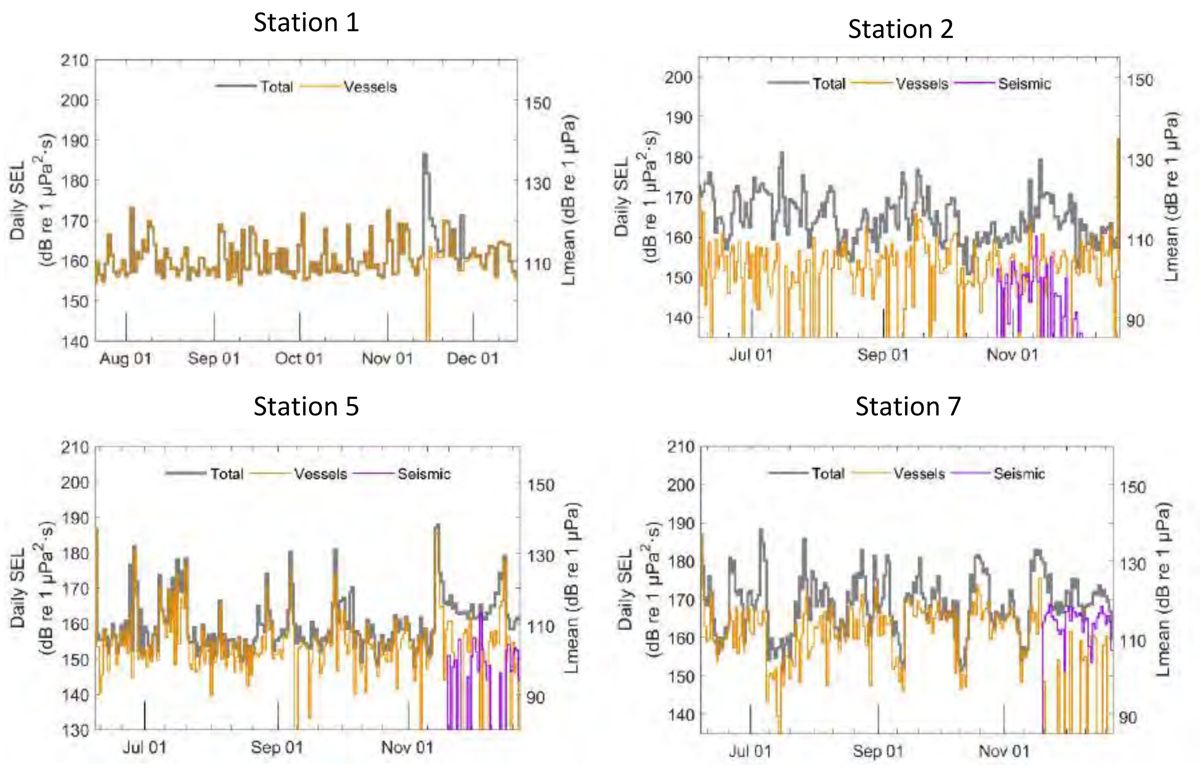

Figure 4-8: Total, vessel, and seismic-associated daily sound exposure level (SEL) and equivalent continuous noise levels (L*mean*). Stations 1 and 2 (top row) and stations 5 and 7 (bottom row).

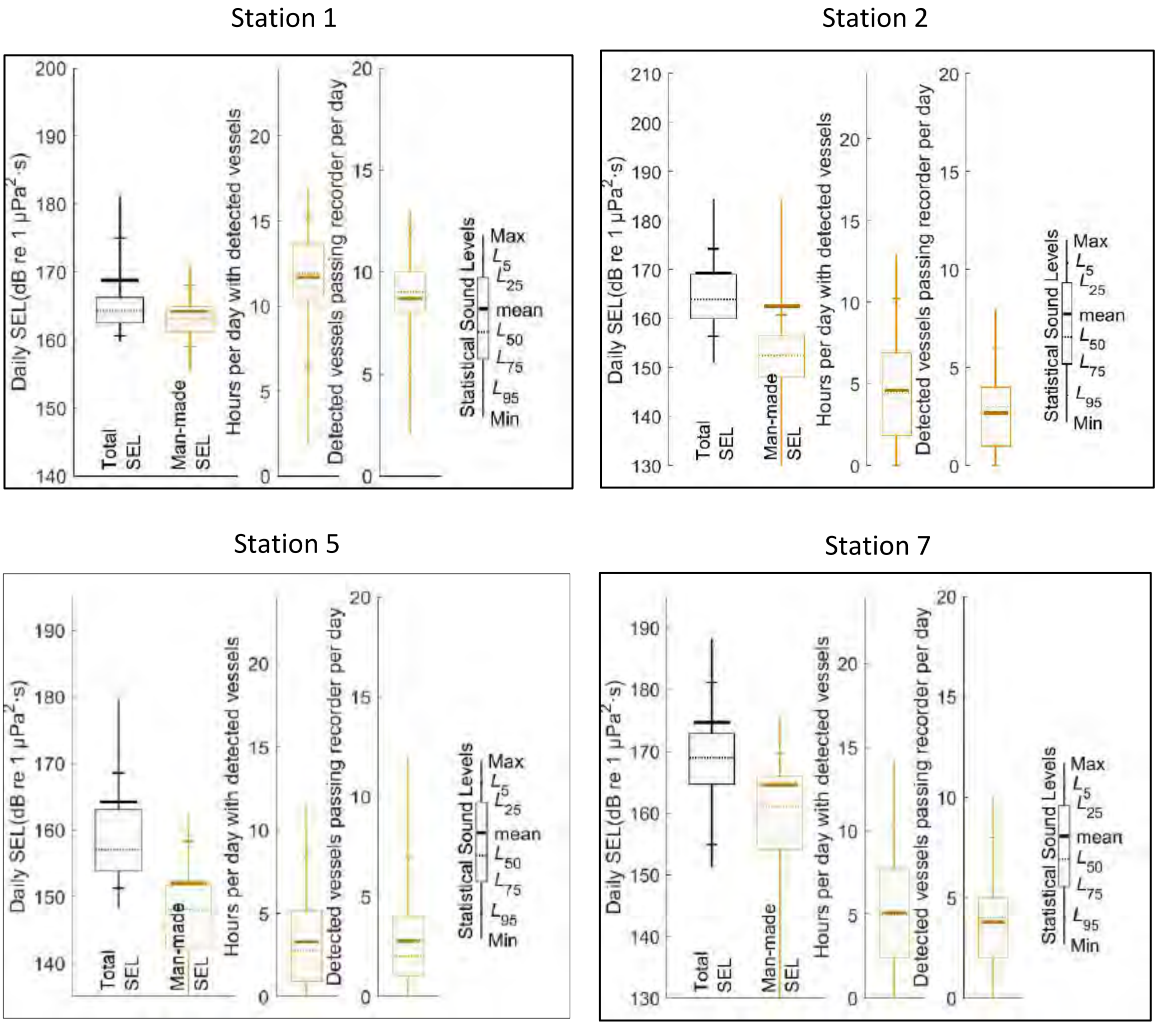

Figure 4-9: Total and man-made associated sound exposure level (SEL), with daily total hours of vessel detection and daily vessel detections. Stations 1 and 2 (top row) and stations 5 and 7 (bottom row).

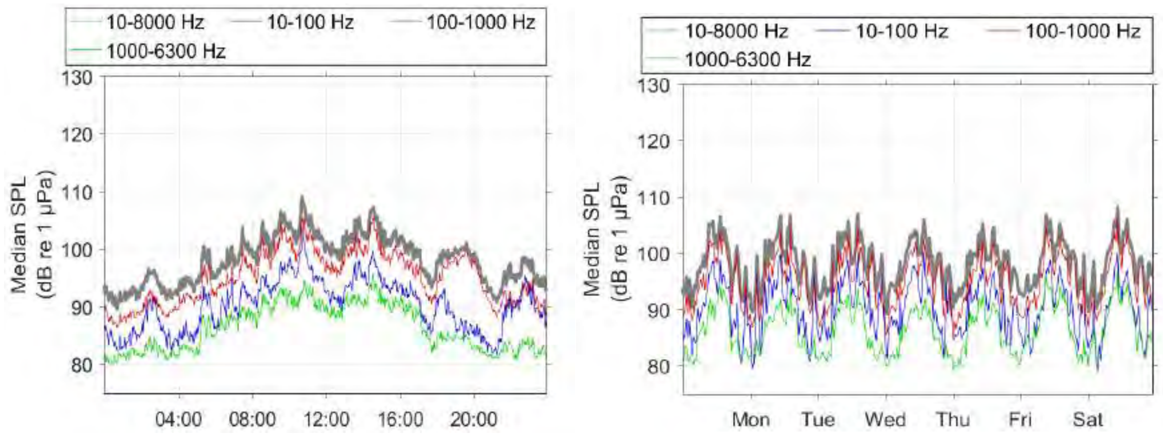

Figure 4-10: Daily (left) and weekly (right) median 1-min sound pressure level (SPL) in approximate-decade-bands for station 1.

4.3 Marine Mammal Detections

Table 4-1 summarizes the cetacean species that were detected in the greater Cook Strait region. Of these species, only Hector's and unidentified dolphin and delphinid species were detected at station 1 in QCS. Hector's dolphin clicks (Figure 4-11**)** were not detected outside of QCS. Automated detections occurred on 57 days, or 38.5% of the recording days with detections peaking between mid-July and mid-August (Figure 4-12**)**. Though not as frequent, Hector's dolphin clicks were also detected throughout October. Outside these periods, detections of Hector's dolphin clicks were less frequent.

Automated detections of whistles from unidentified dolphins (Figure 4-13**)** were detected on 69% of the recording days (Figure 4-14**)**. Despite chain noise, likely from a nearby mooring or other unknown underwater equipment, ~ 70% of the true calls were able to be detected. Echolocation clicks produced by unidentified delphinids (Figure 4-15**)** were automatically detected every day (Figure 4-16**)** but this result did not match the manual validation and the presence of clicks did not conform to the diel pattern typically observed. Therefore, results for unidentified dolphin clicks should be viewed with caution. An examination of the detector's performance indicated that 24% of the detections were incorrect. Further investigation revealed that impulsive signals emitted by small craft powered by outboard engines (Figure 4-17**)** were the main cause for false detections and partly explains the increased number of detections during daylight hours. In order to accurately represent the acoustic occurrence of delphinids near station 1, at least 7% of the data will need to be manually analysed.

Marine mammal observations were also made during the Queen Charlotte Sound / Tōtaranui and Tory Channel / Kura Te Au Hydrographic Survey (HS51), the period of which overlaps with station 1 acoustic detections for seven weeks from 24th October to 13th December 2016 (see Appendix A; Davey et al., 2017; 2017a). During the survey period, sightings recorded in QCS included Hector's dolphins, bottlenose dolphins, dusky dolphins, common dolphins, unidentified dolphins, and Orca (killer whale). These recorded sightings, as well as the sightings over the full duration of HS51, provide a qualitative visual validation of the automated detections at station 1.

Table 4-1: Automated detections and manual validation of cetaceans recorded at various stations in the Cook Strait, New Zealand. Station 4 was excluded from this table because of the high proportion of false detections induced by vessel and flow noise. Abbreviations: na denotes data that was 'not available' due to the poor performance of some detectors; *indicates detections that should be interpreted with caution due to the influence of noise on the automated detectors; **indicates species where automated detectors were ran but no detections were made at any of the stations.

Species grouping	Common name	Scientific name	Stations with automated detections	Stations with manual validation
Odontocetes (toothed whales)	Cuvier's beaked whale	*Ziphius cavirostris*	5, 6, 7	5, 6, 7
	Unidentified beaked whale 1	-	*na*	5, 6, 7
	Unidentified beaked whale 2	-	5, 6, 7	5, 6, 7
	Hector's dolphin	*Cephalorhynchus hectori*	*1**	1
	Pilot whale	*Globicephala* sp.	2, 5, 6, 7	2, 5, 6, 7
	Sperm whale	*Physeter macrocephalus*	3, 5, 6, 7	3, 5, 6, 7
	Unidentified dolphins (whistles)	-	1, 2, 3, 5, 6, 7	1, 2, 3, 5, 6, 7
	Unidentified delphinids (clicks)	-	1*, 2, 3, 5, 6, 7	1*, 2, 3, 5, 6, 7
Mysticetes (baleen whales)	Antarctic blue whale	*Balaenoptera musculus intermedia*	*na*	2, 5, 6, 7
	New Zealand blue whale	*Balaenoptera musculus*	*na*	2, 3, 5, 6
	Humpback whale	*Megaptera novaeangliae*	2, 3, 5, 6, 7	2, 3, 5, 6, 7
	Antarctic minke whale	*Balaenoptera bonaerensis*	*na*	2, 3, 5, 6, 7
	Southern right whale	*Eubalaena australis*	*na*	3
	Sei whale	*Balaenoptera borealis*	*na*	2
	Fin whale	*Balaenoptera physalus*	**	-

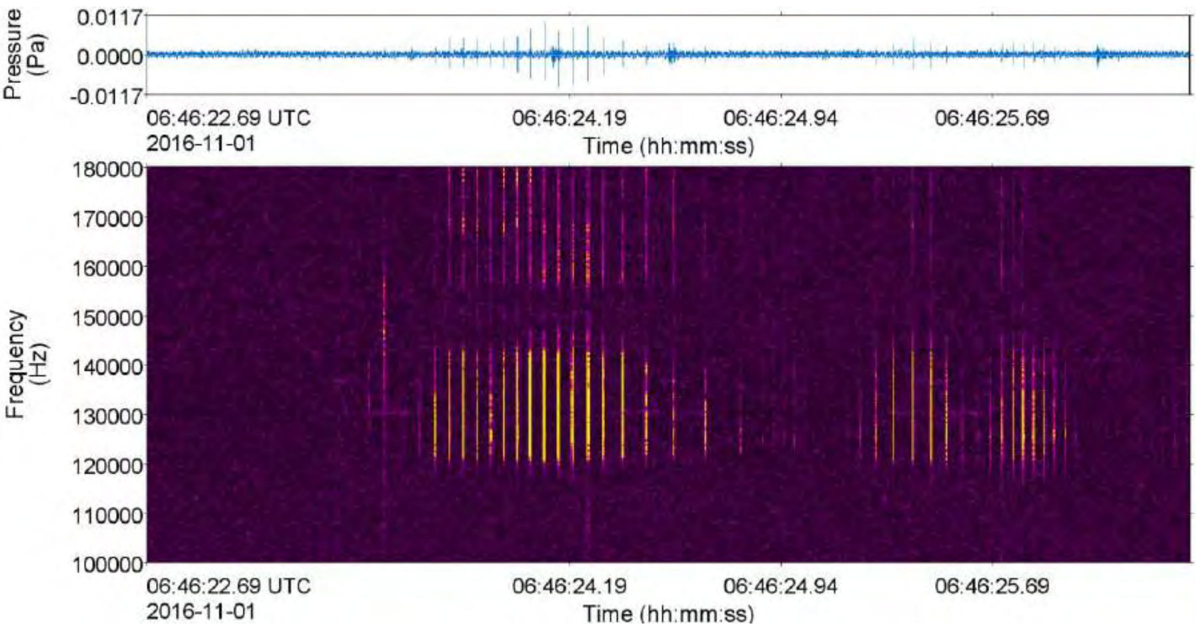

Figure 4-11: Spectrogram of Hector's dolphin click train recorded at station 1 on 01 November 2016.

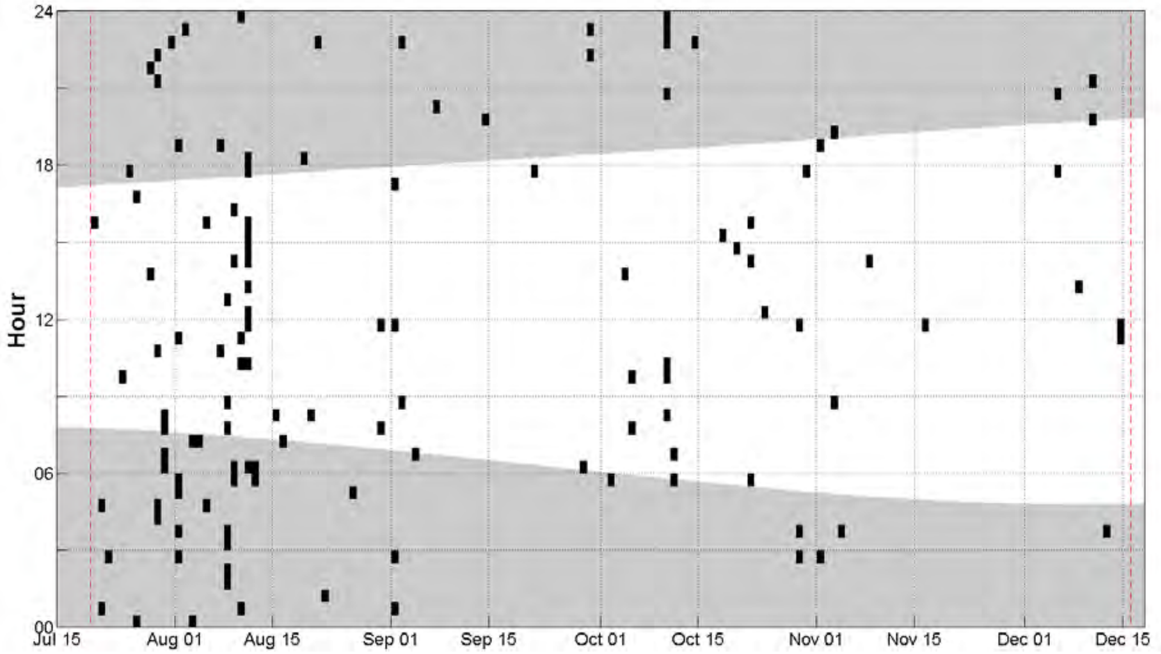

Figure 4-12: Daily and hourly occurrence of automatically detected Hector's dolphin clicks recorded at station 1 from 20 July to 15 December 2016. Shaded areas indicate night and the red dashed lines demark the start and the end of the recording period.

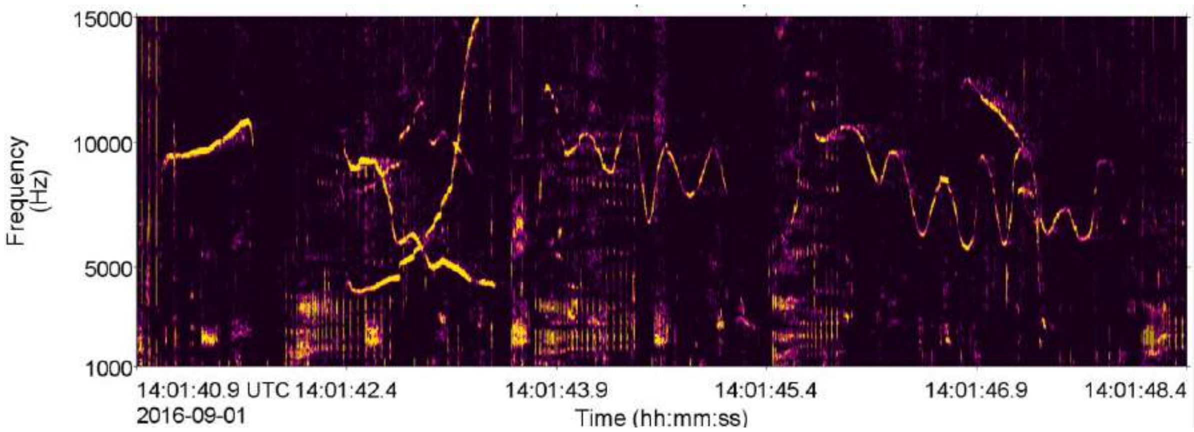

Figure 4-13: Spectrogram of unidentified dolphin whistles recorded at station 1 on 01 September 2016.

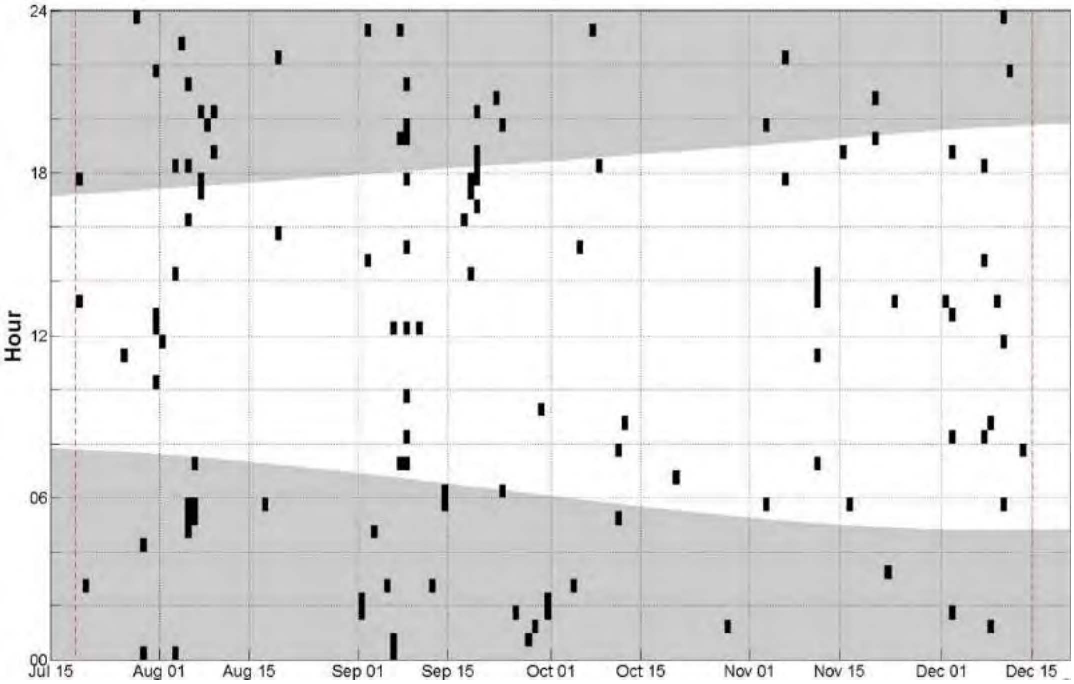

Figure 4-14: Daily and hourly occurrence of automatically detected unidentified dolphin whistles recorded at station 1 from 20 July to 15 December 2016. Shaded areas indicate night and the red dashed lines demark the start and the end of the recording period.

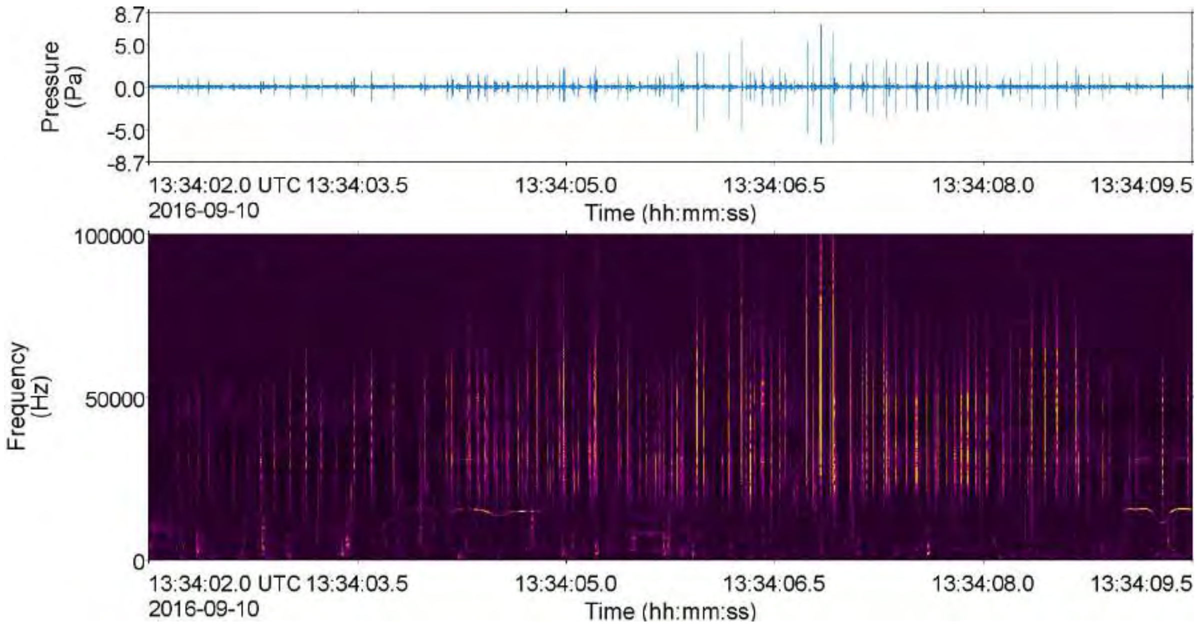

Figure 4-15: Spectrogram of unidentified delphinid click trains recorded at station 1 on 10 September 2016.

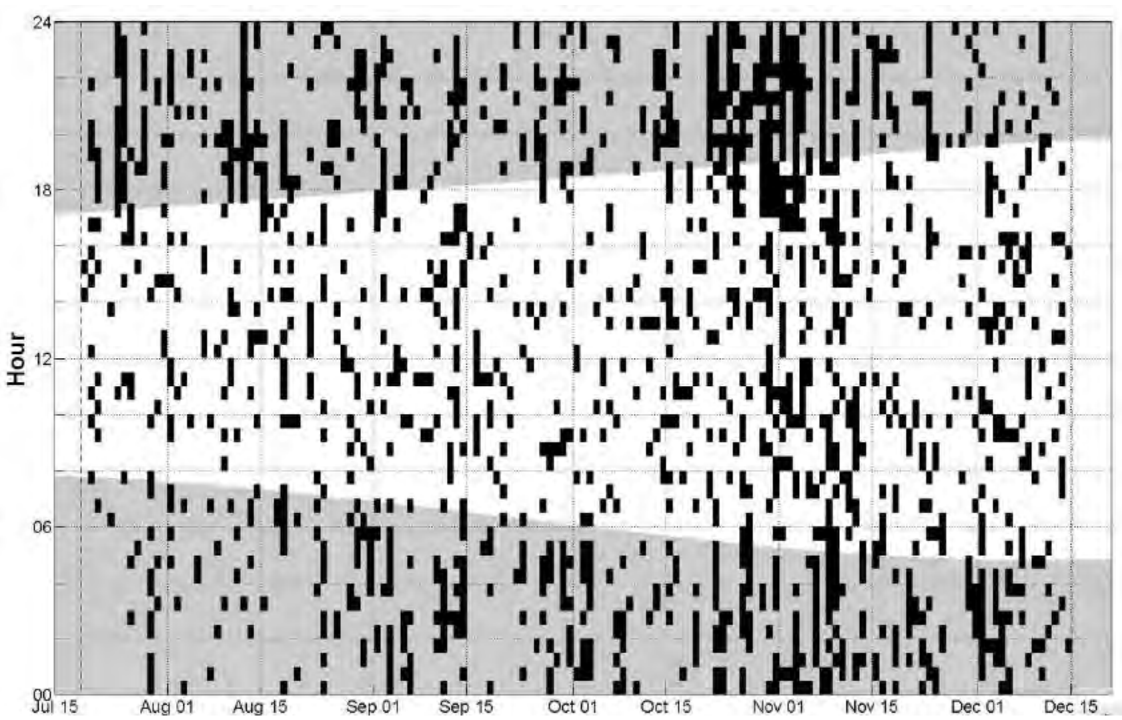

Figure 4-16: Daily and hourly occurrence of automatically detected unidentified delphinid clicks recorded at station 1 from 20 July to 15 December 2016. Shaded areas indicate night and the red dashed lines demark the start and the end of the recording period.

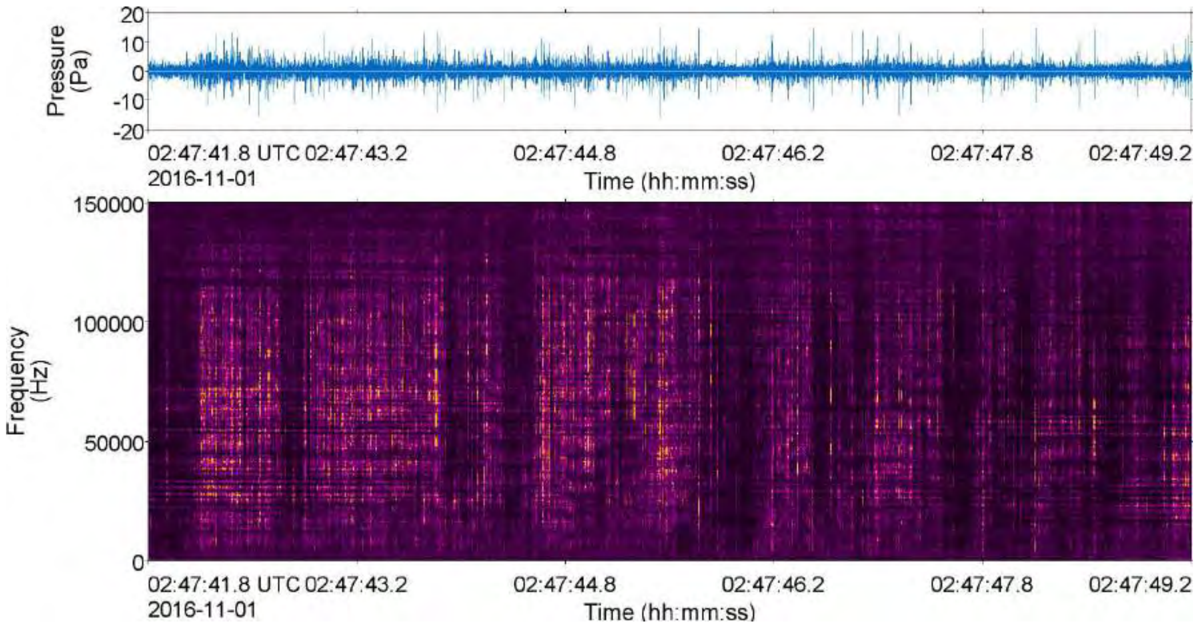

Figure 4-17: Spectrogram of impulsive sounds associated with the transit of a small craft powered by an outboard engine recorded at station 1 on 01 November 2016.

4.4 Fish Chorusing

Fish chorusing events were detected at all stations, including QCS despite increased levels of vessel traffic. These events are typically denoted through the elevated levels from 600–1000 Hz. Fish choruses were detected around dawn and dusk throughout the deployment period and are visible on daily spectrograms (Figure 4-18). The influence of fish chorus events on the soundscape in evident despite occurring for only ~2 hours each day (Figure 4-19).

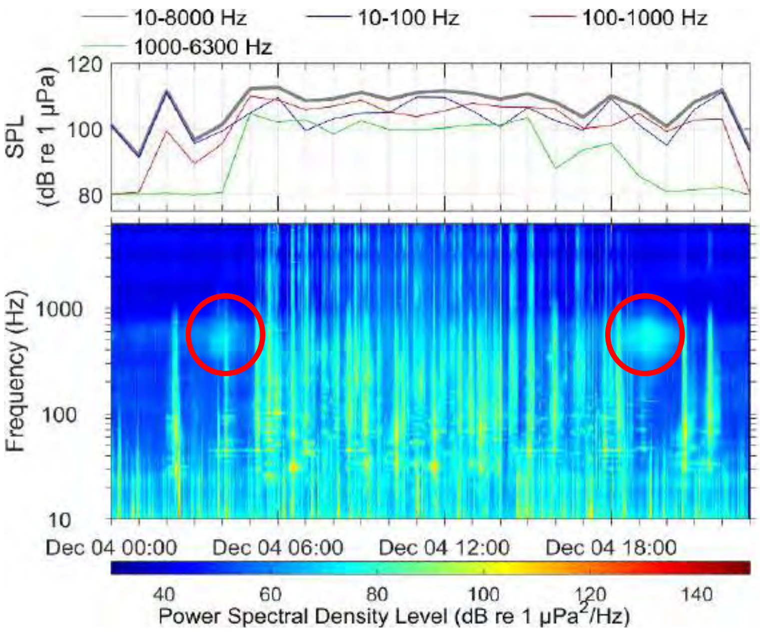

Figure 4-18: Sound level summary from 04 December 2016 recorded on station 1. In-band summary sound pressure level (SPL) (top) and spectrogram of underwater sound (bottom). Red circles denote fish chorusing events.

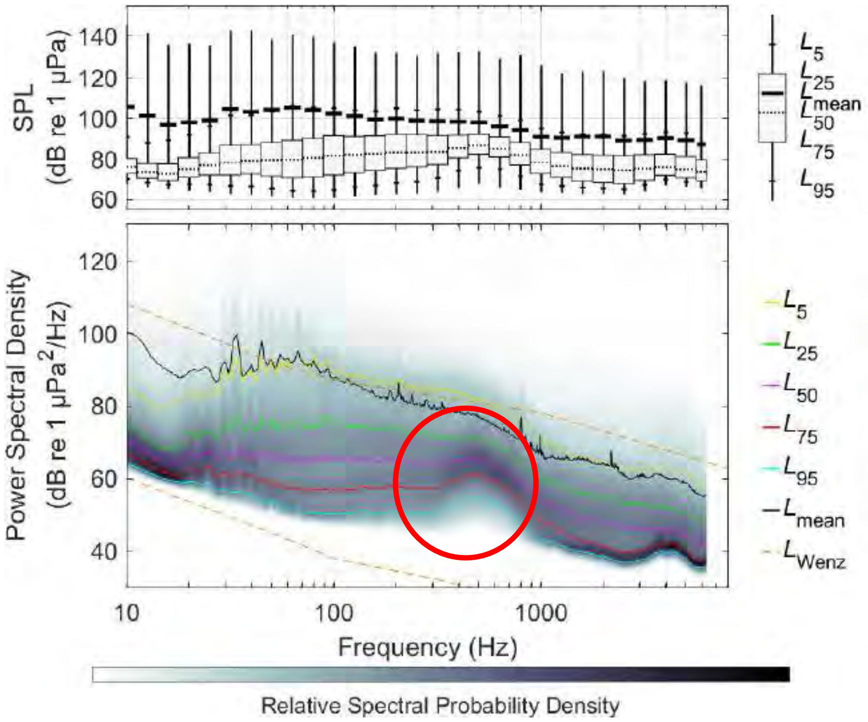

Figure 4-19: Station 1 September 2016. Exceedance percentiles and mean 1/3 octave-band sound presssure level (SPL) (top) and probability density (grayscale) of 1-min power spectral density (PSD) levels comparted to the limits of prevailing noise (Wenz, 1962) shown as dashed lines. The red circle denotes the contribution from fish chorusing events.

5 Summary and Conclusions

The soundscape of the Cook Strait region is influenced by noise from natural (wind, waves and geological seismic events), biological (including marine mammals and fish) and anthropogenic (including shipping and seismic surveys) sources. Weather and anthropogenic noise sources were prominent in this region, and noise from vessels were the dominant man-made contributor to the soundscape. Of all stations, station 1 in QCS had the highest amount of boat traffic. Recreational boating, traffic associated with fish farms, ferries, and large vessels heading in and out of the Sound all contributed to noise levels. Because of the extent and persistent nature of vessel traffic in QCS, the influence of weather (through wind and wave action) was not readily detectable.

The bathymetry at each station significantly affected the levels of shipping noise detected and the time period over which individual vessels were detected. In shallower waters (i.e. stations 1-3) vessels were detected for a shorter period, whereas deeper waters (i.e. stations 4-7) vessel detections lasted several hours. This is due to the location of shipping lanes in Cook Strait and greater sound propagation along the continental shelf in deep water. The shallow and sheltered location of the recorder at station 1 suggests that vessels in transit were detected for a relatively short period. This was compensated by the high frequency of vessels passaging near the recorder.

Although there was no seismic survey activity recorded at station 1 in QCS, seismic surveys did influence the soundscape of the greater Cook Strait region. For example, seismic surveys detected at station 2 in the South Taranaki Bight were found to have less influence on the overall soundscape as they used strong frequency modes. In comparison, the east coast Pegasus Basin survey (near stations 4-7) had more influence on the overall soundscape due to its use of a strong multi-path.

Despite often elevated levels of noise, cetaceans and fish chorusing events were detected at all stations. In QCS, both Hector's dolphins and at least one unidentified species of dolphin were detected throughout the recording period near station 1. Hector's dolphins are known to occur in QCS though not as frequently as in other parts of their range (Dawson, Slooten et al. 2004). A corrected abundance estimate of 20 Hector's dolphins (95% CI: 4-110) was produced from a boat based survey by Dawson et al. (2004). The restricted range of these animals in QCS in combination with the limited hearing range of the acoustic device (a few hundred meters) suggests that the number of Hector's dolphins at station 1 may be less than 20. This result is consistent with current knowledge of Hector's dolphins in QCS, and with sightings recorded by Davey et al. (2017b, 2017a; Appendix A) during 24th October to 13 December 2016.

At station 1, both Hector's and unidentified dolphin detections were common in the first two weeks of August. However, in September and toward the end of the recording period, detections of unidentified dolphins was relatively high while detection's of Hector's dolphins were scarce. Interestingly, the opposite pattern was found in October in which Hector's dolphin detections were more common.

At least three other dolphin species which could have produced whistles detected at station 1 have been sighted in QCS: Dusky (*Lagenorhynchus obscurus*), common (*Delphinus sp.*), and bottlenose dolphins (e.g. Childerhouse 2005; Davey, Neil et al. 2017b; Davey, Neil et al. 2017a). Dusky dolphins typically prefer the Admiralty Bay region to the west of QCS, where several hundred individuals aggregate to feed in winter (Markowitz, Harlin et al. 2004). In addition, this species is not known to produce whistles (Vaughn-Hishorn, Hodge et al. 2012) and therefore would not have contributed to the whistles detected in QCS.

Other than Hector's dolphins, the majority of dolphin sightings in QCS are bottlenose dolphins (Merriman, Markowitz et al. 2009; Davey, Neil et al. 2017b; Davey, Neil et al. 2017a) (Appendix A). The population of bottlenose dolphins in the Marlborough Sounds was estimated to be 211 animals, with the most sightings occurring in QCS (Merriman, Markowitz et al. 2009). These animals are presumed to be part of a larger coastal population. Both bottlenose (Smolker, Mann et al. 1993; Janik and Slater 1998) and common (Petrella, Martinez et al. 2012) dolphins produce whistles. However, because common dolphins are typically found offshore, it is more likely that the whistles detected at station 1 were produced by bottlenose dolphins. It is also worth noting that approximately 200 bottlenose dolphins were encountered shorty after leaving the deployment site on 20 July 2016 (see cover photo).

Detections of unidentified dolphin whistles and delphinid clicks occurred at all stations outside of QCS, with the exception of station 4 which was excluded due to high flow noise. Outside of QCS, it is unknown which species of dolphin produced whistles as both common and bottlenose dolphins produce whistles and occur in New Zealand waters. However, bottlenose dolphins primarily occur in three regions around New Zealand: Northland, Marlborough Sounds and Fiordland (Tezanos-Pinto, Baker et al. 2008), while common dolphins are widely distributed throughout New Zealand waters (Stockin, Pierce et al. 2008). Due to their preferred habitats, the whistles detected outside of QCS are likely attributed to common dolphins. Detections of unidentified delphinid clicks were most likely to be from common dolphins (*Delphinus sp.*) and bottlenose dolphins (*Tursiops truncatus*), based on known occurrence patterns in New Zealand, but it is possible that other species are present.

Other toothed whales detected in the greater Cook Strait region include sperm whales and beaked whales. Sperm whales were detected at multiple stations but were most common at station 5 located near Kaikoura Canyon, where the species' year-round occurrence is well documented (Jacquet and Whitehead 1999). In addition, three types of beaked whales (Cuvier's and two unidentified species) were detected at the three deep water stations (5, 6, and 7). Based on published studies, the unidentified beaked whale species are likely to be Gray's (*Mesoplodon grayi*) (Trickey, Reyes et al. 2014; Trickey, Baumann-Pickering et al. 2015) and straptoothed (*M. layardii*) beaked whales.

Five species of baleen whales were detected in the greater Cook Strait region. Humpback whales were detected at all stations (except for station 1) predominantly between July and August. This is consistent with the literature which reports this species being present in New Zealand waters between May and August (Dawbin 1956) before migrating north to tropical waters. The greatest detections were at stations 2 and 3. This suggests that the Cook Strait is an important migratory path for this species that is used more regularly than the north-east coast of the North Island.

New Zealand blue whales were dominant at station 2, particularly from June to August. The seasonality of these detections is consistent with the winter peak and summer absence in song production by this species (Stafford, Bohnenstiehl et al. 2004; Oleson, Wiggins et al. 2007). These detections are not surprising since New Zealand blue whales are thought forage in this area (Torres 2013). In contrast, Antarctic blue whales were primarily recorded at the deep water stations east of the Cook Strait during July, August and October. This species has been previously been recorded off northern (McDonald 2006) and southern (Double, Barlow et al. 2013) New Zealand. While blue whale calls can travel vast distances, these vocalisations were likely produced in New Zealand waters based on the characteristics of the recordings.

While Antarctic minke whales occur throughout much of the Southern Hemisphere, this study presents the first records of this species in New Zealand waters. This species has been recorded acoustically in Australia during winter and spring (Risch, Gales et al. 2014), and therefore it is not surprising that detections occurred here during winter months. It has been suggested that only some animals may undertake a seasonal migration while others remain in Antarctica (Matthews, Macleod et al. 2004; McCauley, R. D., Bannister et al. 2004; Erbe, Verma et al. 2015). Considering this, it is plausible that Antarctic minke whales migrate through the Cook Strait region, and possibly over-winter in New Zealand waters.

Southern right whales are primarily found in the sub-Antarctic Auckland Islands where they go to calve, with smaller numbers wintering at Campbell Island and around the New Zealand mainland (Rayment, Davidson et al. 2011). The single detection of southern right whales may be due to the low number of individuals near recording sites in the Cook Strait. Historical records indicate that this species was hunted in sheltered bays of the Cook Strait (Richards 2009) and therefore low numbers detected in this region may indicate recolonization of an area inhabited prior to whaling.

Sei whales are distributed worldwide and are primarily found offshore (Rice 1998). Like many other baleen whales, sei whales migrate between tropical waters in the winter and subpolar waters in the summer. In January-February, sei whales are typically found between 45°S and 60°S within the South Pacific Ocean (Miyashita, Kato et al. 1995) while their winter distribution in the southern hemisphere is largely unknown. The single detection of a sei whale in the Cook Strait region occurred at station 2 during July indicates that this species is either transiting through or inhabiting New Zealand waters in winter.

In addition to cetaceans, fish choruses made a biological contribution to the soundscape at all stations. Many species of fish produce sound for purposes such as communication, feeding, swimming, and reproduction (Busnel 1963). Fish produce sounds using a variety of mechanisms but most commonly form striking two bony structures together to produce broadband sounds which is then amplified by the swim bladder, an organ that regulates buoyancy, to produce a fundamental frequency and its harmonics (National Research Council 2003). It is not known how many fish species produce sound. However, studies have shown that deep-sea fish of the family *Myctophidae* (lantern fish) have specialized muscles connected to the swim batter for sound production (Marshall 1962; Marshall 1967). In New Zealand waters, red gurnard (*Chelidonichthys kumu*), in the family *Triglidae,* are also known to vocalise (Ghazali 2011). Choruses typically occur when many individuals produce noise in spatial-temporal proximity to one another to produce a cacophony of sounds (McCauley, Robert D. and Cato 2016). Although uncertain, given the characteristics and timing of the chorusing events observed, it is likely that fish species responsible belong to the *Myctophidae* family at the deep water stations and red gurnard at shallow water stations, including QCS.

Results presented in this report demonstrate that PAM is a cost-effective and autonomous method to monitor natural, biological and anthropogenic sound sources. Specifically, acoustics can be used to monitor marine mammal populations and to monitor the ambient soundscape. The data recorded during this project represents an acoustic snapshot of the greater Cook Strait region in space and time. Because the detection range was not modelled, results presented in this report are only relevant to areas proximate to the seven stations and are not necessarily representative of areas outside the listening radii of the acoustic instruments. Furthermore, future efforts should focus on increasing the level of manual data analysis in order to overcome challenges associated with species for which little is known about their vocal repertoire or for which automated detectors either performed poorly or have not yet been developed.

6 Acknowledgements

We acknowledge the sponsors of this project which include OMV New Zealand Ltd, Marlborough District Council, Chevron New Zealand Holdings LLC, and Woodside Energy Ltd. We would like to thank the captain and crew of the *RV Ikatere*, *RV Tangaroa*, and *RV Kaharoa* as well as the many technicians that made the deployment of the acoustic moorings possible. Craig McPherson was instrumental in providing advice and guidance throughout this project.

7 Glossary of Abbreviations and Terms

AMAR	Autonomous Multichannel Acoustic Recorders
LINZ	Land Information New Zealand
MDC	Marlborough District Council
NIWA	National Institute of Water and Atmospheric Research
PAM	Passive Acoustic Monitoring
PSD	Power Spectral Density
QCS	Queen Charlotte Sound / Tōtaranui
SEL	Sound Exposure Level
SPL	Sound Pressure Level

8 References

Busnel, R.G. (1963) *Acoustic behaviour of animals*. Elsevier, Amsterdam.

Childerhouse, S. (2005) Cetacean research in New Zealand 2003/2004. *DOC Science Internal Series*, 214.

Davey, N., Neil, H., HS51 Survey team (2017a) Queen Charlotte Sound / Tōtaranui and Tory Channel / Kura Te Au Hydrographic Survey, LINZ Project HYD-2016/17-01 (HS51), Marine Mammal Observations. OBIS at https://nzobisipt.niwa.co.nz/resource?r=hs51marinemammalobs&v=1.0, GBIF at https://doi.org/10.15468/s7ctpf. 10.15468/s7ctp

Davey, N., Neil, H., HS51 Survey team (2017b) Queen Charlotte Sound / Tōtaranui and Tory Channel / Kura Te Au Hydrographic Survey, LINZ Project HYD-2016/17-01 (HS51), Marine Mammal Report. NIWA Client Report 2017208WN.,

Dawbin, W.H. (1956) The migrations of humpback whales which pass the New Zealand coast. *Transactions of the Royal Society of New Zealand*.

Dawson, S., Slooten, E., DuFresne, S., Wade, P., Clement, D. (2004) Small-boat surveys for coastal dolphins: line-transect surveys for Hector's dolphins (*Cephalorhynchus hectori*). *Fishery Bulletin*, 102(3): 441-451. <Go to ISI>://WOS:000223030100004

Deane, G.B. (2000) Long time-base observations of surf noise. *Journal of the Acoustical Society of America*, 107(2): 758-770.

Double, M., Barlow, J., Miller, B., Olson, P., Andrews-Goff, V., Leaper, R., Ensor, P., Kelly, N., Lindsay, M., Peel, D. (2013) Cruise report of the 2013 Antarctic blue whale voyage of the Southern Ocean Research Partnership. *Report SC65a/SH/21 submitted to the Scientific Committee of the International Whaling Commission. Jeju Island, Republic of Korea*.

Erbe, C., Verma, A., McCauley, R., Gavrilov, A., Parnum, I. (2015) The marine soundscape of the Perth Canyon. *Progress in Oceanography*, 137: 38-51.

Jacquet, N., Whitehead, H. (1999) Movements, distribution and feeding success of sperm whales in the Pacific Ocean, over scales of days and tens of kilometers. *Aquatic Mammals*, 25(1): 1-13.

Janik, V., Slater, P. (1998) Context-specific use suggests that bottlenose dolphin signature whistles are cohesion calls. *Animal Behaviour*, 56: 829-838.

Markowitz, T., Harlin, A., Wursig, B., Mcfadden, C. (2004) Dusky dolphin foraging habitat: overlap with aquaculture in New Zealand. *Aquatic Conservation: Marine and Freshwater Ecosystems*, 14(2): 133-149. <Go to ISI>://000220495900003

Marshall, N. (1962) The biology of sound-producing fishes. *Symp. Zool. Soc. Lond*.

Marshall, N. (1967) Sound-producing mechanisms and the biology of deep-sea fishes. *Marine bio-acoustics*, 2: 123-133.

Matthews, D., Macleod, R., McCauley, R. (2004) Bio-duck activity in the Perth Canyon. An automatic detection algorithm. *Proceedings of Acoustics*, 2004: 63-66.

McCauley, R.D., Bannister, J., Burton, C., Jenner, C., Rennie, S., Kent, C.S. (2004) Western Australian exercise area blue whale project. Final summary report: Milestone 6.

McCauley, R.D., Cato, D.H. (2016) Evening choruses in the Perth Canyon and their potential link with Myctophidae fishes. *The Journal of the Acoustical Society of America*, 140(4): 2384-2398. 10.1121/1.4964108

McDonald, M.A. (2006) An acoustic survey of baleen whales off Great Barrier Island, New Zealand. *Zealand Journal of Marine and Freshwater Research*, 40(4): 519-529.

McPherson, C., Delarue, J., Whitt, C., Maxner, E., Kowarski, K., Mouy, X. (2017) Acoustic Monitoring in the Cook Strait Region: Document 01391, Version 1.0. Technical report by JASCO Applied Sciences for NIWA.,

Merriman, M.G., Markowitz, T.M., Harlin-Cognato, A.D., Stockin, K.A. (2009) Bottlenose dolphin (*Tursiops truncatus*) abundance, site fidelity, and group dynamics in the Marlborough Sounds, New Zealand. *Aquatic Mammals*, 35(4): 511.

Miyashita, T., Kato, H., Kasuya, T. (1995) *Worldwide Map of Cetacean Distribution Based on Japanse Sighting Data*. National Research Institute of Far Sea Fisheries.

National Research Council (2003) *Ocean noise and marine mammals*. National Academies Press.

Oleson, E.M., Wiggins, S.M., Hildebrand, J.A. (2007) Temporal separation of blue whale call types on a southern California feeding ground. *Animal Behaviour*, 74(4): 881-894.

Petrella, V., Martinez, E., Anderson, M.G., Stockin, K.A. (2012) Whistle characteristics of common dolphins (Delphinus sp.) in the Hauraki Gulf, New Zealand. *Marine Mammal Science*, 28(3): 479-496. 10.1111/j.1748-7692.2011.00499.x

Rayment, W., Davidson, A., Dawson, S., Slooten, E., Webster, T. (2011) Distribution of southern right whales on the Auckland Islands calving grounds. *New Zealand Journal of Marine and Freshwater Research*, 46(3): 431-436.

Rice, D. (1998) Marine mammals of the world: systematics and distribution, special publication number 4, the Society for Marine Mammalogy. Allen Press, USA. 231pp.

Richards, R. (2009) Past and present distributions of Southern right whales (*Eubalaena australis*). *New Zealand Journal of Zoology*, 36(4): 447-459.

Risch, D., Gales, N.J., Gedamke, J., Kindermann, L., Nowacek, D.P., Read, A.J., Siebert, U., Van Opzeeland, I.C., Van Parijs, S.M., Friedlaender, A.S. (2014) Mysterious bio-duck sound attributed to the Antarctic minke whale (*Balaenoptera bonaerensis*). *Biology Letters*, 10(4): 20140175.

Ross, D. (1976) *Mechanics of Underwater Noise*. Pergamon Press, New York.

Smolker, R.A., Mann, J., Smuts, B.B. (1993) Use of signature whistles during separations and reunions by wild bottlenose dolphin mothers and infants. *Behavioral Ecology and Sociobiology*, 33: 393-402.

Stafford, K.M., Bohnenstiehl, D.R., Tolstoy, M., Chapp, E., Mellinger, D.K., Moore, S.E. (2004) Antarctic-type blue whale calls recorded at low latitudes in the Indian and eastern Pacific Oceans. *Deep Sea Research Part I: Oceanographic Research Papers*, 51(10): 1337-1346.

Stockin, K.A., Pierce, G.J., Binedell, V., Wiseman, N., Orams, M.B. (2008) Factors affecting the occurrence and demographics of common dolphins (*Delphinus* sp.) in the Hauraki Gulf, New Zealand. *Aquatic Mammals*, 34(2): 200.

Tezanos-Pinto, G., Baker, C.S., Russell, K., Martien, K., Baird, R.W., Hutt, A., Stone, G., Mignucci-Giannoni, A.A., Caballero, S., Endo, T. (2008) A worldwide perspective on the population structure and genetic diversity of bottlenose dolphins (*Tursiops truncatus*) in New Zealand. *Journal of Heredity*, 100(1): 11-24. Torres, L. (2013) Evidence for an unrecognised blue whale foraging ground in New Zealand. *New Zealand Journal of Marine and Freshwater Research*, 47(2): 235-248.

Trickey, J.S., Baumann-Pickering, S., Hildebrand, J.A., Reyes Reyes, M.V., Melcón, M., Iñíguez, M. (2015) Antarctic beaked whale echolocation signals near South Scotia Ridge. *Marine Mammal Science*, 31(3): 1265-1274.

Trickey, J.S., Reyes, M.V.R., Baumann-Pickering, S., Melcón, M.L., Hildebrand, J.A., Iñíguez, M.A. (2014) Acoustic encounters of killer and beaked whales during the 2014 SORP cruise. *IWC Report SC/65b/SM12*.

Vaughn-Hishorn, R.L., Hodge, K.B., Wursig, B., Sappenfield, R.H., Lammers, M.O., Dudzinski, K.M. (2012) Characterizing dusky dolphin sounds from Argentina and New Zealand. *Journal of the Acoustical Society of America*, 132(1): 498-506.

Wenz, G.M. (1962) Acoustic ambient noise in the ocean: Spectra and sources. *Journal of the Acoustical Society of America*, 34(12): 1936-1956.

Appendix A Marine Mammal Observations from HS51

The National Institute of Water and Atmospheric Research (NIWA) was contracted in October 2016 by Land Information New Zealand (LINZ) to undertake hydrographic surveying services for the Queen Charlotte Sound / Tōtaranui (QCS) and Tory Channel / Kura Te Au Hydrographic Survey (HS51).

This survey comprises both hydrographic (LINZ) and habitat mapping (Marlborough District Council (MDC)) using multibeam sounders. The frequency of the sound emitted by a multibeam echo sounder used in HS51 is outside the hearing range of marine mammals in the Sounds, however as a precaution, NIWA ensured best practice for minimising survey activities in the immediate proximity of marine mammals, including logging all sightings while on multibeam effort and reporting to a Marine Mammal Liaison Group.

Observations were recorded between 24th October 2016 to 18th June 2017, across all survey areas of HS51 (Davey et al., 2017; 2017a). This period of observations overlap with the data collected at the Station 1 acoustic mooring deployment in QCS which spanned from 20 July 2016 to 15 December 2016 (Table 3-1).

Overall, HS51 recorded 229 sightings which included bottlenose dolphins (*Tursiops truncatus*), dusky dolphins (*Lagenorhynchus obscurus*), common dolphins (*Delphinus delphis*), Hector's dolphins (*Cephalorhynchus hectori*) and New Zeand fur seals (*Arctocephalus forsteri*). Also sighted were Orca (killer whale, *Orcinus orca*), unidentified dolphins, an unidentified marine mammal and a Rorqual whale (Sei or Brydes), (Figure A-1). During the overlapping period of HS51 observations with the acoustic mooring deployment in QCS, 66 sightings were recorded and were comprised of bottlenose dolphins, dusky dolphins, common dolphins, Hector's dolphins, unidentified dolphins, Orca (killer whale), and New Zealand fur seals (Figure A-2). A Roqual whale was also recorded but not within QCS.

The distribution of sightings for all species together and individually (excluding New Zealand fur seal) are also provided for the period of the entire HS51 survey and for the period overlapping with the acoustic mooring deployment in QCS (Figure A-3 to Figure A-14).

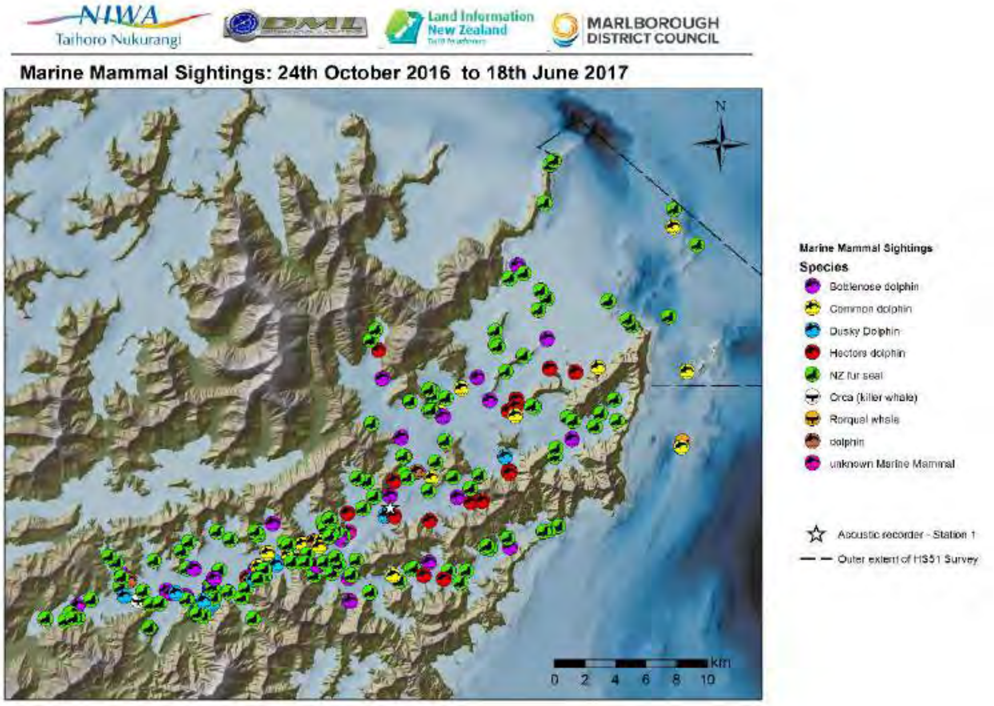

Figure A-1: HS51 sightings for the period 24th October 2016 to 18th June 2017. Acoustic mooring deployment location indicated by white star.

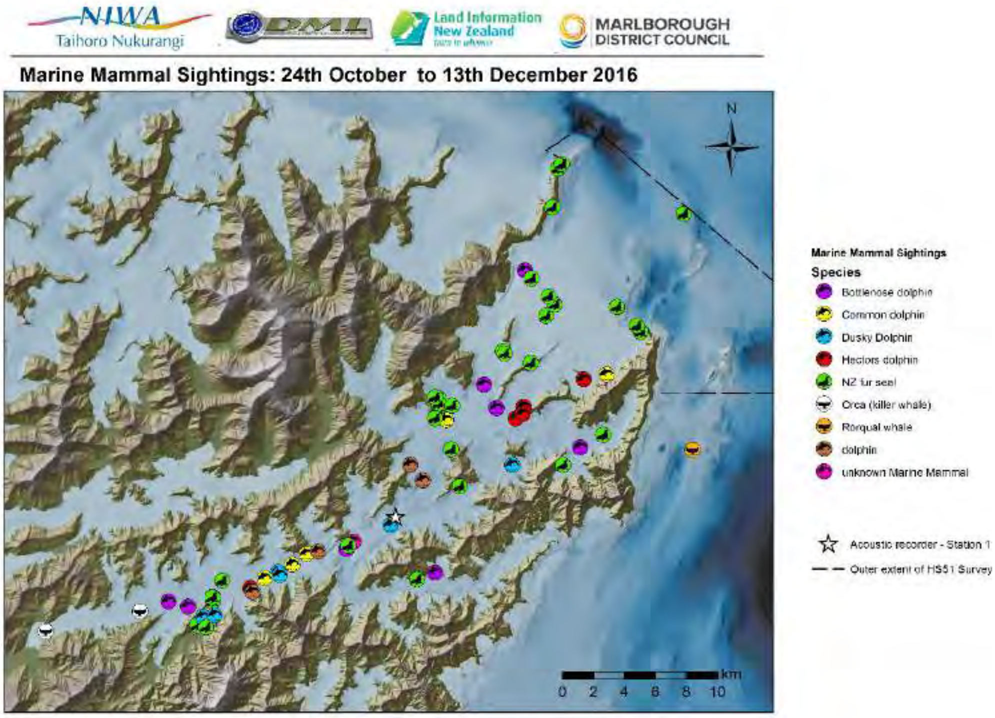

Figure A-2: HS51 sightings for the period 24th October to 13th December 2016 overlapping with acoustic monitoring. Acoustic mooring deployment location indicated by white star.

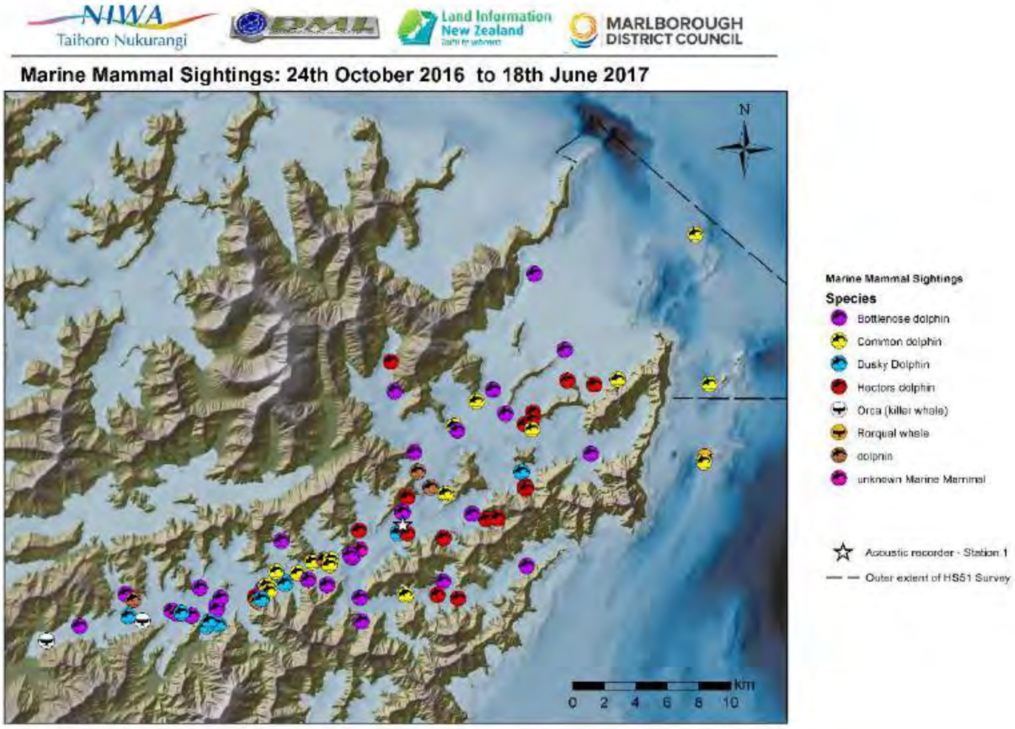

Figure A-3: HS51 sightings for the period 24th October 2016 to 18th June 2017, excluding New Zealand fur seal sightings. Acoustic mooring deployment location indicated by white star.

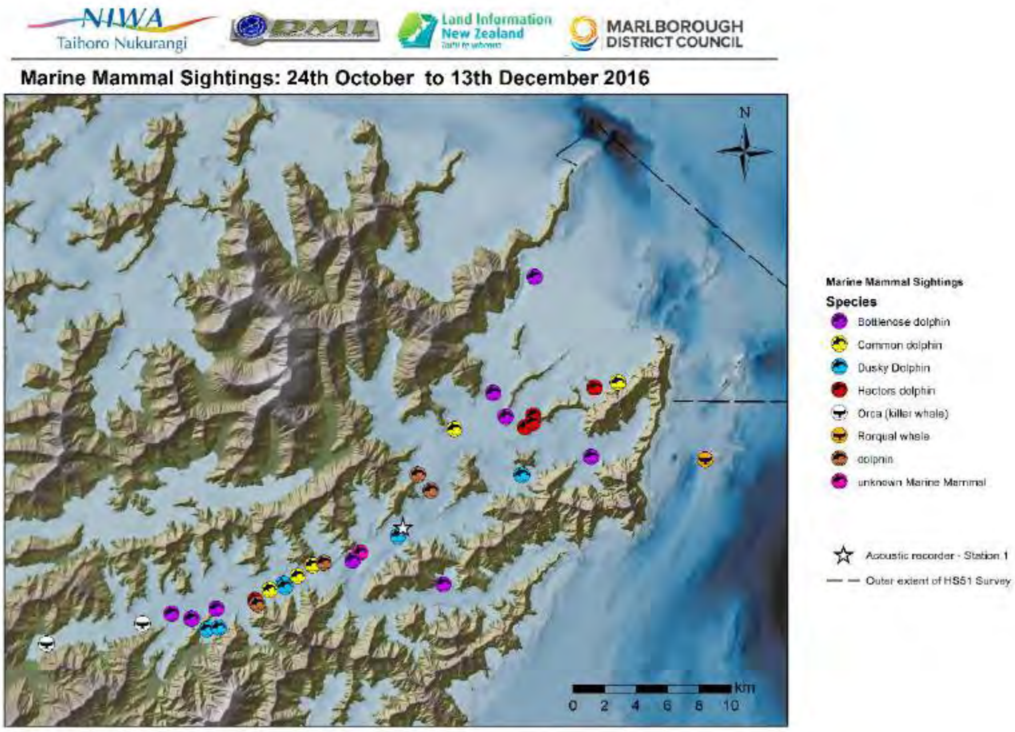

Figure A-4: HS51 sightings for the period 24th October to 13th December 2016 overlapping with acoustic monitoring, excluding NZ Fur Seal sightings. Acoustic mooring deployment location indicated by white star.

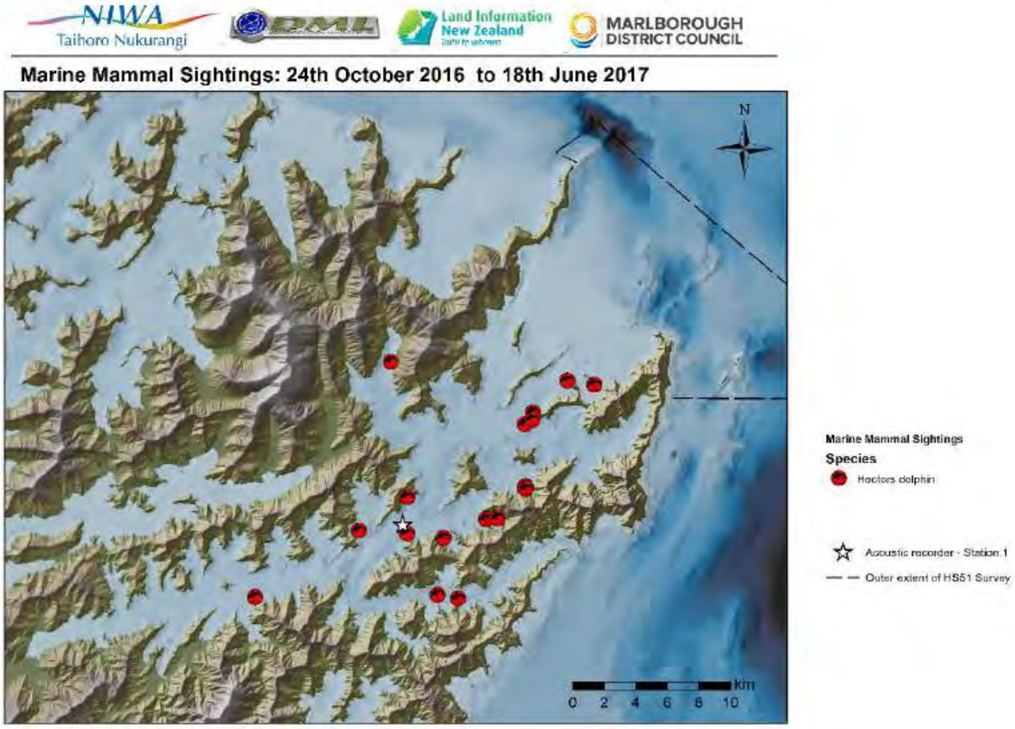

Figure A-5: Hector's dolphin sightings for the period 24th October 2016 to 18th June 2017. Acoustic mooring deployment location indicated by white star.

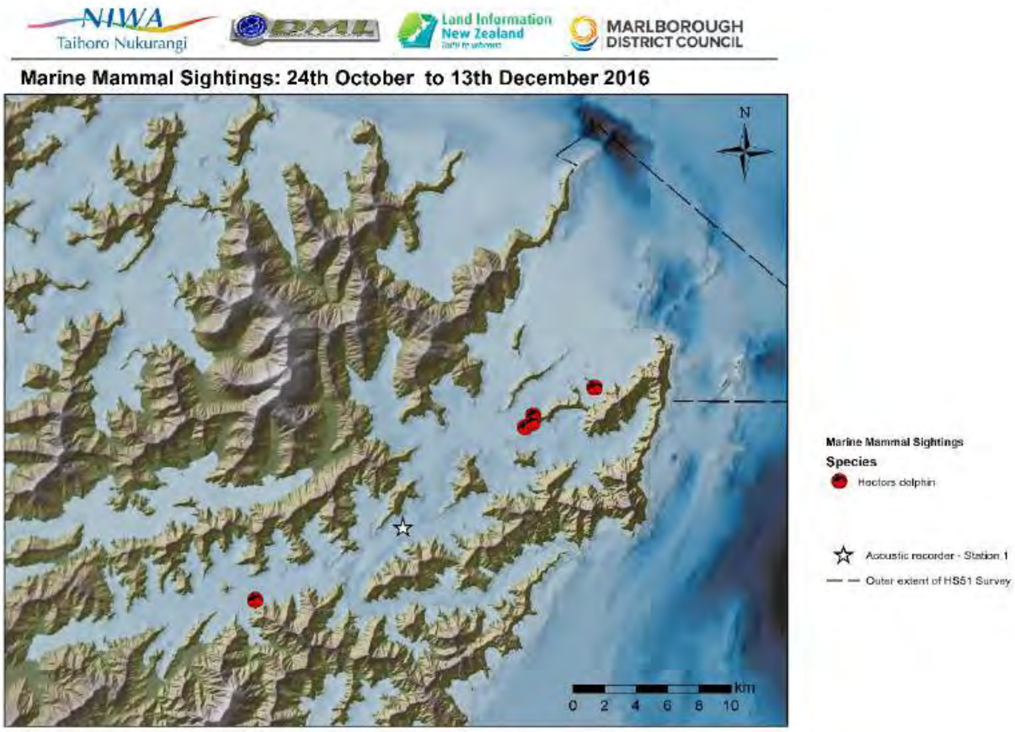

Figure A-6: Hector's dolphin sightings for the period 24th October to 13th December 2016 overlapping with acoustic monitoring. Acoustic mooring deployment location indicated by white star.

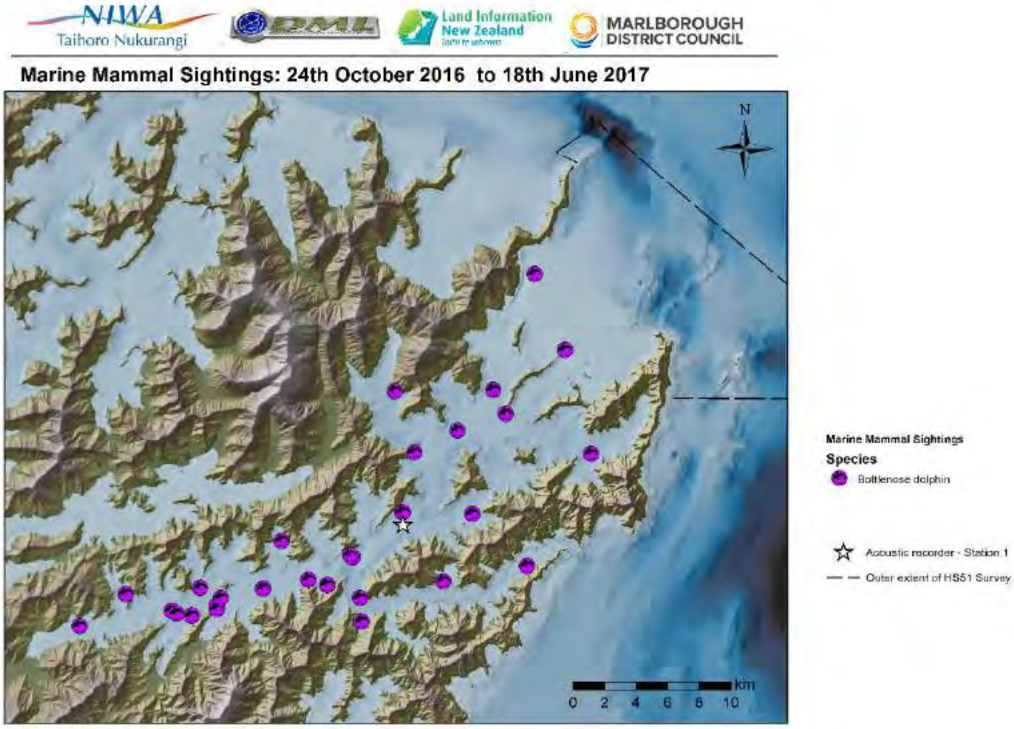

Figure A-7: Bottlenose dolphin sightings for the period 24th October 2016 to 18th June 2017. Acoustic mooring deployment location indicated by white star.

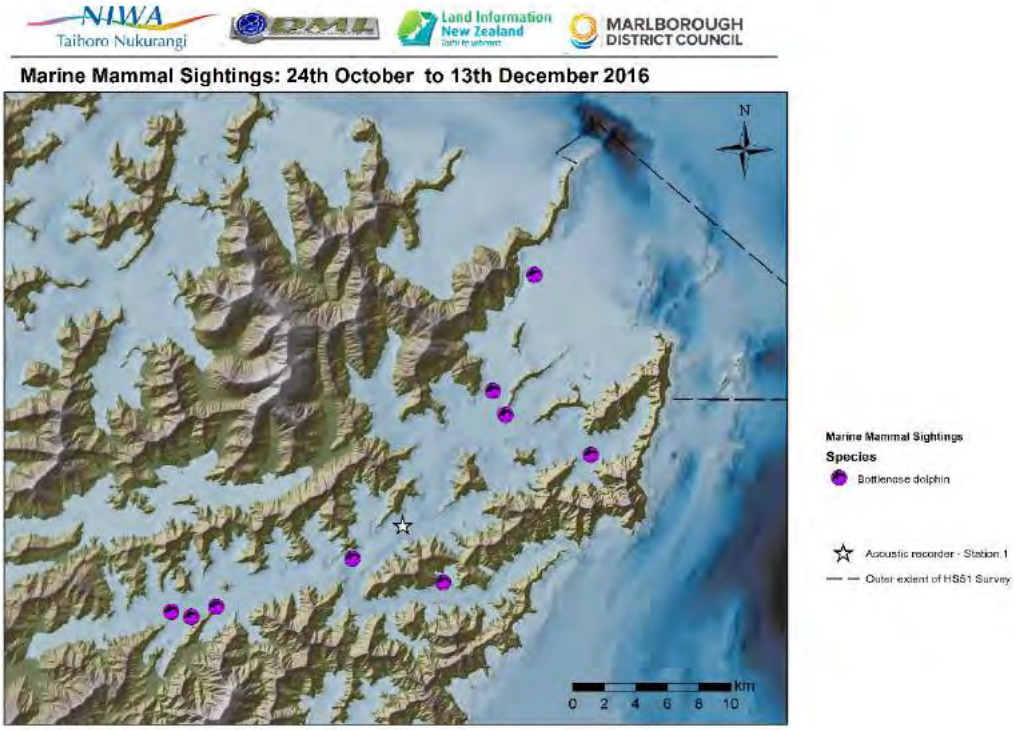

Figure A-8: Bottlenose dolphin sightings for the period 24th October to 13th December 2016 overlapping with acoustic monitoring. Acoustic mooring deployment location indicated by white star.

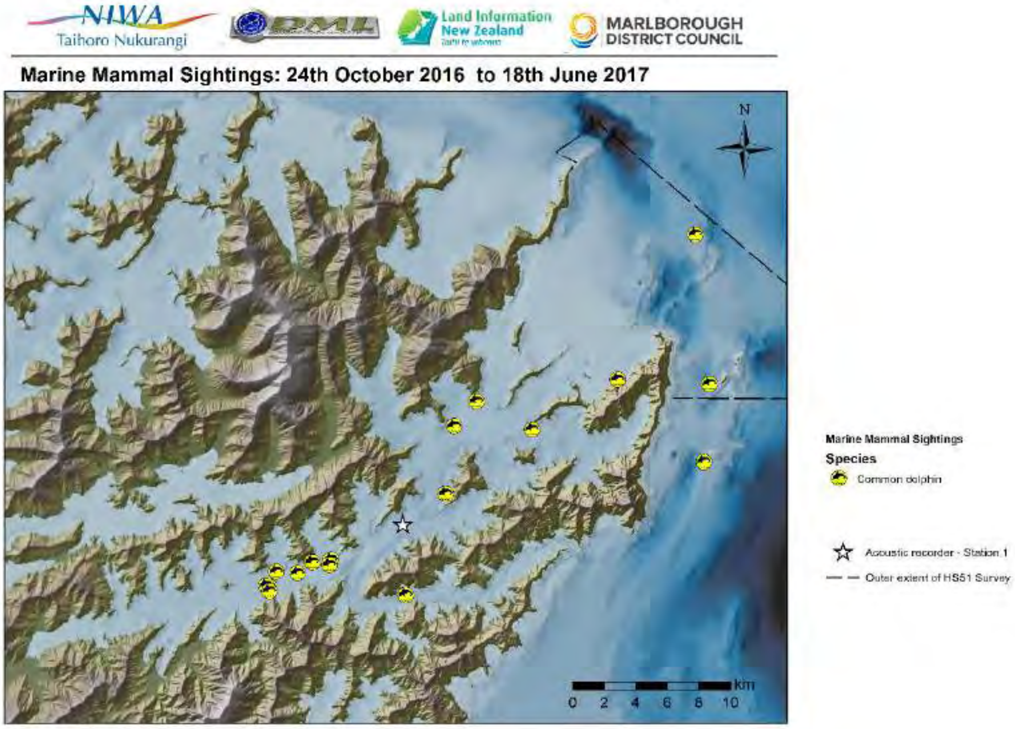

Figure A-9: Common dolphin sightings for the period 24th October 2016 to 18th June 2017. Acoustic mooring deployment location indicated by white star.

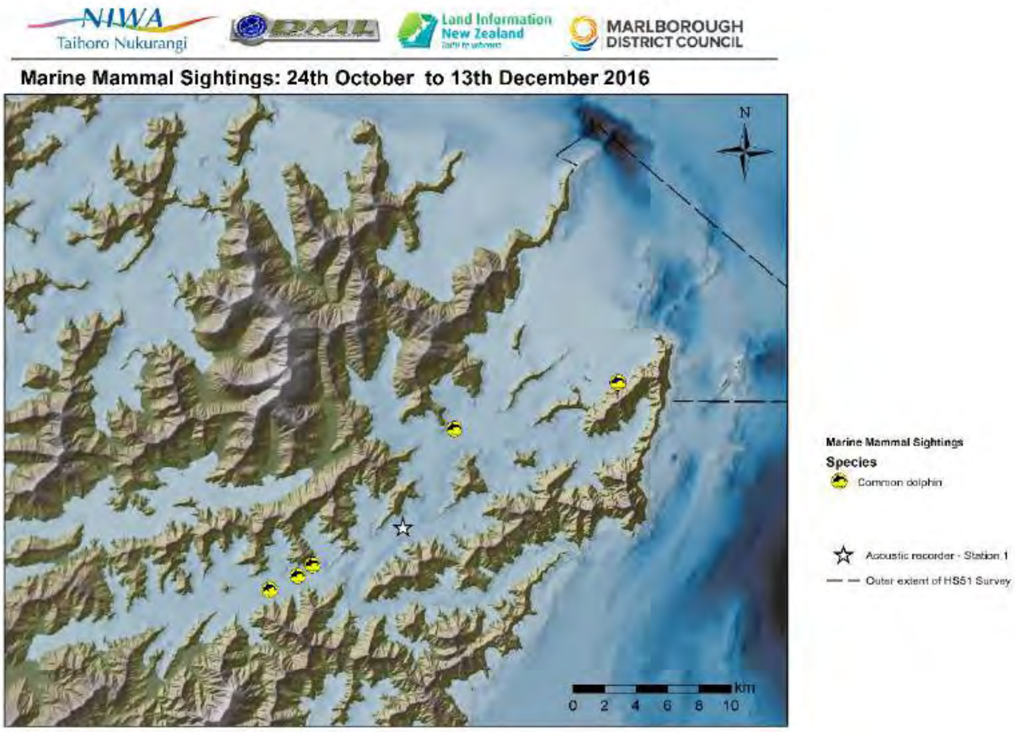

Figure A-10: Common dolphin sightings for the period 24th October to 13th December 2016 overlapping with acoustic monitoring. Acoustic mooring deployment location indicated by white star.

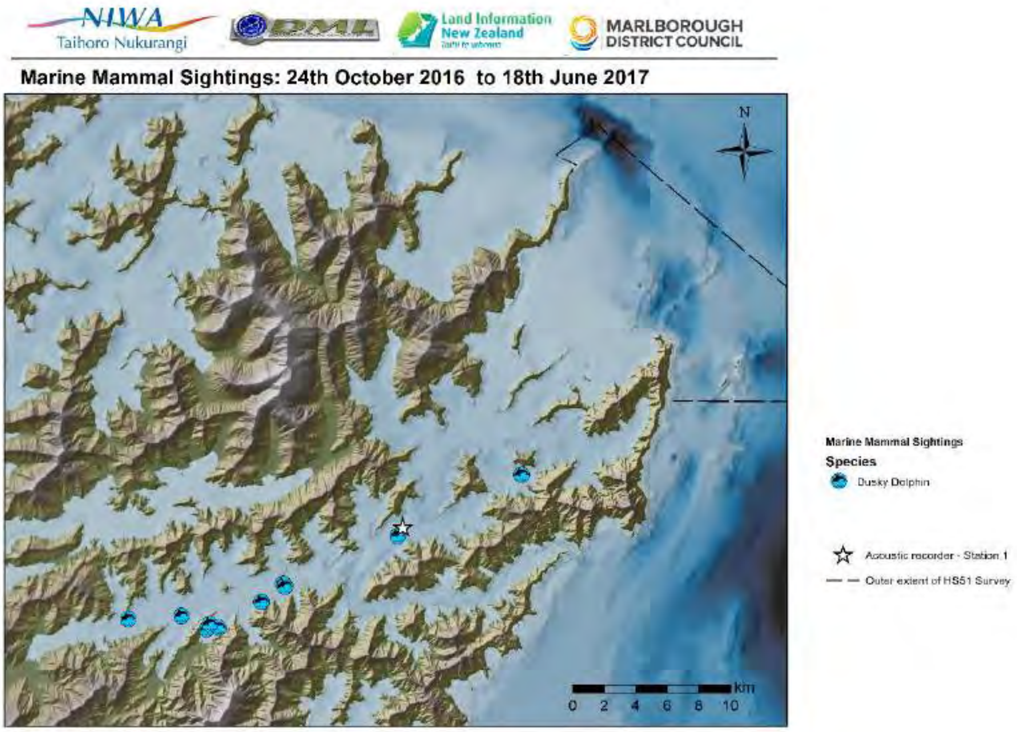

Figure A-11: Dusky dolphin sightings for the period 24th October 2016 to 18th June 2017. Acoustic mooring deployment location indicated by white star.

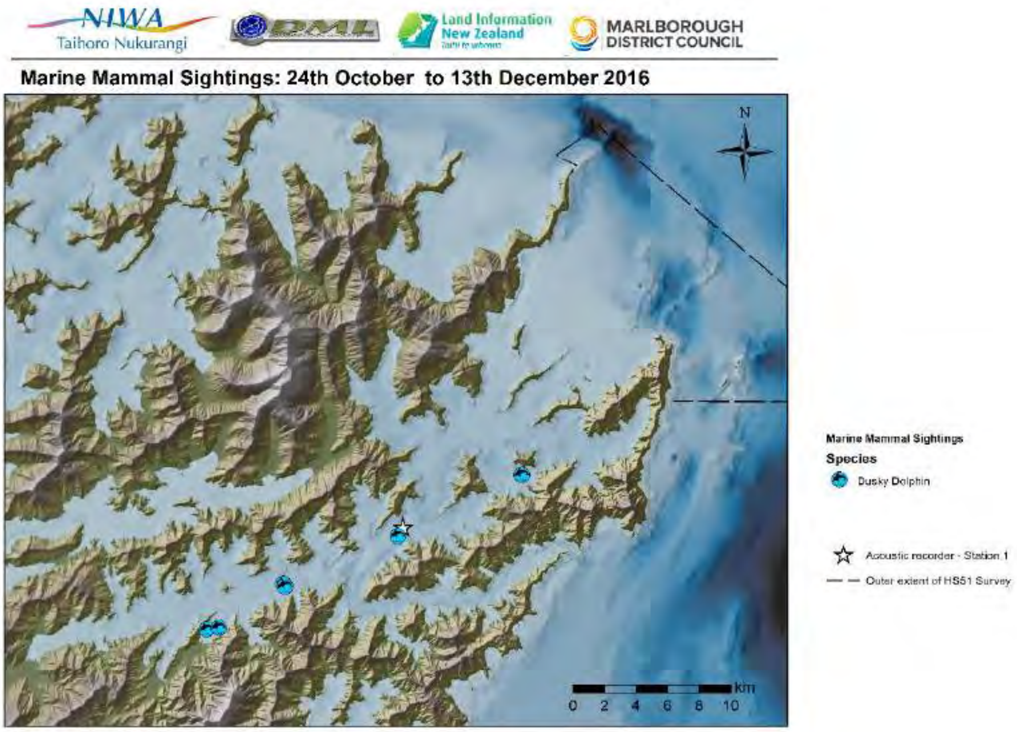

Figure A-12: Dusky dolphin sightings for the period 24th October to 13th December 2016 overlapping with acoustic monitoring. Acoustic mooring deployment location indicated by white star.

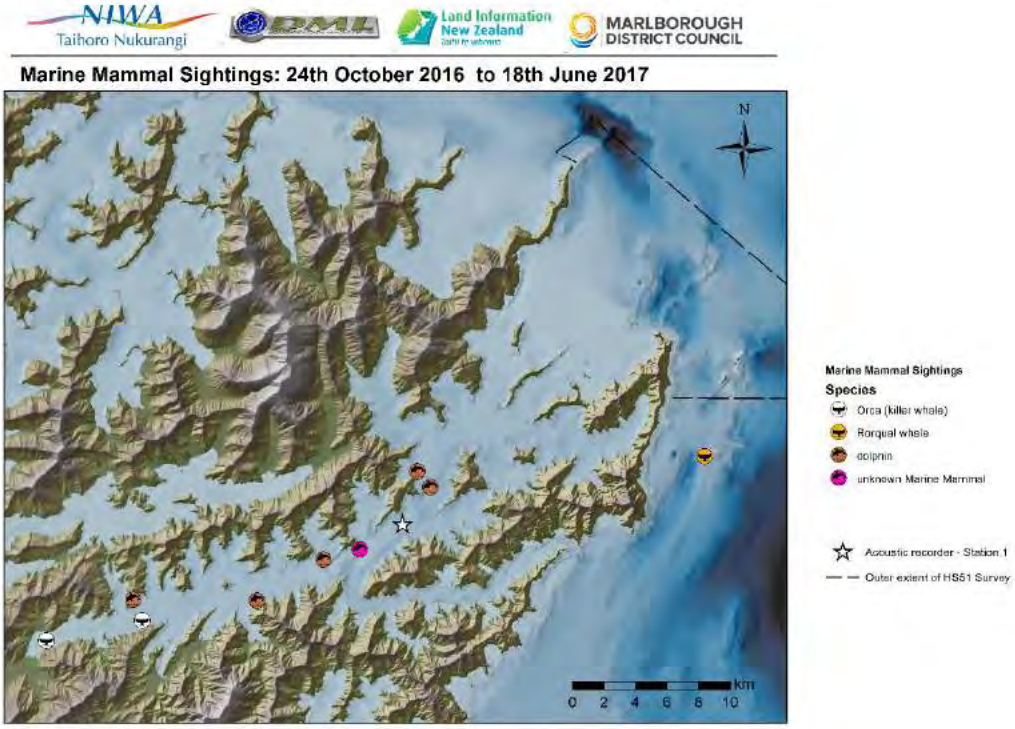

Figure A-13: Other cetacean sightings for the period 24th October 2016 to 18th June 2017. Acoustic mooring deployment location indicated by white star.

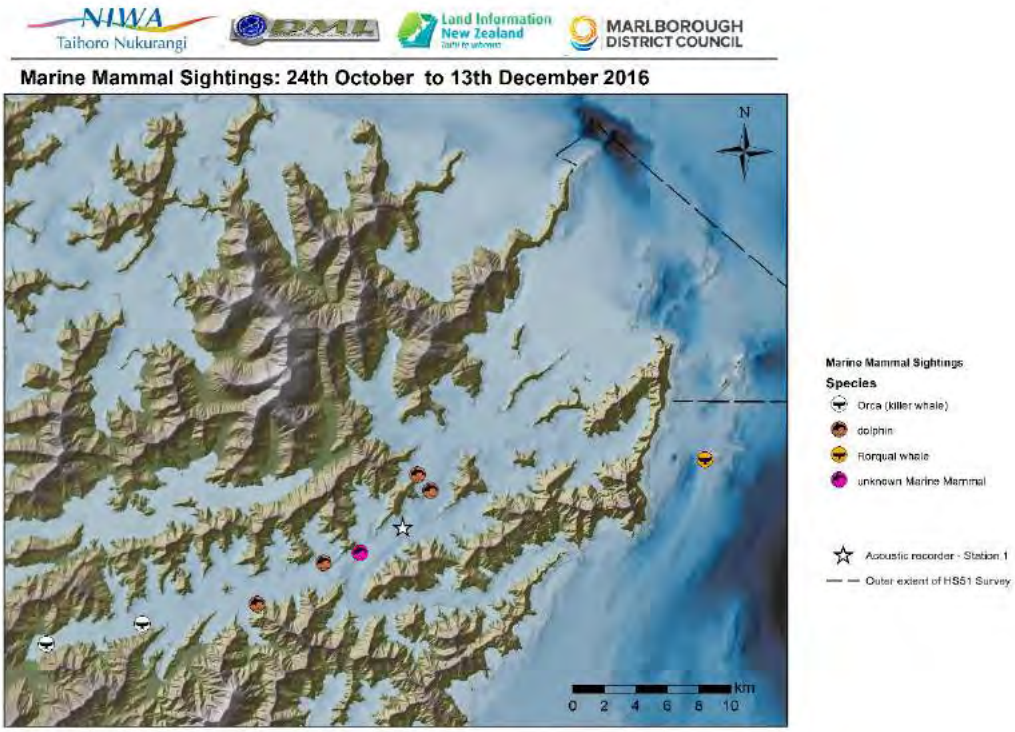

Figure A-14: Other cetacean sightings for the period 24th October to 13th December 2016 overlapping with acoustic monitoring. Acoustic mooring deployment location indicated by white star.

Appendix B Report from JASCO Applied Sciences

Acoustic Monitoring in the Cook Strait Region

June 2016 to December 2016, Summary Report

Submitted to:

Kimberly Goetz
NIWA
Greta Point, Wellington

Authors:

Craig McPherson
Julien Delarue
Christopher Whitt
Emily Maxner
Katie Kowarski
Xavier Mouy

24 May 2017

JASCO Applied Sciences (Australia) Pty Ltd.
Unit 4, 61-63 Steel Street
Capalaba, Queensland, 4157
Tel: +61 7 3823 2620
Mob: +61 4 3812 8179
www.jasco.com

P001307-002
Document 01391
Version 1.0

Document Version Control

Version	Date	Name	Change
1.0 DRAFT	2017 May 9	C. McPherson	Draft released to client.
1.0 FINAL	2017 May 24	C. McPherson	Final submitted to client

Disclaimer:

The results presented herein are relevant within the specific context described in this report. They could be misinterpreted if not considered in the light of all the information contained in this report. Accordingly, if information from this report is used in documents released to the public or to regulatory bodies, such documents must clearly cite the original report, which shall be made readily available to the recipients in integral and unedited form.

Suggested citation:

McPherson, C., J. Delarue, C. Whitt., E. Maxner, K. Kowarski, and X. Mouy. 2017. *Acoustic Monitoring in the Cook Strait Region: June 2016 to December 2016, Summary Report*. Document 01391, Version 1.0. Technical report by JASCO Applied Sciences for NIWA.

Contents

Figures

Tables

1. Introduction

The National Institute of Water and Atmosphere (NIWA) contracted JASCO Applied Sciences (JASCO) to provide a summary of information regarding the underwater acoustic environment in Cook Strait.

The data presented in this report were collected as part of the NIWA Cook Strait acoustic monitoring project and were analysed by JASCO. They consisted of seven months of acoustic recordings obtained from seven locations in, and near the entrances of, Cook Strait (Figure 1). The recordings were used to characterise the main contributors to the marine soundscape: ambient noise, marine mammal sounds, and anthropogenic noise. The mooring locations were selected as a result of discussions between NIWA and JASCO, and they accounted for regional coverage, bathymetry, and fishing operations.

This report details the methods used to analyse the data and presents a summary of the data with overview explanations. The report has been provided to give some context and explanation to the analysis results being delivered to NIWA. It does not represent a detailed synthesis of the results contained within it.

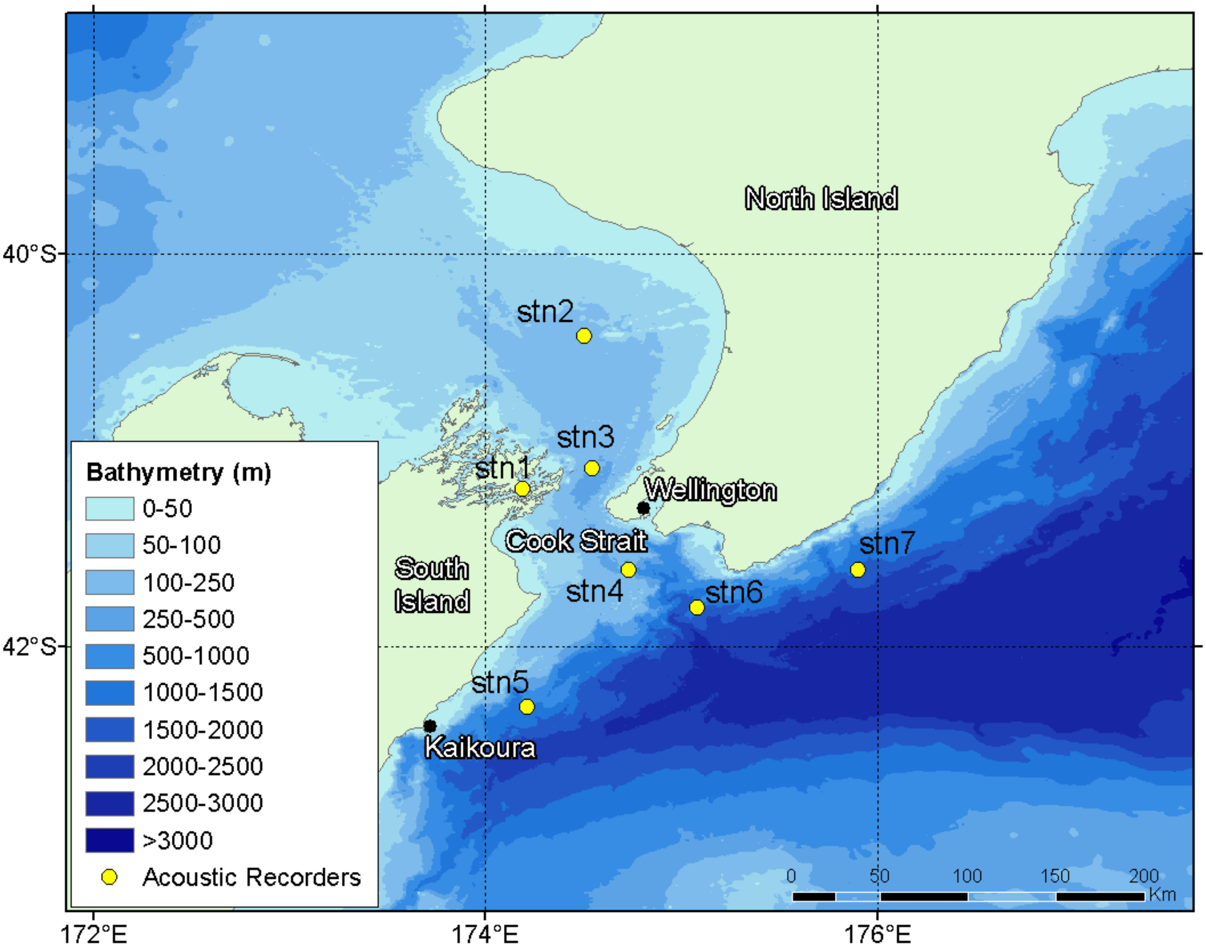

Figure 1. Overview map of region showing deployment locations.

2. Methods

2.1. Data Collection

2.1.1. Acoustic Recorders

The NIWA Cook Strait acoustic monitoring program occurred from June to December 2016. Autonomous Multichannel Acoustic Recorders (AMARs) (http://www.jasco.com/amar/) were deployed at seven locations across the Cook Strait region.

Each AMAR was fitted with an M36-V35-100 omnidirectional hydrophone (GeoSpectrum Technologies Inc.; −164 dB re 1 V/µPa sensitivity), and deployed in a mooring configuration suitable for the deployment location. An example of the AMAR section of the mooring for Stations 1–3 is shown in Figure 2. Table 1 reports deployment dates and duty cycles for each station. Further details on the AMAR configuration and calibration are provided in Appendix B.

Figure 2. JASCO AMARs on baseplates prior to deployment at Station 2 and 3 by NIWA, June 2016 (Image Credit: NIWA).

Table 1. Deployment details for each station.

Station	Latitude	Longitude	Depth (m)	Deployment	Retrieval/ end of data	Duty cycle
1	−41.200067	174.190317	48.5	20 Jul 2016	15 Dec 2016	630 s at 16 ksps 125 s at 375 ksps 145 s sleep
2	−40.419567	174.5074	110	4 Jun 2016	20 Dec 2016	630 s at 16 ksps 125 s at 250 ksps 145 s sleep
3	−41.0927	174.5469	252	3 Jun 2016	19 Dec 2016	
4	−41.61233	174.7353	711	6 Jun 2016	20 Dec 2016	
5	−42.3087	174.2145	1251	6 Jun 2016	21 Dec 2016	
6	−41.805017	175.081	1188	6 Jun 2016	21 Dec 2016	
7	−41.6098	175.9029	1481	5 Jun 2016	21 Dec 2016	

2.2. Automated Data Analysis

During the seven-month deployment period, 11.14 TB of acoustic data (totalling 3 years and 24.1 days or 256,974 files) were collected. Data were analysed using a specialised computing platform capable of processing acoustic data hundreds of times faster than real-time. The system performs automated analysis of total ocean noise and sounds from vessels, seismic surveys, and (possible) marine mammal calls. Figure 3 outlines the stages of the automated analysis.

We also classify the dominant sound source in each minute of data as "Vessel", "Seismic", or "Ambient". To minimise the influence of anthropogenic sources on ambient sound level estimates, we define ambient levels from individual minutes of data that did not have an anthropogenic detection within one hour on either side of that minute. This results in more accurate estimates of daily sound exposure levels from each source class, cumulative distribution functions of sound pressure levels, and exceedance spectra.

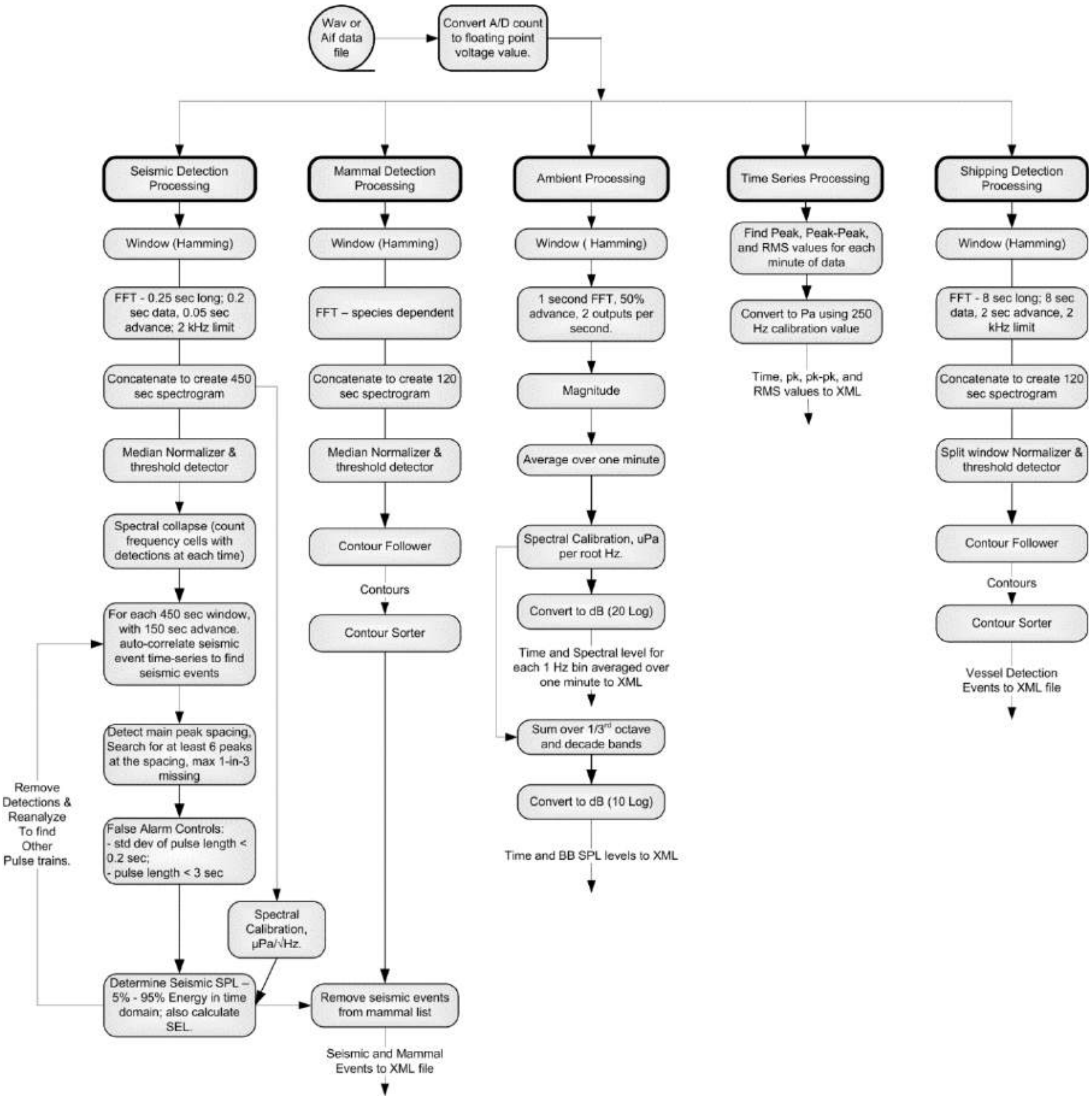

Figure 3. Major stages of the automated acoustic analysis software suite.

2.2.1. Total Ocean Noise and Time Series Analysis

Ambient noise levels at the recording stations were examined to document the local baseline underwater sound conditions. In Section 3.1, ambient noise levels at each recording station are presented as:

1. Spectrograms: Ambient noise at each station was analysed by Hamming-windowed fast Fourier transforms (FFTs), with 1 Hz resolution and 50% window overlap. The 120 FFTs performed with these settings are averaged to yield 1 min average spectra.
2. Broadband and approximate-decade-band sound pressure levels (SPL) over time for these frequency bands: 10 Hz to 8 kHz, 10–100 Hz, 100 Hz to 1 kHz, and 1–6.3 kHz.
3. Statistical distribution of SPL in broadband, approximate-decade-bands, and 1/3-octave-bands: The boxes of the statistical distributions indicate the first (L_{25}), second (L_{50}), and third (L_{75}) quartiles. The whiskers indicate the maximum and minimum range of the data. The solid line indicates the mean SPL, or L_{mean}, in each band.
4. Spectral density level percentiles: Histograms of each frequency bin per 1 min of data. The L_{mean}, L_5, L_{25}, L_{50}, L_{75}, and L_{95} percentiles are plotted. The L_5 percentile curve is the frequency-dependent level exceeded by 5% of the 1 min averages. Equivalently, 95% of the 1 min spectral levels are above the 95th percentile curve.
5. Daily sound exposure levels (SEL): Computed for the total received sound energy and the detected shipping energy. The SEL is the linear sum of the 1 min SEL. For shipping, the 1 min SEL values are the linear 1 min squared SPL values multiplied by the duration, 60 s. For seismic survey pulses, the 1 min SEL is the linear sum of the per-pulse SEL.

The 50th percentile (median of 1 min spectral averages) can be compared to the well-known Wenz ambient noise curves (Figure 4), which show the variability of ambient spectral levels off the US Pacific coast as a function of frequency of measurements for a range of weather, vessel traffic, and geologic conditions. The Wenz curve levels are generalised and are used for approximate comparisons only (see Section 2.2.1.1).

The 1 min averaged, 1 Hz spectral density levels are summed over the 1/3-octave and decade bands to calculate the 1 min averaged broadband levels (dB re 1 µPa) and presented with the density levels.

Table A-1 lists the 1/3-octave-band frequencies. Table A-2 lists the decade-band frequencies.

2.2.1.1. Sound Level Statistics

The ambient, or background, sound levels that create the ocean soundscape are comprised of many natural and anthropogenic sources. The main environmental sources of sound are wind and precipitation. Wind-generated noise in the ocean is well-described (e.g., Wenz 1962, Ross 1976), and surf noise is known to be an important contributor to near-shore soundscapes (Deane 2000). Precipitation is a frequent noise source, with contributions typically concentrated at frequencies above 500 Hz. At low frequencies (<100 Hz), earthquakes and other geological activities contribute to the soundscape.

Sound level statistics quantify the observed distribution of recorded sound levels, and they are presented in terms of SPL and SEL in this report. Following standard acoustical practice, the *n*th percentile level (L_n) is the sound level exceeded by *n*% of the data. L_{max} is the maximum recorded sound level. L_{mean} is the equivalent continuous sound level that represents the level of a continuous constant sound that produces the same sound power as the time varying signal level being measured over the same time period. In this report, the median level (L_{50}) is considered most representative of the nominal case, since it is less affected by high level outliers that can more strongly affect mean sound levels. The L_{50} is compared to the Wenz curves (Figure 4) for the upper and lower limits on prevailing ambient noise. L_5, the level exceeded by only 5% of the data, generally represents the highest typical sound levels measured. Sound levels between L_5 and L_{max} are due to close passes of vessels, intense weather, or other abnormal conditions. L_{95} represents the quietest typical conditions.

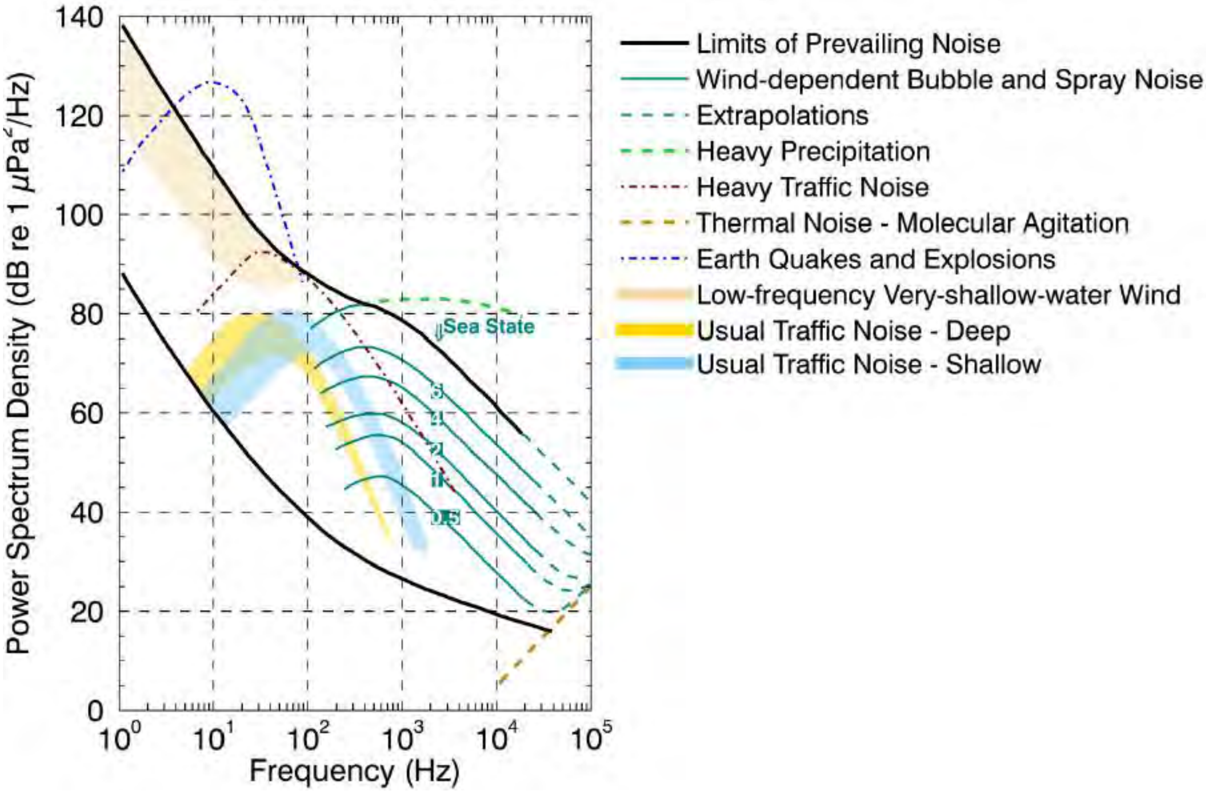

Figure 4. Wenz curves (NRC 2003), adapted from (Wenz 1962), describing pressure spectral density levels of marine ambient noise from weather, wind, geologic activity, and commercial shipping.

2.2.1.2. One-Third-Octave-Band Analysis

It is common practice to examine sound levels in small frequency ranges (bands) that represent the frequency filtering capabilities of mammalian auditory systems. For example, a noise at 500 Hz has less effect on the ability to hear other sounds at 1000 Hz because the auditory system separates them by sensing these different frequency sounds at different sections of the cochlea. The frequency filtering resolution of the mammalian ear has a bandwidth approximately 1/3 of an octave wide. Hence, the division of noise into 1/3-octave-bands is useful for determining how noise will interfere with hearing in the same bands. Statistical distributions of SPL in each 1/3-octave-band are presented as boxplots (Section 3.1). The boxes of the statistical distributions indicate the first (L_{25}), second (L_{50}), and third (L_{75}) quartiles in each band. The whiskers indicate the maximum and minimum range of the data. The solid lines indicate the SPL, or L_{mean}, in each 1/3-octave-band.

A similar approach is to divide the noise into decade bands. In this analysis, we used the 10–100 Hz, 100 Hz to 1 kHz, and 1–6.3 kHz bands.

Further details on 1/3-octave and decade band analyses are provided Appendix A.2.

2.2.2. Vessel Noise Detection

Vessels are detected in two steps:

1. Constant, narrowband tones produced by a vessel’s propulsion system and other rotating machinery (Arveson and Vendittis 2000) are detected. These sounds are also referred to as tonals. We detect the tonals as lines in a 0.125 Hz resolution spectrogram of the data.
2. The root-mean-square SPL are assessed for each minute in the 40–315 Hz frequency band, which commonly contains most sound energy produced by mid-sized to large vessels. Background estimates of the shipping band SPL and broadband SPL are then compared to their median values over the 12 h window, centred on the current time.

Vessel detections are defined by three criteria:

- The SPL in the shipping band is at least 3 dB above the median.
- At least 5 shipping tonals (0.125 Hz bandwidth) are present.
- The SPL in the shipping band is within 8 dB of the broadband SPL (Figure 5).

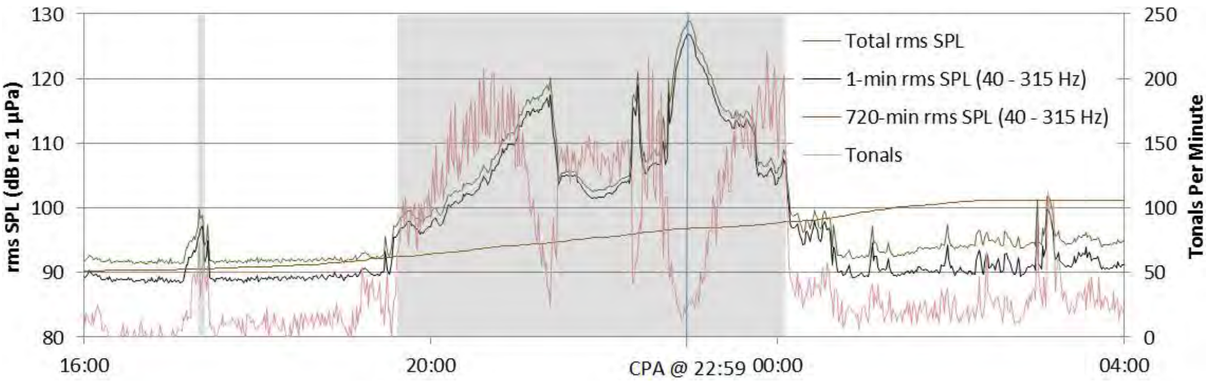

Figure 5. Example of broadband and 40–315 Hz band SPL, as well as the number of tonals detected per minute as a ship approached a recorder, stopped, and then departed. The shaded area is the period of shipping detection. Fewer tonals are detected at the ship's closest point of approach (CPA) at 22:59 because of masking by broadband cavitation noise and due to Doppler shift that affects the tone frequencies.

2.2.3. Seismic Survey Event Detection

Seismic pulse sequences are detected using correlated spectrogram contours. We calculate spectrograms using a 300-s long window with 4 Hz frequency resolution and a 0.05 s time resolution (Reisz window). All frequency bins are normalised by their medians over the 300-s window. The detection threshold is three times the median value at each frequency. Contours are created by joining the time-frequency bins above threshold in the 7–1000 Hz band using a 5 × 5 bin kernel. Contours 0.2–6 s in duration with a bandwidth of at least 60 Hz are retained for further analysis.

An "event" time series is created by summing the normalised value of the frequency bins in each time step that contained detected contours. The event time series is auto-correlated to look for repeated events. The correlated data space is normalised by its median and a detection threshold of 3 is applied. Peaks larger than their two nearest neighbours are identified, and the peaks list is searched for entries with a set repetition interval. The allowed spacing between the minimum and maximum time peaks is 4.8 to 65 s, which captures the normal range of seismic pulse periods. Where at least six regularly spaced peaks occur, the original event time series is searched for all peaks that match the repetition period within a tolerance of 0.25 s. The duration of the 90% SPL window of each peak is determined from the originally sampled time series, and pulses more than 3 s long are rejected.

2.2.4. Marine Mammal Detection

Detections of marine mammal calls were based on automated detections and the validation of those results by experienced analysts. Odontocete clicks and whistles were recorded and detected on the high-frequency (250 and 375 ksps) data, whilst the low-frequency data (16 ksps) was used to detect baleen whale calls. Species-specific stereotyped calls were targeted by specific detectors (e.g., blue whale songs or Cuvier's beaked whale clicks), whilst more variable signals, such as dolphin whistles, were targeted by tonal detectors searching for energy and contours in pre-defined frequency bands.

2.2.4.1. *Automated Click Detector*

We apply an automated click detector/classifier to the high-frequency data to detect clicks from sperm whales, beaked whales, porpoise, and delphinids (Figure 6). This detector/classifier is based on the zero-crossings in the acoustic time series. Zero-crossings are the rapid oscillations of a click's pressure waveform above and below the signal's normal level (e.g., Figure 6). Clicks are detected by the following steps (Figure 6):

1. The raw data is high-pass filtered to remove all energy below 8 kHz. This removes most energy from other sources such as shrimp, vessels, wind, and cetacean tonal calls, whilst allowing the energy from all marine mammal click types to pass. Faint sperm whale clicks with no energy above 8 kHz cannot be detected.
2. The filtered samples are summed to create a 0.5 ms rms time series. Most marine mammal clicks have a 0.1–1 ms duration.
3. Possible click events are identified with a Teager-Kaiser energy detector.
4. The maximum peak signal within 1 ms of the detected peak is found in the high-pass filtered data.
5. The high-pass filtered data is searched backwards and forwards to find the time span where the local data maxima are within 12 dB of the maximum peak. The algorithm allows for two zero-crossings to occur where the local peak is not within 12 dB of the maximum before stopping the search. This defines the time window of the detected click.
6. The classification parameters are extracted. The number of zero crossings within the click, the median time separation between zero crossings, and the slope of the change in time separation between zero crossings are computed. The slope parameter helps to identify beaked whale clicks, as beaked whale clicks increase in frequency (upsweep).
7. The Mahalanobis distance between the extracted classification parameters and the templates of known click types is computed. The covariance matrices for the known click types, computed from thousands of manually identified clicks for each species, are stored in an external file. Each click is classified as a type with the minimum Mahalanobis distance, unless none of them are less than the specified distance threshold.
8. The click detector was optimised for the NIWA dataset by incorporating templates of the local species' signals, in particular the echolocation clicks of Hector's dolphins and two unidentified beaked whale species. These species were identified during a preliminary review of the data.
9. Because of the difficulty of distinguishing clicks from different species of the family *Delphinidae,* these clicks are detected as a single class, called delphinid click.

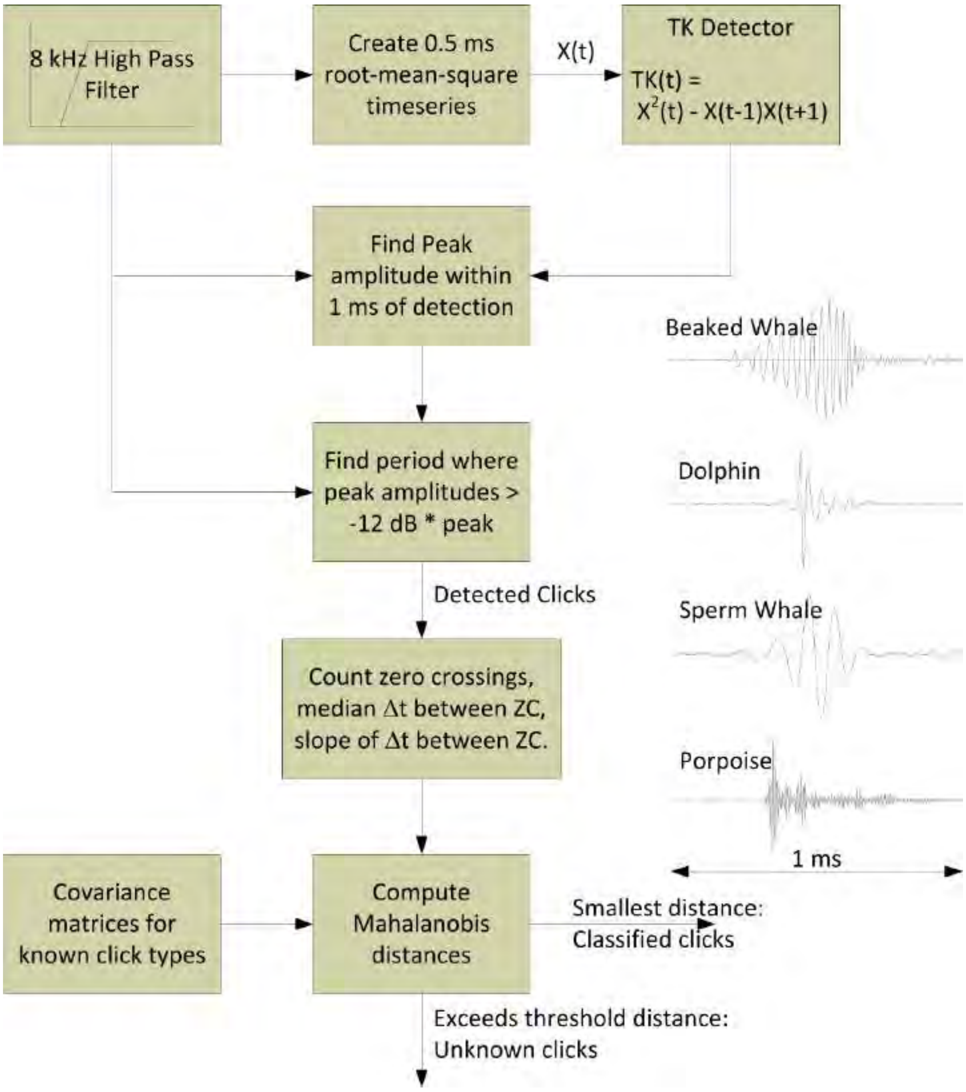

Figure 6. The click detector/classifier and a 1 ms time-series of four click types.

2.2.4.2. Tonal Call Detection

The tonal call detector identifies data likely to contain marine mammal moans, songs, and whistles. The detector identifies delphinid whistles in the high-frequency recordings and baleen whales in the low-frequency recordings. Tonal calls are detected and classified by the following steps:

1. Spectrograms are created of the appropriate resolution for each mammal call type that are normalised by the median value in each frequency bin for each detection window (Table 2).
2. Adjacent bins are joined and contours are created via a contour-following algorithm (Figure 7).
3. A call sorting algorithm determines if the contours match the definition of a marine mammal call type (Table 3).

The calls of humpback whales, pilot whales, dolphins (tonal calls), fin whales, and southern right whales were targeted specifically (Table 3). The sei whale (*Balaenoptera borealis*) template is built using calls described for North Atlantic sei whales (Baumgartner et al. 2008). The description of sei whale calls in the Southern Hemisphere remain limited (McDonald et al. 2005, Calderan et al. 2014), and no attempt was made to automatically detect these signals. The manual detection review (Section 2.2.4.4) did not positively identify any signals resembling these descriptions, although on one occasion (stn 3, 23 Nov around 1600 UTC), analysts annotated calls similar to those described in Calderan et al. (2014) as "possibly sei whale".

The distinction between pilot and dolphin tonal calls is largely based on frequency. Pilot whale calls have lower frequencies than dolphin whistles (Steiner 1981, Rendell et al. 1999). Killer whale (*Orcinus orca*) pulsed calls are lower in frequency than pilot whale calls (Ford 1989) and would be merged with pilot whale detections. False killer whale (*Pseudorca crassidens*) tonal calls also have energy below 6 kHz (Murray et al. 1998, Oswald et al. 2003), and they would likely be detected as pilot whales. The true dolphin species that produce whistles do so at higher frequencies and are detected separately. No attempts were made at separating detections from different dolphin species due to the limited understanding of the vocal repertoire of local species. In the study area, the species most likely to be detected based on known patterns of occurrence are common dolphins (*Delphinus delphis*) and bottlenose dolphins (*Tursiops truncatus*), but it is possible that other species are present.

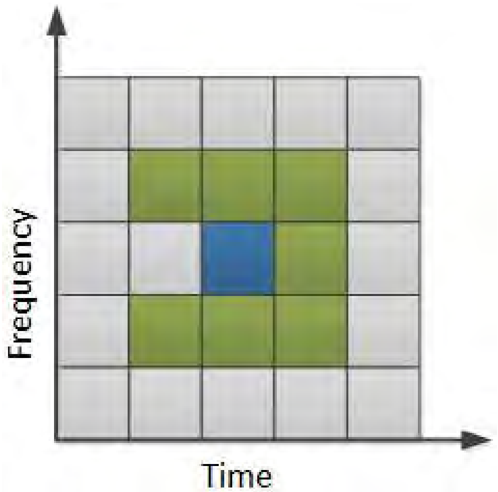

Figure 7. Illustration of the search area used to connect spectrogram bins. The blue square represents a bin of the binary spectrogram equalling 1 and the green squares represent the potential bins it could be connected to. The algorithm advances from left to right so grey cells left of the test cell need not be checked.

Table 2. Fast Fourier Transform and detection window settings used to detect tonal calls of marine mammal species expected in the data. Values are based on JASCO's experience and empirical evaluation on a variety of data sets.

Possible species	Call type	FFT			Detection window (s)	Detection threshold
		Resolution (Hz)	Frame length (s)	Timestep (s)		
Pilot whales	Whistle	16	0.03	0.015	5	3
Dolphins	Whistle	64	0.015	0.005	5	3
Humpback whales	Moan	4	0.2	0.05	5	3
Southern Right whales	Upcall	2	0.2	0.05	5	3
Fin whales	20-Hz note	1	0.2	0.05	5	4
Sei whales	Downsweep	3.25	0.2	0.035	5	3.5

Table 3. Call sorter definitions for the tonal calls of cetacean species expected in the area.

Possible species	Call type	Frequency (Hz)	Duration (s)	Bandwidth (Hz)	Other detection parameters
Pilot whales	Whistle	1,000–10,000	0.5–5	>300	Minimum frequency <5,000 Hz
Dolphins	Whistle	4,000–20,000	0.3–3	>700	Maximum instantaneous bandwidth = 5,000 Hz
Humpback whales	Moan	100–700	0.5–5	>50	Maximum instantaneous bandwidth = 200 Hz
Right whales	Upcall	50–300	0.4–2.2	60–250	Minimum frequency <120 Hz Maximum instantaneous bandwidth = 80 Hz Sweep rate = 30 to 200 Hz/s
Fin whales	20-Hz downsweep	8–40	0.3–3	> 6	Minimum frequency <17 Hz Sweep rate = −100 to 0 Hz/s
Sei whales	Downsweep	20–150	0.5–1.7	19–120	Maximum instantaneous bandwidth = 100 Hz Sweep rate = −100 to −6 Hz/s

2.2.4.3 *Blue Whale Detector*

The spectrogram correlation technique used for detecting New Zealand (Miller et al. 2014) and Antarctic (Sirovic et al. 2004) blue whale song notes as well as audible downsweeps (D calls; Oleson et al. 2007)) is based on Mouy et al. (2009) and Martin et al. (2014). The technique is as follows:

1. The spectrogram is computed and normalised using a split-window normaliser (Struzinski and Lowe 1984).
2. The spectrogram is then binarised by calculating the variance of energy values around each spectrogram bin on a time-frequency kernel of size 1 s by 10 Hz. Bins of the spectrogram with a local variance less than 0.4 and a normalised energy value less than 2.5 are set to zero. Remaining spectrogram bins are set to 1.
3. A set of synthetic binary time-frequency templates representing typical blue whale calls are created as successions of linear time-frequency segments defined by their starting frequency, ending frequency, duration, frequency width, frequency span, and silence duration before and after the call (Figure 8).
4. To create a detection function, a correlation index that measures how well the synthetic templates match the binary spectrogram is defined for each time step of the spectrogram and for each of the templates (Figure 9). The occurrences of blue whale call detections are defined by parts of the detection function that exceed an empirically chosen threshold, *Tdetec*. Detection thresholds for Antarctic, New Zealand, and downsweep blue whale calls were 0.13, 0.12, and 0.29, respectively.

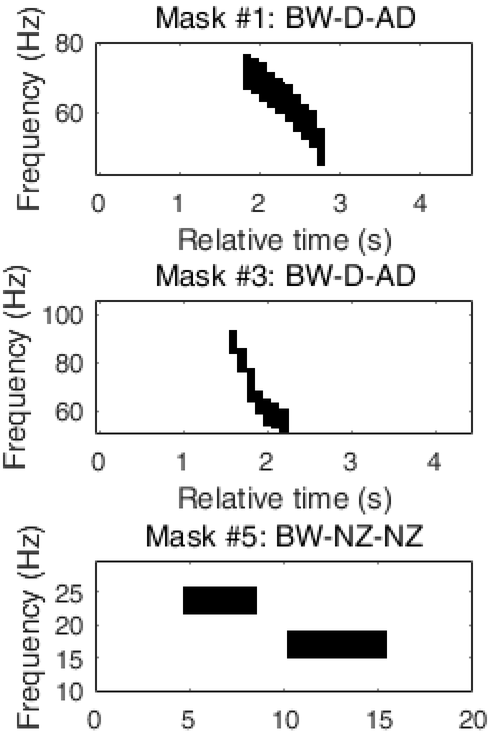

Figure 8. Examples of synthetic binary time-frequency templates used to detect New Zealand and audible downsweep blue whale calls.

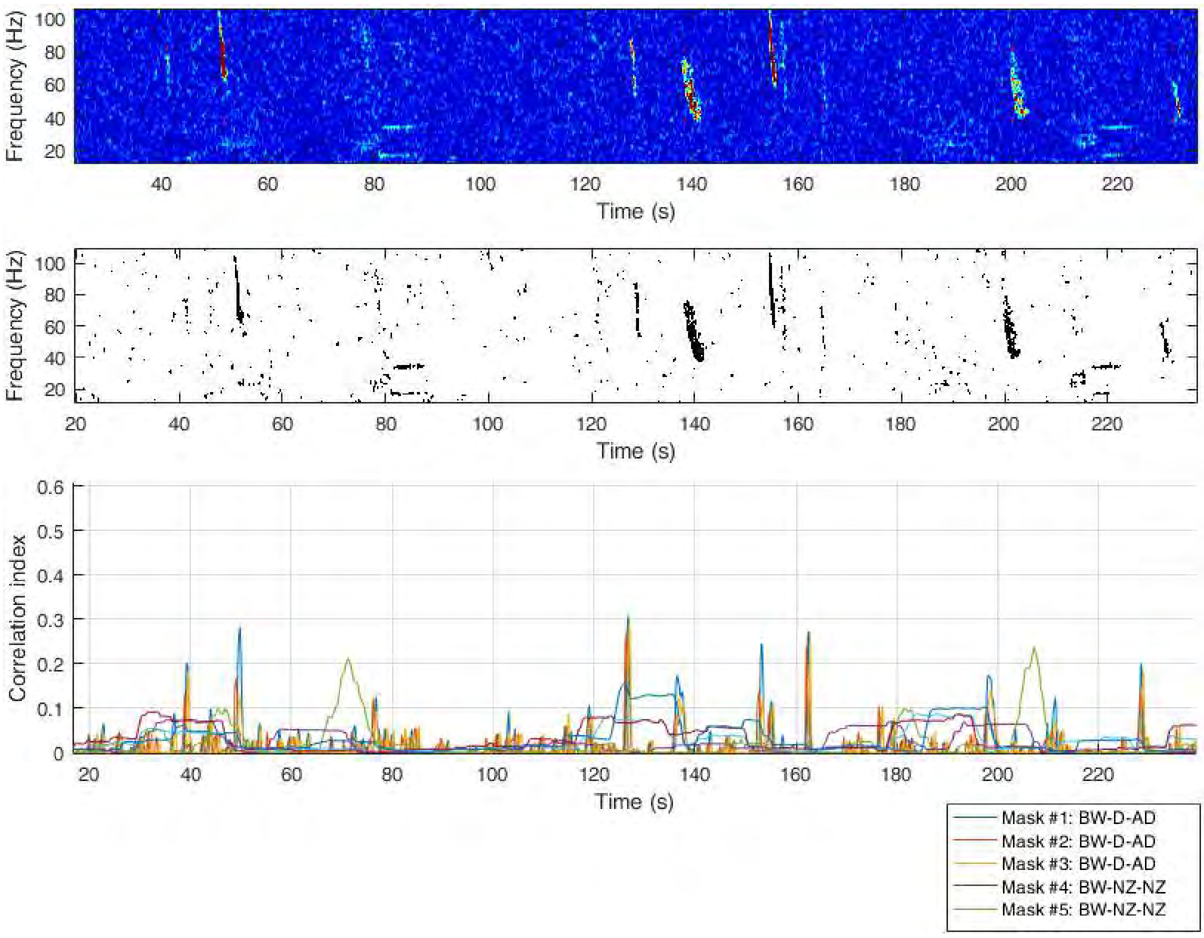

Figure 9. Blue whale call detection process. Top: Spectrogram with blue whale calls. Middle: Binarised spectrogram. Bottom: Detection functions for each template.

2.2.4.4. Validation of Automated Detectors

We develop and test automated detectors with example data files that contain a range of vocalisation types and background noise conditions. However, test files cannot cover the full range of possible call and noise conditions. Therefore, a selection of files is manually validated to check each detector's performance for a specific data set and to determine the parameters, such as minimum number of detections per sound file (further referred to as detection threshold), required to accept the detector's results.

2.2.4.4.1. Selection of Data for Manual Validation

To standardise the file selection process, we developed an algorithm that automatically selects a sample of files for review. The sample size *N* is set based on the amount of time allocated to the review effort. In this study, 1% of the 10.5 min 16 ksps files and 1% of the 2 min 250/375 ksps files per station were reviewed, resulting in *N* = 2,600 files, or about 260 hr of acoustic data, manually reviewed. It is important to note that this level of effort is distributed across all detected species. Therefore, individual species receive only a fraction of the manual review effort.

The algorithm selects files to manually review based on the following criteria:

1. All species targeted by a detector whose performance needs to be assessed must be represented within a minimum of 10 files (unless fewer than 10 files have detections).
2. The sample should not include more than one file per day unless *N* is greater than the number of recording days or the "minimum 10 file per species" rule dictates that more than one file per day be reviewed.
3. Files must contain low, medium, and high numbers of detected species. Files with no detected species are excluded from the pool of eligible files. Files are selected such that the proportion of each species count bin within the sample matches the per-file species count distribution in the whole data set.
4. Files must contain low, medium, and high numbers of detections per file for each species. The number of detections per file is split into low (but at least one), medium, and high bins, which corresponded to the lower, middle, and upper third percentile of the range, respectively. Files with no detection for each species will appear among those with detections of other species, allowing us to evaluate false negatives. We choose to slightly oversample the high detection counts (40% of files compared with 30% from the medium and low bins) to avoid biasing the detection threshold high. The three files with the highest detection counts are automatically included in those selected from the high bins for the same reason.

We score the goodness of fit of a sample of files according to how well it conforms to the "preferred" distribution of detections, as determined by the initial distribution and the preferred final sampling. A lower score implies a better fit. To score the goodness of fit, we perform the following step for a selected sample of files:

1. Determine the diversity (species count per file) proportions (Pc) of the selected sample of files, and calculate a diversity score based on how much the current proportions differ from the original diversity proportions (Po).

   DiversityScore = average(abs(Pc[i]–Po[i]))

2. For each species, determine the proportion of files (C) that have detection counts in the low/medium/high original species count distributions. Files with no detections are not included in the calculation for each species (0-detection files for a species will unavoidably be included in files selected for other species).

   PerSpeciesScore[i] = abs(C_{low}–0.3) + abs(C_{medium}–0.3) + abs(C_{high}–0.4)

   DetectionScore = average(PerSpeciesScore[1..n]), where n is the number of species

   FitScore = (DiversityScore + DetectionScore)/2

2.2.4.4.2. Detector Performance Calculation and Optimisation

All files selected for manual validation are reviewed using JASCO's PAMlab software to determine the true presence or absence of every species. The automated detector results are then compared to the manually reviewed results for each species to determine 1) the performance of the detector and 2) if the detector performance can be maximised by applying any restrictions spatially, temporally, and/or using a detection threshold, which is the number of detections per file at and above which detections of species are considered valid.

To determine the performance of each detector and any necessary detector thresholds, the results of the comparison of automated compared with manual detections were fed to a maximum likelihood estimation algorithm that maximises the probability of detection and minimises the number of false alarms using the 'F-score':

$$F = \frac{(1+\beta^2)P * R}{(\beta^2)P + R}; P = \frac{TP}{TP+FP}; R = \frac{TP}{TP+FN}$$

where *TP* (true positive) is the number of correctly detected files, *FP* (false positive) is the number of files that are false detections, and *FN* (false negatives) is the number of files with missed detections. *P* is the classifier's precision, representing the proportion of detected calls that are true positives. A *P* value of 0.9 means that 90% of the detections are correctly classified, but says nothing about whether all calls in the dataset were identified. *R* is the classifier's recall, representing the proportion of calls in the dataset that are detected by the detector. An *R* value of 0.8 means that 80% of all calls in the dataset were detected, but says nothing about how many classifications were wrong. Thus, a perfect detector/classifier would have *P* and *R* values equal to 1. An F-score is a combined measure of *P* and *R* where an F-score of 1 indicates perfect performance–all events are detected with no false alarms. The algorithm determines a classification threshold for each species that maximises the F-score. Table 4 shows the dependence of the classification threshold on the β-parameter and its effect on the precision and recall of the detector and classifier system. β is the relative weight between the recall and precision. Here, we have made precision more important than recall as a β of 0.5 means the recall has half the weight of the precision.

Table 4. Effects of changing the F-score β-parameter on the classification threshold, precision, and recall for the odontocete clicks.

β	Classification threshold	Precision $P = \frac{TP}{TP+FP}$	Recall $R = \frac{TP}{TP+FN}$	F-score
2	25	0.87	0.95	0.93
0.5	50	0.91	0.91	0.91

To maximise the sample size used to estimate the performance metrics, we combine the validation results of all stations for each species. This has the benefit of allowing an unbiased comparison of automated detections across stations. However, several station-specific factors can potentially affect the precision and recall values. Higher noise levels at some stations could affect these metrics due to masking. Alternatively, the location of each station relative to each species' preferred habitat may disproportionately affect recall. Indeed, the farther a station is from a species' preferred habitat, the more calls may fall below the detector's noise threshold although analysts can still classify them. Within a species' preferred habitat where we expect more calls to be produced within the recorder's detection range, analysts and detectors are likely much more closely matched in terms of classification abilities. Because several interacting factors influence detector performance at each station, we believe the chosen approach is the least biased. However, the results presented in this report should be viewed with an understanding of its potential effects on the relative occurrence of species across stations.

The size of the area monitored in this project coupled with different levels and types of anthropogenic activities across stations result in a range of acoustic conditions that can greatly challenge automated detectors. By restricting detections spatially and/or temporally in some cases, we can maximise the detectors' performance and the reliability of the results. The following restrictions increase detector performance and are applied to our automated detector results:

1. If a species is automatically detected at a station, but is never confirmed to occur at the station during the manual validation process, all automated detections at that station are considered false and removed.
2. If a species is automatically detected over a specific timeframe, but manual validation reveals all detections to be falsely triggered by another noise or species, all automated detections during that time at that station are considered false and removed.

Detection time series based on the restrictions above are plotted using JASCO's ADPT software and critically reviewed. Questionable detections based on time of year and location or overlap with the detection period of other species are manually reviewed and removed from the plots if they are found to be false. The detector performance metrics presented in Section 3.2.1 are based on the fully revised and edited results as shown in the detection time series.

It is important to note that additional systematic manual analysis and validation beyond the 1% conducted by JASCO may confirm automated detections or allow further optimisation to occur.

3. Summary Results

A summary of the results from the monitoring project is provided in the following section. All images and csv files generated through the analysis process have been provided to NIWA as a separate deliverable to assist in future analysis of the data (Appendix C).

3.1. Ambient and Anthropogenic Noise Measurements

3.1.1. Overview

The data for each station is presented as described in Section 2.2.1. For clarity, the relevant description is linked to each of the listed representations for Station 1:

- Spectrogram and broadband and approximate-decade-band sound pressure levels example: Figure 10.
- Statistical distribution of SPL in broadband, approximate-decade-bands example: Figure 11.
- Spectral density level percentiles and statistical distribution of SPL in 1/3-octave-bands example: Figure 12.
- Daily sound exposure levels (SEL) example: Figure 13.
- Total and man-made associated SEL statistics, with daily total hours of vessel or seismic detection and daily vessel or seismic detections example: Figure 14.
- Statistical analysis of SPL and daily SEL example: Table 5 and Table 6.

Marine mammal contributions and anthropogenic events are discussed in Sections 3.2 and 3.4.

The spectrogram and band-level plots (e.g., Figure 10) provide an overview of the sound variability in time and frequency, and the presence and level of contribution from different sources. Short-term events appear as vertical stripes on the spectrograms and spikes on the band level plots. Long-term events appear in the spectrograms as horizontal bands of colour. They affect (increasing or decreasing accordingly) the band level over the event period. A significant example is the 14 Nov 2016 earthquake, visible as a large increase in the levels in the 10–100 Hz at all stations except stn 2. Seismic activity can be seen at stns 5, 6, and 7 at the end of the recording periods below 200 Hz. Tonals induced by vessel and flow noise can be seen as horizontal lines at stns 3 and 4.

Overall, median broadband SPL were lowest at stn 1 (98.1 dB re 1µPa) and highest at stn 4 (115.8 dB re 1µPa). High flow-induced pseudo-noise as well as vessel traffic were responsible for the high level of noise at the low frequencies at stn 4. Vessel noise was usually the dominant man-made contributor to background noise, except at stns 6 and 7 where the contribution of seismic surveys to daily SEL was higher than that of vessels at the end of the recording period. Although stn 1 had the highest daily number vessel detections and hours with vessel detections, the associated SEL levels were lower or on par with other stations. The seismic survey detected at stns 5–7 using the un-optimised detector was also recorded at stn 4; however, as there were no detections, its presence is not reflected in the daily SEL plot (Figure 29). The 14 Nov earthquake is visible in all daily SEL plots, including stn 2. The percentile power spectral density (PSD) levels were generally within the limits of the Wenz curves, except below 50 Hz for the 5th and 25th percentile at stations experiencing flow noise, and up to 300 Hz at stn 4 caused by high level of vessel noise.

3.1.2. Station 1

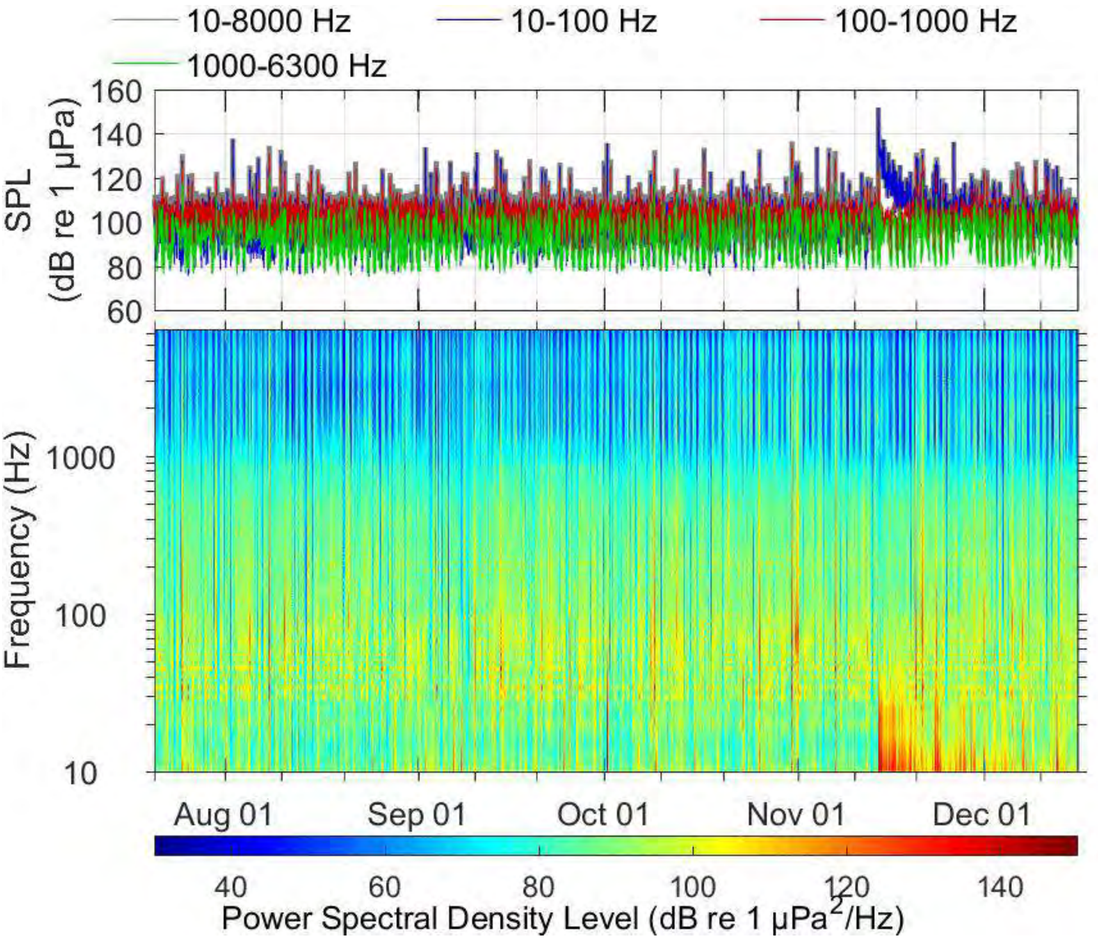

Figure 10. Station 1: Sound level summary from 20 Jul to 15 Dec 2016.(Top) In-band SPL and (bottom) spectrogram of underwater sound.

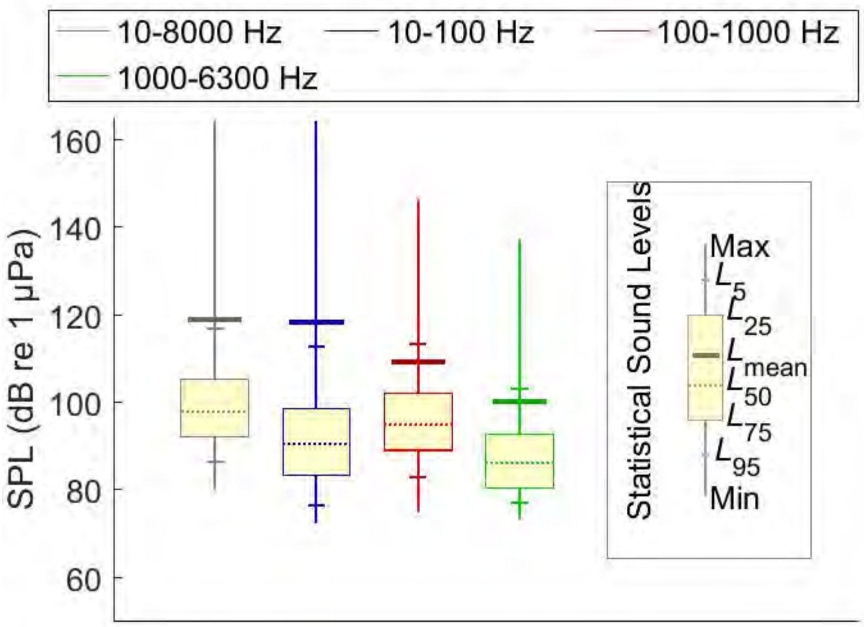

Figure 11. Station 1: Broadband and in-band 1-min SPL.

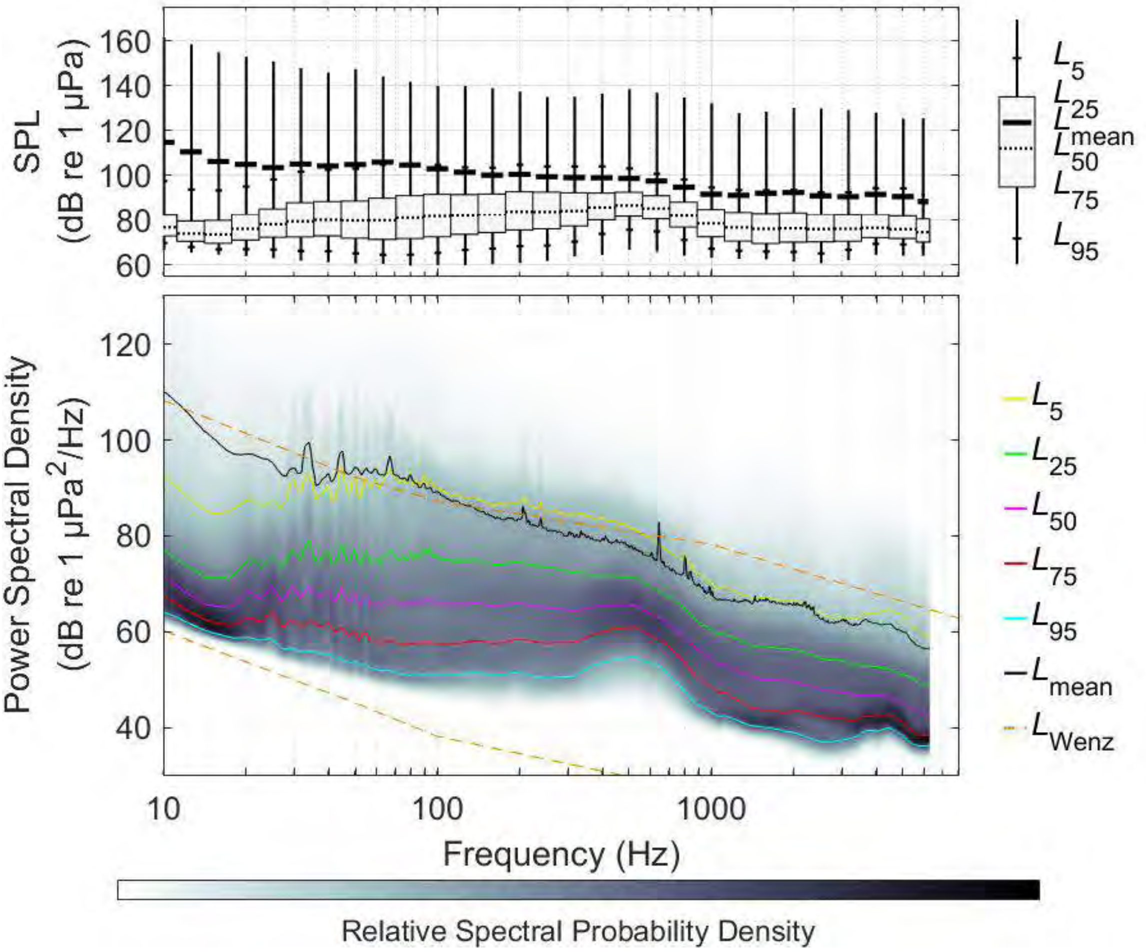

Figure 12. Station 1: (Top) Exceedance percentiles and mean of 1/3-octave-band SPL and (bottom) exceedance percentiles and probability density (grayscale) of 1-min PSD levels compared to the limits of prevailing noise (Wenz 1962).

Table 5. Station 1: Statistical analysis of SPL. SPL units: dB re 1 µPa.

Sound level statistic	SPL			
	10–8000 Hz	10–100 Hz	100–1000 Hz	1000–6300 Hz
Minimum	80.1	72.5	75.1	73.5
L_{95}	86.5	76.7	83.1	77.3
L_{75}	92.4	83.4	89.2	80.6
L_{50}	98.1	90.6	95	86.2
L_{25}	105.4	98.7	102.2	92.8
L_{5}	116.9	112.8	113.4	103.1
Maximum	164.4	164.4	146.4	137.5
Mean (L_{mean})	119	118.4	109.4	100.3

Table 6. Station 1: Statistical analysis of daily SEL (10–8000 Hz). SEL units: dB re 1 µPa²·s, presented as unweighted levels.

Sound level statistic	Daily SEL
	Unweighted
Minimum	153.1
L_{95}	154.3
L_{75}	155.9
L_{50}	158.7
L_{25}	162
L_{5}	168.6
Maximum	185.2
Mean	166.6

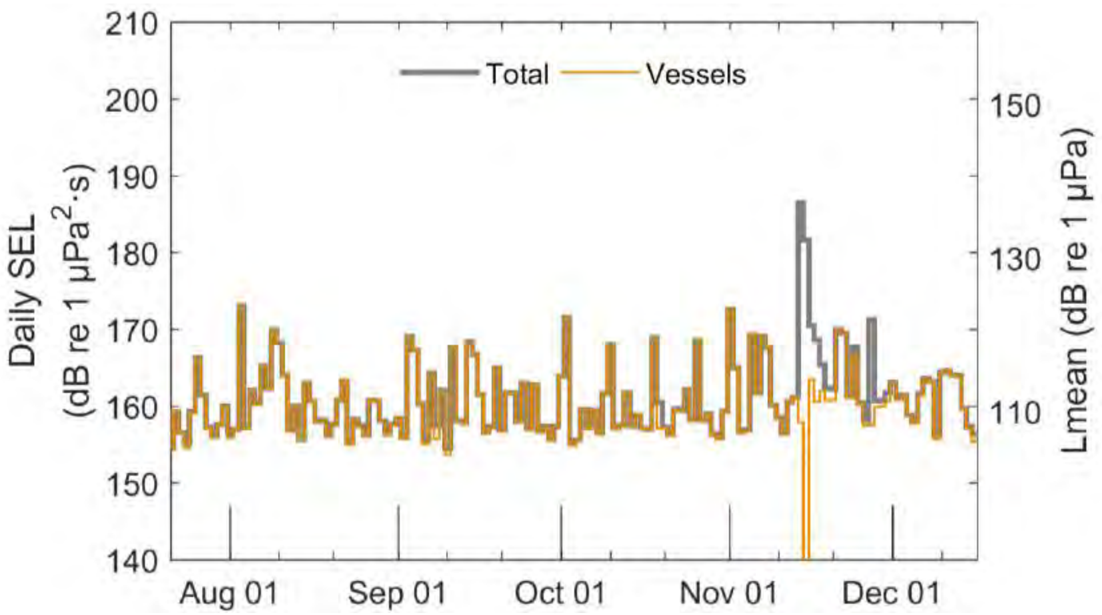

Figure 13. Station 1: Total, vessel, and seismic-associated daily SEL and equivalent continuous noise levels (L_{mean}).

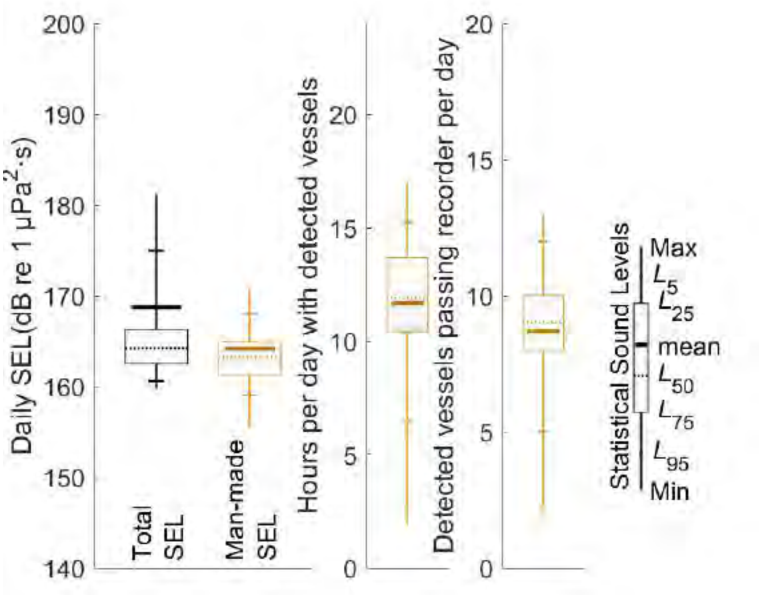

Figure 14. Station 1: Total and man-made associated SEL, with daily total hours of vessel detection and daily vessel detections.

3.1.3. Station 2

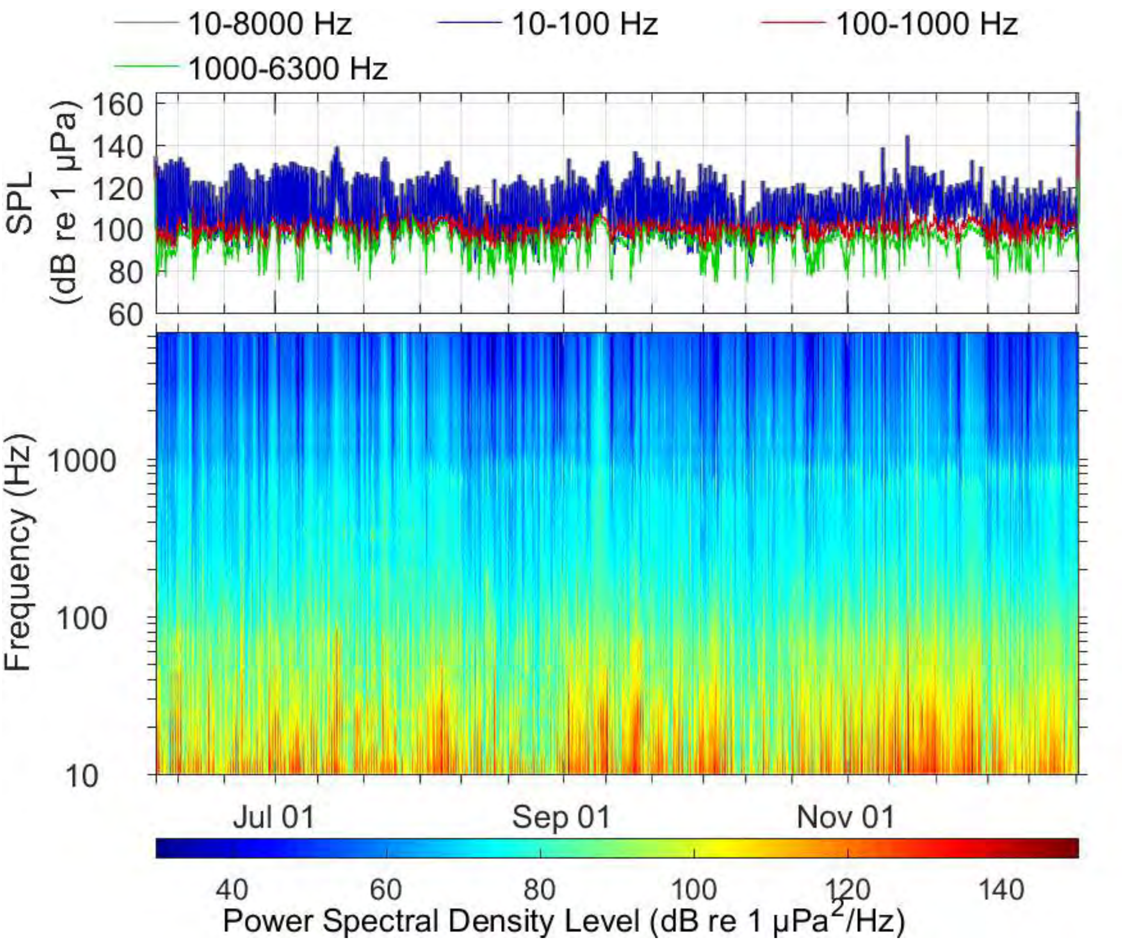

Figure 15. Station 2: Sound level summary from 4 Jun to 20 Dec 2016.(Top) In-band SPL and (bottom) spectrogram of underwater sound.

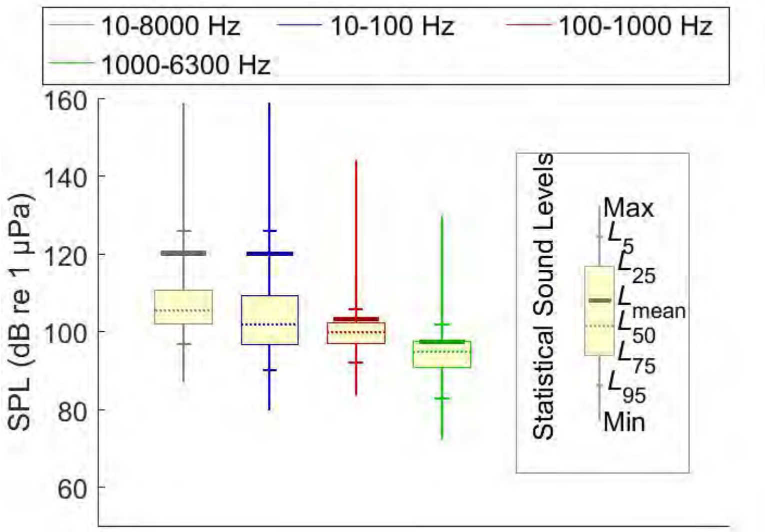

Figure 16. Station 2: Broadband and in-band 1-min SPL.

Table 7. Station 2: Statistical analysis of SPL. SPL units: dB re 1 µPa.

Sound level statistic	SPL			
	10–8000 Hz	10–100 Hz	100–1000 Hz	1000–6300 Hz
Minimum	87.1	79.9	83.9	72.6
L_{95}	97.2	90.4	92.3	83.0
L_{75}	102.3	96.9	97.3	91.1
L_{50}	105.6	102.0	100.1	95.2
L_{25}	110.9	109.5	102.6	97.9
L_{5}	126.2	126.2	106.0	102.0
Maximum	159.1	159.1	143.4	130.0
Mean (L_{mean})	120.4	120.2	103.2	97.6

Table 8. Station 2: statistical analysis of daily SEL (10–8000 Hz). SEL units: dB re 1 µPa²·s, presented as unweighted levels.

Sound level statistic	Daily SEL
	Unweighted
Minimum	149.6
L_{95}	155
L_{75}	158.7
L_{50}	162.5
L_{25}	167.6
L_{5}	172.9
Maximum	183.1
Mean	167.9

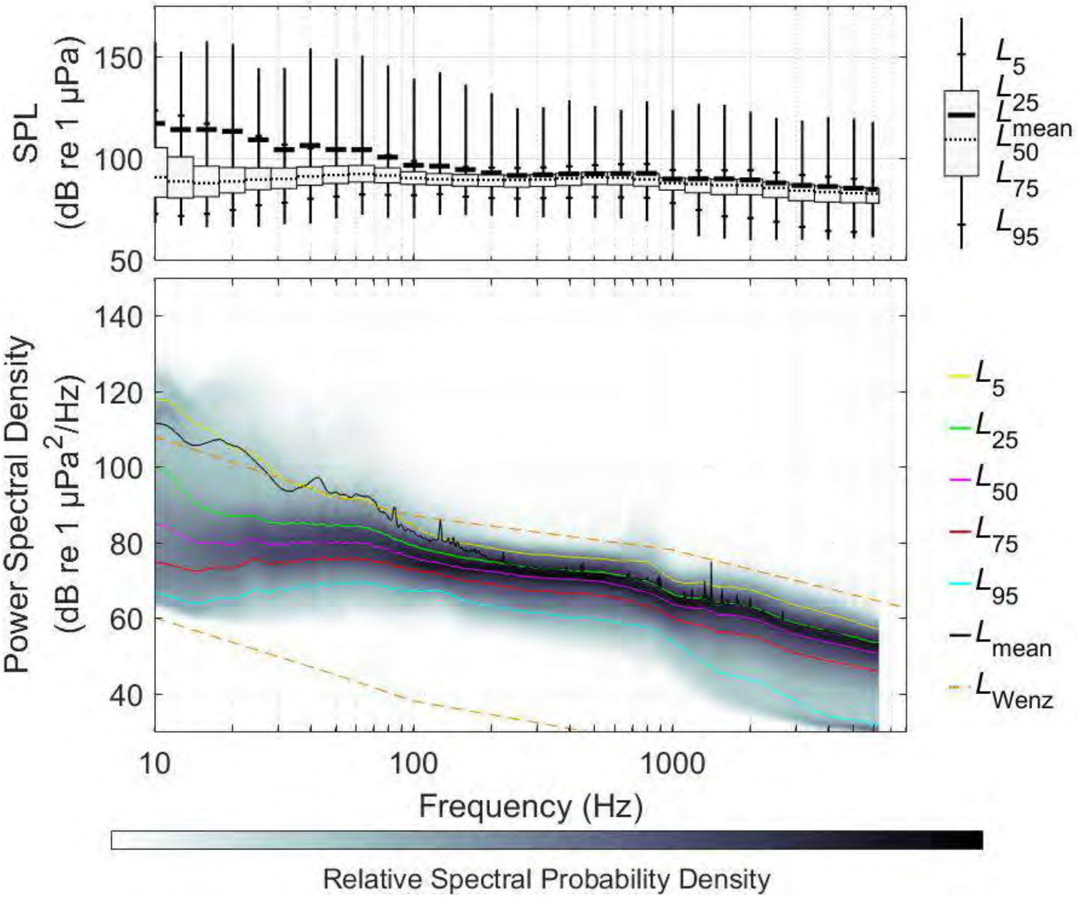

Figure 17. Station 2: (Top) Exceedance percentiles and mean of 1/3-octave-band SPL and (bottom) exceedance percentiles and probability density (grayscale) of 1-min PSD levels compared to the limits of prevailing noise (Wenz 1962).

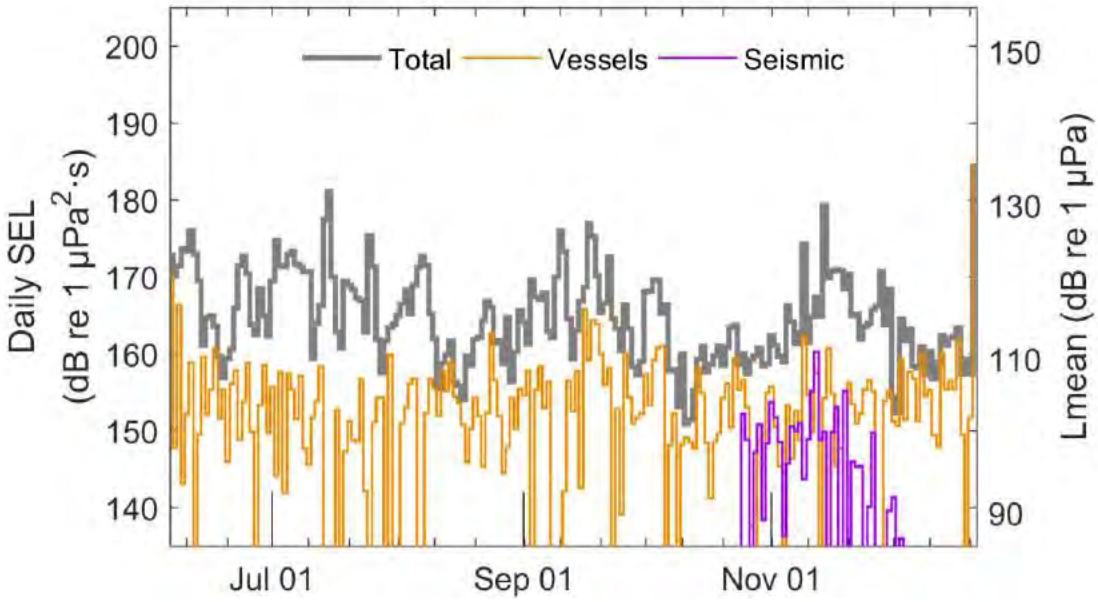

Figure 18. Station 2: Total, vessel, and seismic-associated daily SEL and equivalent continuous noise levels (L_{mean}).

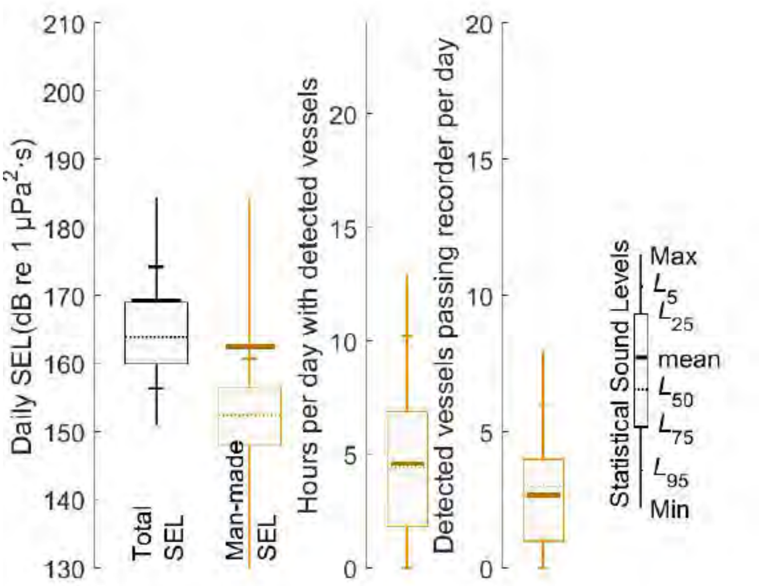

Figure 19. Station 2: Total and man-made associated SEL, with daily total hours of vessel detection and daily vessel detections.

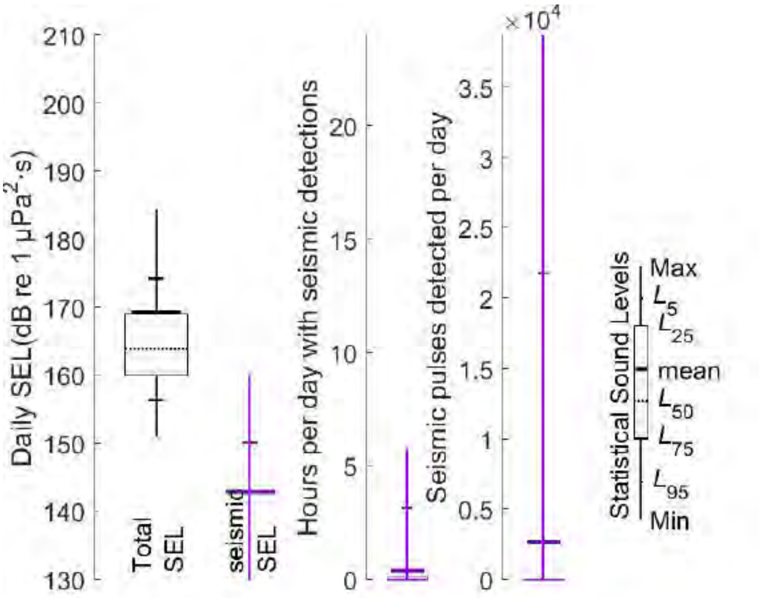

Figure 20. Station 2: Total and seismic associated SEL, with daily total hours of seismic detection and daily seismic pulses detections.

3.1.4. Station 3

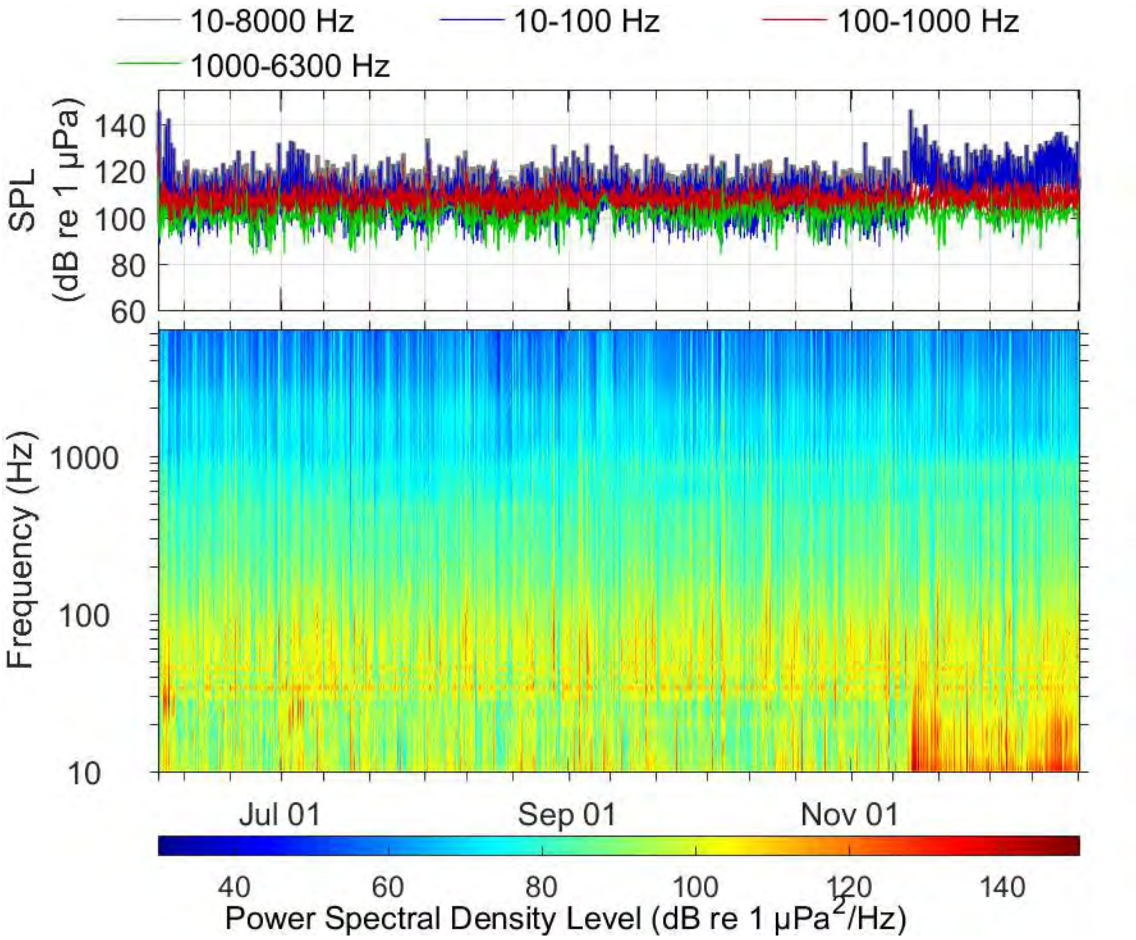

Figure 21. Station 3: Sound level summary from 3 Jun to 19 Dec 2016.(Top) In-band SPL and (bottom) spectrogram of underwater sound.

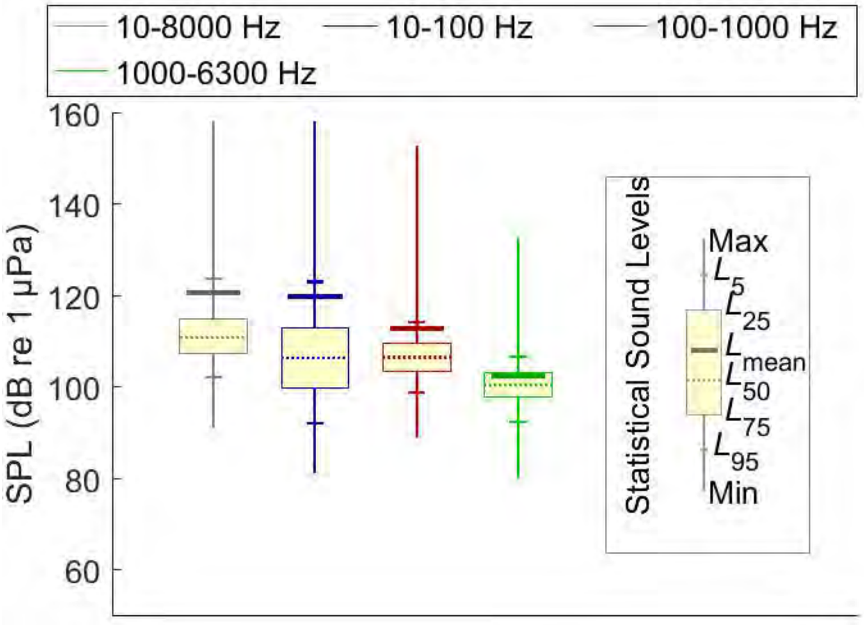

Figure 22. Station 3: Broadband and in-band 1-min SPL.

Table 9. Station 3: Statistical analysis of SPL. SPL units: dB re 1 µPa.

Sound level statistic	SPL			
	10–8000 Hz	10–100 Hz	100–1000 Hz	1000–6300 Hz
Minimum	91.1	81.5	89.1	80.4
L_{95}	102.4	92.2	99	92.6
L_{75}	107.4	99.9	103.6	98.1
L_{50}	111	106.7	106.7	100.7
L_{25}	115.2	113	109.7	103.3
L_{5}	124	123.2	114.5	106.7
Maximum	158.3	158.3	152.9	132.8
Mean (L_{mean})	120.8	119.9	112.9	102.6

Table 10. Station 3: Statistical analysis of daily SEL (10–8000 Hz). SEL units: dB re 1 µPa²·s, presented as unweighted levels.

Sound level statistic	Daily SEL
	Unweighted
Minimum	158.4
L_{95}	159.2
L_{75}	161.1
L_{50}	162.9
L_{25}	164.9
L_{5}	173.6
Maximum	179.8
Mean	167.4

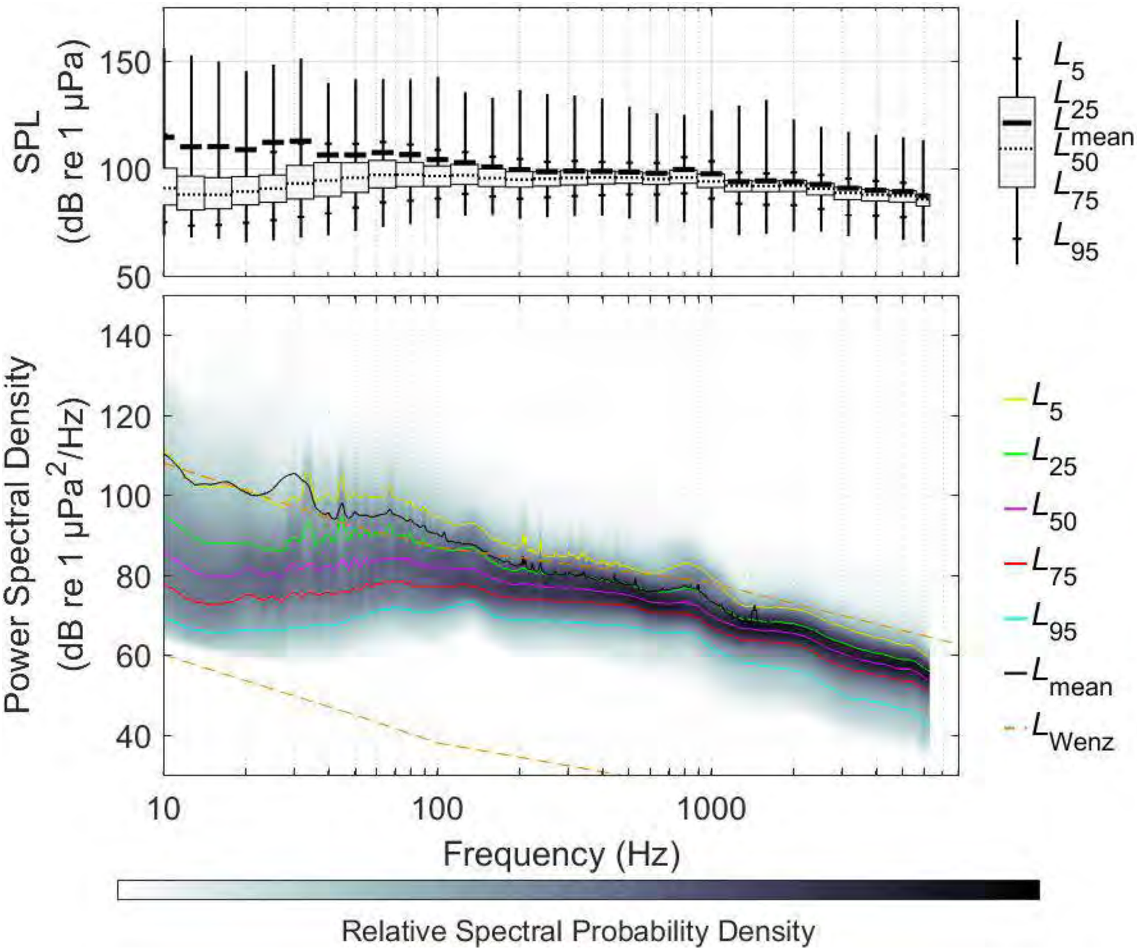

Figure 23. Station 3: (Top) Exceedance percentiles and mean of 1/3-octave-band SPL and (bottom) exceedance percentiles and probability density (grayscale) of 1-min PSD levels compared to the limits of prevailing noise (Wenz 1962).

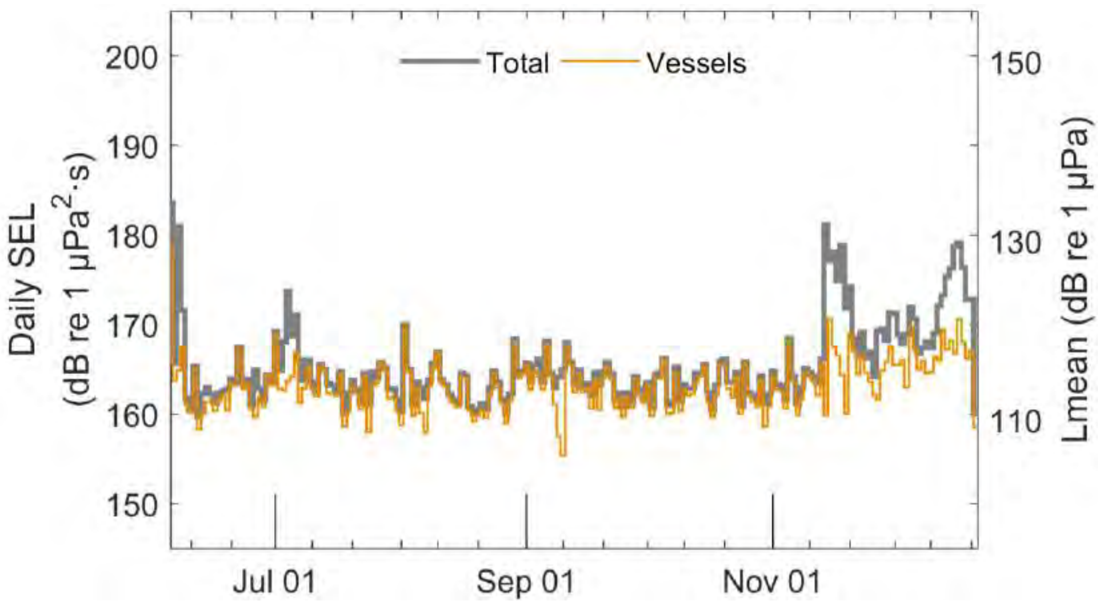

Figure 24. Station 3: Total, vessel, and seismic-associated daily SEL and equivalent continuous noise levels (L_{mean}).

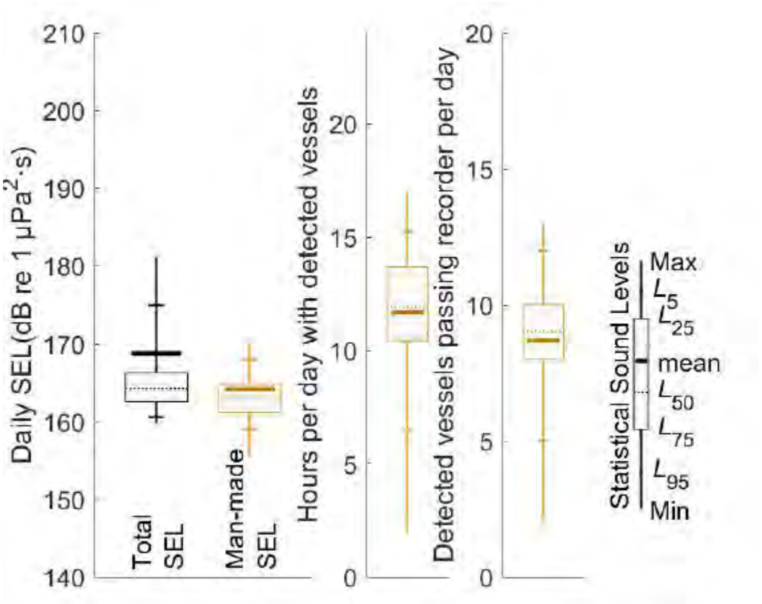

Figure 25. Station 3: Total and man-made associated SEL, with daily total hours of vessel detection and daily vessel detections.

3.1.5. Station 4

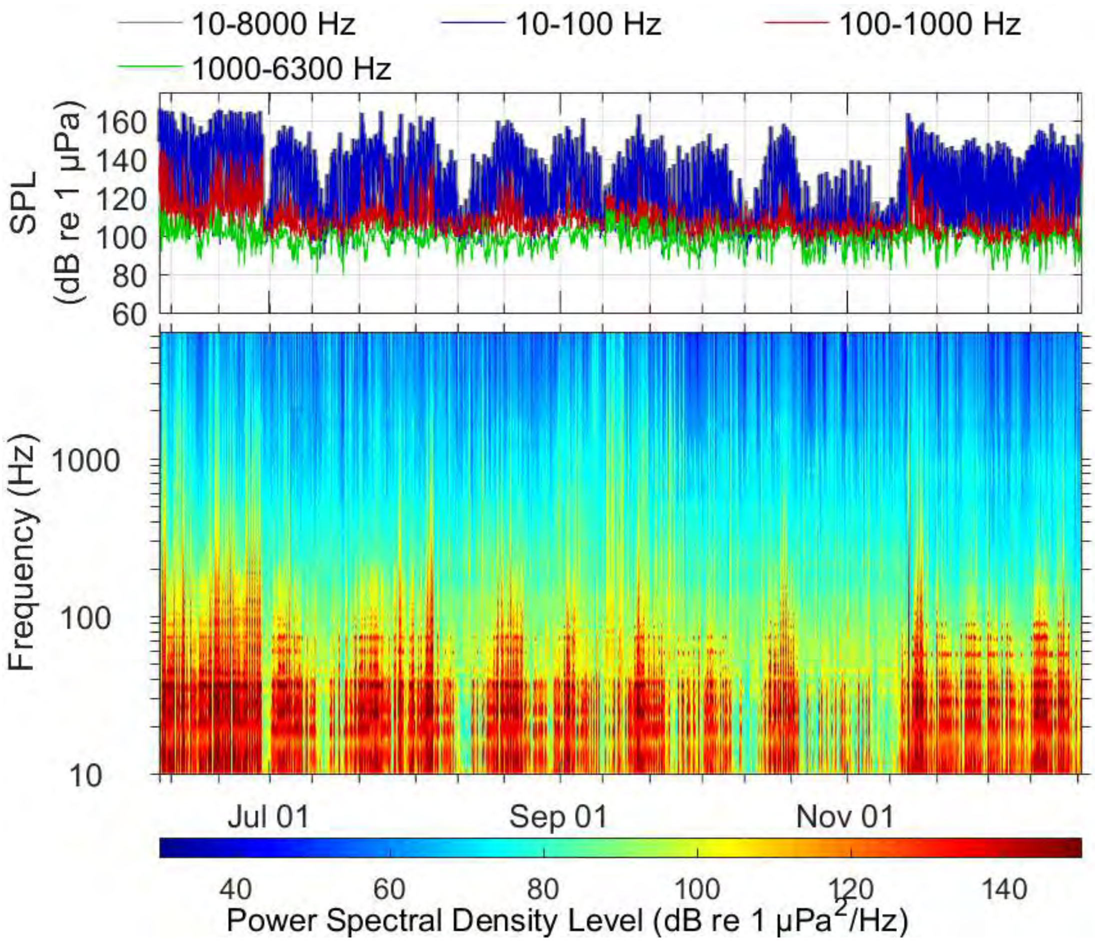

Figure 26. Station 4: Sound level summary from 6 Jun to 20 Dec 2016.(Top) In-band SPL and (bottom) spectrogram of underwater sound.

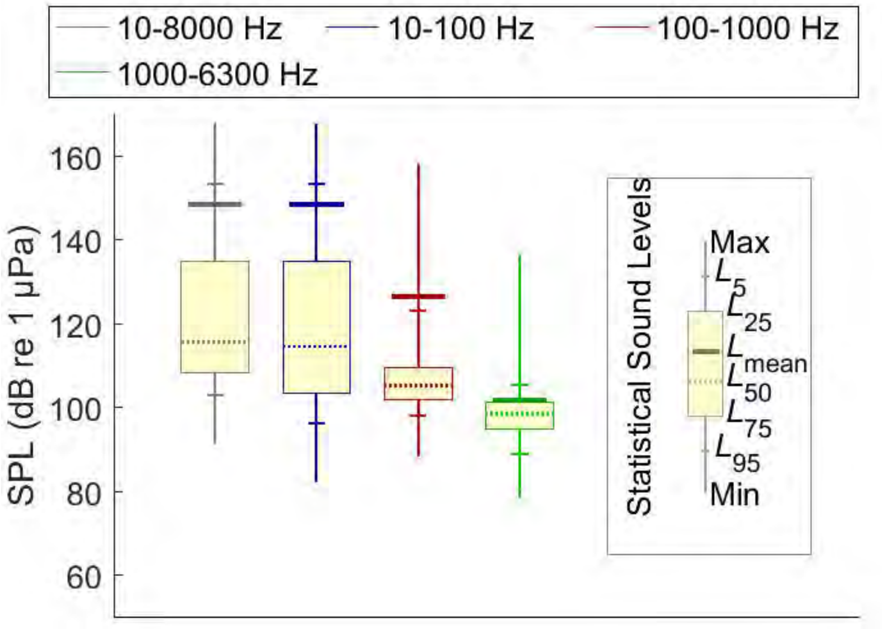

Figure 27. Station 4: Broadband and in-band 1-min SPL.

Table 11. Station 4: Statistical analysis of SPL. SPL units: dB re 1 µPa.

Sound level statistic	SPL			
	10–8000 Hz	10–100 Hz	100–1000 Hz	1000–6300 Hz
Minimum	91.4	82.4	88.4	78.7
L_{95}	103.2	96.4	98.1	88.9
L_{75}	108.4	103.5	102.2	95.1
L_{50}	115.8	114.6	105.4	98.7
L_{25}	134.9	134.9	109.7	101.5
L_{5}	153.4	153.4	123.2	105.7
Maximum	168	167.9	158.3	136.7
Mean (L_{mean})	148.6	148.6	126.6	102

Table 12. Station 4: Statistical analysis of daily SEL (10–8000 Hz). SEL units: dB re 1 µPa²·s, presented as unweighted levels.

Sound level statistic	Daily SEL
	Unweighted
Minimum	155.9
L_{95}	157.7
L_{75}	178.3
L_{50}	186.4
L_{25}	194
L_{5}	203.1
Maximum	208
Mean	195.9

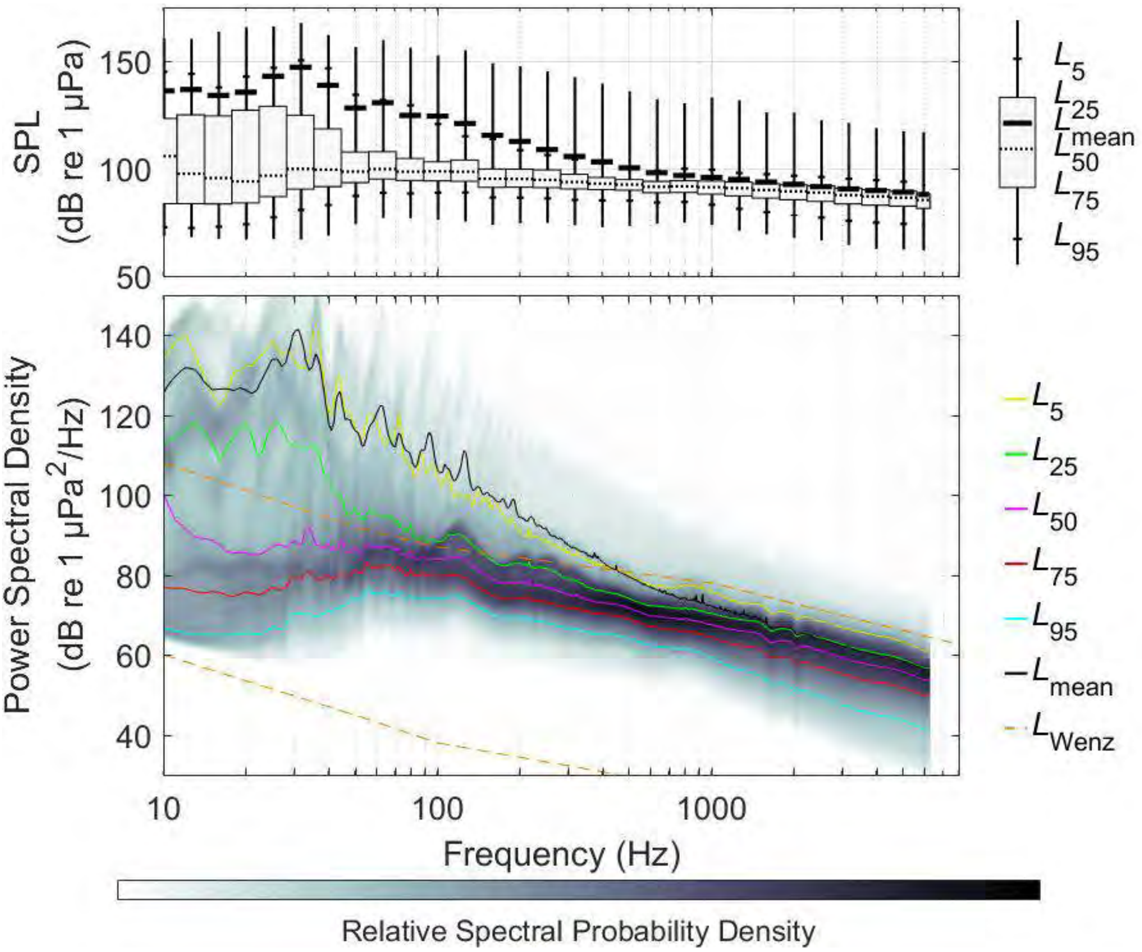

Figure 28. Station 4: (Top) Exceedance percentiles and mean of 1/3-octave-band SPL and (bottom) exceedance percentiles and probability density (grayscale) of 1-min PSD levels compared to the limits of prevailing noise (Wenz 1962).

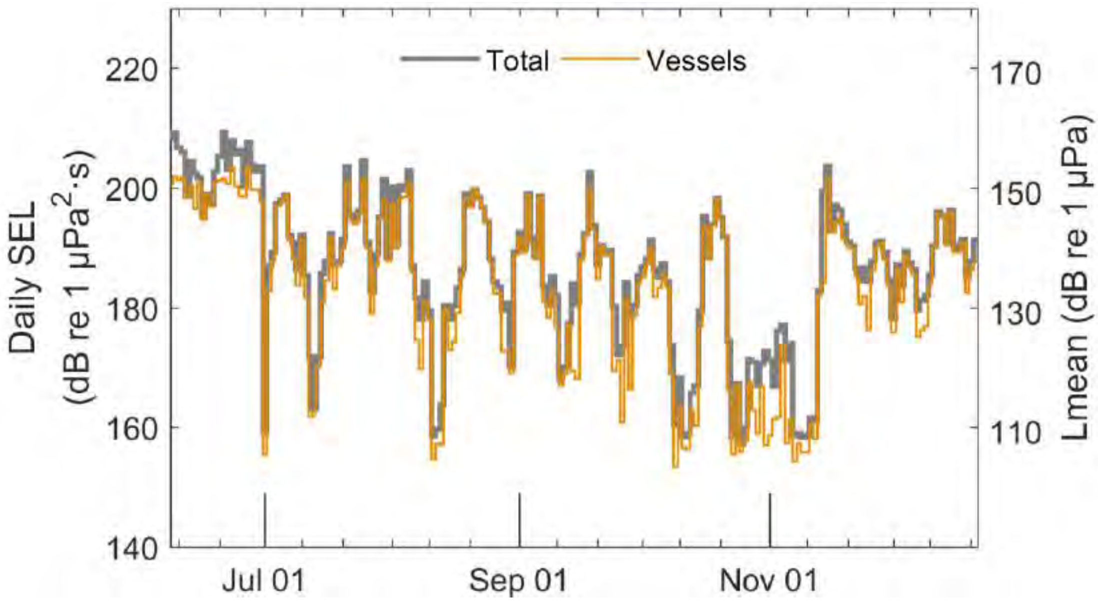

Figure 29. Station 4: Total and vessel SEL and equivalent continuous noise levels (L_{mean}).

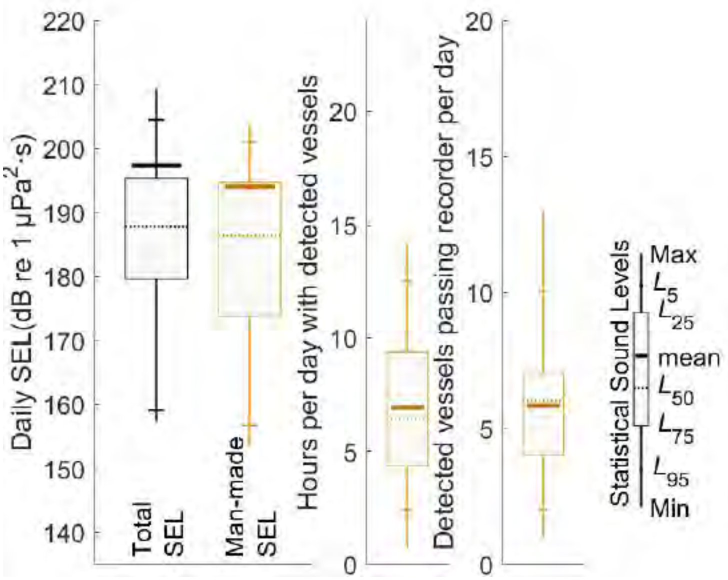

Figure 30. Station 4: Total and man-made associated SEL, with daily total hours of vessel detection and daily vessel detections.

3.1.6. Station 5

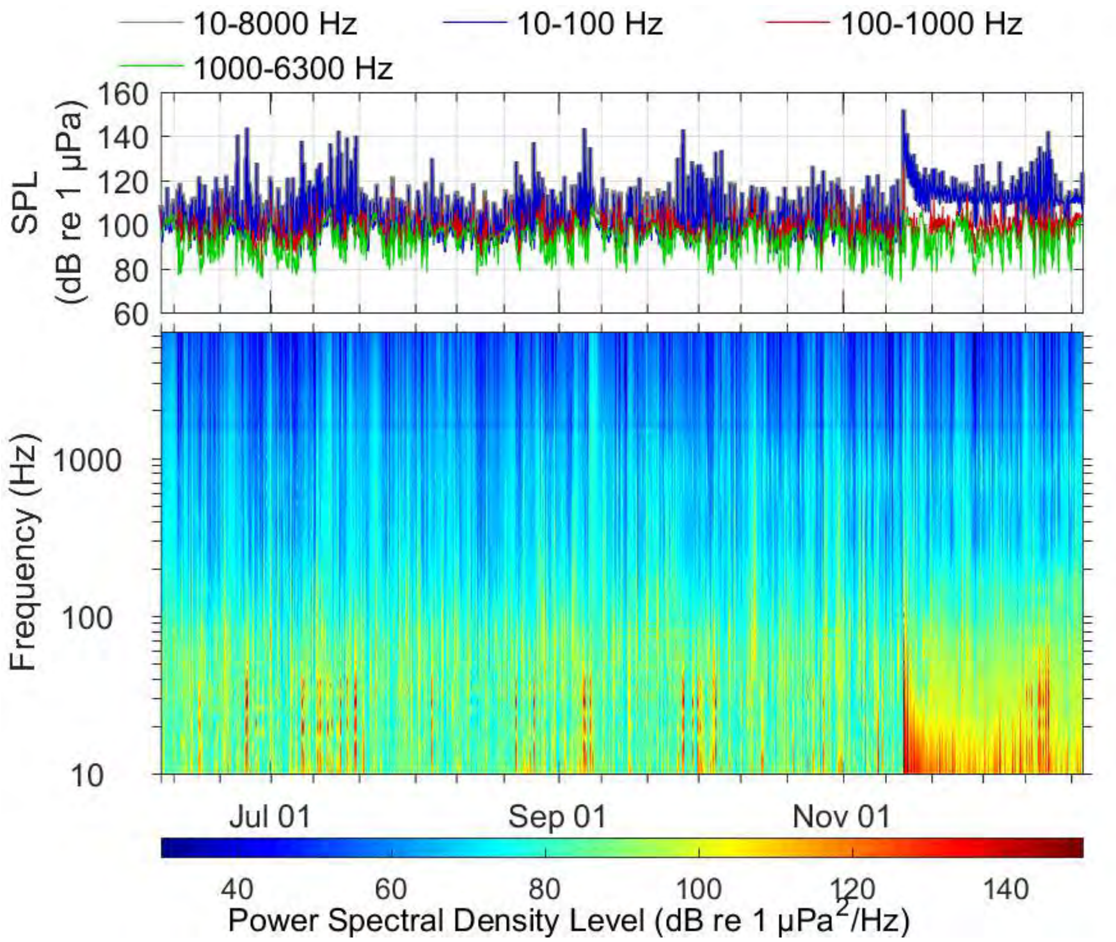

Figure 31. Station 5: Sound level summary from 6 Jun to 21 Dec 2016.(Top) In-band SPL and (bottom) spectrogram of underwater sound.

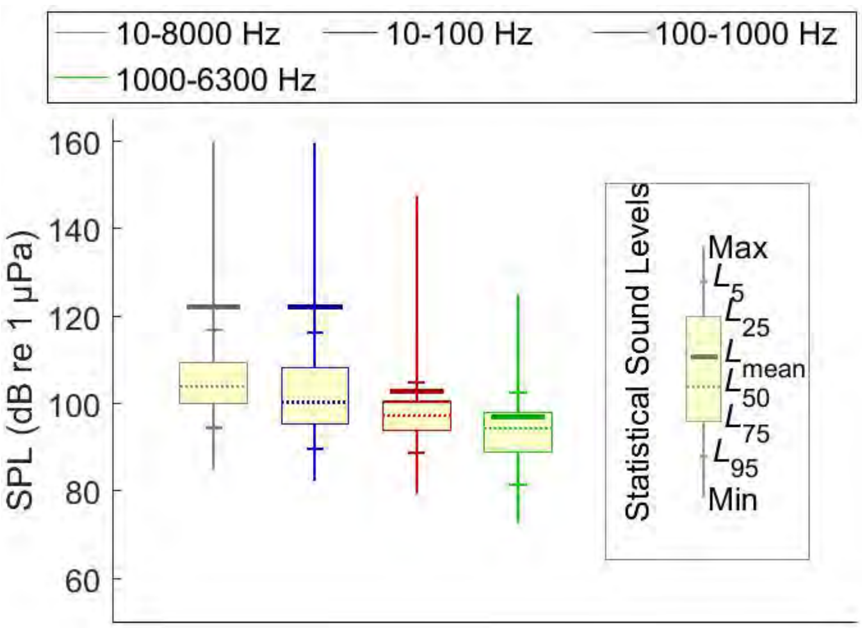

Figure 32. Station 5: Broadband and in-band 1-min SPL.

Table 13. Station 5: Statistical analysis of SPL. SPL units: dB re 1 µPa.

Sound level statistic	SPL			
	10–8000 Hz	10–100 Hz	100–1000 Hz	1000–6300 Hz
Minimum	85.2	82.5	79.5	72.9
L_{95}	94.6	89.8	88.9	81.5
L_{75}	100.2	95.6	93.9	89.1
L_{50}	104	100.5	97.4	94.4
L_{25}	109.6	108.3	100.6	98.1
L_{5}	116.9	116.5	105.1	102.7
Maximum	160.1	159.8	147.9	125.2
Mean (L_{mean})	122.3	122.2	102.9	97.2

Table 14. Station 5: Statistical analysis of daily SEL (10–8000 Hz). SEL units: dB re 1 µPa²·s, presented as unweighted levels.

Sound level statistic	Daily SEL
	Unweighted
Minimum	146.2
L_{95}	149.6
L_{75}	153.7
L_{50}	157.1
L_{25}	161.9
L_{5}	173.1
Maximum	186.6
Mean	169.1

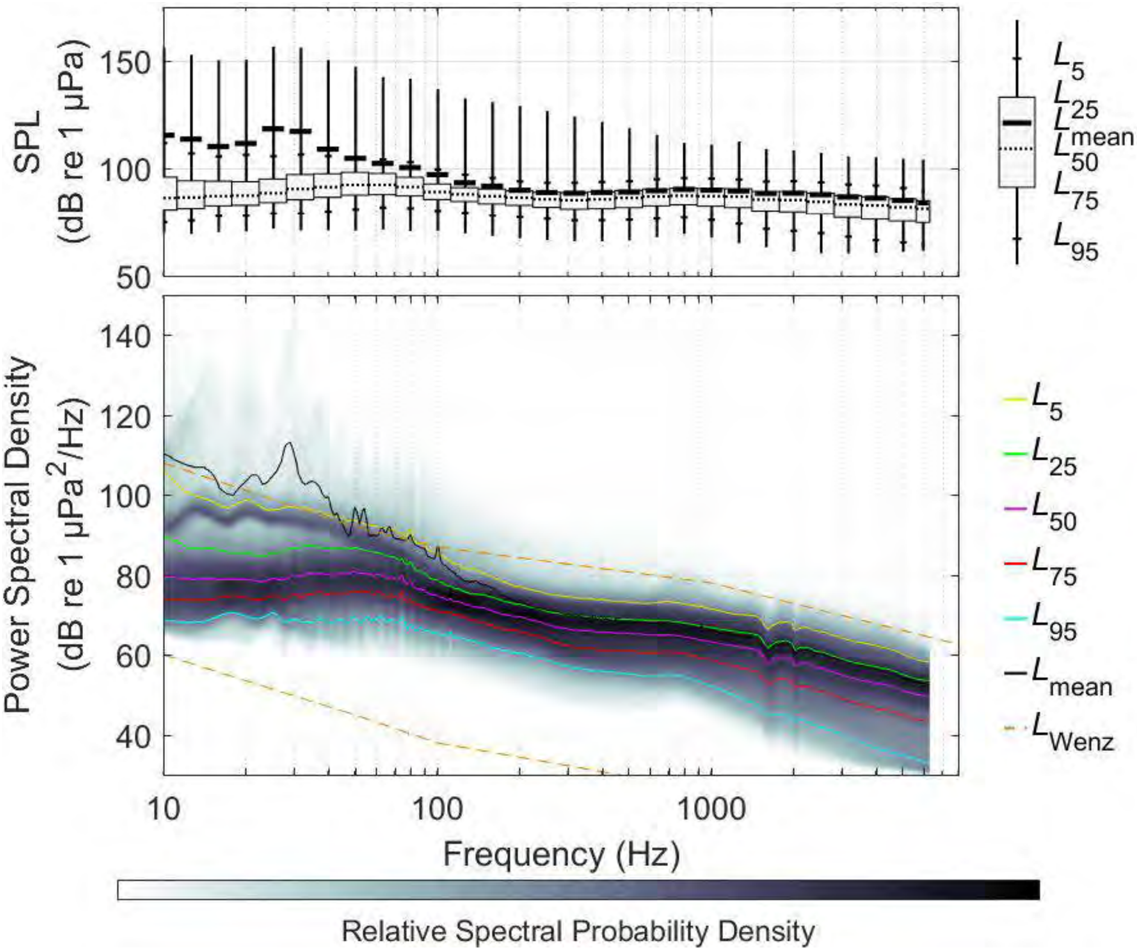

Figure 33. Station 5: (Top) Exceedance percentiles and mean of 1/3-octave-band SPL and (bottom) exceedance percentiles and probability density (grayscale) of 1-min PSD levels compared to the limits of prevailing noise (Wenz 1962).

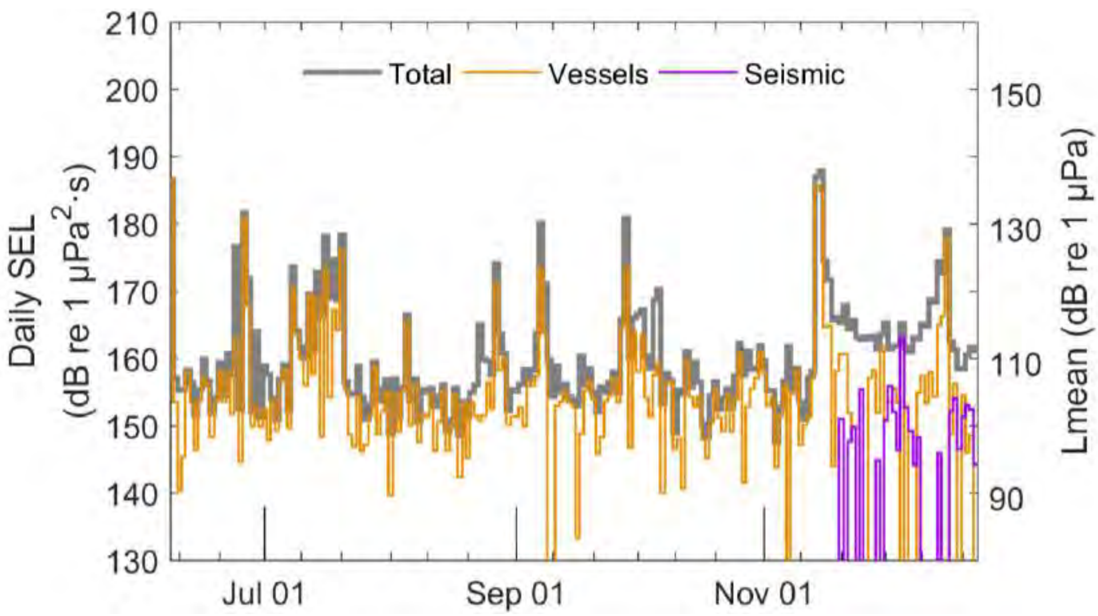

Figure 34. Station 5: Total, vessel, and seismic-associated daily SEL and equivalent continuous noise levels (L_{mean}).

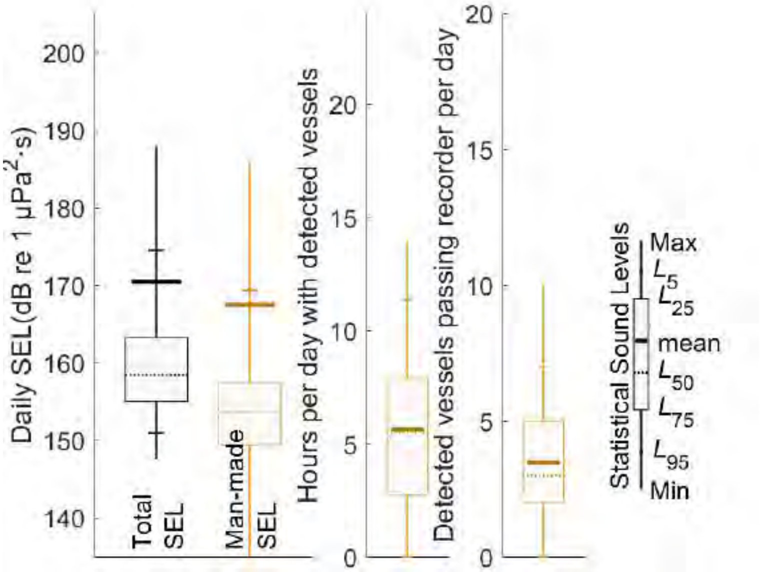

Figure 35. Station 5: Total and man-made associated SEL, with daily total hours of vessel detection and daily vessel detections.

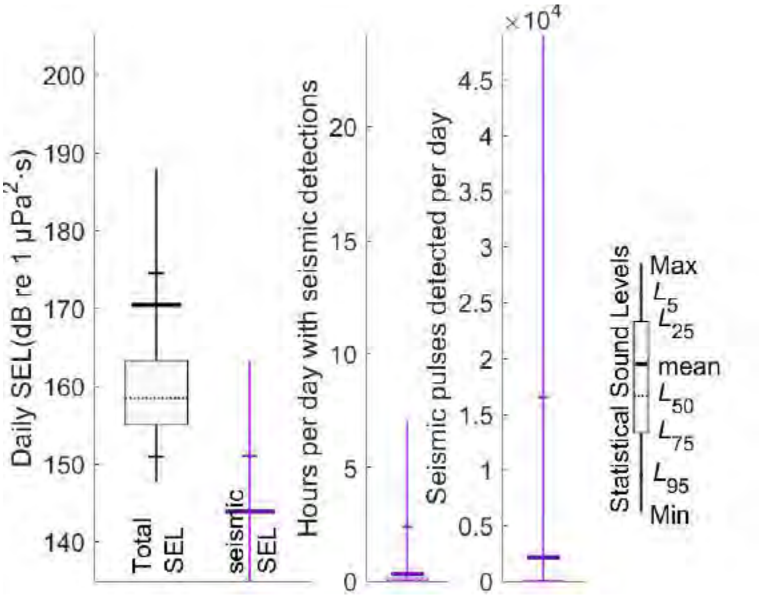

Figure 36. Station 5: Total and seismic associated SEL, with daily total hours of seismic detection and daily seismic pulse detections.

3.1.7. Station 6

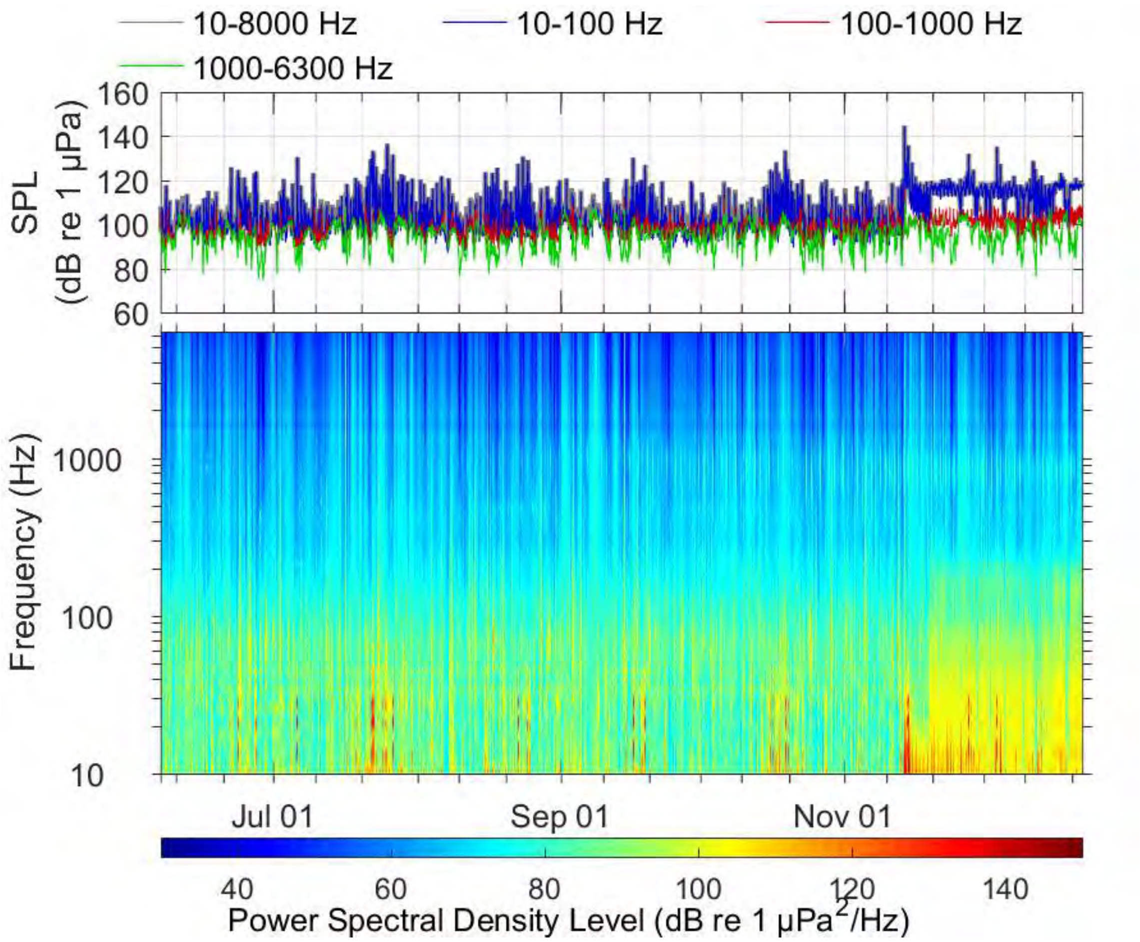

Figure 37. Station 6: Sound level summary from 6 Jun to 21 Dec 2016.(Top) In-band SPL and (bottom) spectrogram of underwater sound.

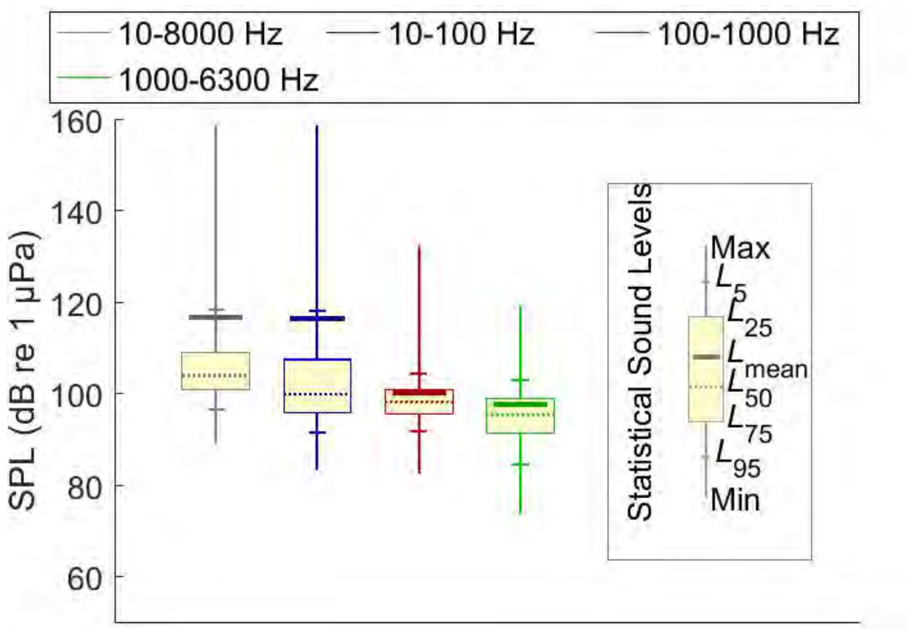

Figure 38. Station 6: Broadband and in-band 1-min SPL.

Table 15. Station 6: Statistical analysis of SPL. SPL units: dB re 1 µPa.

Sound level statistic	SPL			
	10–8000 Hz	10–100 Hz	100–1000 Hz	1000–6300 Hz
Minimum	89.3	83.5	82.9	73.9
L_{95}	96.9	91.7	92	84.8
L_{75}	101	96.1	95.7	91.6
L_{50}	104.2	100.1	98.5	95.6
L_{25}	109.3	107.7	101.2	99
L_{5}	118.6	118.4	104.6	103.1
Maximum	158.8	158.8	132.5	119.4
Mean (L_{mean})	116.8	116.6	100.5	97.9

Table 16. Station 6: Statistical analysis of daily SEL (10–8000 Hz). SEL units: dB re 1 µPa²·s, presented as unweighted levels.

Sound level statistic	Daily SEL
	Unweighted
Minimum	146.8
L_{95}	149.9
L_{75}	152.4
L_{50}	155.6
L_{25}	161.7
L_{5}	167.2
Maximum	178.2
Mean	162.8

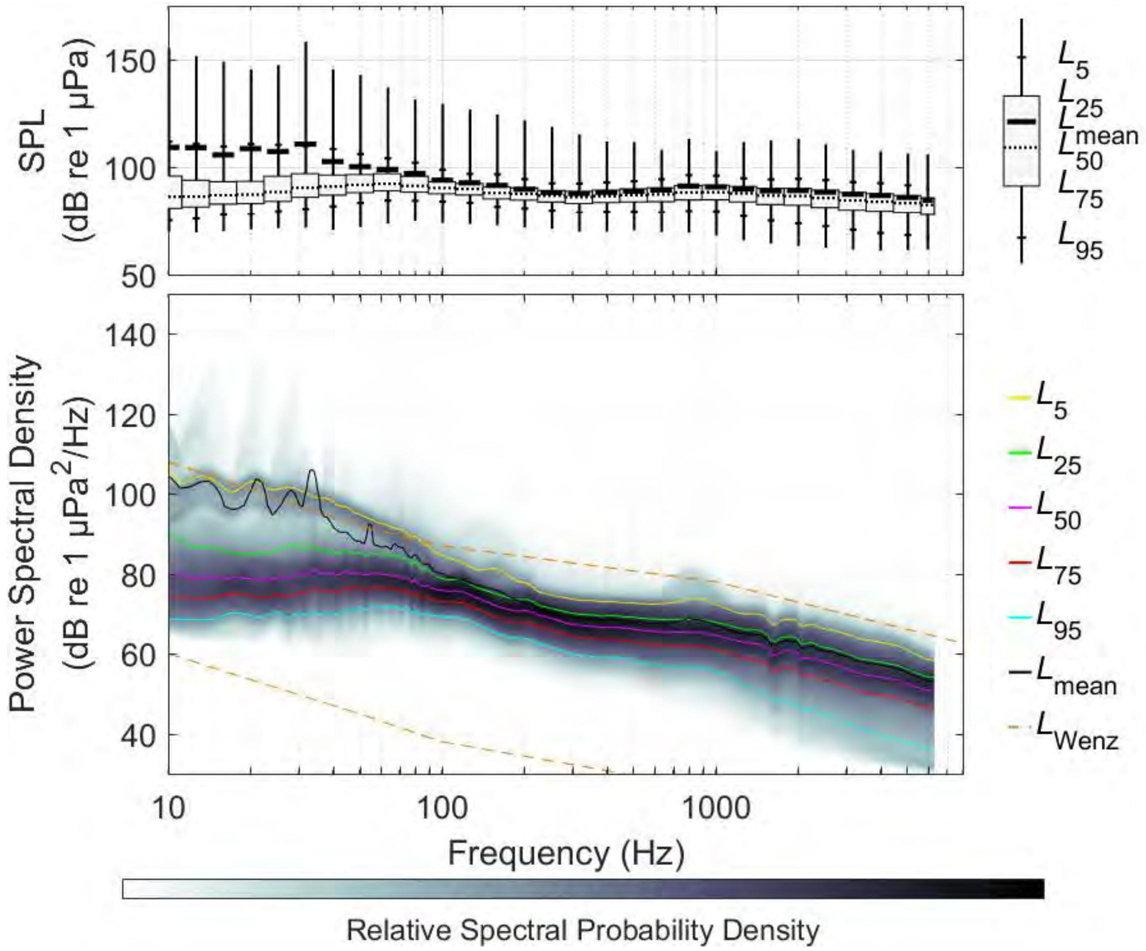

Figure 39. Station 6: (Top) Exceedance percentiles and mean of 1/3-octave-band SPL and (bottom) exceedance percentiles and probability density (grayscale) of 1-min PSD levels compared to the limits of prevailing noise (Wenz 1962).

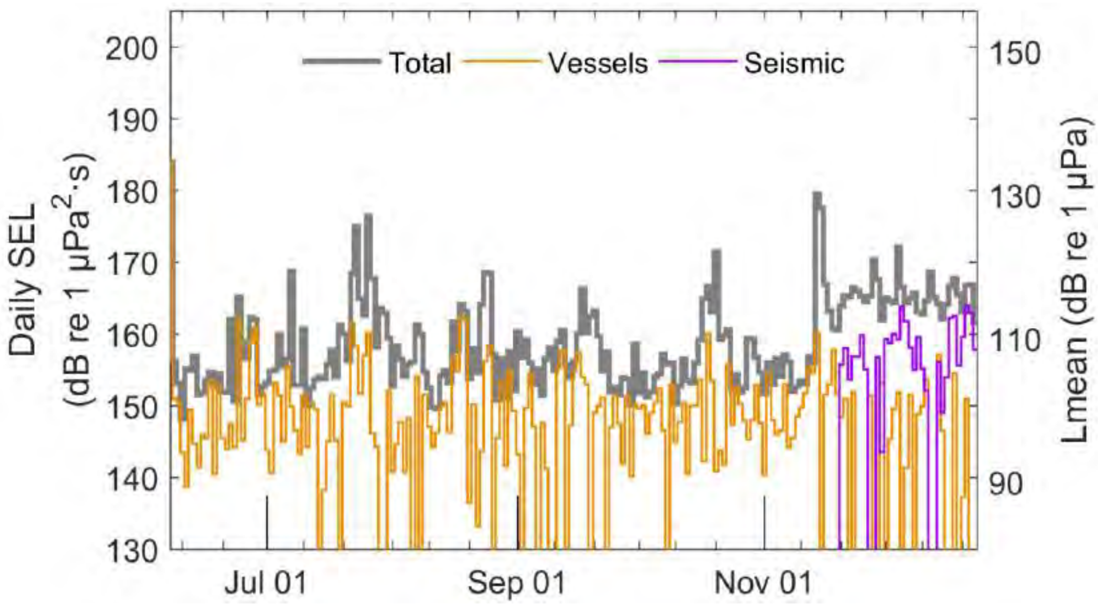

Figure 40. Station 6: Total, vessel, and seismic-associated daily SEL and equivalent continuous noise levels (L_{mean}).

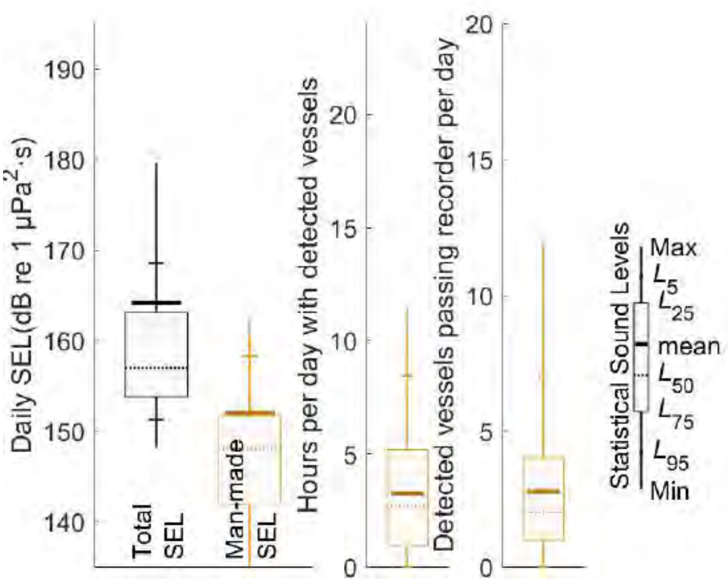

Figure 41. Station 6: Total and man-made associated SEL, with daily total hours of vessel detection and daily vessel detections.

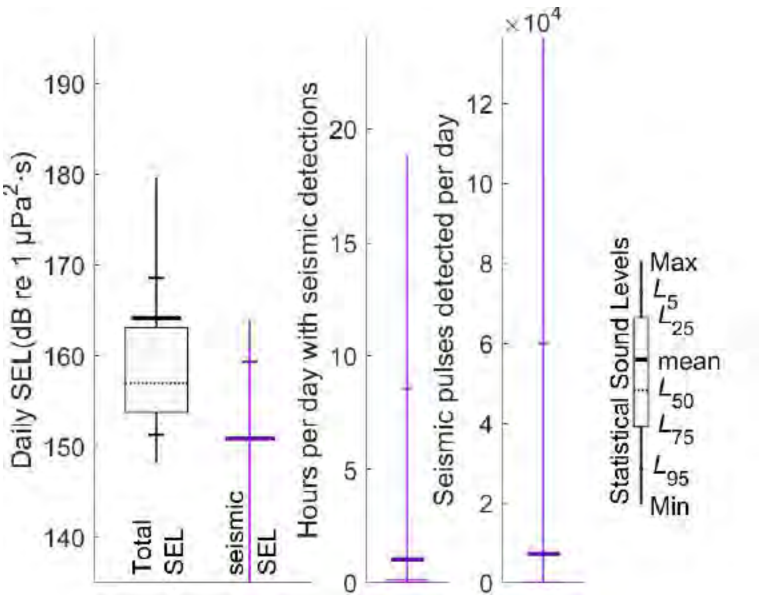

Figure 42. Station 6: Total and seismic associated SEL, with daily total hours of seismic detection and daily seismic pulse detections.

3.1.8. Station 7

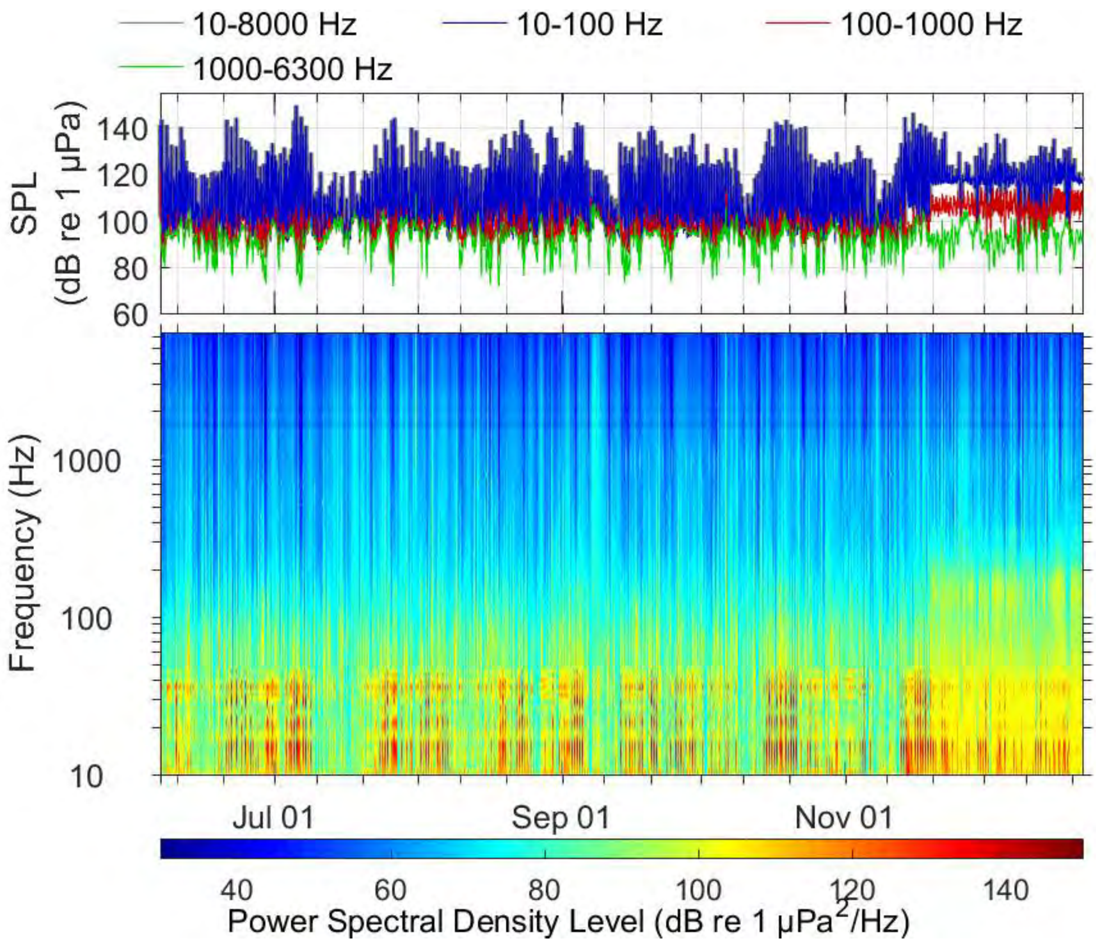

Figure 43. Station 7: Sound level summary from 5 Jun to 21 Dec 2016.(Top) In-band SPL and (bottom) spectrogram of underwater sound.

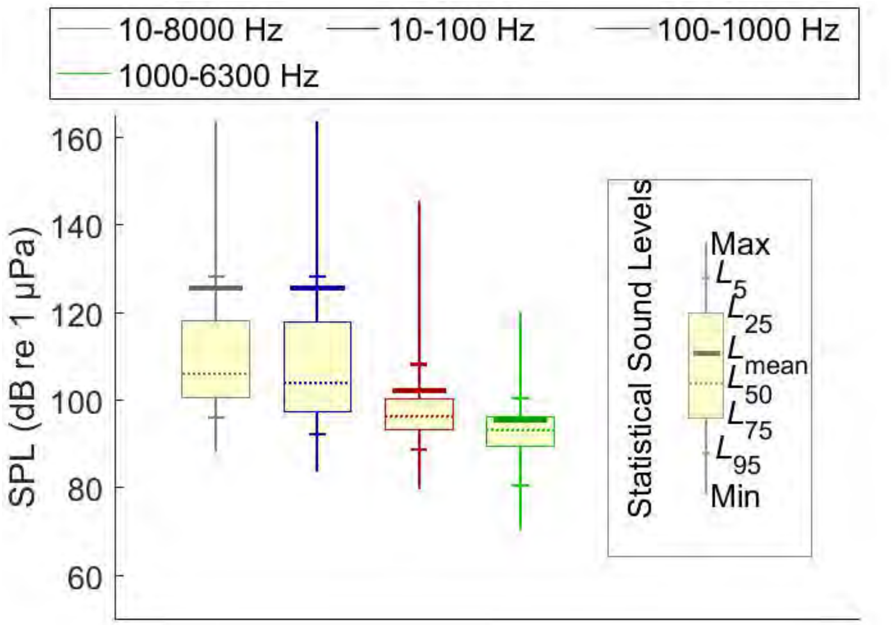

Figure 44. Station 7: Broadband and in-band 1-min SPL.

Table 17. Station 7: Statistical analysis of SPL. SPL units: dB re 1 µPa.

Sound level statistic	SPL			
	10–8000 Hz	10–100 Hz	100–1000 Hz	1000–6300 Hz
Minimum	88.2	83.9	79.8	70.4
L_{95}	96.1	92.3	88.8	80.7
L_{75}	100.7	97.5	93.3	89.7
L_{50}	106.1	104.3	96.5	93.4
L_{25}	118.4	118	100.4	96.3
L_{5}	128.5	128.5	108.4	100.7
Maximum	163.9	163.9	145.7	120.2
Mean (L_{mean})	125.9	125.9	102.5	95.5

Table 18. Station 7: Statistical analysis of daily SEL (10–8000 Hz). SEL units: dB re 1 µPa²·s, presented as unweighted levels.

Sound level statistic	Daily SEL
	Unweighted
Minimum	149.8
L_{95}	153.5
L_{75}	163.2
L_{50}	167.5
L_{25}	171.5
L_{5}	179.7
Maximum	186.8
Mean	173.2

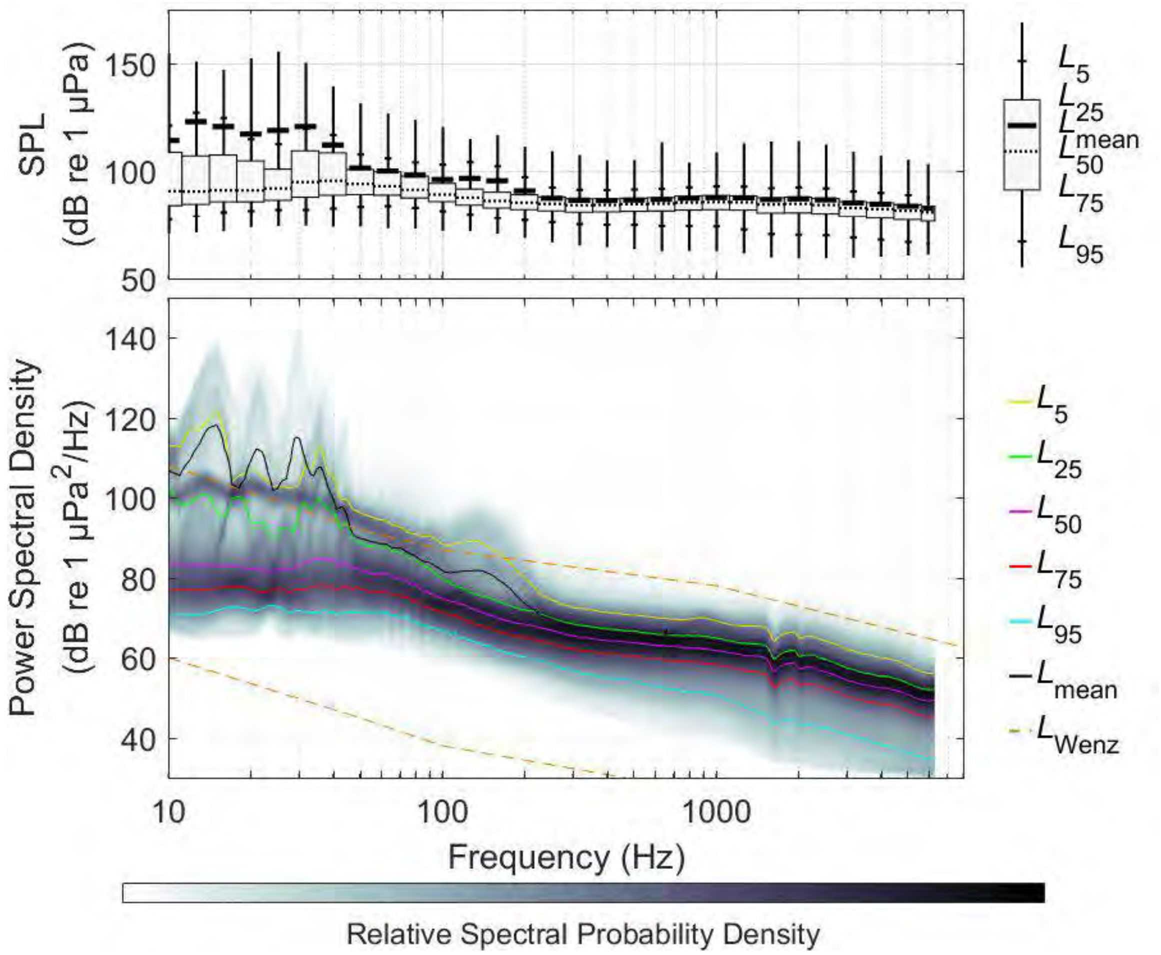

Figure 45. Station 7: (Top) Exceedance percentiles and mean of 1/3-octave-band SPL and (bottom) exceedance percentiles and probability density (grayscale) of 1-min PSD levels compared to the limits of prevailing noise (Wenz 1962).

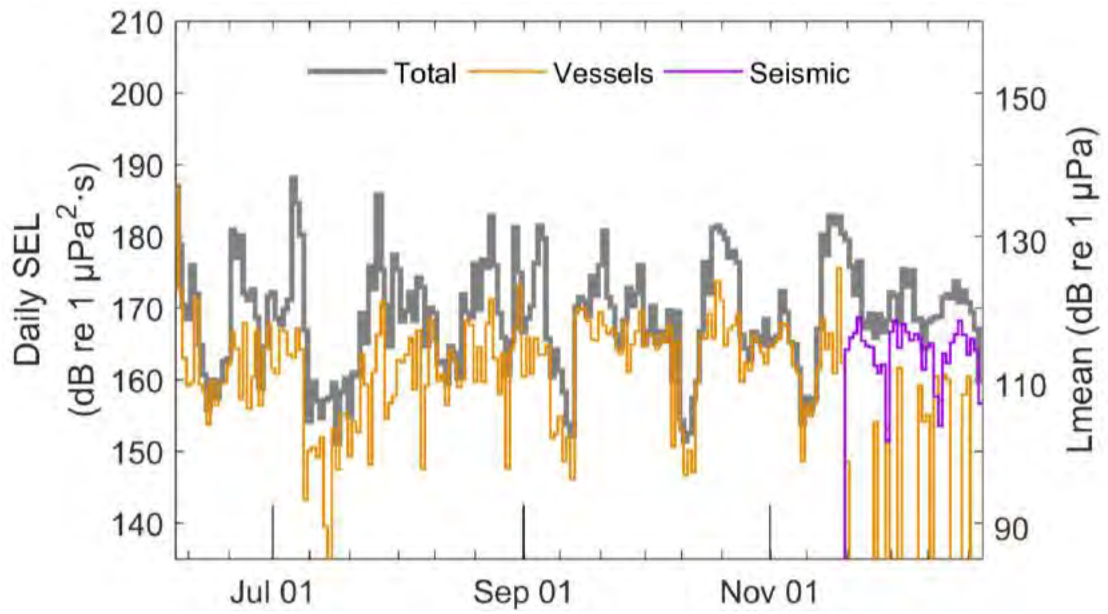

Figure 46. Station 7: Total, vessel, and seismic-associated daily SEL and equivalent continuous noise levels (L_{mean}).

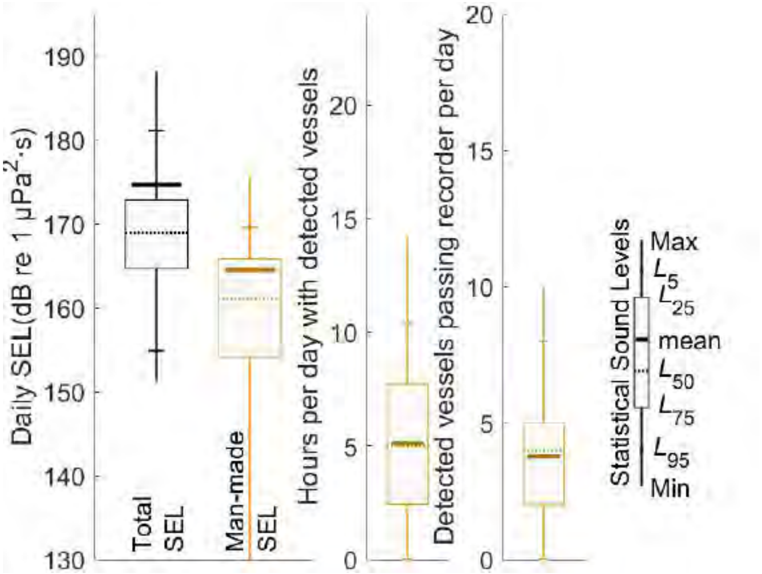

Figure 47. Station 7: Total and man-made associated SEL, with daily total hours of vessel detection and daily vessel detections.

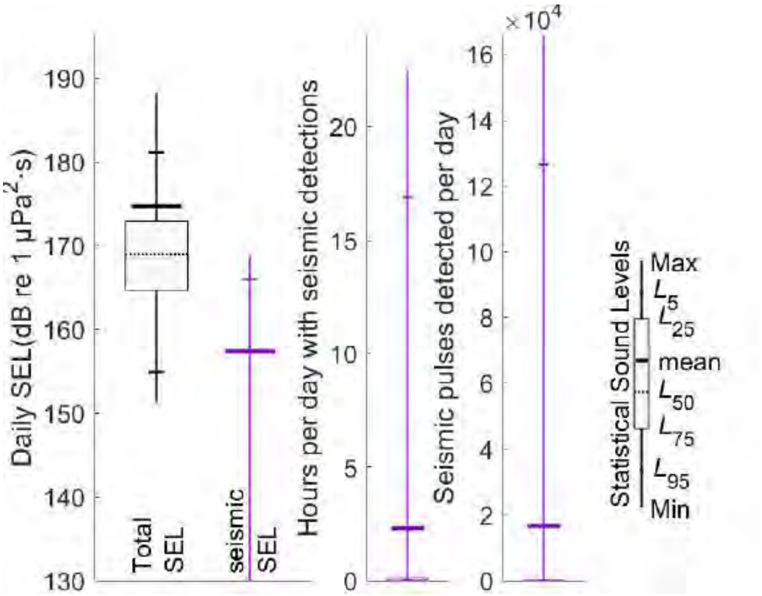

Figure 48. Station 7: Total and seismic associated SEL, with daily total hours of seismic detection and daily seismic pulse detections.

3.2. Marine Mammals

The acoustic presence of marine mammals was identified automatically by JASCO's detectors (Section 2.2.4) and verified by the manual analysis of ~300 h of acoustic data. The manual review of data revealed the presence of 11 species or species groups: blue whales (New Zealand (*Balaenoptera musculus)* and Antarctic (*B. m. intermedia*) sub-species); humpback whales (*Megaptera novaeangliae*); Antarctic minke whales (*B. bonaerensis*); southern right whales (*Eubalaena australis*); pilot whales (*Globicephala sp.*); sperm whales (*Physeter macrocephalus*); Cuvier's beaked whales (*Ziphius cavirostris*); and two unidentified species of beaked whales; as well as Hector's dolphins (*Cephalorhynchus hectori*) and unidentified dolphins. The low number of annotations at stn 4 reflects the masking effect of high local background noise conditions. When present, manual annotations were plotted to note which species were detected at this station. Stn 5 had the highest number of annotations, followed by stn 7. Delphinid clicks were the most commonly encountered acoustic signals, followed by anthropogenic noises (either airgun shots or vessels). The Cuvier's beaked whale was the most commonly recorded species, followed by sperm and pilot whales (Table 19).

Table 19. Summary of annotations created during the validation of automated detections.

Species/call	stn1	stn2	stn3	stn4	stn5	stn6	stn7	Total
Blue whales		115	25	6	12	14	10	182
Humpback whales		52	32	8	36	11	2	141
Antarctic minke whales		1	2	1	6	7	12	29
Right whales			3					3
Sperm whales			37	29	174	33	50	323
Cuvier's beaked whales					147	110	113	370
UnkBkd38					2	21	26	49
UnkBkd55					15	14	18	47
Unidentified beaked whales					28	7	33	68
Hector's dolphins	51							51
Delphinid click	78	92	40		201	157	152	720
Dolphin whistle		10	13	16	38	11	25	113
Pilot whale whistle		29	1	3	69	48	158	308
Unidentified click	7	10	3		21	10	13	64
Unidentified whistle	19	10	16	2	12	70	33	162
Anthropogenic	216	86	20	9	122	94	120	667
Unknown	130	94	45	23	85	38	61	476
Total	501	499	237	97	968	645	826	3773

3.2.1. Detector Performance

The validation of acoustic detections for stn 4 was excluded from the detector performance assessment because of the high proportion of false detections induced by vessel and flow noise at that station. Automated detection results are not presented for this station.

When multiple versions of a detector were applied to this dataset, the results of the best version are provided here.

The evaluation of the click detector targeting Cuvier's beaked whale and two unknown beaked whale signals whose frequencies centre around ~38 and 55 kHz (UnkBkd38 and UnkBkd50) was restricted to stn 5, 6, and 7 because they were not manually detected at any other stations. Similarly, Hector's dolphin clicks were only manually confirmed at stn 1 and detections at other stations were excluded. The sperm whale click detector and pilot whale whistle detector were evaluated using only the stations where these species occurred (i.e., stns 3, 5, 6, 7 and stns 2, 5, 6, 7, respectively). Dolphin whistles and delphinid clicks occurred at all stations.

For humpback whale calls, we excluded periods during which airgun pulses were detected because of the high number of false detections they induced, and because no detections were manually validated during these periods. At stns 5, 6, and 7, airgun pulse detections occurred from 10 Nov until the end of the deployment. At stn 2, airgun pulses were detected from 25 Oct to 24 Nov.

When the F-score of a detector is below 0.6, the results are considered as providing a poor representation of the actual acoustic occurrence of a species; however, the P and R values provide an opportunity to evaluate the potential magnitude of the misrepresentation. The choice of presenting automated detection results if F <0.6 usually relies on the overlap between manual and automated detections. In this study, sperm whale and blue whale detections were both concerned with a low F-score; however, sperm whale manual and automated detections were in relatively good agreement, while this was not the case for blue whales. Ultimately, all automated detection results have to be interpreted with the corresponding detector performance values in mind.

Table 20. Detection thresholds determined from validating the automated detector outputs. Considering only sound files with a number of detected call equal or greater than the detection threshold yields precision ($P_{threshold}$) and recall ($R_{threshold}$) values that maximise the F-score $F_{threshold}$. For comparison, the precision ($P_{original}$) and recall ($R_{original}$) values without threshold are shown as well.

Species/call	$P_{original}$	$R_{original}$	Detection threshold	$P_{threshold}$	$R_{threshold}$	$F_{threshold}$
Sperm whales	0.43	0.66	2	0.50	0.52	0.50
Pilot whale whistles	0.64	0.52	1	0.64	0.52	0.61
Dolphin whistles	0.66	0.50	1	0.66	0.50	0.62
Delphinid clicks	0.59	0.74	7	0.85	0.46	0.73
Cuvier's beaked whales	0.81	0.76	1	0.81	0.76	0.80
Hector's dolphins	0.26	1.00	11	0.97	0.60	0.86
UnkBkd38	0.12	1.00	109	0.93	0.33	0.68
UnkBkd50	0.66	1.00	2	0.79	0.88	0.81
Blue whales (NZ)	0.19	0.87	5	0.52	0.26	0.44
Blue whales (Antarctic)	0.07	0.45	7	0.44	0.27	0.39
Humpback whales	0.83	0.56	4	0.96	0.47	0.80

3.2.2. Odontocetes

Beaked Whales

Three distinct beaked whale click types were recorded. One belonged to Cuvier's beaked whales (Zimmer et al. 2005). The other two, with peak frequencies respectively centred around ~38 and 55 kHz, have been targeted by detectors developed using "template" signals extracted from the data. Suggestions regarding the potential source of each of these signals are discussed in Section 4.2.1.

3.2.2.1.

3.2.2.1.1. Cuvier's Beaked Whales

Cuvier's beaked whale clicks (Figure 49) were recorded at stns 5, 6, and 7 on 67 to 74% of recording days (Table 21). Automated detections suggest a slightly higher occurrence of that species at stn 5. The manual and automated detection time series do not indicate any seasonal variations in occurrence of Cuvier's beaked whale east of Cook Strait during the recording period (Figure 50 and Figure 51).

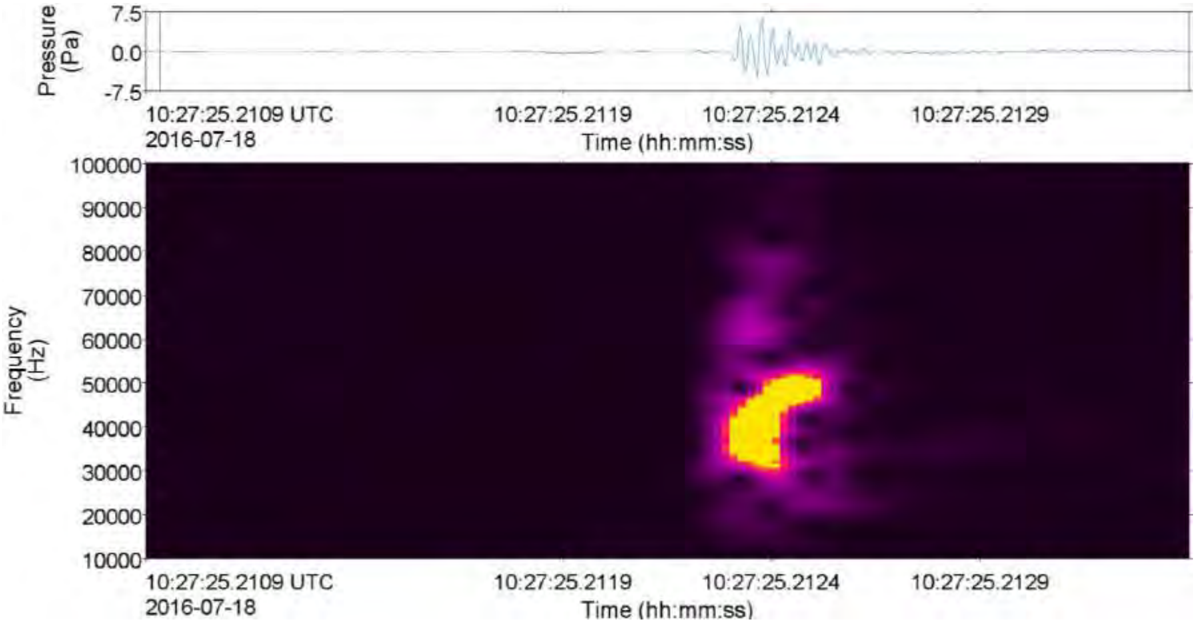

Figure 49. Spectrogram of a Cuvier's beaked whale click recorded at stn 6 on 18 Jul 2016. (488 Hz frequency resolution, 0.26 ms time window, 0.02 ms time step, Hamming window).

Table 21. Cuvier's beaked whale clicks: Summary of automated detections.

Station	Deployment	First detection	Last detection	Record end	Number of detection days	Days with detections (%)	Number of detections
Stn 5	6 Jun	7 Jun	21 Dec	21 Dec	147	73.9	1641
Stn 6	6 Jun	8 Jun	18 Dec	21 Dec	134	67	1364
Stn 7	5 Jun	6 Jun	20 Dec	21 Dec	133	66.5	1218

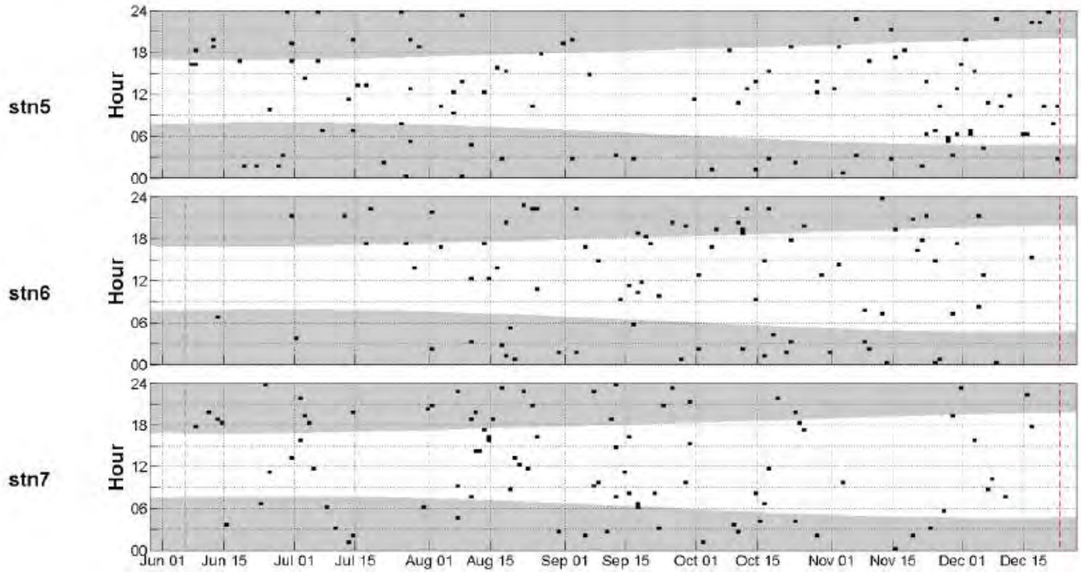

Figure 50. Daily and hourly distribution of manual detections of Cuvier's beaked whale clicks at stns 5, 6, and 7 from 5 Jun to 21 Dec 2016. The grey areas show hours of darkness. The red dashed lines show the deployment and retrieval times. One percent was manually analysed.

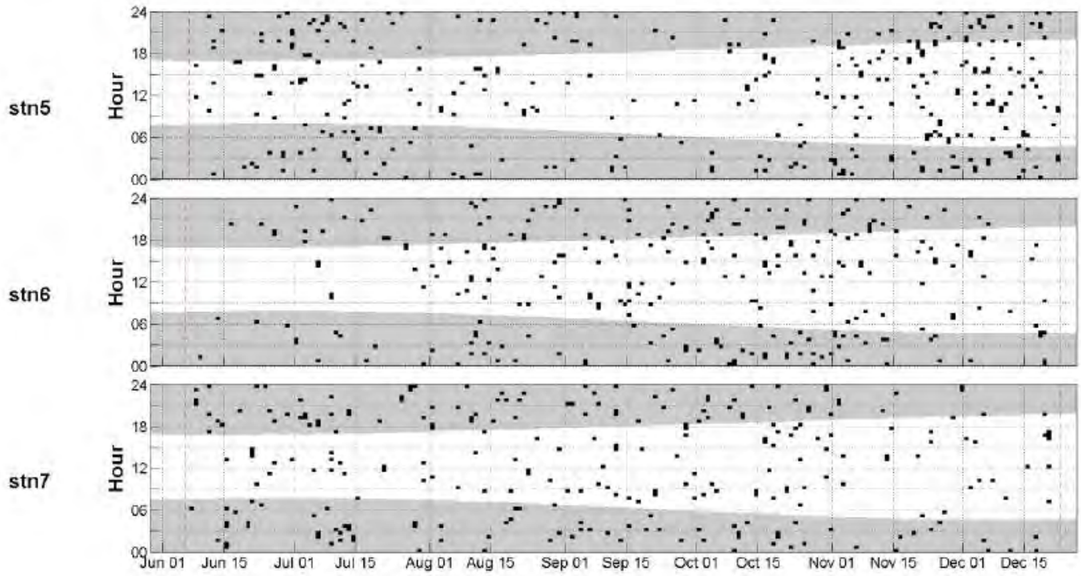

Figure 51. Daily and hourly occurrence of automatically detected Cuvier's beaked whale clicks at stns 5, 6, and 7 from 5 Jun to 21 Dec 2016. Shaded areas indicate periods of darkness. The red dashed lines indicate AMAR deployment and retrieval dates.

3.2.2.1.2. Unknown Beaked Whale 38 kHz (UnkBkd38)

The detector built to target these signals (Figure 52) performed poorly, possibly as the result of the overlap in peak/dominant frequencies with Cuvier's beaked whale clicks. The high threshold required to ensure acceptable detector performance yielded only 11 automated detections for the three deep stations combined (stns 5, 6, and 7). Therefore, the occurrence of the species producing these signals is assessed using manually validated calls (Figure 53). We recorded these clicks once at stn 5 and over 13 and 16 days at stns 7 and 6, respectively. Although a seasonal trend is difficult to detect considering the scarcity of the detections, it is worth noting that 71% of these signals were recorded after 1 Oct 2016.

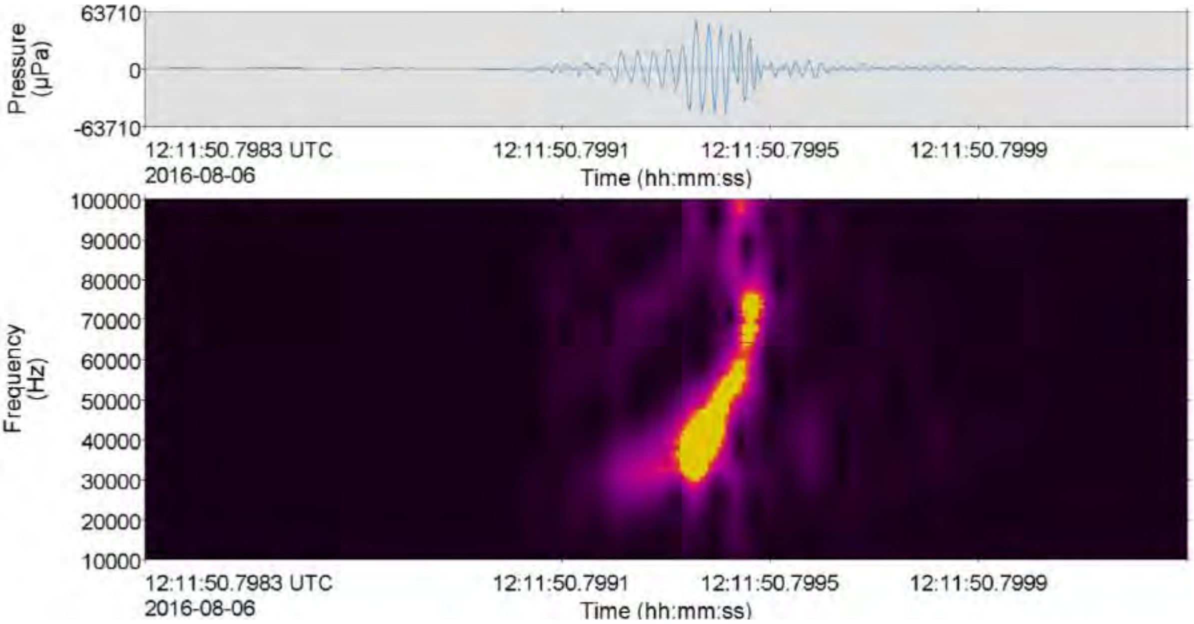

Figure 52. Spectrogram of an unknown UnkBkd38click recorded at stn 6 on 6 Aug 2016 (488 Hz frequency resolution, 0.1 ms time window, 0.01 ms time step, Hamming window). The window length is 2 ms.

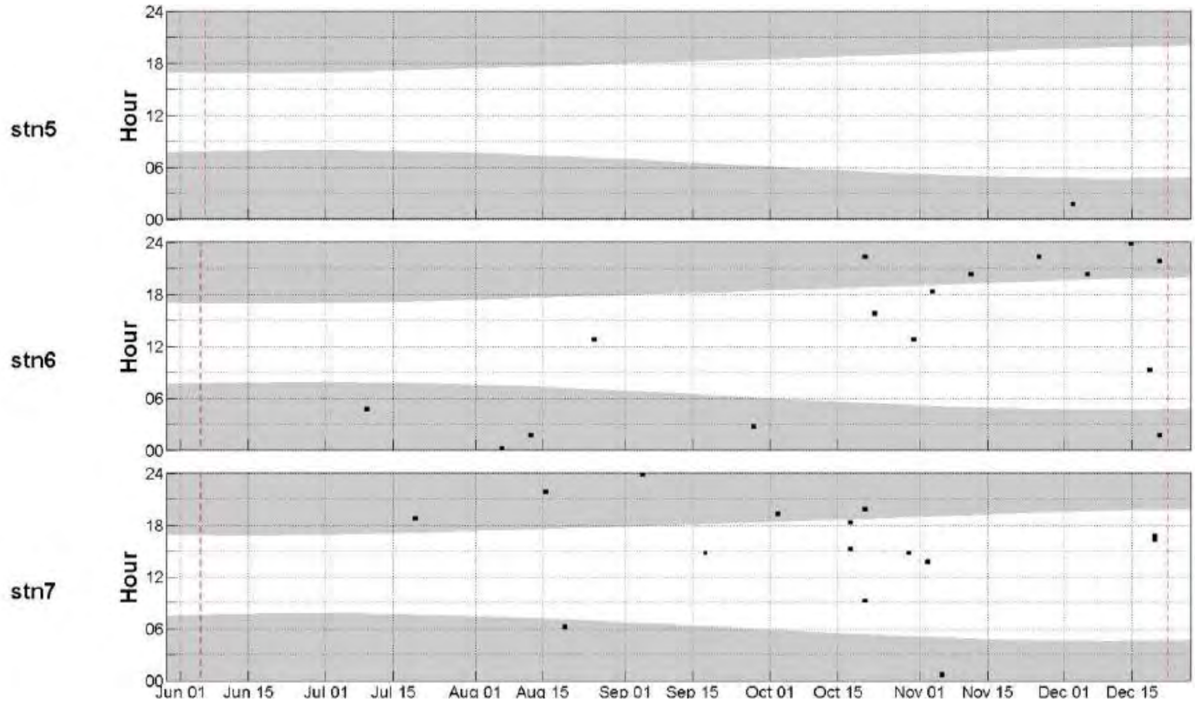

Figure 53. Daily and hourly distribution of manual detections of unkBkd38 clicks at stns 5, 6, and 7 from 5 Jun to 21 Dec 2016. The grey areas show hours of darkness. The red dashed lines show the deployment and retrieval times. One percent was manually analysed.

3.2.2.1.3. Unknown Beaked Whale 55 kHz (UnkBkd55)

The detector developed to target the unknown beaked whale click centred around 55 kHz (Figure 54) performed reasonably well, allowing us to use automated detections to assess the acoustic occurrence of these signals, which provided results consistent with the manual detections (Figure 55 and Figure 56). Stn 7 had the highest number of detections, almost three times higher than stn 6 (Table 22). Detections were scarce before August, peaked from August to November, and declined past mid-Nov.

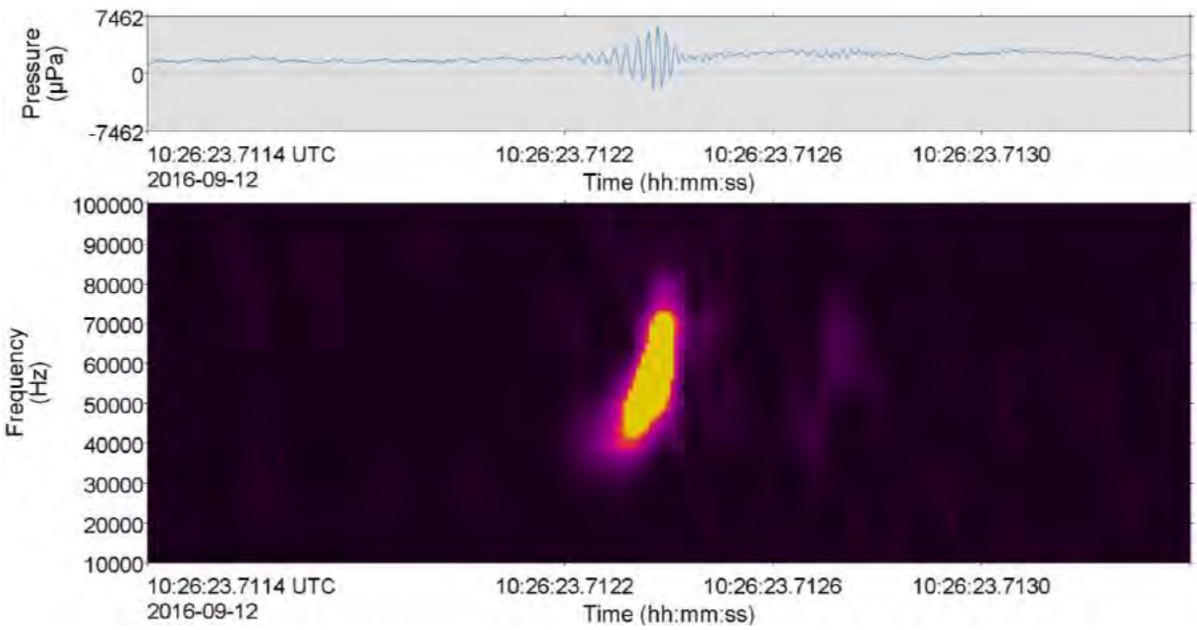

Figure 54. Spectrogram of a click from the unknown UnkBkd55recorded at stn 5 on 12 Sep 2016 (488 Hz frequency resolution, 0.1 ms time window, 0.01 ms time step, Hamming window). The window length is 2 ms.

Table 22. Unknown beaked whale click (55 kHz): Summary of automated detections.

Station	Deployment	First detection	Last detection	Record end	Number of detection days	Days with detections (%)	Number of detections
stn 5	6 Jun	11 Jun	17 Dec	21 Dec	16	8	222
stn 6	6 Jun	6 Aug	18 Dec	21 Dec	10	5	100
stn 7	5 Jun	19 Jun	20 Dec	21 Dec	23	11.5	292

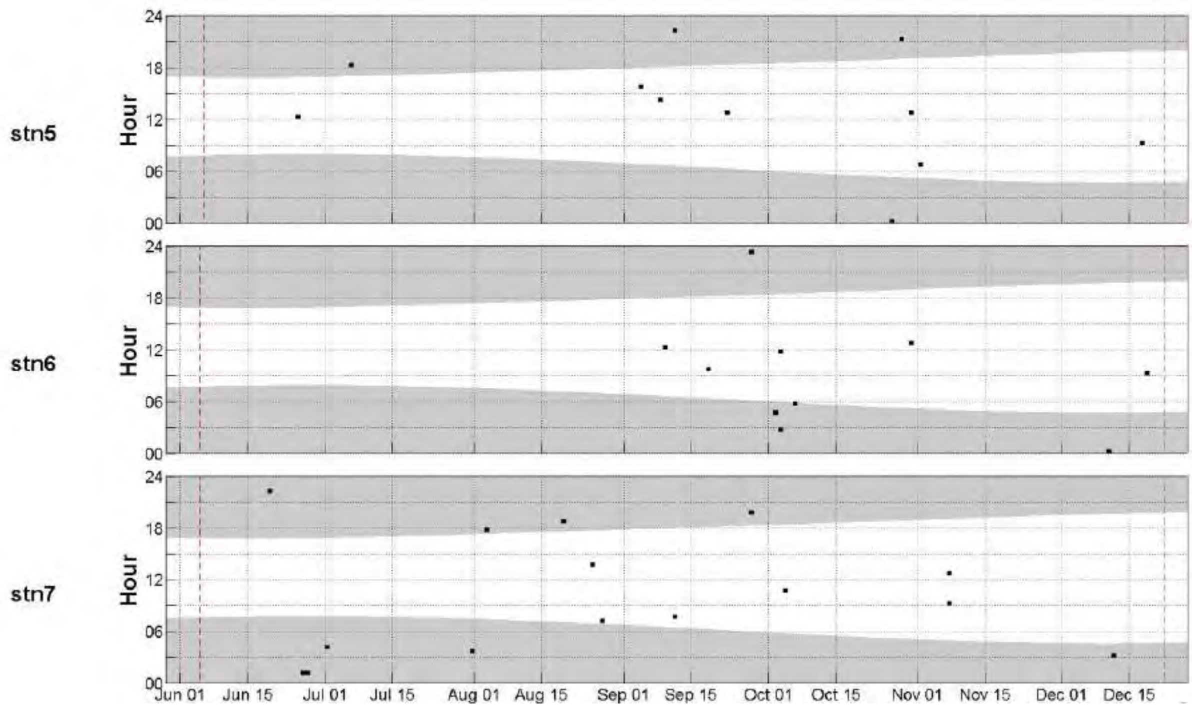

Figure 55. Daily and hourly distribution of manual detections of unkBkd55 clicks at stns 5, 6, and 7 from 5 Jun to 21 Dec 2016. The grey areas show hours of darkness. The red dashed lines show the deployment and retrieval times. One percent was manually analysed.

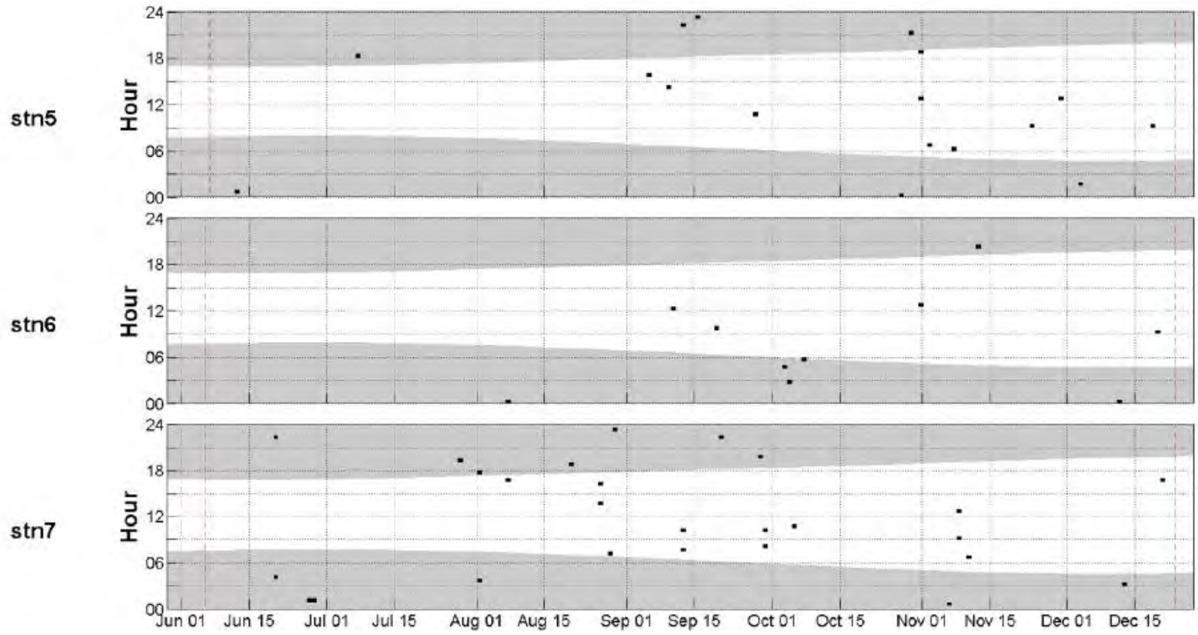

Figure 56. Daily and hourly distribution of automated detections of unkBkd55 clicks at stns 5, 6, and 7 from 5 Jun to 21 Dec 2016. The grey areas show hours of darkness. The red dashed lines show the deployment and retrieval times.

3.2.2.2. Delphinids

3.2.2.2.1. Hector's Dolphins

Hector's dolphin clicks (Dawson and Thorpe 1990) (Figure 57) were only detected at stn 1. Automated detections occurred on 57 days (38.5% of recording days). Manual and automated detections (Figure 58 and Figure 59) both peaked between the start of the recording period (mid-July) and mid-August and later from late October to early November. Detections were scarce between or after these periods.

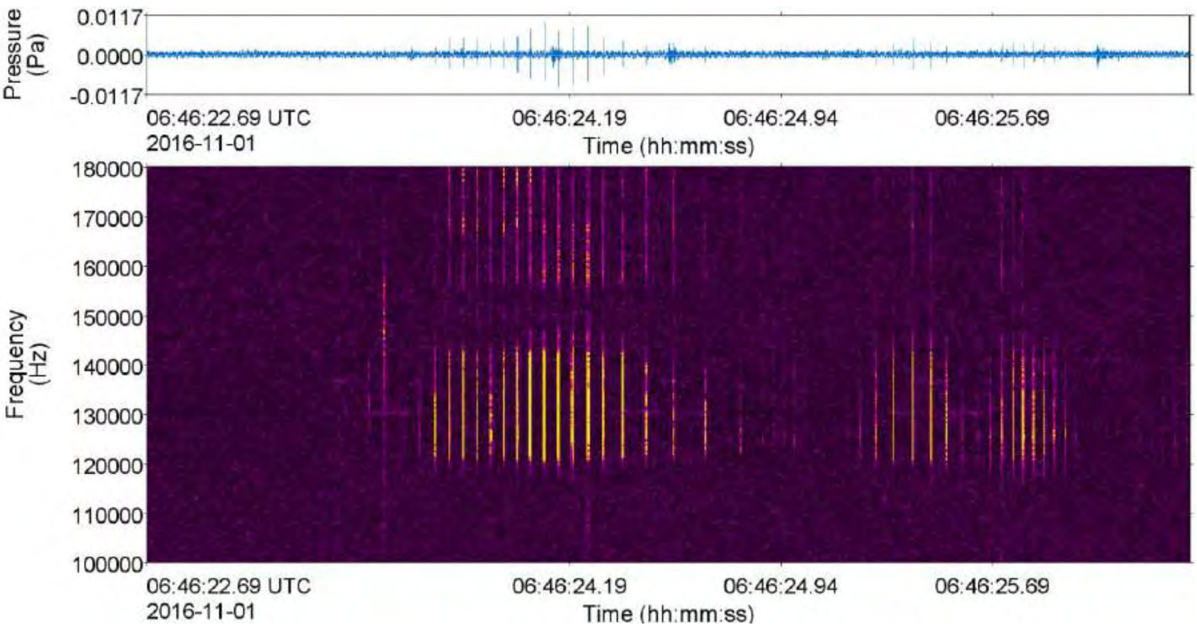

Figure 57. Spectrogram of Hector's dolphin click train recorded at stn 1 on 1 Nov 2016 (46 Hz frequency resolution, 0.01 s time window, 0.005 s time step, Hamming window).

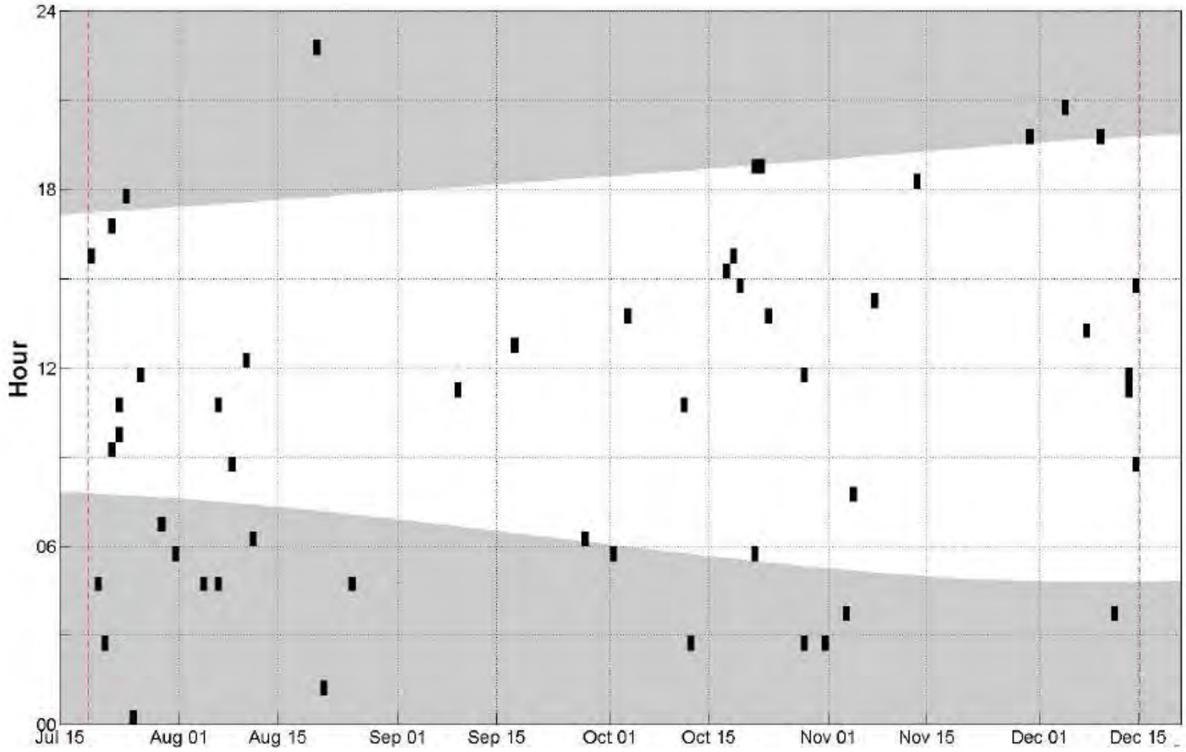

Figure 58. Daily and hourly occurrence of manually detected Hector's dolphin clicks recorded at stn 1 from 20 Jul to 15 Dec 2016. Shaded areas indicate periods of darkness. The red dashed lines indicate AMAR deployment and retrieval dates. One percent was manually analysed.

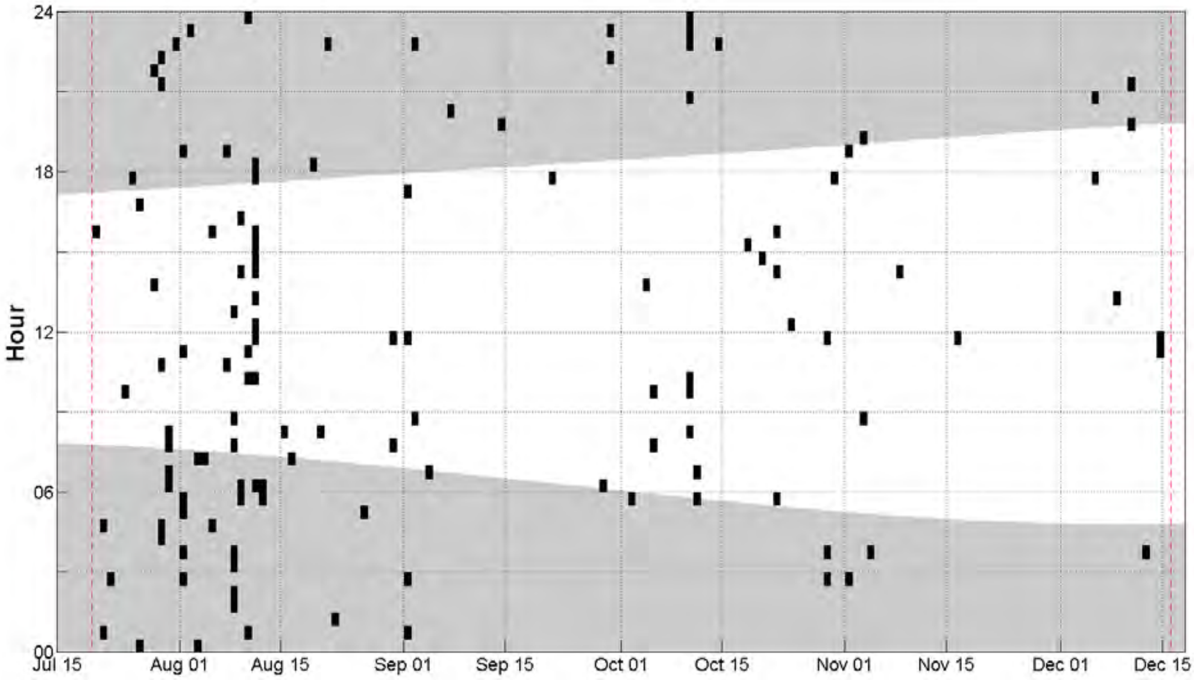

Figure 59. Daily and hourly occurrence of automatically detected Hector's dolphin clicks recorded at stn 1 from 20 Jul to 15 Dec 2016. Shaded areas indicate periods of darkness. The red dashed lines indicate AMAR deployment and retrieval dates.

3.2.2.2.2. *Pilot Whales (Tonal Signals)*

Pilot whale whistles (Figure 60) and other tonal signals (Rendell et al. 1999, Nemiroff and Whitehead 2009) were automatically detected at stns 2, 5, 6, and 7. Stn 2 had the lowest number of detection days, but the second highest number of automated detections. Pilot whale detections were highest at stn 7, detections occurring on 52% of recording days (Table 23). Detections at stn 7 were also the most evenly distributed across the recording period. Most detections at stn 2 occurred after mid-October (Figure 61 and Figure 62).

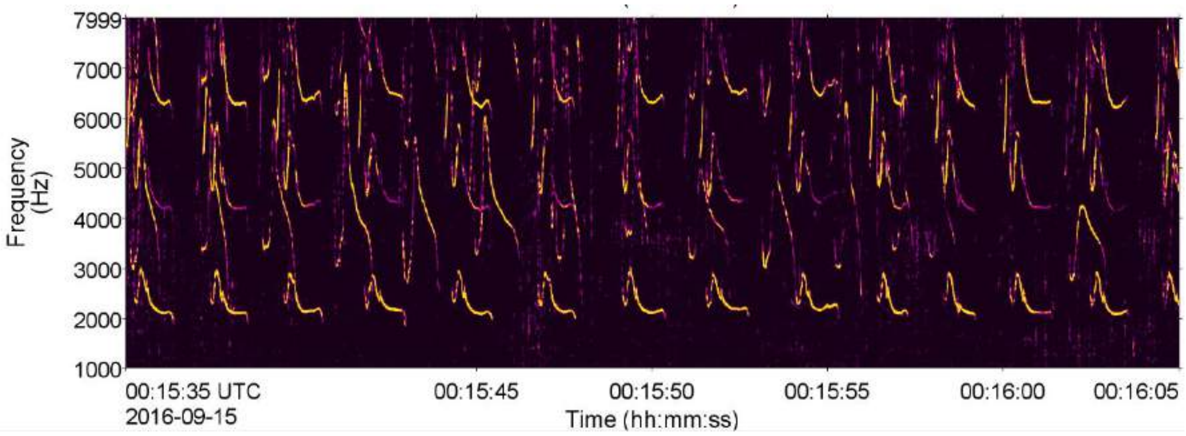

Figure 60. Spectrogram of pilot whale calls recorded at stn 7 on 15 Sep 2016 (4 Hz frequency resolution, 0.05 s time window, 0.01 s time step, Hamming window).

Table 23. Pilot whale whistles: Summary of automated detections

Station	Deployment	First detection	Last detection	Record end	Number of detection days	Days with detections (%)	Number of detections
stn 2	4 Jun	12 Jun	20 Dec	20 Dec	46	23	1190
stn 5	6 Jun	11 Jun	16 Dec	21 Dec	62	31	872
stn 6	6 Jun	6 Jun	20 Dec	21 Dec	61	30.5	499
stn 7	5 Jun	6 Jun	19 Dec	21 Dec	104	52	1708

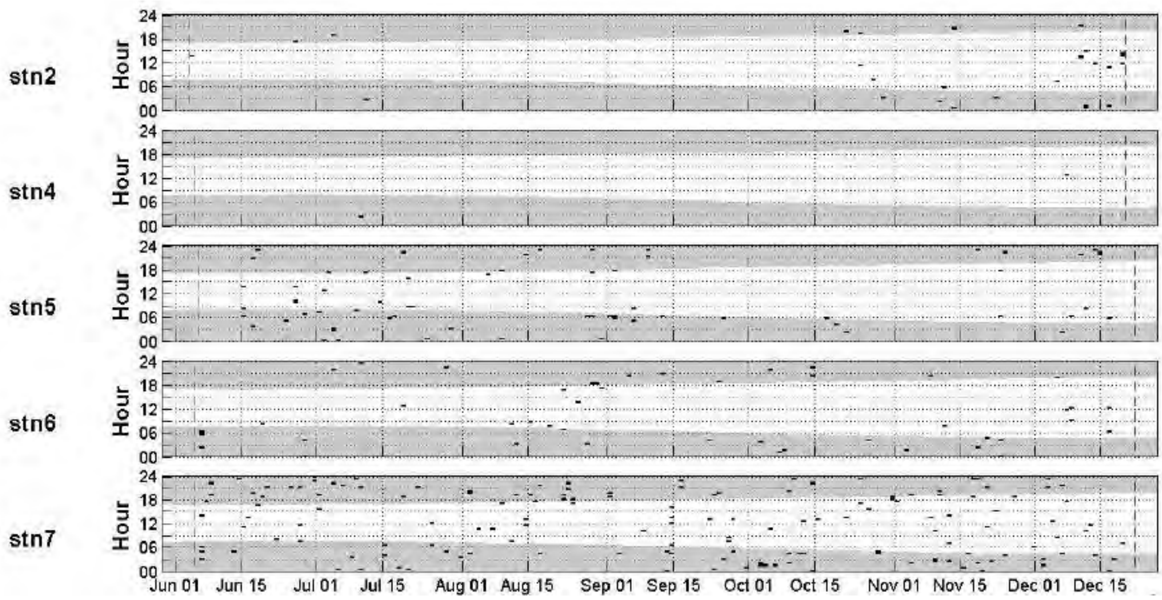

Figure 61. Daily and hourly occurrence of manually detected pilot whale whistles recorded at stns 2, 4, 5, 6, and 7 from 5 Jun to 21 Dec 2016. Shaded areas indicate periods of darkness. The red dashed lines indicate AMAR deployment and retrieval dates. One percent was manually analysed.

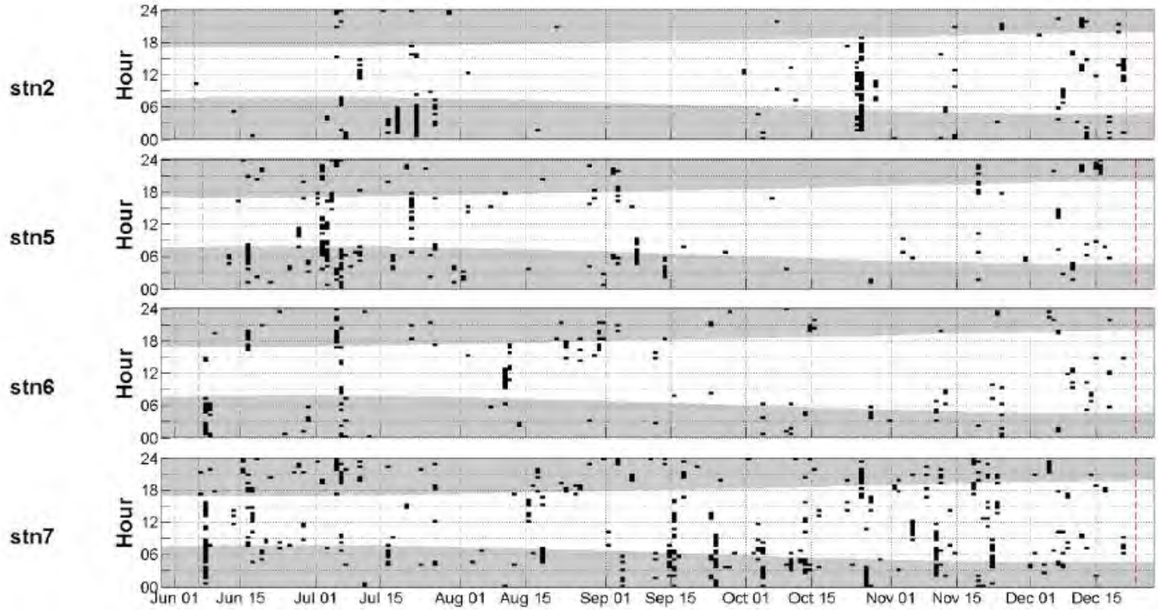

Figure 62. Daily and hourly occurrence of automatically detected pilot whale whistles recorded at stns 2, 5, 6, and 7 from 5 Jun to 21 Dec 2016. Shaded areas indicate periods of darkness. The red dashed lines indicate AMAR deployment and retrieval dates.

3.2.2.2.3. Unidentified Dolphins (Tonal Signals)

Automated detections of whistles produced by unidentified dolphins (Rendell et al. 1999, Oswald et al. 2003) (Figure 63) were most common at stn 1 and least common at stn 2 (Table 24). Manual detections were in good agreement with the automated detections, except at stn 1, where a closer evaluation of the data revealed that chain noise (presumably from a nearby mooring) was triggering the dolphin whistle detector. Therefore, the high detection count at stn 1 is to be interpreted with caution since the actual contribution of true dolphin whistles to the detection results is unknown. We consider the combined manual detections of dolphin whistles (Figure 64) and delphinid clicks (Figure 67) to provide a more accurate and conservative assessment of dolphin occurrence at stn 1. Excluding stn 1, stns 3 and 6 had the highest and similar number of automated detections (Table 24), despite large differences in the number of detections days. We noted a strong seasonal pattern of occurrence at stn 2 and, to a lesser extent, at stn 3, with detections restricted to the beginning and end of the recording period. Detections at stns 5 and 6 were generally more common in the first half of the study, and more evenly distributed at stn 7 (Figure 64 and Figure 65).

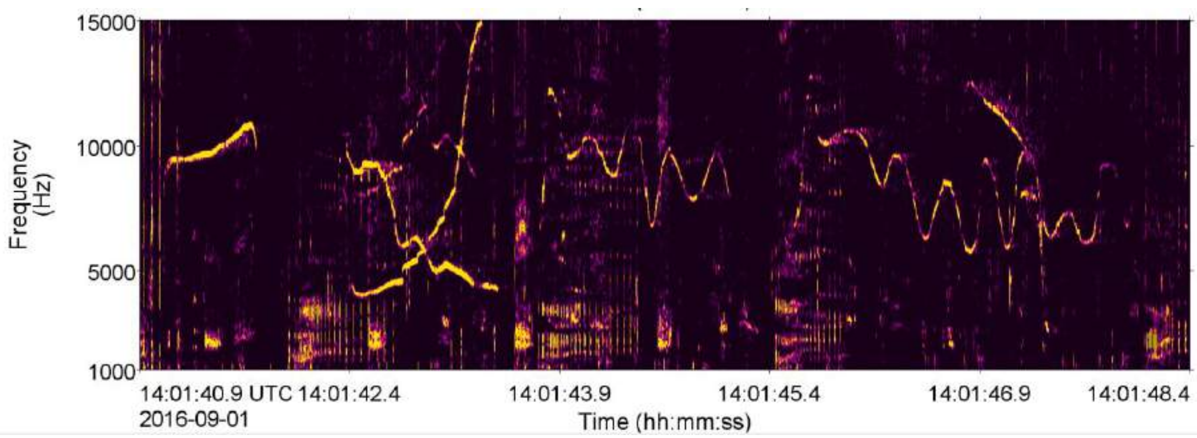

Figure 63. Spectrogram of unidentified dolphin whistles recorded at stn 1 on 1 Sep 2016 (92 Hz frequency resolution, 0.001 s time window, 0.0005 s time step, Hamming window).

Table 24. Unidentified dolphin tonal signal: Summary of automated detections

Station	Deployment	First detection	Last detection	Record end	Number of detection days	Days with detections (%)	Number of detections
stn 1	20 Jul	20 Jul	14 Dec	15 Dec	103	69.1	1300
stn 2	4 Jun	12 Jun	20 Dec	20 Dec	19	9.5	582
stn 3	3 Jun	5 Jun	19 Dec	19 Dec	57	28.5	1146
stn 5	6 Jun	11 Jun	16 Dec	21 Dec	39	19.5	301
stn 6	6 Jun	6 Jun	20 Dec	21 Dec	39	19.5	1113
stn 7	5 Jun	6 Jun	19 Dec	21 Dec	68	34	539

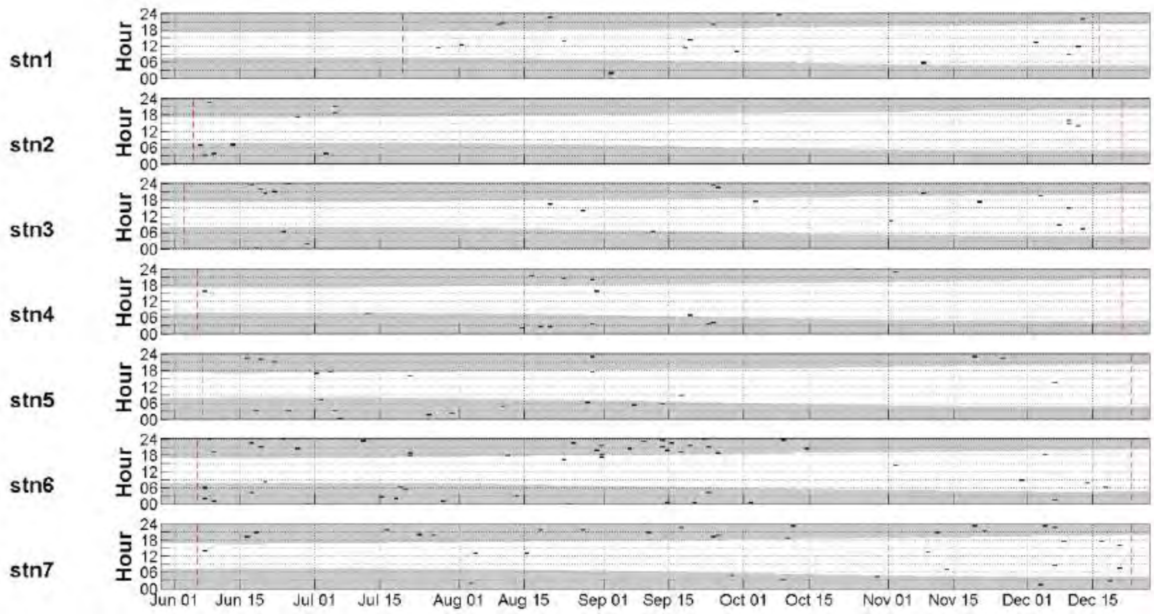

Figure 64. Daily and hourly occurrence of manually detected unidentified dolphin whistles recorded at all stations from 5 Jun to 21 Dec 2016. Shaded areas indicate periods of darkness. The red dashed lines indicate AMAR deployment and retrieval dates. One percent was manually analysed.

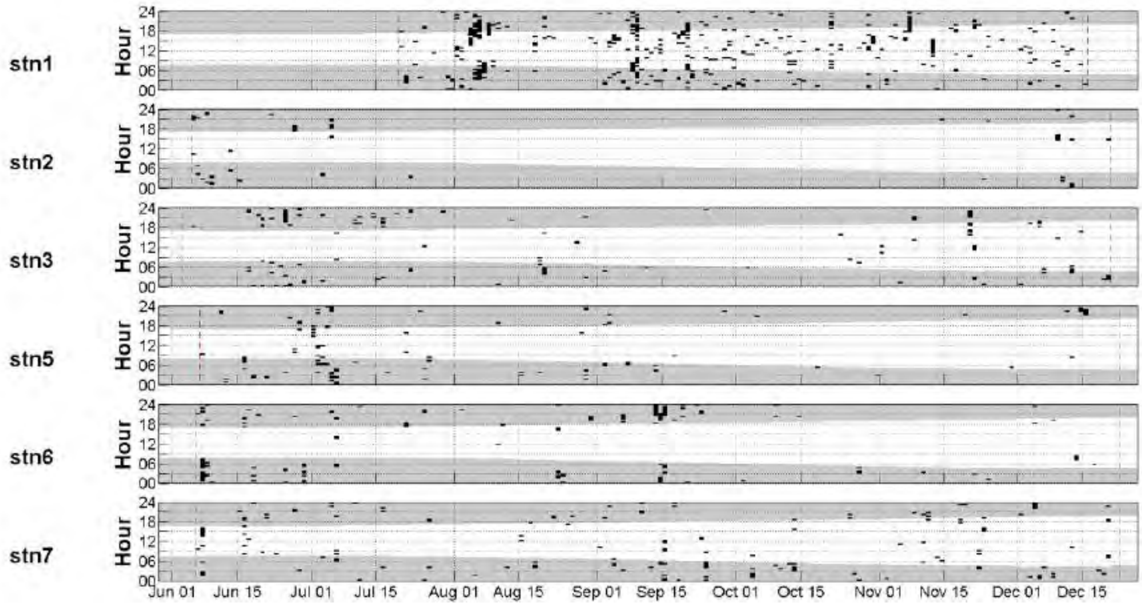

Figure 65. Daily and hourly occurrence of automatically detected unidentified dolphin whistles recorded at stns 1, 2, 3, 5, 6, and 7 from 5 Jun to 21 Dec 2016. Shaded areas indicate periods of darkness. The red dashed lines indicate AMAR deployment and retrieval dates.

3.2.2.3. Delphinid Clicks

Echolocation clicks produced by unidentified delphinids (Au and Wursig 2004, Eskesen et al. 2011) (Figure 66) were recorded at all stations. The high click detection counts and 100% daily occurrence at stn 1 (Table 25) do not match the manual detections (Figure 67 and Figure 68) and lack the diel pattern observed at other stations and typical of delphinid clicks. As for the dolphin whistles, automated detections at that station were largely induced by noise instead of true delphinid signals. Clicks were detected on 48% of days at stn 2, and on 71 to 84% of days at stns 3–7. Detection counts were highest at stn 7, followed by 5 and 6. Despite relatively a high number of detection days, stn 3 had comparatively few detections (Table 25). Detections occurred fairly evenly across the recording period at stns 5, 6, and 7, but were more pronounced at the beginning and end of the study at stn 2 (Figure 67 and Figure 68).

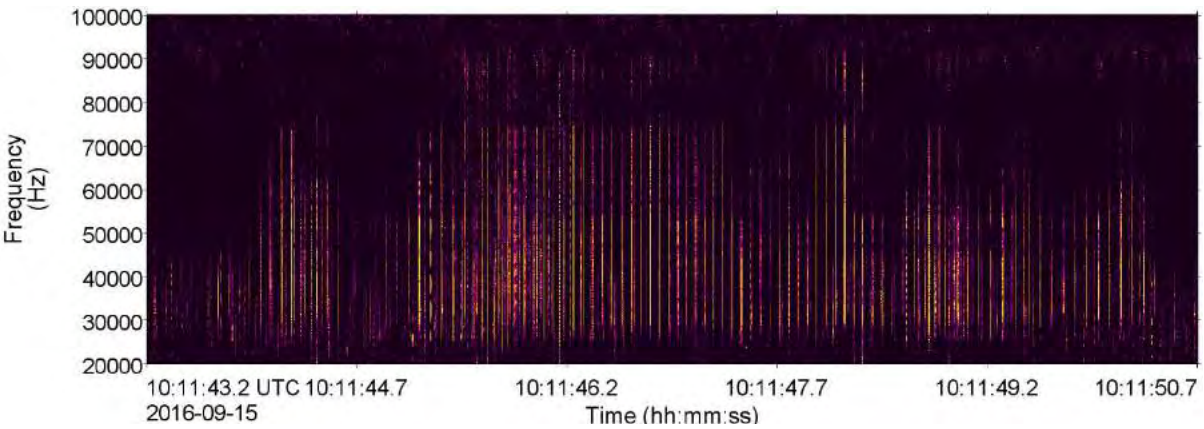

Figure 66. Spectrogram of unidentified delphinid click trains recorded at stn 6 on 15 Sep 2016 (122 Hz frequency resolution, 0.001 s time window, 0.0005 s time step, Hamming window).

Table 25. Delphinid clicks: Summary of automated detections

Station	Deployment	First detection	Last detection	Record end	Number of detection days	Days with detections (%)	Number of detections
stn 1	20 Jul	20 Jul	14 Dec	15 Dec	150	100	210743
stn 2	4 Jun	12 Jun	20 Dec	20 Dec	96	48	40106
stn 3	3 Jun	5 Jun	19 Dec	19 Dec	151	75.5	47403
stn 5	6 Jun	11 Jun	16 Dec	21 Dec	168	84.5	145527
stn 6	6 Jun	6 Jun	20 Dec	21 Dec	142	71	97127
stn 7	5 Jun	6 Jun	19 Dec	21 Dec	161	81	250283

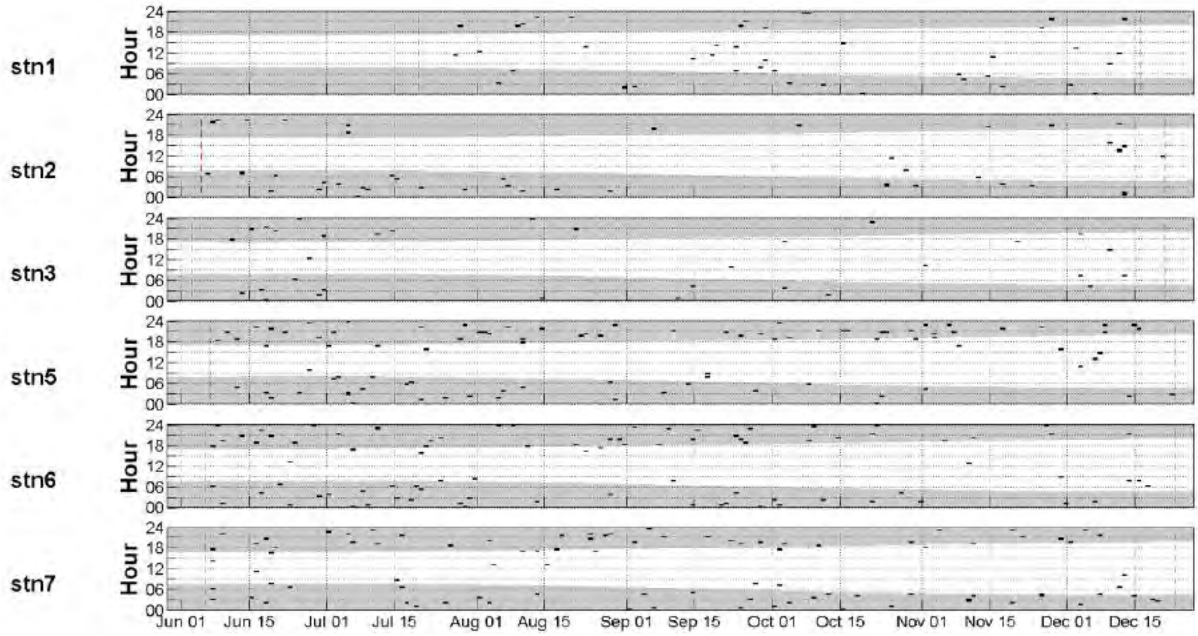

Figure 67. Daily and hourly distribution of manual detections of unidentified delphinid clicks recorded at stns 1, 2, 3, 5, 6, and 7 from 5 Jun to 21 Dec 2016. Shaded areas indicate periods of darkness. The red dashed lines indicate AMAR deployment and retrieval dates. One percent was manually analysed.

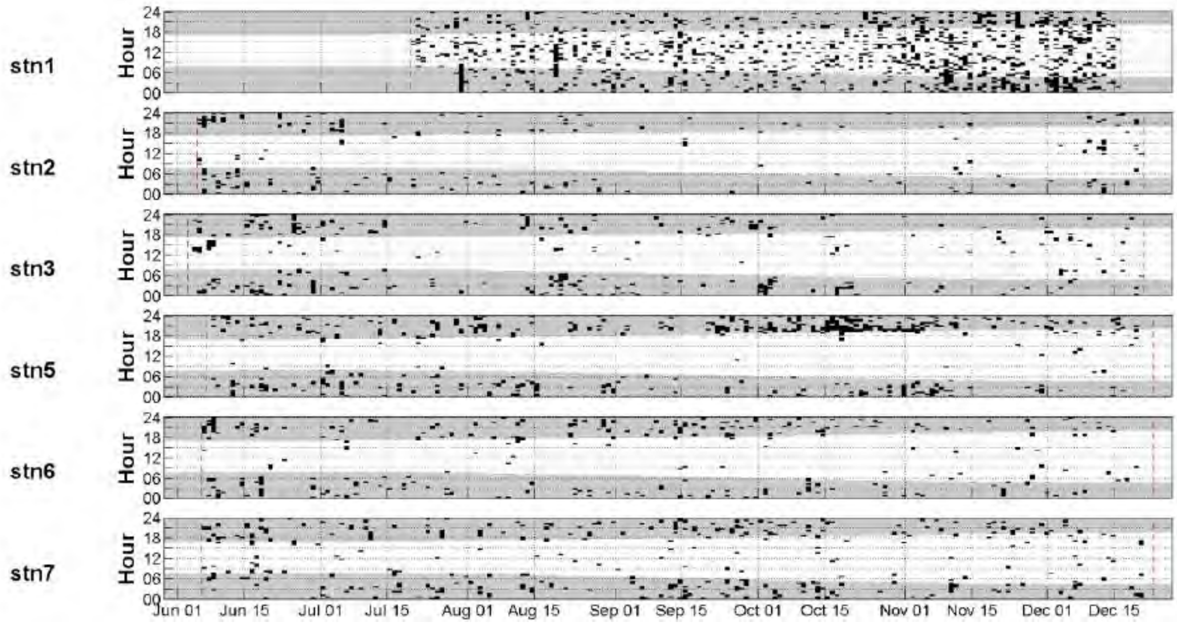

Figure 68. Daily and hourly distribution of automated detections of unidentified delphinid clicks recorded at stns 1, 2, 3, 5, 6, and 7 from 5 Jun to 21 Dec 2016. Shaded areas indicate periods of darkness. The red dashed lines indicate AMAR deployment and retrieval dates.

3.2.2.4. *Sperm Whales*

Sperm whale clicks (Madsen et al. 2002, Mohl et al. 2003) (Figure 69) were automatically detected at stns 3, 5, 6, and 7. Manual detections occurred at these stations plus stn 4. Stn 3 had the highest number of detection days, but the lowest number of detections. Stn 5 recorded clicks on 87% of days and had the highest click detection counts (Table 26). Stns 3 and 5 showed similar temporal patterns of click occurrence, with the bulk of the detections occurring from mid-August to late October and additional detections at the beginning and end of the recording period. In contrast, clicks were detected fairly evenly, though sporadically, throughout the study at stns 6 and 7 (Figure 70 and Figure 71). It is worth noting that the sperm whale click detector performed relatively poorly in comparison to other species, with an F-score of 0.5. Therefore, the automated detections in Figure 71, although in relatively good agreement with manual detections, contain some false detections and should be interpreted with caution.

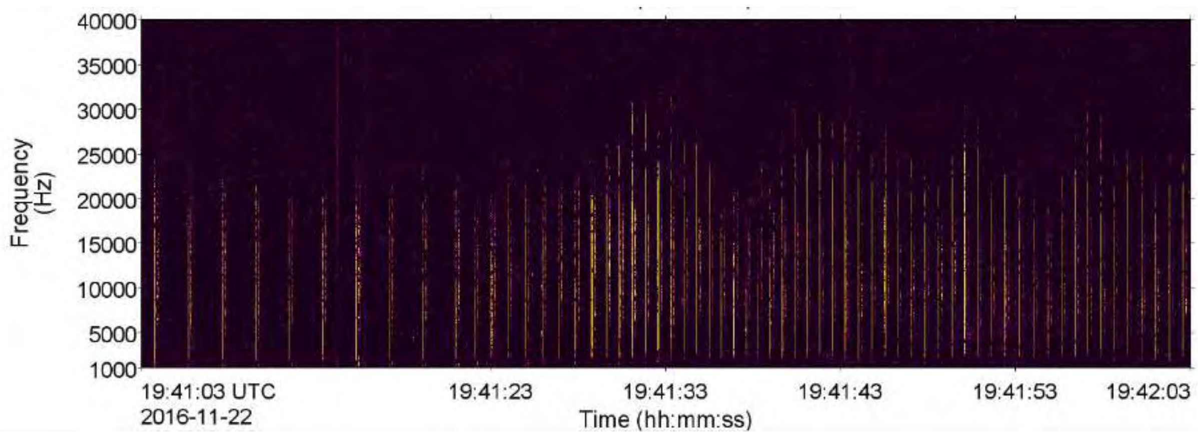

Figure 69. Spectrogram of sperm whale click train recorded at stn 7 on 22 Nov 2016. (122 Hz frequency resolution, 0.001 s time window, 0.0005 s time step, Hamming window).

Table 26. Sperm whale clicks: Summary of automated detections.

Station	Deployment	First detection	Last detection	Record end	Number of detection days	Days with detections (%)	Number of detections
stn 3	3 Jun	5 Jun	19 Dec	19 Dec	190	95	26675
stn 5	6 Jun	11 Jun	16 Dec	21 Dec	173	87	57481
stn 6	6 Jun	6 Jun	20 Dec	21 Dec	136	68	44875
stn 7	5 Jun	6 Jun	19 Dec	21 Dec	147	73.5	44856

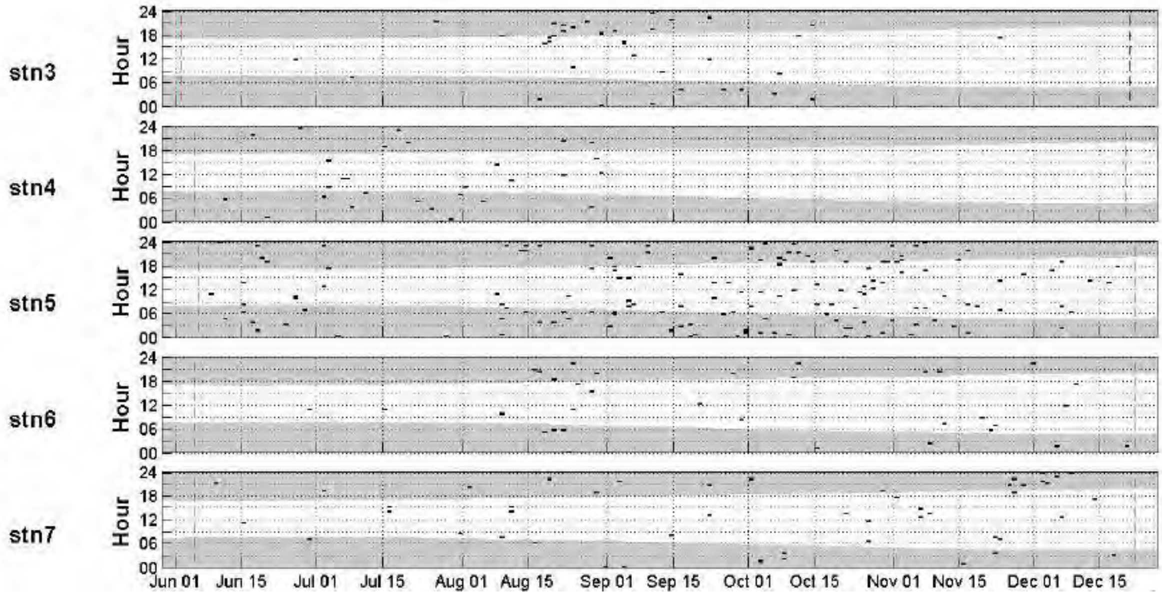

Figure 70. Daily and hourly occurrence of manually detected sperm whale clicks recorded at stns 3, 4, 5, 6, and 7 from 5 Jun to 21 Dec 2016. Shaded areas indicate periods of darkness. The red dashed lines indicate AMAR deployment and retrieval dates. One percent was manually analysed.

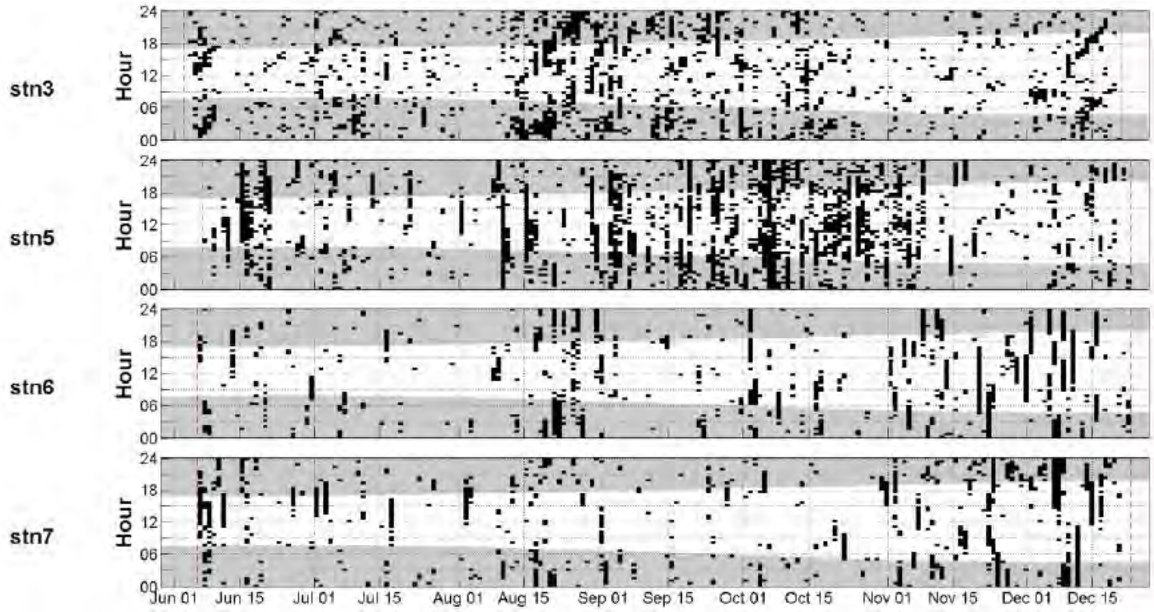

Figure 71. Daily and hourly occurrence of automatically detected sperm whale clicks recorded at stns 3, 5, 6, and 7 from 5 Jun to 21 Dec 2016. Shaded areas indicate periods of darkness. The red dashed lines indicate AMAR deployment and retrieval dates.

3.2.3. Mysticetes

3.2.3.1 *Blue Whales*

Signals from Antarctic (Figure 72) (Sirovic et al. 2004) and New Zealand (Figure 73) (Miller et al. 2014) blue whales were recorded in the data. Audible downsweeps, or D-calls, (Figure 74) (Oleson et al. 2007) were also recorded. The performance of the respective automated detectors was too low to consider their outputs. This was largely the results of vessel activity in the area, and the associated tonals triggering the detectors. Temporal patterns of acoustic occurrence are therefore described based on the manual review of ~1% of sound files. Although the actual number of possible detections is underestimated, the main periods of occurrence are believed to be reliably identified by the manual review. Isolated detections were likely missed.

The New Zealand song type was dominant at stn 2, particularly from June to Aug. Sporadic manual detections resumed after November, although D-calls were more commonly detected during that period. D-calls were also recorded at stn 3 in latter part of the recording period. New Zealand songs were also recorded at stns 3, 5, and 6. The Antarctic song type was detected at stns 2, 5, 6, and 7. Detections at stn 2 were few and isolated. A first period of detections occurred at stns 5, 6, and 7 from mid-June to early July. A second cluster of detections occurred at stn 6 in the second half of August. A third cluster of detections occurred at stns 6 and 7 in late October. The low number of manual detections at stn 4 is attributed to vessel noise masking blue whale calls.

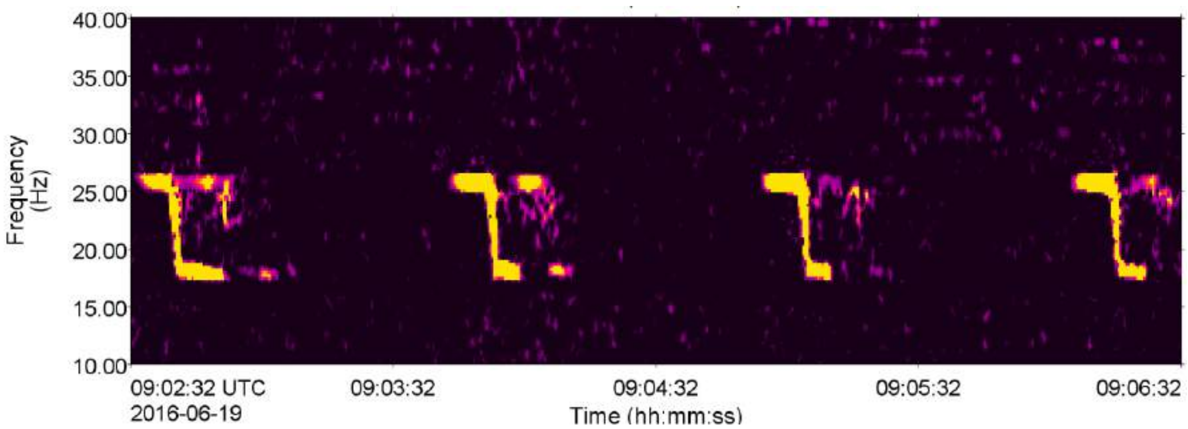

Figure 72. Spectrogram of Antarctic blue whale song notes recorded at stn 6 on 1 Jul 2016. (0.122 Hz frequency resolution, 1 s time window, 0.5 s time step, Hamming window).

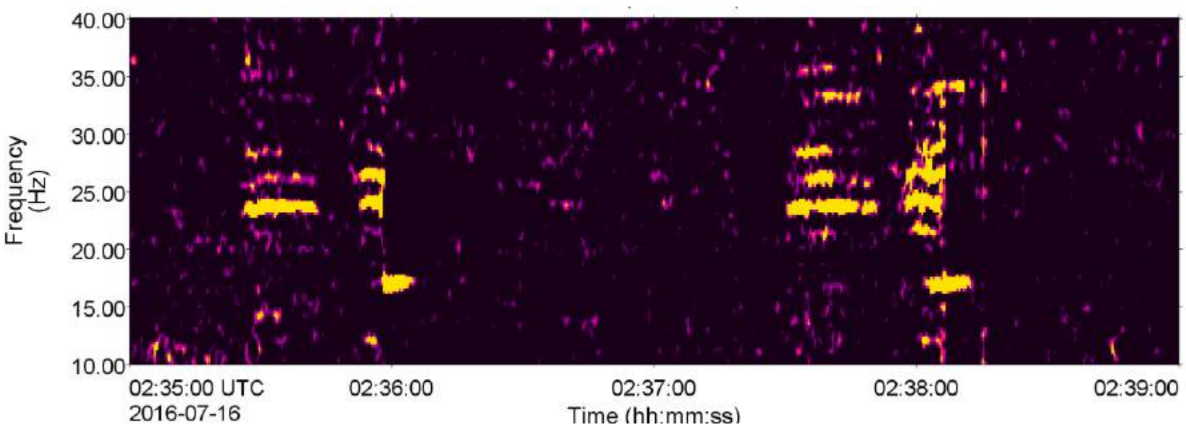

Figure 73. Spectrogram of New Zealand blue whale song notes recorded at stn 2 on 16 Jul 2016. (0.122 Hz frequency resolution, 1 s time window, 0.5 s time step, Hamming window).

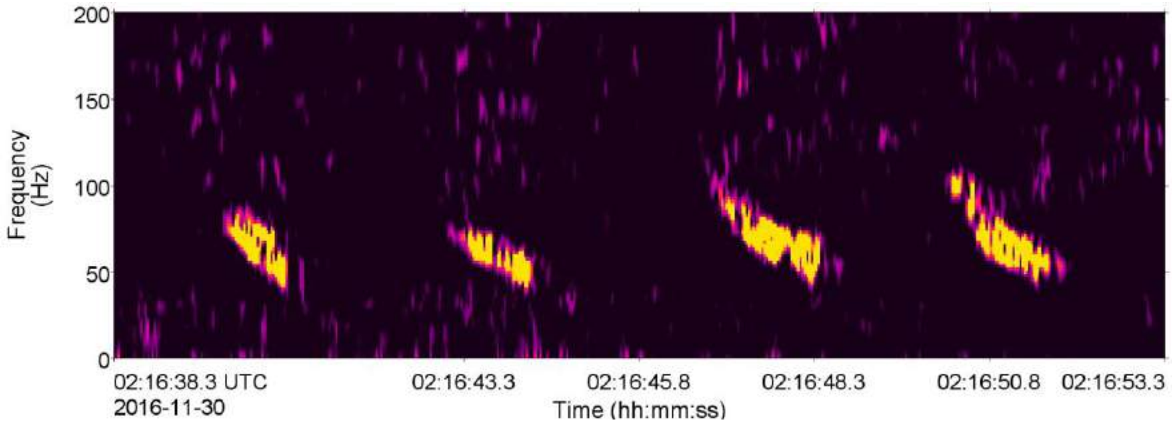

Figure 74. Spectrogram of New Zealand blue whale D-calls recorded at stn 3 on 30 Nov 2016. (2 Hz frequency resolution, 0.128 s time window, 0.032 s time step, Hamming window).

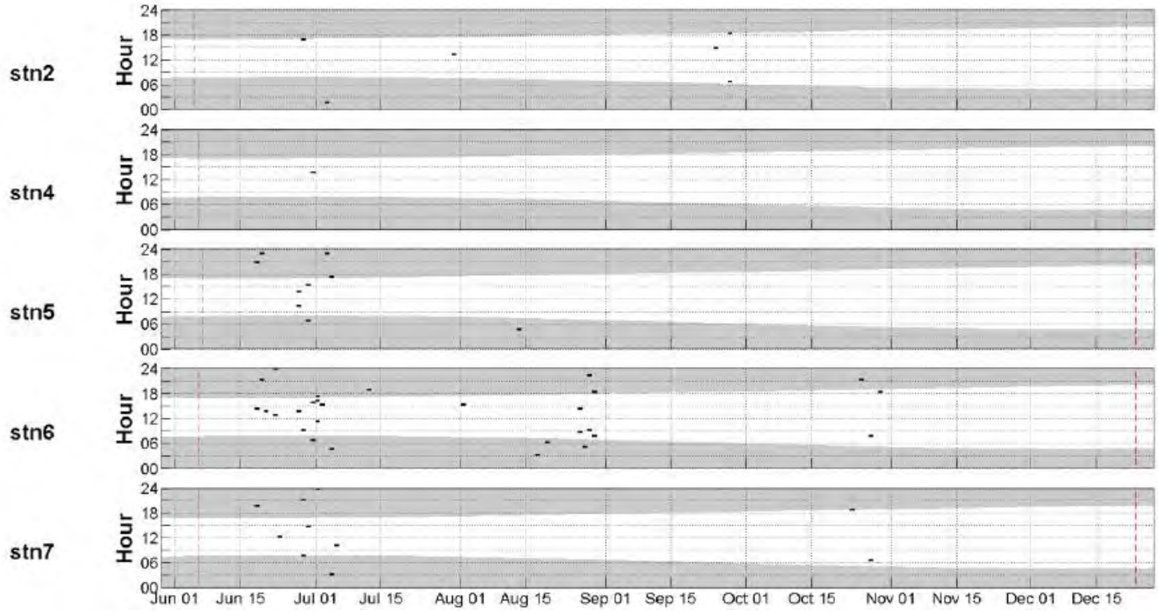

Figure 75. Daily and hourly occurrence of manually detected Antarctic blue whale song note recorded at stns 2, 5, 6, and 7 from 4 Jun to 21 Dec 2016. Shaded areas indicate periods of darkness. The red dashed lines indicate AMAR deployment and retrieval dates. One percent was manually analysed.

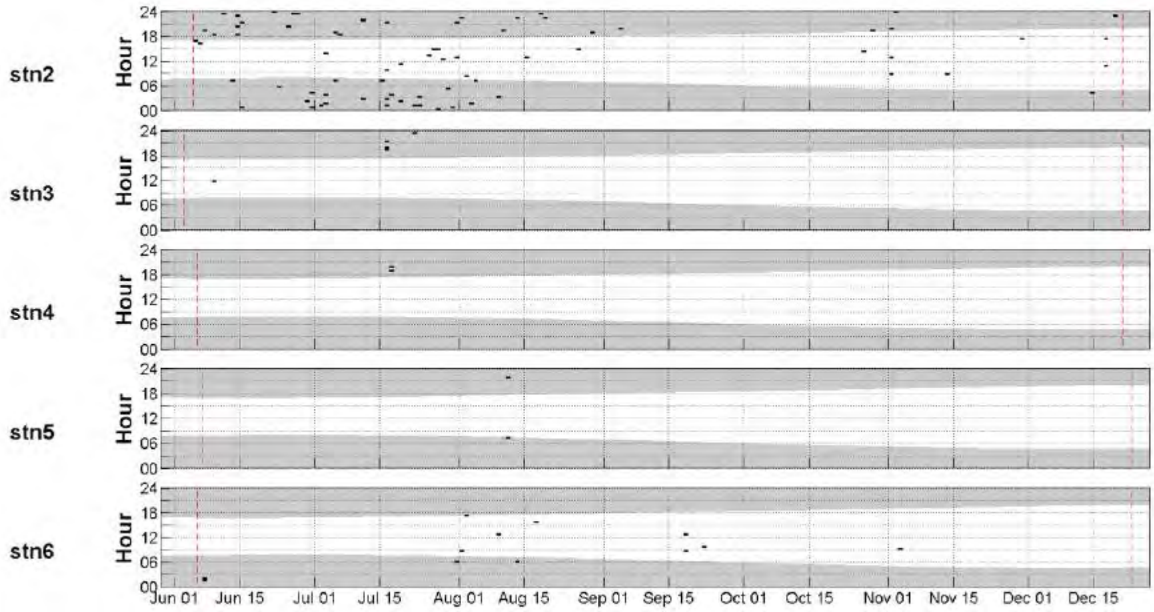

Figure 76. Daily and hourly occurrence of manually detected New Zealand blue whale song notes recorded at stns 2, 3, 5, and 6 from 4 Jun to 21 Dec 2016. Shaded areas indicate periods of darkness. The red dashed lines indicate AMAR deployment and retrieval dates. One percent was manually analysed.

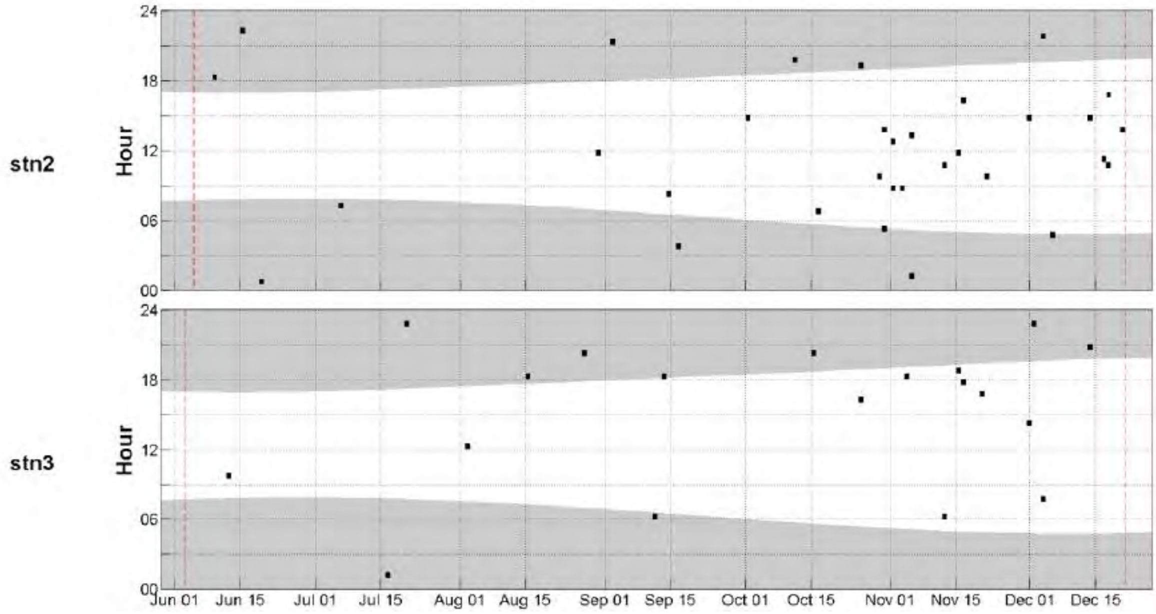

Figure 77. Daily and hourly occurrence of manually detected audible blue whale calls (D-calls) recorded at stns 2 and 3 from 4 Jun to 21 Dec 2016. Shaded areas indicate periods of darkness. The red dashed lines indicate AMAR deployment and retrieval dates. One percent was manually analysed.

3.2.3.2. Humpback Whales

Most humpback whale detections consisted of songs (Payne and McVay 1971, McDonald 2006) (Figure 78). Songs were detected at stns 2, 3, 4, 5, 6, and 7. Stn 2 had the highest number of detections. The other four stations (automated detections at stn4 were excluded) had lower and similar proportions of days with detections, with differed in the number of call detections. Stn 3, nearest to the stn 2, had the highest count after stn 2 and stn 7 the lowest count. Stn 5 and 6 had intermediate detection counts (Table 27). The vast majority of both manual and automated detections occurred between 1 Jul and 5 Aug 2016.

Table 27. Humpback whale tonal calls: Summary of automated detections

Station	Deployment	First detection	Last detection	Record end	Number of detection days	Days with detections (%)	Number of detections
stn 2	4 Jun	12 Jun	20 Dec	20 Dec	69	34.5	51150
stn 3	3 Jun	5 Jun	19 Dec	19 Dec	42	21	13645
stn 5	6 Jun	11 Jun	16 Dec	21 Dec	50	25	6276
stn 6	6 Jun	6 Jun	20 Dec	21 Dec	46	23	6559
stn 7	5 Jun	6 Jun	19 Dec	21 Dec	40	20	836

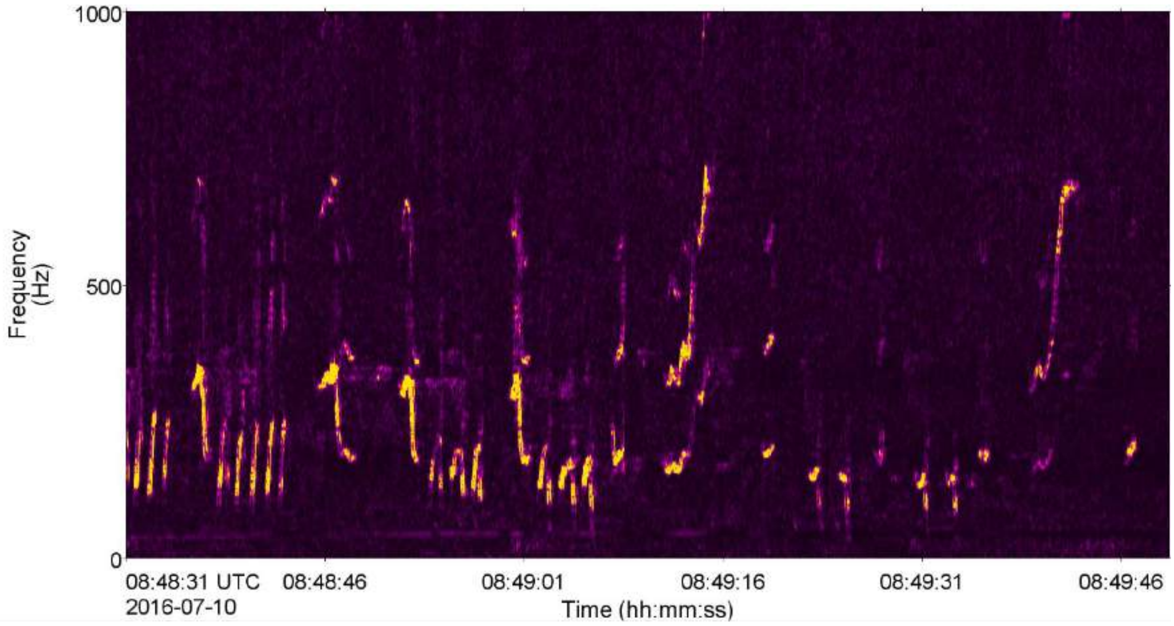

Figure 78. Spectrogram of a humpback whale song segment recorded at stn 3 on 10 Jul 2016 (1 Hz frequency resolution, 0.2 s time window, 0.05 s time step, Hamming window). The window length is 79 s.

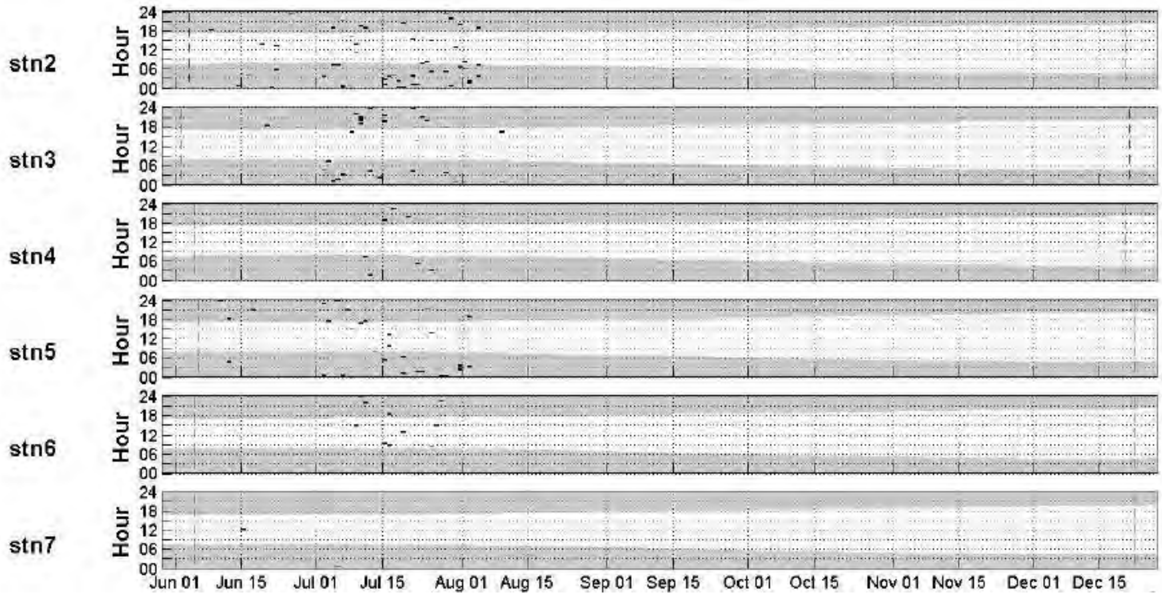

Figure 79. Daily and hourly occurrence of manually detected humpback whale calls recorded at stns 2, 3, 4, 5, 6, and 7 from 5 Jun to 21 Dec 2016. Shaded areas indicate periods of darkness. The red dashed lines indicate AMAR deployment and retrieval dates. One percent was manually analysed.

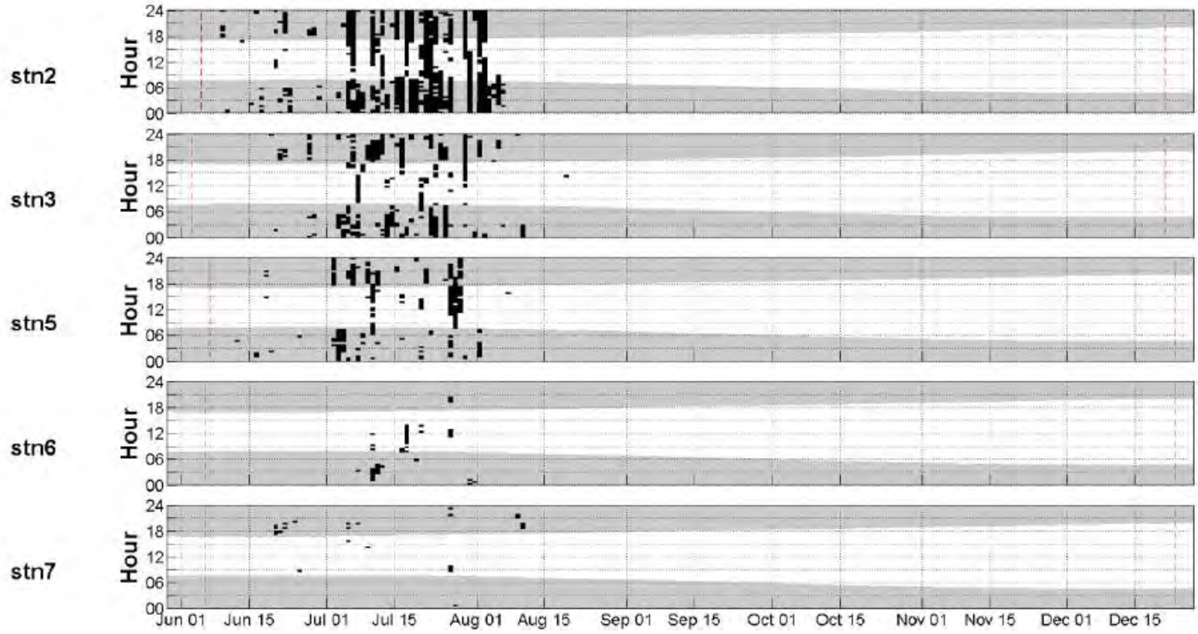

Figure 80. Daily and hourly occurrence of automatically detected humpback whale calls recorded at stns 2, 3, 5, 6, and 7 from 5 Jun to 21 Dec 2016. Shaded areas indicate periods of darkness. The red dashed lines indicate AMAR deployment and retrieval dates.

3.2.3 *Antarctic Minke Whales*

Antarctic minke whale bioduck signals (Risch et al. 2014) (Figure 81) were manually detected stns 2, 3, 4, 5, 6, and 7 (Figure 82). Because these signals were not expected in the data, we did not attempt to develop an automated detector for these calls. Manual detections, although sporadic, were most common at stns 5, 6, and 7. Most calls were recorded between mid-July and mid-September.

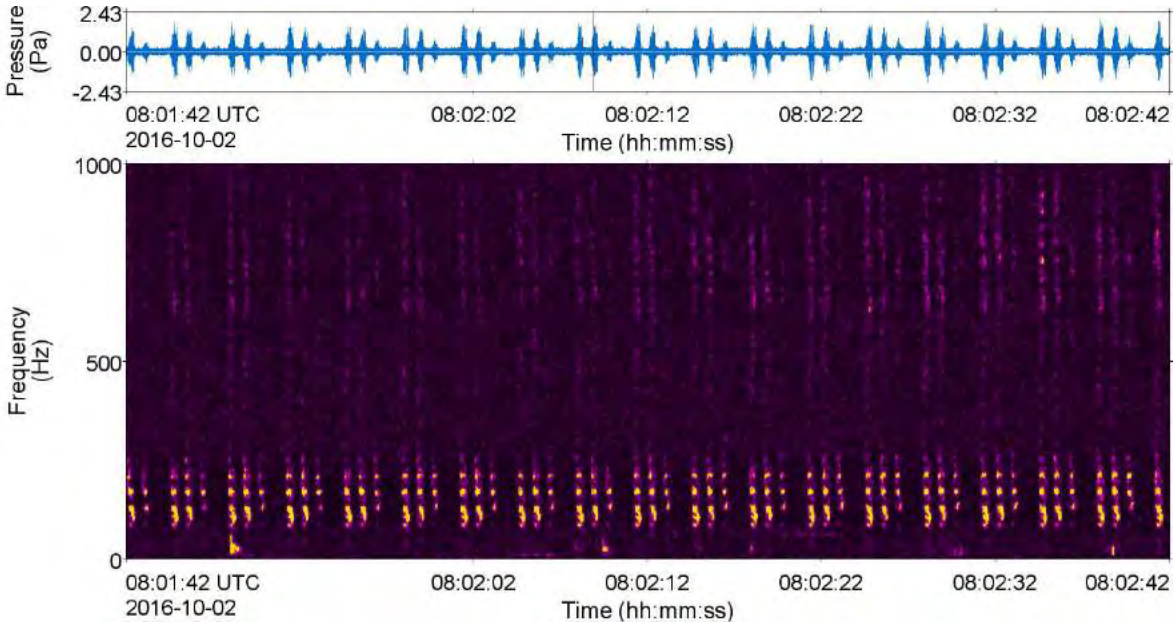

Figure 81. Spectrogram of Antarctic minke whale bioduck calls recorded at stn 2 on 2 Oct 2016 (1 Hz frequency resolution, 0.2 s time window, 0.05 s time step, Hamming window). The window length is 60 s.

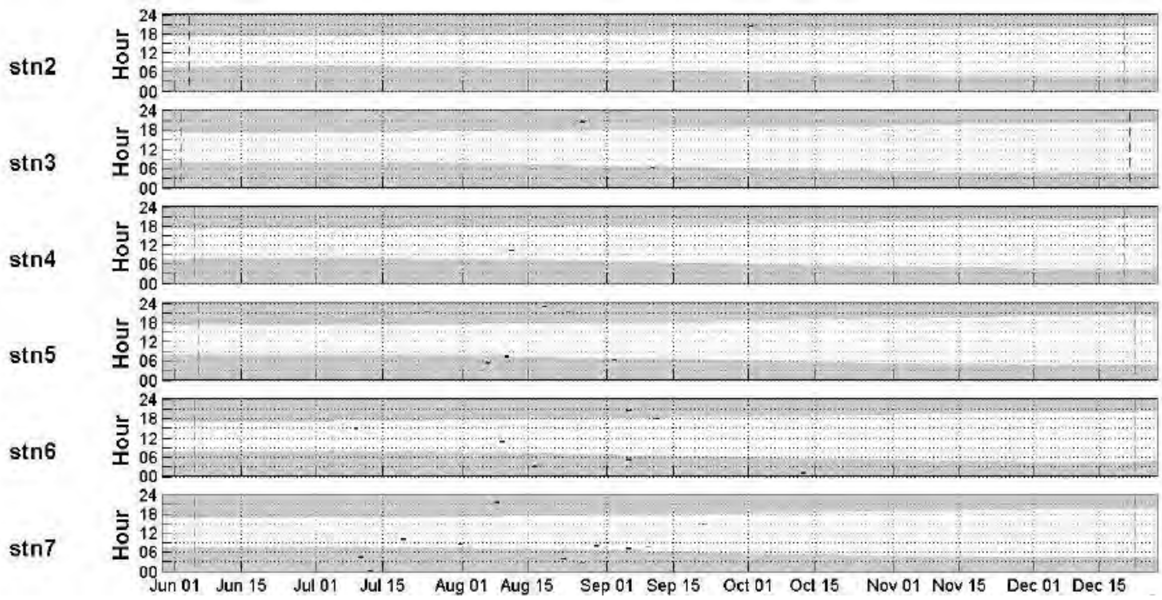

Figure 82. Daily and hourly occurrence of manually detected Antarctic minke whale bioduck calls recorded at stns 2-7 from 5 Jun to 21 Dec 2016. Shaded areas indicate periods of darkness. The red dashed lines indicate AMAR deployment and retrieval dates. One percent was manually analysed.

3.2.3 Southern Right Whales

Southern right whale upcalls (Webster et al. 2016) (Figure 83) were manually detected once over a period of one hour at Stn 3 on 24 Aug 2016. These calls were faint and had not been detected by the automated detector targeting right whale upcalls. All other automated detections proved to be false detections caused by humpback whale calls or noise.

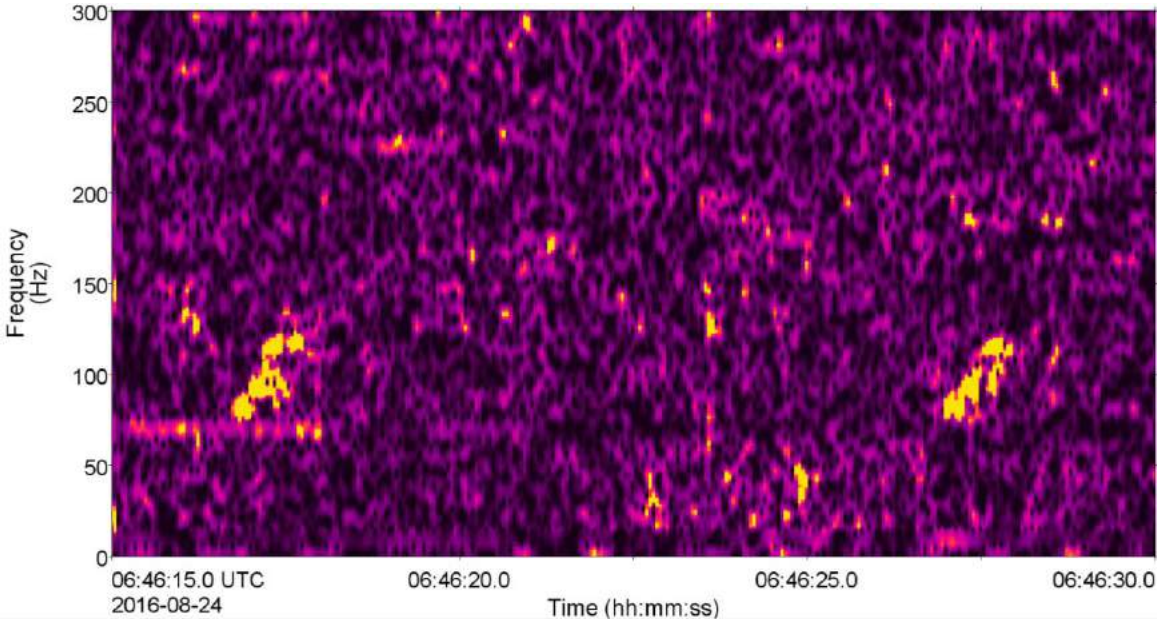

Figure 83. Spectrogram of two right whale upcalls recorded at stn 3 on 24 Aug 2016 (1 Hz frequency resolution, 0.2 s time window, 0.05 s time step, Hamming window). The window length is 15 s.

3.3. Fish Chorusing

The number of fish chorusing events increased as the water temperature increased. These events are typically denoted through the elevated levels from 600–1000 Hz. At stn 6, no chorusing was observed in winter (Figure 84); however, by mid-September the nightly chorusing increased in intensity (Figure 85). By December, while there were peaks in the intensity at dawn and dusk, there was often chorusing occurring throughout the day (Figure 86). The contribution of the fish choruses to the overall soundscape can be seen in the increased levels in all percentiles around 700-900 Hz during the period 11–17 Dec 2016 (Figure 87). Similar trends occurred at all stations, and even at the station with the highest levels of vessel traffic during the day (stn 1) the chorusing events were still visible at dawn and dusk (Figure 88).

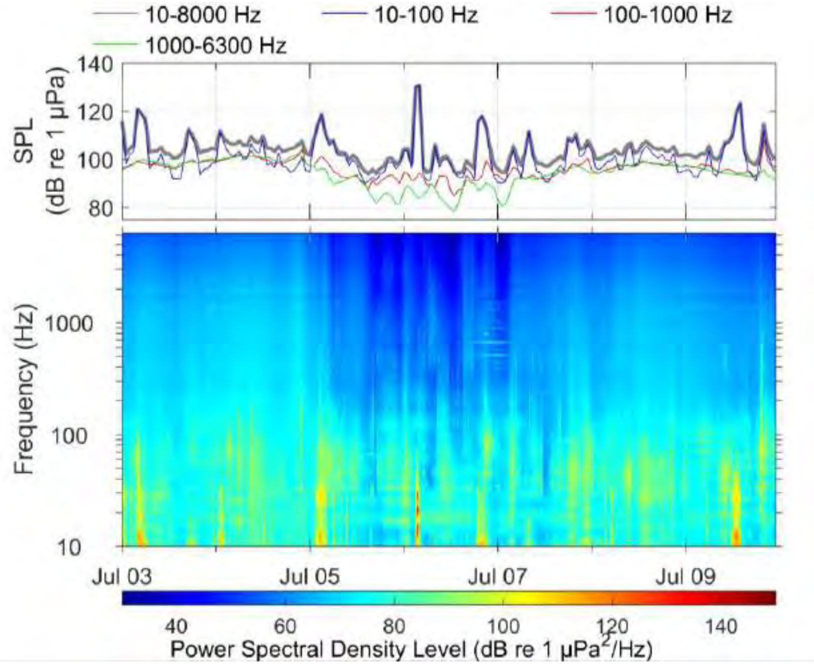

Figure 84. Station 6: Sound level summary from 03–09 Jul 2016.(Top) In-band SPL and (bottom) spectrogram of underwater sound.

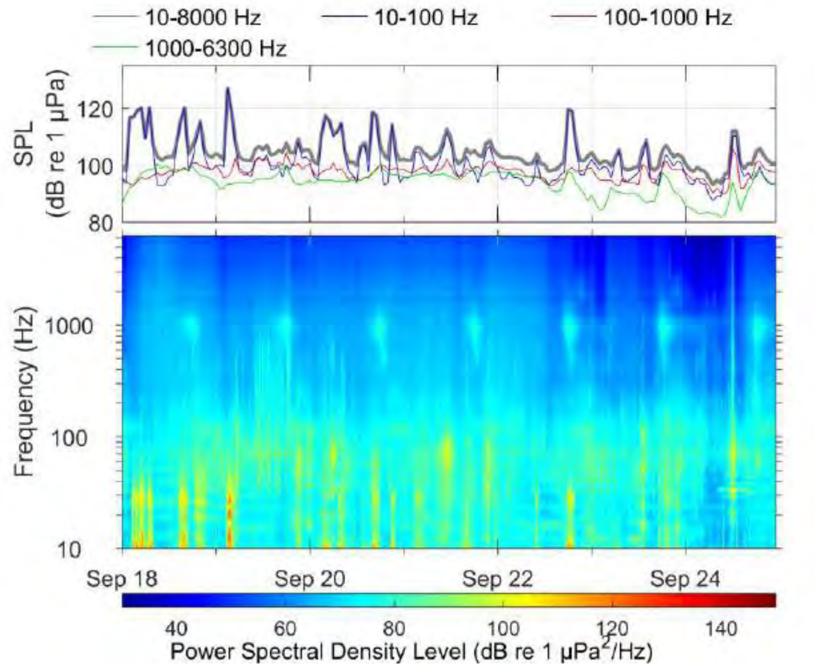

Figure 85. Station 6: Sound level summary from 18–24 Sep 2016.(Top) In-band SPL and (bottom) spectrogram of underwater sound.

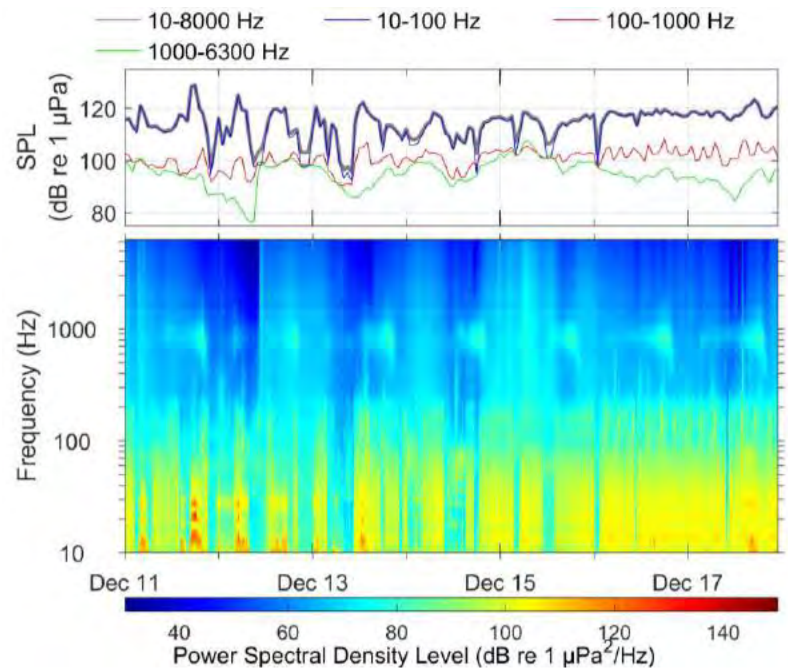

Figure 86. Station 6: Sound level summary from 11–17 Dec 2016.(Top) In-band SPL and (bottom) spectrogram of underwater sound.

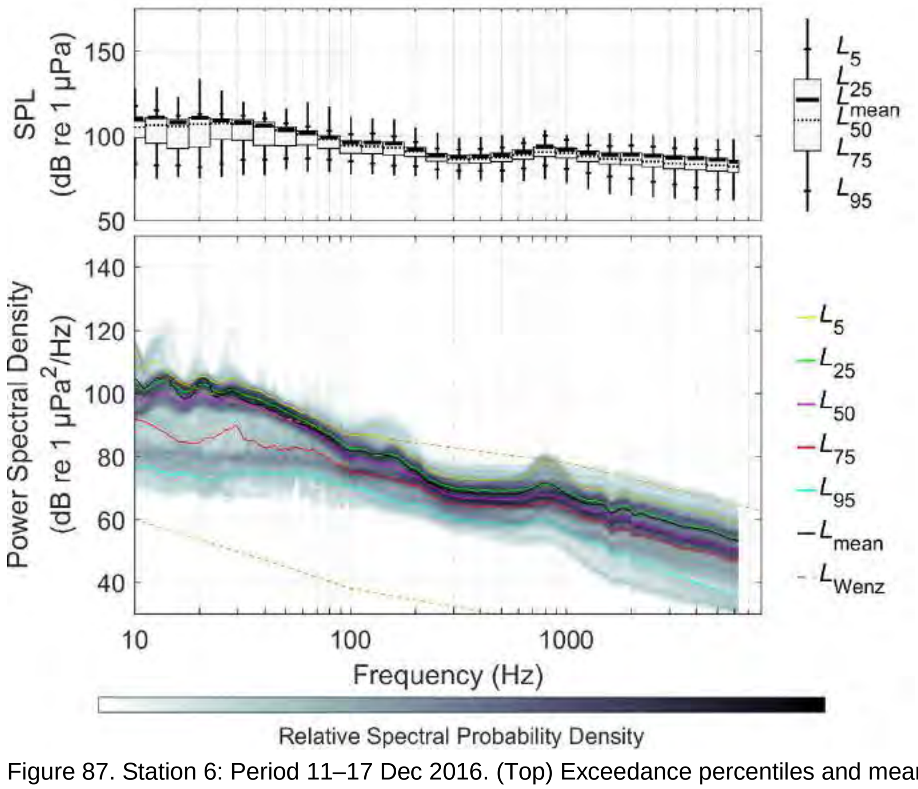

Figure 87. Station 6: Period 11–17 Dec 2016. (Top) Exceedance percentiles and mean of 1/3-octave-band SPL and (bottom) exceedance percentiles and probability density (grayscale) of 1-min PSD levels compared to the limits of prevailing noise (Wenz 1962).

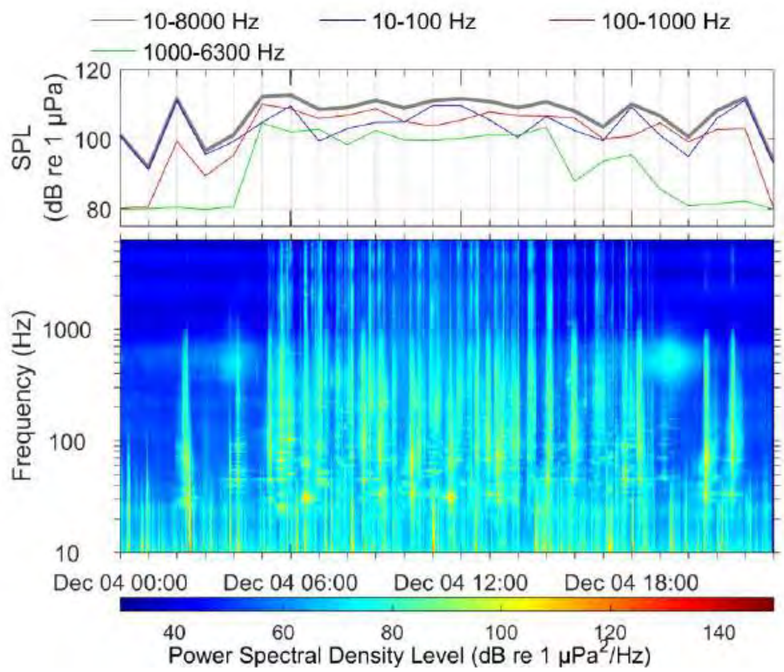

Figure 88. Station 1: Sound level summary from 04 Dec 2016.(Top) In-band SPL and (bottom) spectrogram of underwater sound.

3.4. Anthropogenic Sound Sources

This section provides specific examples of the two main anthropogenic noise contributors recorded during the monitoring program: shipping and seismic surveys.

3.4.1. Shipping

Individual vessels of all classes were a primary contributor to the soundscape. Stns and 3 had the highest number of daily large vessel detections (Figures 14 and 25); however, stn 1 had the greatest number when including small vessel traffic. An example day from stn 1 is shown in Figure 89, with the vessel transit at ~2 a.m. shown in Figure 90. This image clearly shows the tones and increased SPL as described in Section 2.2.2, along with the U-shaped interference patterns caused by constructive and destructive interference from a dipole sound source known as the Lloyd's Mirror Effect (Wales and Heitmeyer 2002).

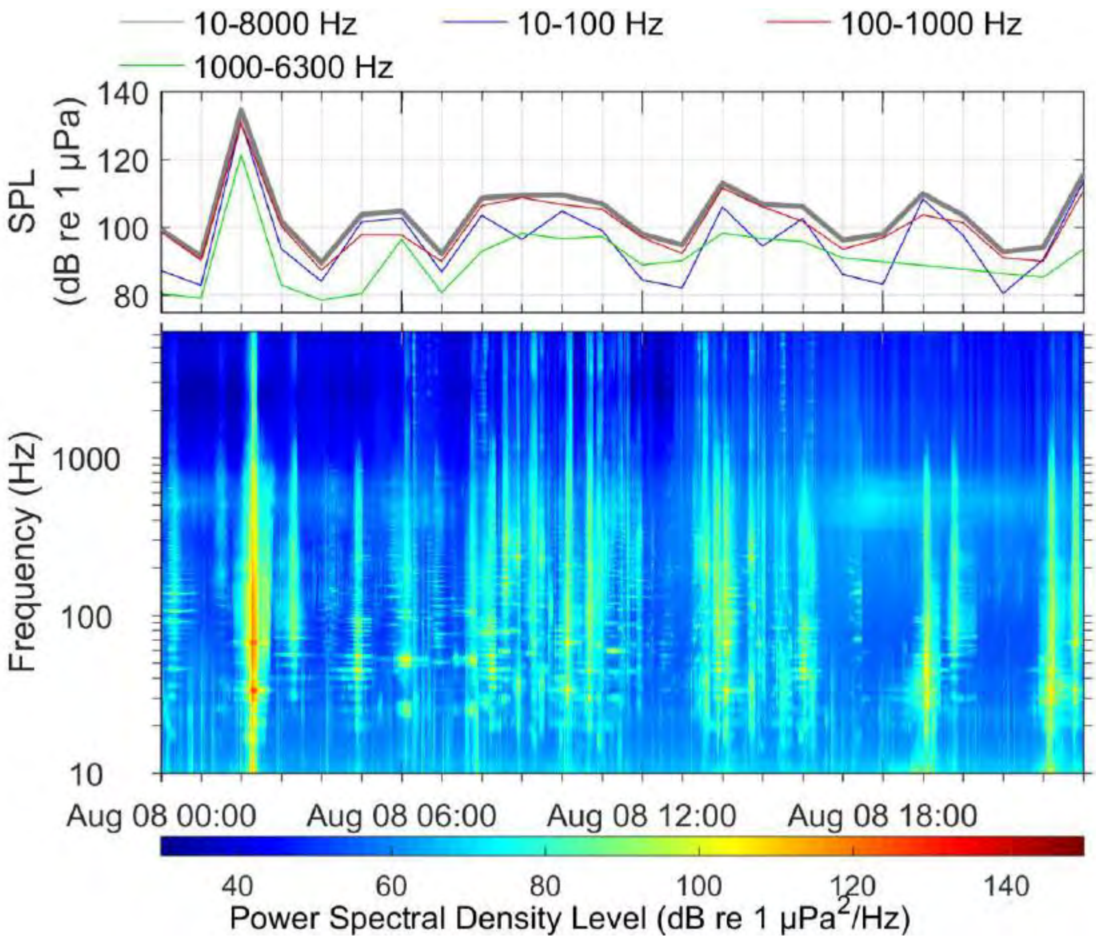

Figure 89. Station 1: Sound level summary from 08 Aug 2016.(Top) In-band SPL and (bottom) spectrogram of underwater sound.

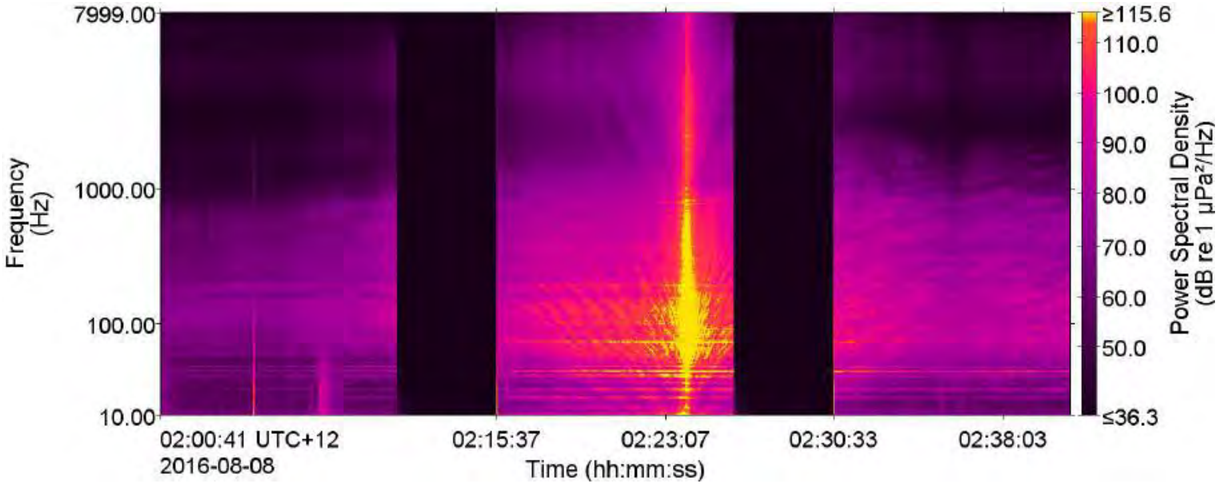

Figure 90. Spectrogram of a vessel recorded at stn 1 on 8 Aug 2016. (0.122 Hz frequency resolution, 1 s time window, 0.5 s time step, Hamming window).

3.4.2. Seismic surveys

Two seismic surveys were detected during the monitoring program. The first survey was only detected at stn 2, between late October and mid-late November. It is likely that this was the PGS Taranaki South 3-D seismic survey. Example impulses recorded from the survey are shown in Figure 91. The second survey was the Schlumberger Pegasus Basin 3-D seismic survey, which was automatically detected at stns 5–7 from mid-November. Example impulses recorded from the survey are shown in Figure 92. The Schlumberger survey is visible on the full period spectrograms for all stations it was detected at (e.g., Figure 43), additionally a weekly spectrogram (Figure 94) and percentile plot (Figure 95) are included in this section. The survey was also recorded at stn 4 (Figure 93); however, the higher noise levels at this station interfered with the performance of the detector.

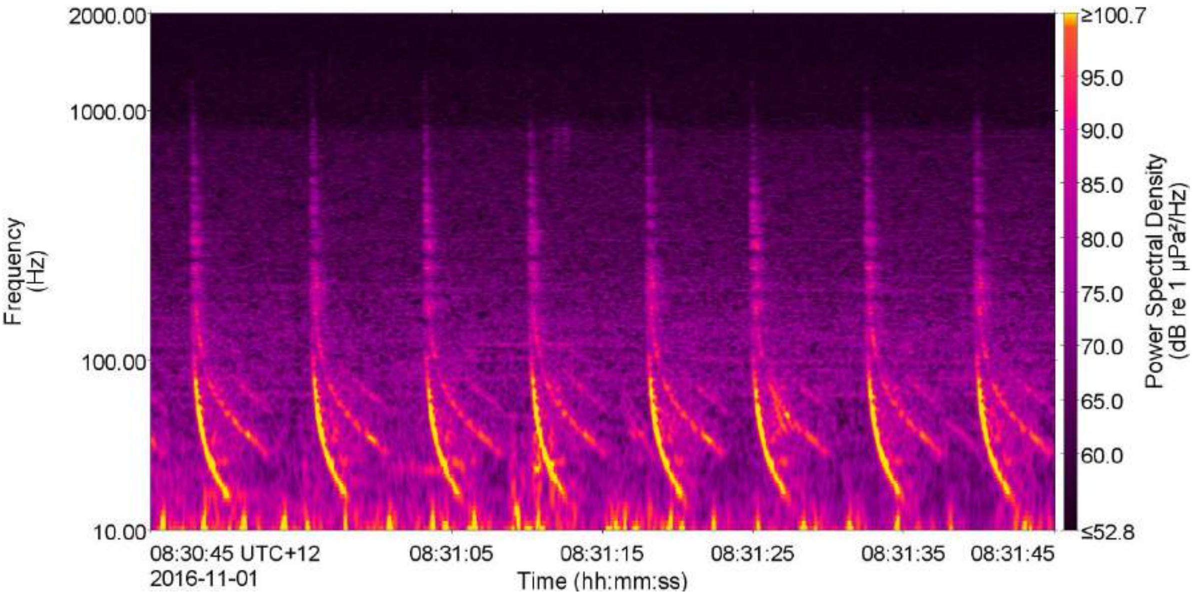

Figure 91. Spectrogram of seismic impulses with inter-pulse interval of seven seconds recorded at stn 2 on 1 Nov 2016. (0.488 Hz frequency resolution, 0.5 s time window, 0.5 s time step, Hamming window).

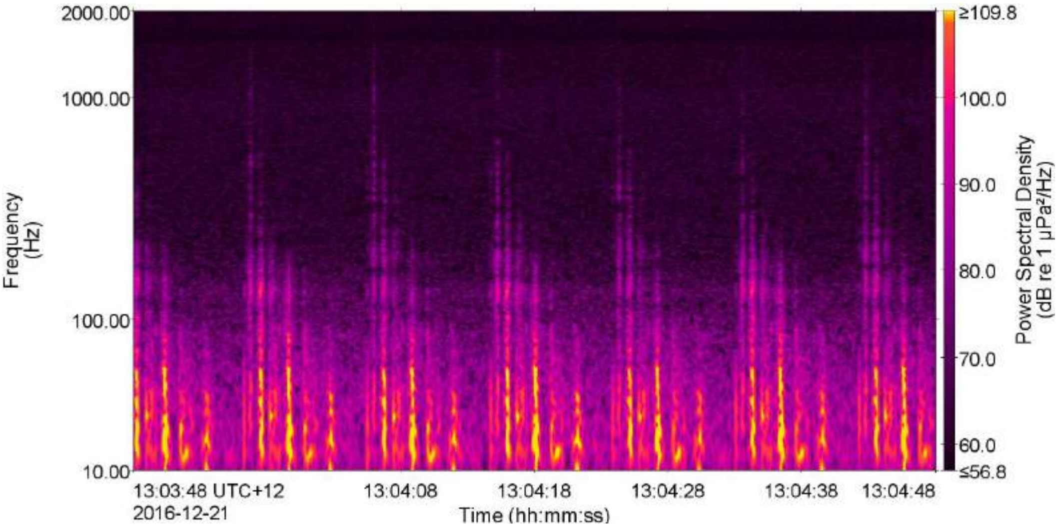

Figure 92. Spectrogram of seismic impulses with inter-pulse interval of nine seconds recorded at stn 7 on 21 Dec 2016. (0.488 Hz frequency resolution, 0.5 s time window, 0.5 s time step, Hamming window).

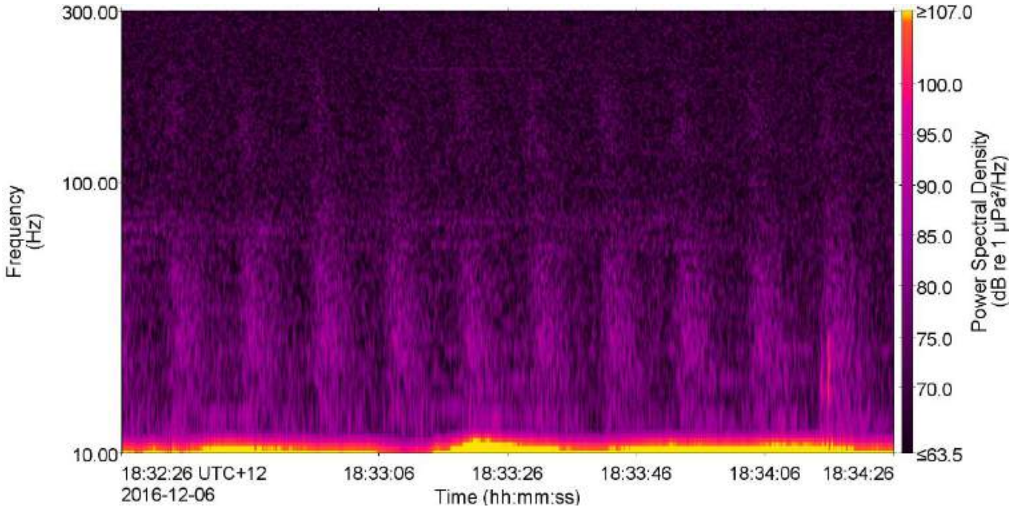

Figure 93. Spectrogram of seismic impulses recorded at stn 4 on 06 Dec 2016. (0.488 Hz frequency resolution, 0.5 s time window, 0.5 s time step, Hamming window).

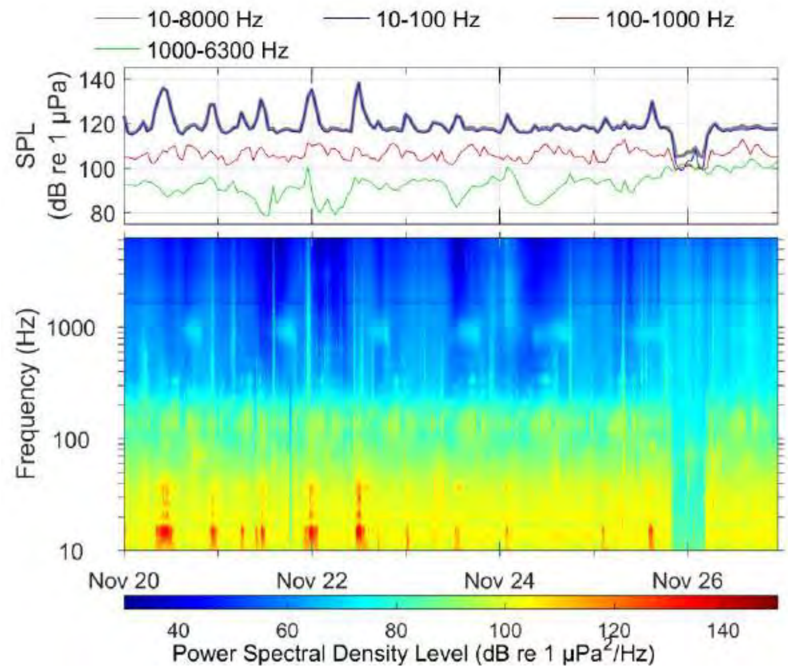

Figure 94. Station 7: Sound level summary from 20–26 Nov 2016.(Top) In-band SPL and (bottom) spectrogram of underwater sound.

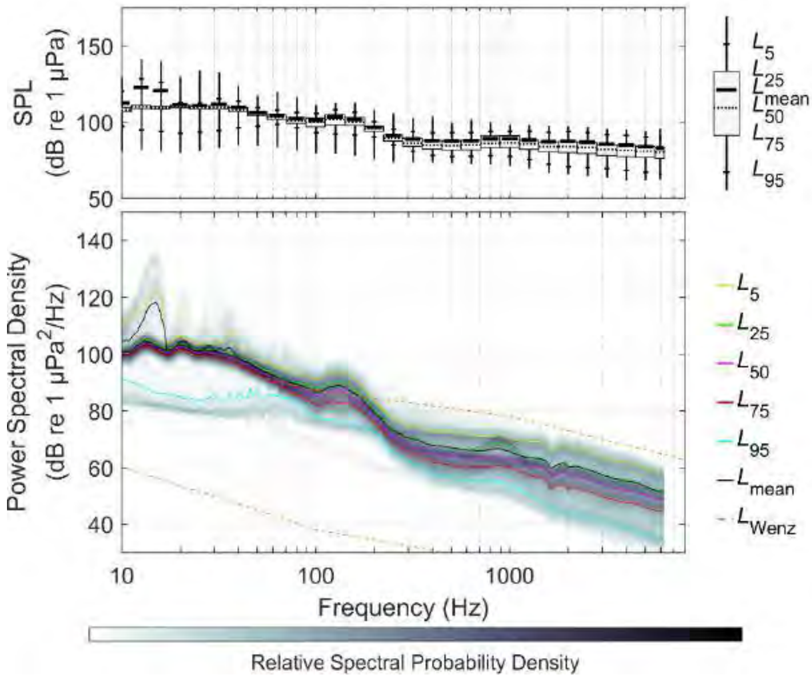

Figure 95. Station 6: Period 11–17 Dec 2016. (Top) Exceedance percentiles and mean of 1/3-octave-band SPL and (bottom) exceedance percentiles and probability density (grayscale) of 1-min PSD levels compared to the limits of prevailing noise (Wenz 1962).

3.5. Rhythmic Pattern Analysis

An analysis of daily (e.g., Figure 96), weekly (e.g., Figure 97), and tidal (e.g., Figure 98) rhythmic patterns was performed for the seven-month recording period for each station to identity potentially recurring contributions to the local soundscapes.

Recurring scheduled daily contributors appear as increased levels at specific hours of the day and are often linked to ferries operating on a schedule. The elevated levels noted for stn 3 around 10 a.m. and 4 p.m. correspond to the inter-island ferry crossings (Figure 102). The elevated mid-day levels observed at stn 1 and attributed to ferry and small boat traffic are visible in the weekly median SPL plots, which indicates that these increased levels are a persistent feature of the soundscape. Elevated levels around dusk in the 1–6.3 kHz band at all stations is due to the fish chorusing events.

The influence of tides, usually through increased flow-induced noise, showed different patterns: no or moderate influence (stn 1, 3, 5, and 6); a single period of increased noise levels during the tidal cycle, which occurred during the period of peak flow after high tide at stn 2 (Figure 101) and around high tide at stn 7 (Figure 116); the latter increase was substantial, increasing levels in the 10–100 Hz band by nearly 25 dB re 1µPa); and twice daily increases in levels at stn 4 (Figure 107), with peaks occurring ~1 hr before high and low tides. Divergence in the timing of elevated levels with respect to the times of high and low tides and the number of peaks may be related to the distance of each station to the relevant tidal station used as reference as well as local bathymetry and interactions with oceanic currents unrelated to tides.

3.5.1. Station 1

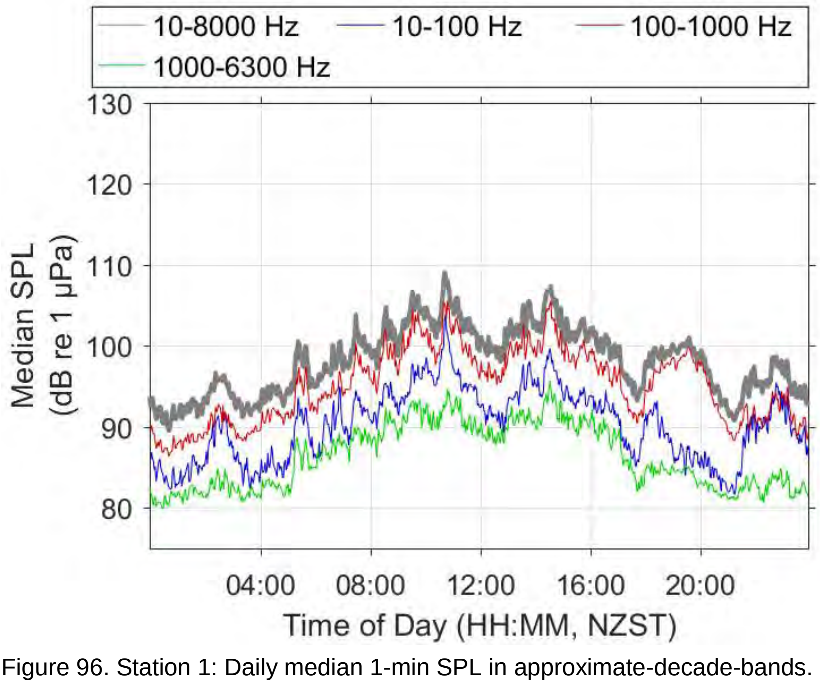

Figure 96. Station 1: Daily median 1-min SPL in approximate-decade-bands.

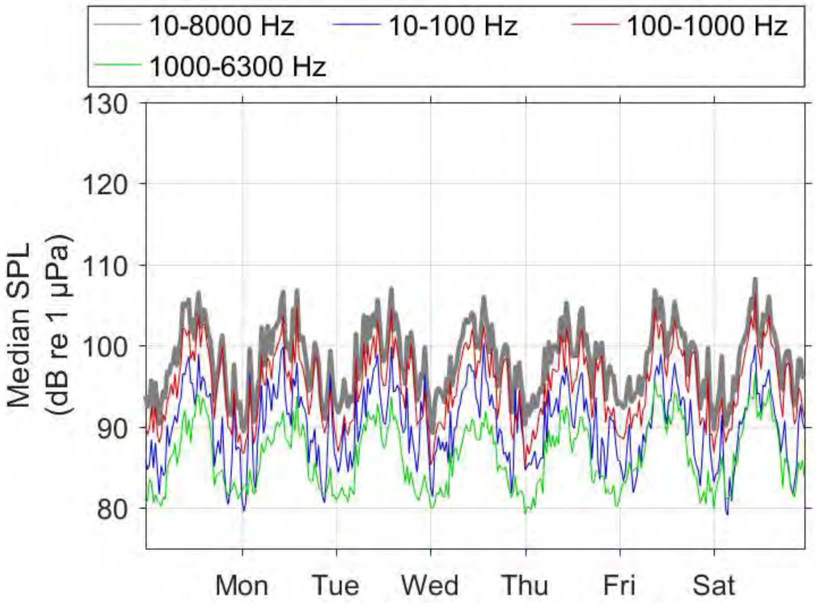

Figure 97. Station 1: Weekly median 1-min SPL in approximate-decade-bands.

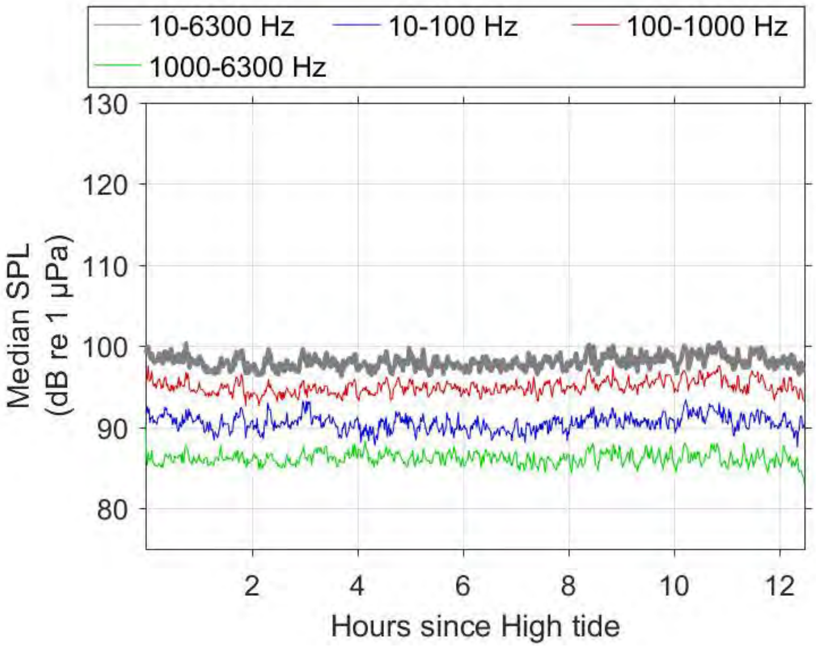

Figure 98. Station 1: Tidal median 1-min SPL in approximate-decade-bands.

3.5.2. Station 2

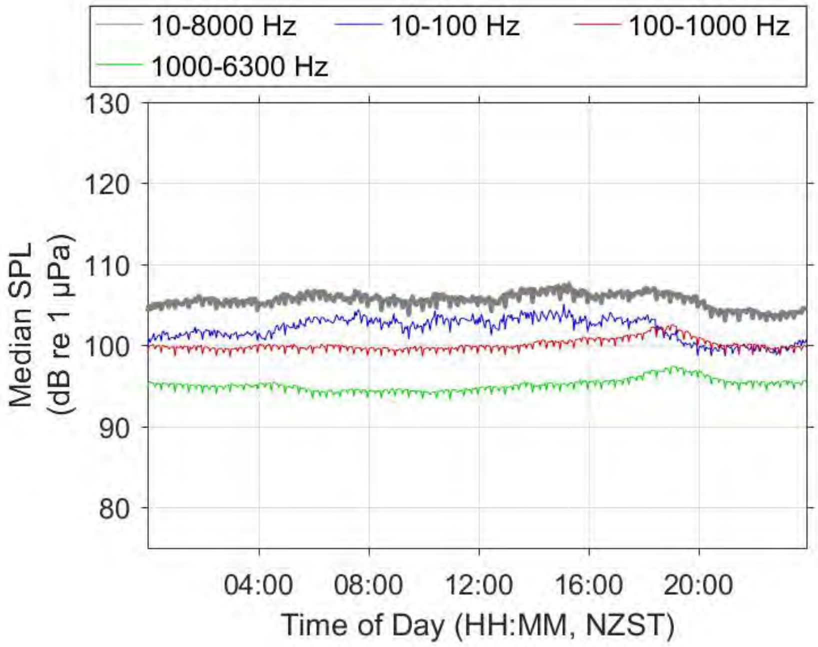

Figure 99. Station 2: Daily median SPL 1-min SPL in approximate-decade-bands.

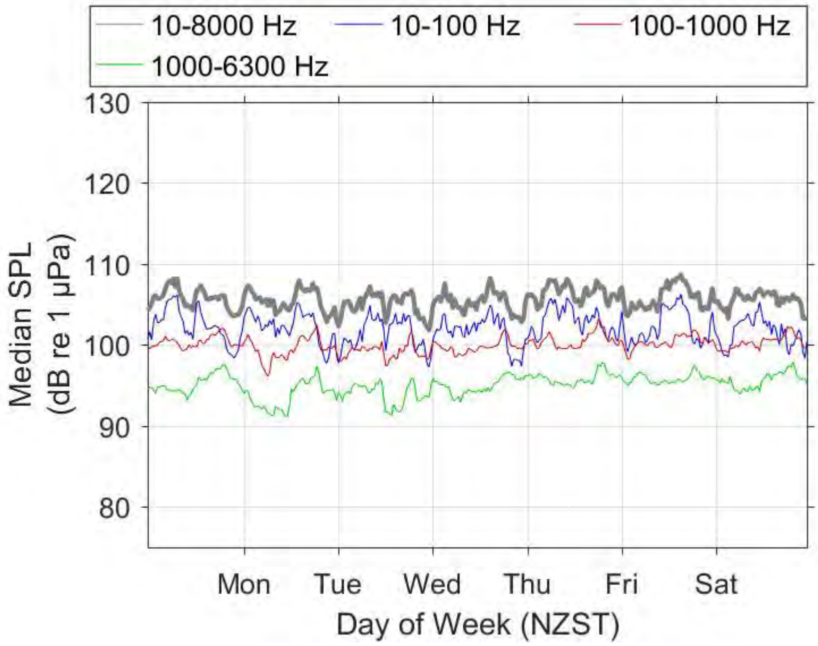

Figure 100. Station 2: Weekly median SPL 1-min SPL in approximate-decade-bands.

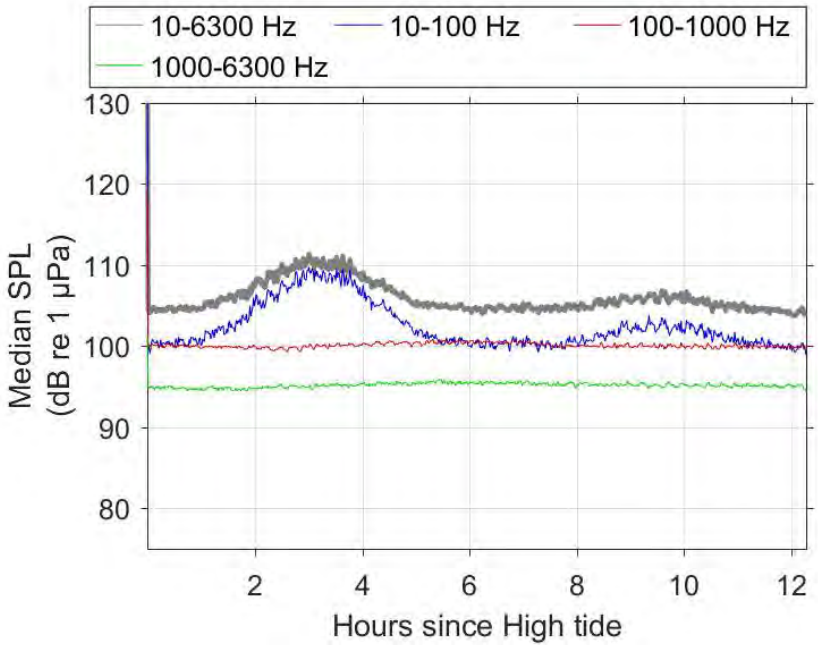

Figure 101. Station 2: Tidal median 1-min SPL in approximate-decade-bands.

3.5.3. Station 3

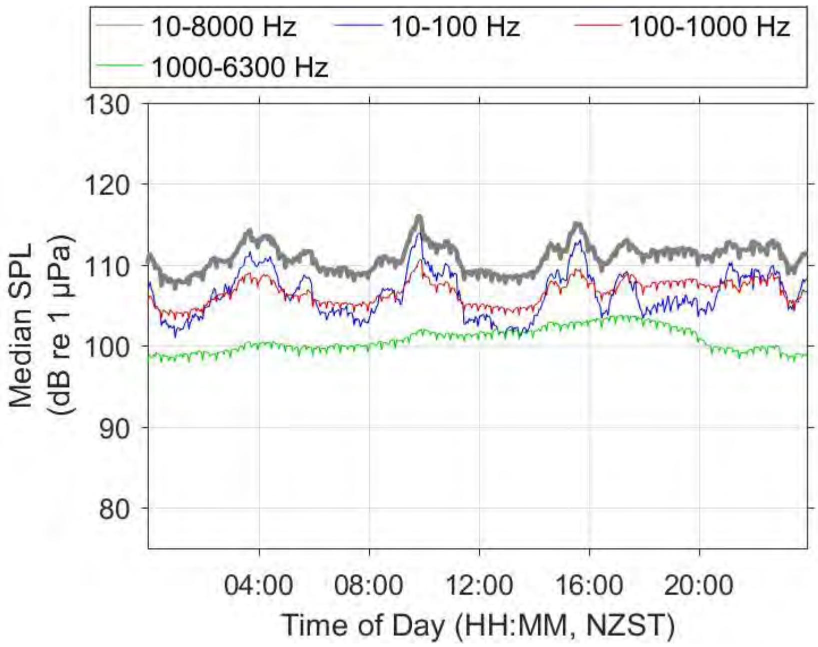

Figure 102. Station 3: Daily median 1-min SPL in approximate-decade-bands.

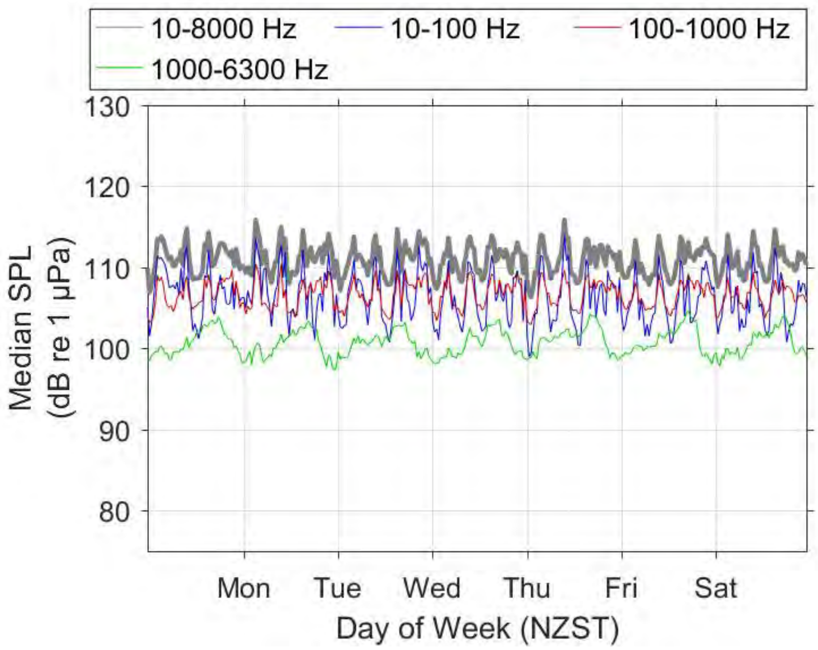

Figure 103. Station 3: Weekly median 1-min SPL in approximate-decade-bands.

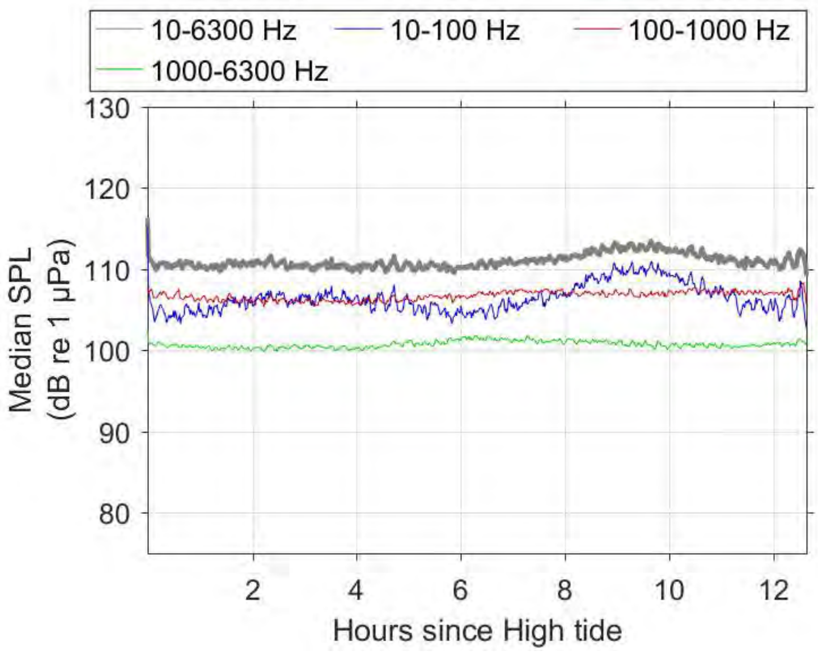

Figure 104. Station 3: Tidal median 1-min SPL in approximate-decade-bands.

3.5.4. Station 4

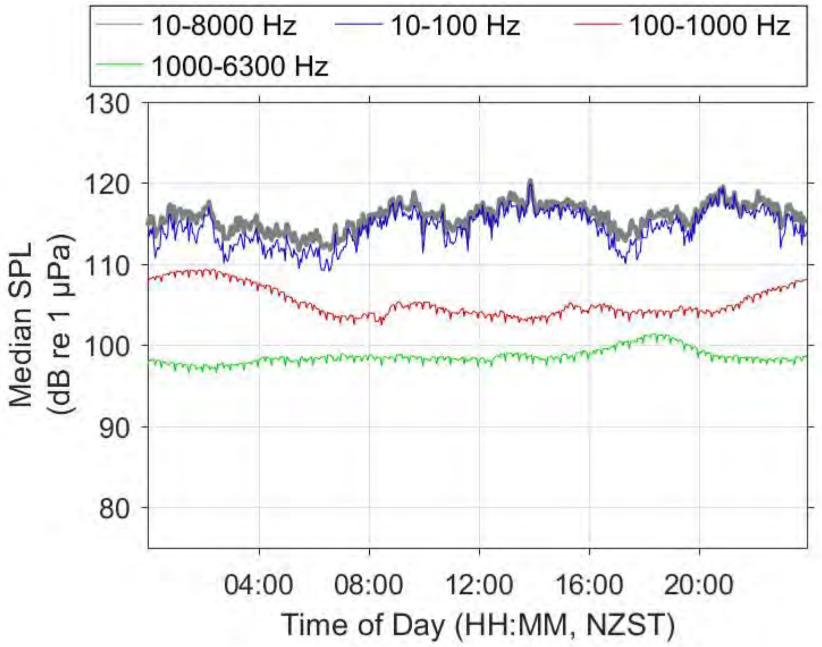

Figure 105. Station 4: Daily median 1-min SPL in approximate-decade-bands.

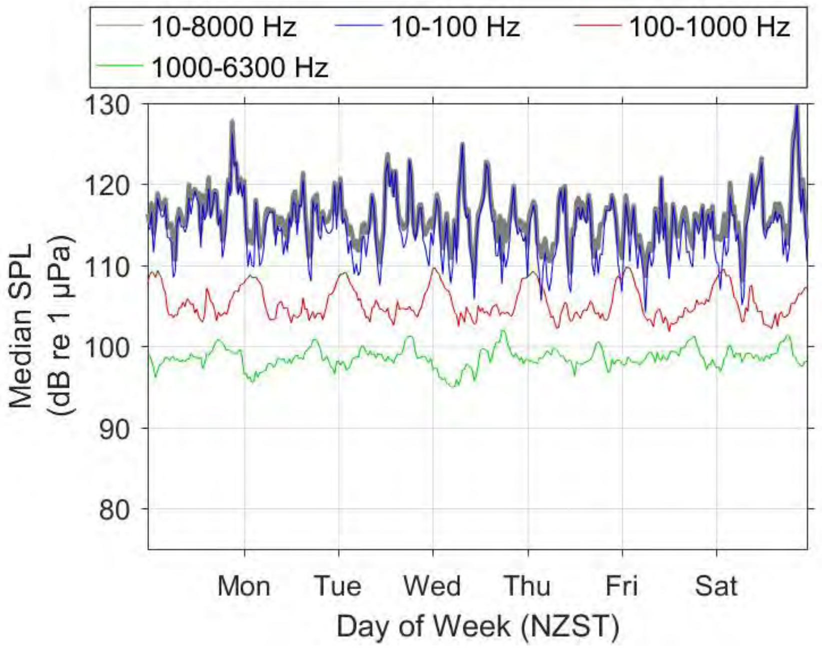

Figure 106. Station 4: Weekly median 1-min SPL in approximate-decade-bands.

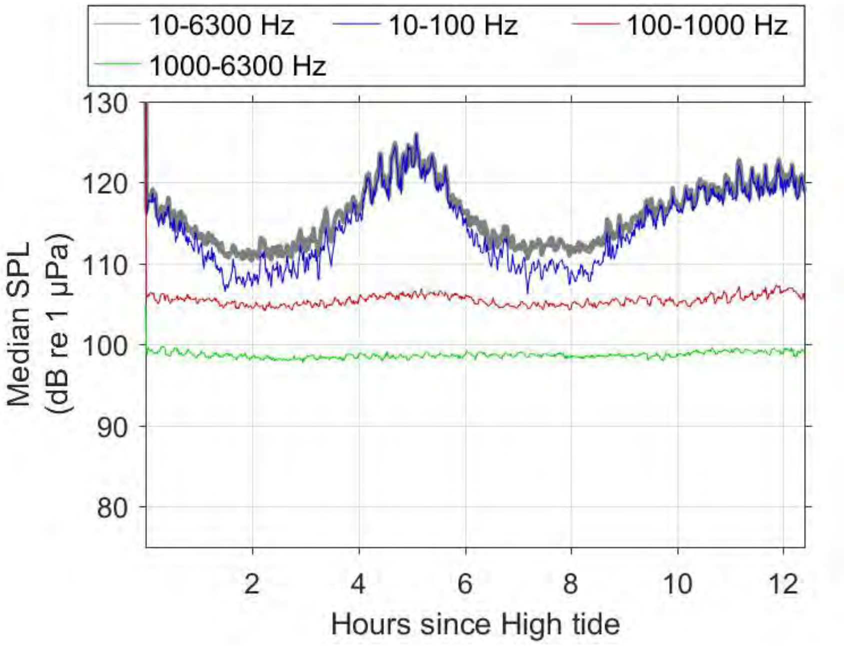

Figure 107. Station 4: Tidal median 1-min SPL in approximate-decade-bands.

3.5.5. Station 5

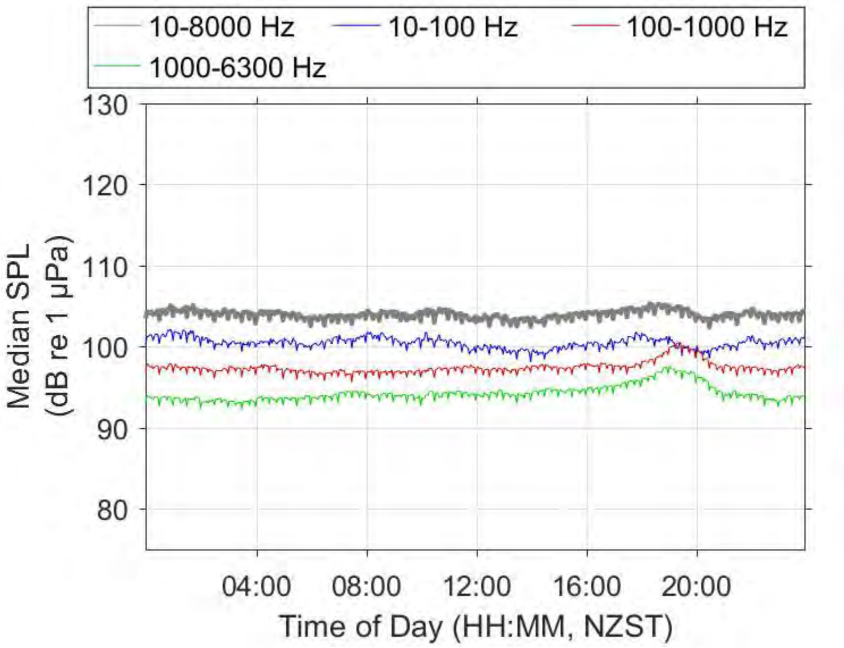

Figure 108. Station 5: Daily median 1-min SPL in approximate-decade-bands.

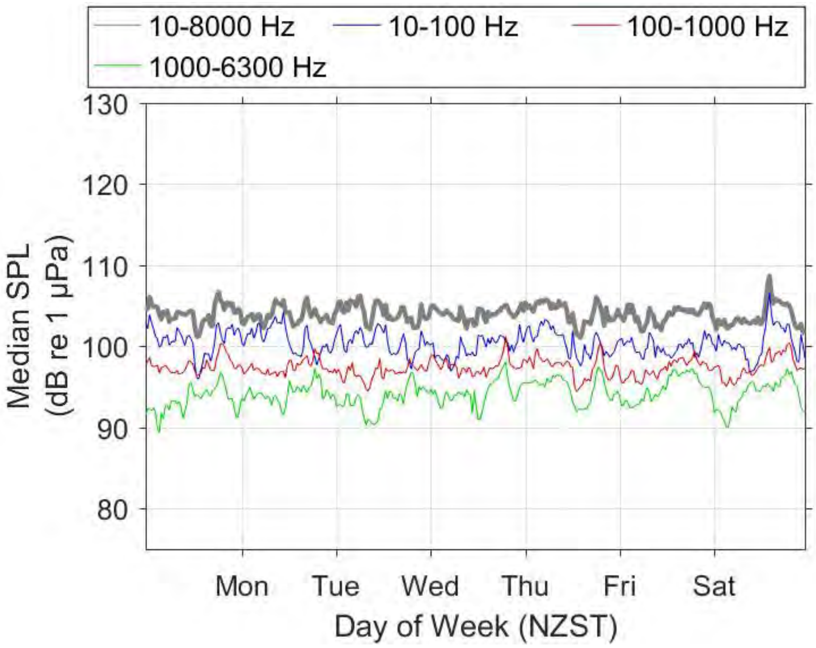

Figure 109. Station 5: Weekly median 1-min SPL in approximate-decade-bands.

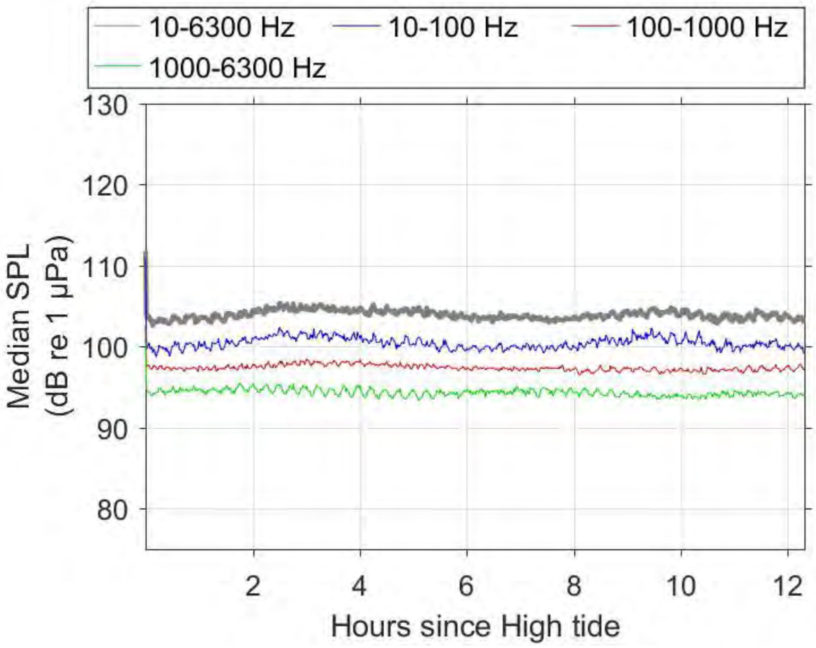

Figure 110. Station 5: Tidal median 1-min SPL in approximate-decade-bands.

3.5.6. Station 6

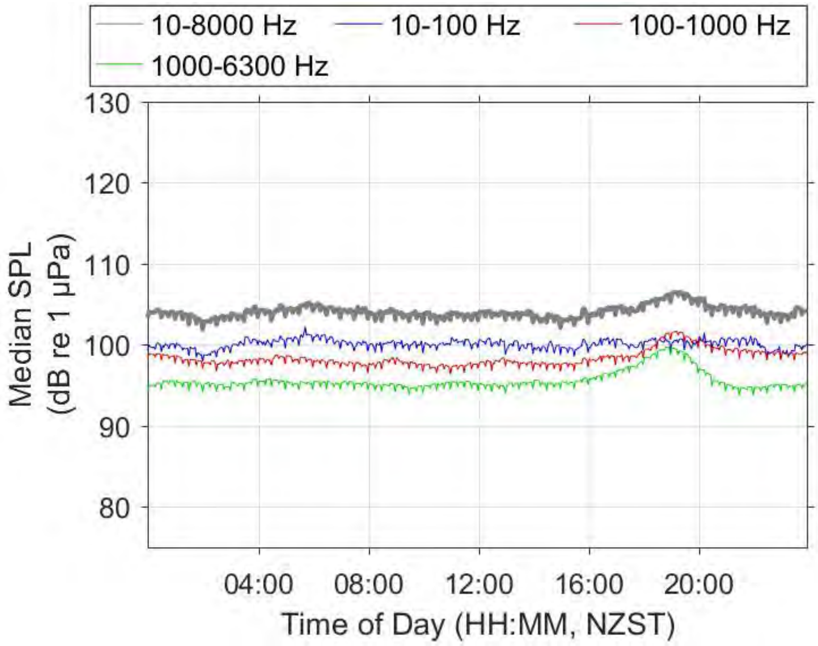

Figure 111. Station 6: Daily median 1-min SPL in approximate-decade-bands.

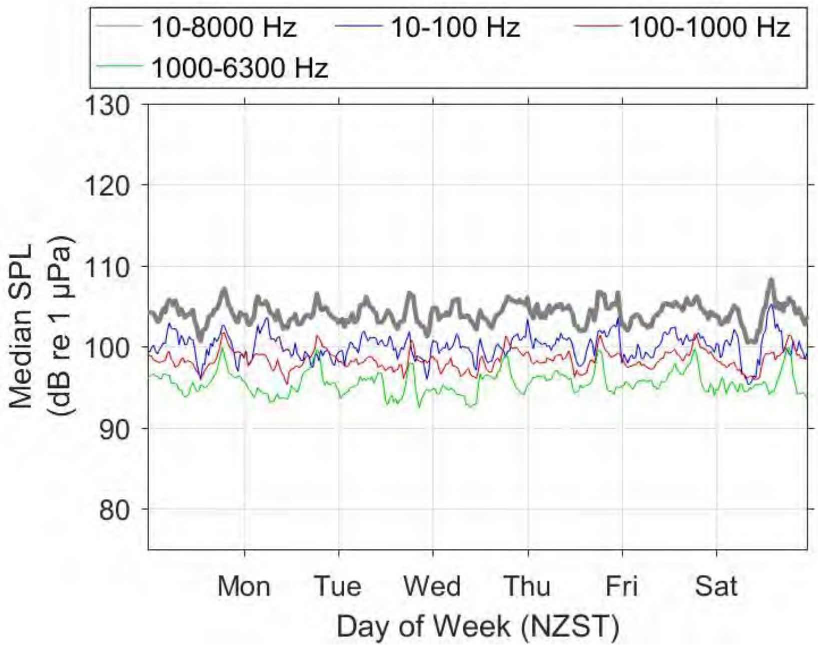

Figure 112. Station 6: Weekly median 1-min SPL in approximate-decade-bands.

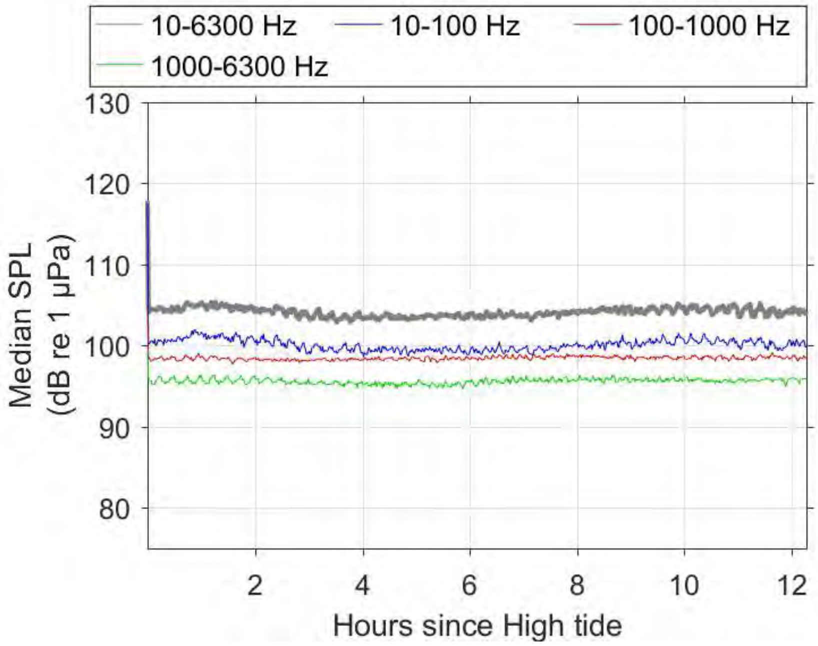

Figure 113. Station 6: Tidal median 1-min SPL in approximate-decade-bands.

3.5.7. Station 7

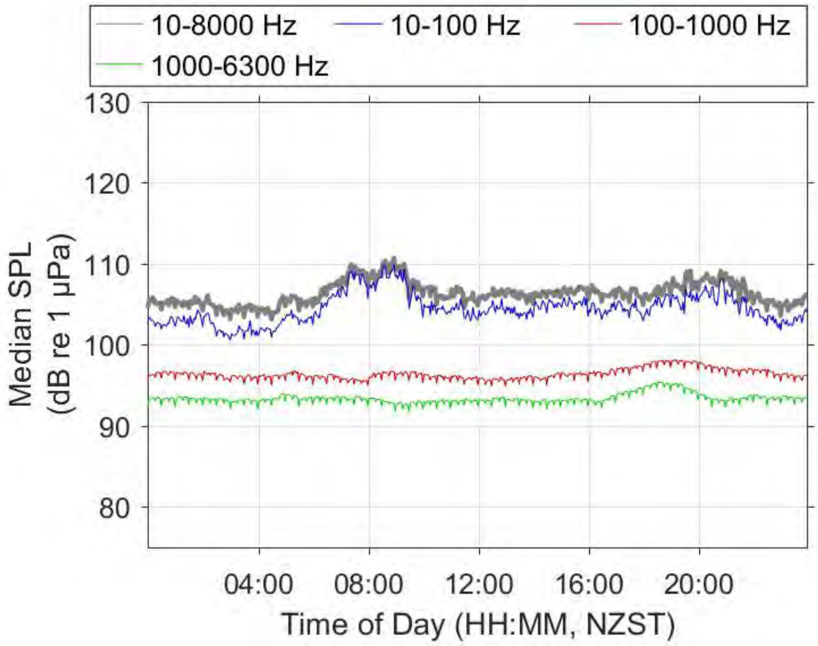

Figure 114. Station 7: Daily median 1-min SPL in approximate-decade-bands.

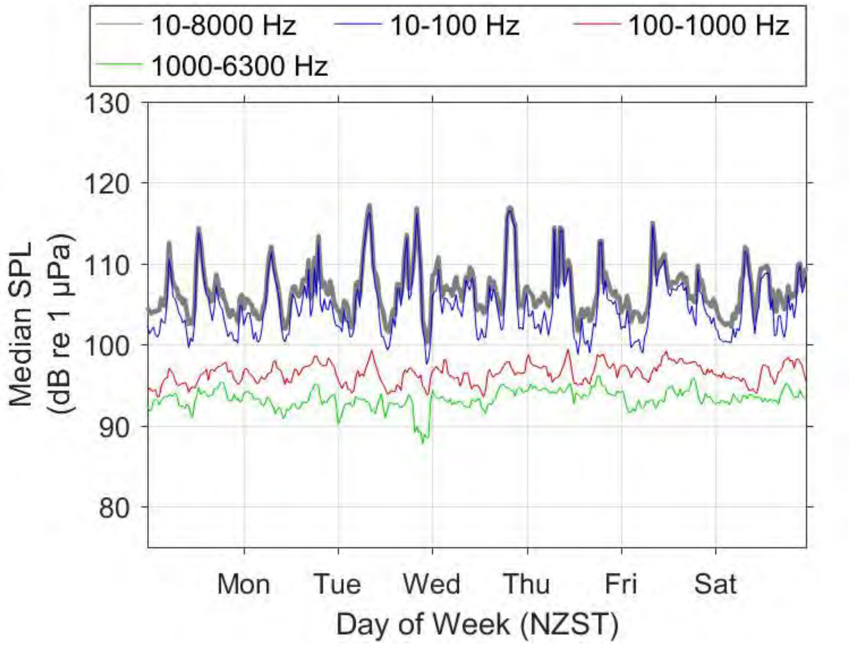

Figure 115. Station 7: Weekly median 1-min SPL in approximate-decade-bands.

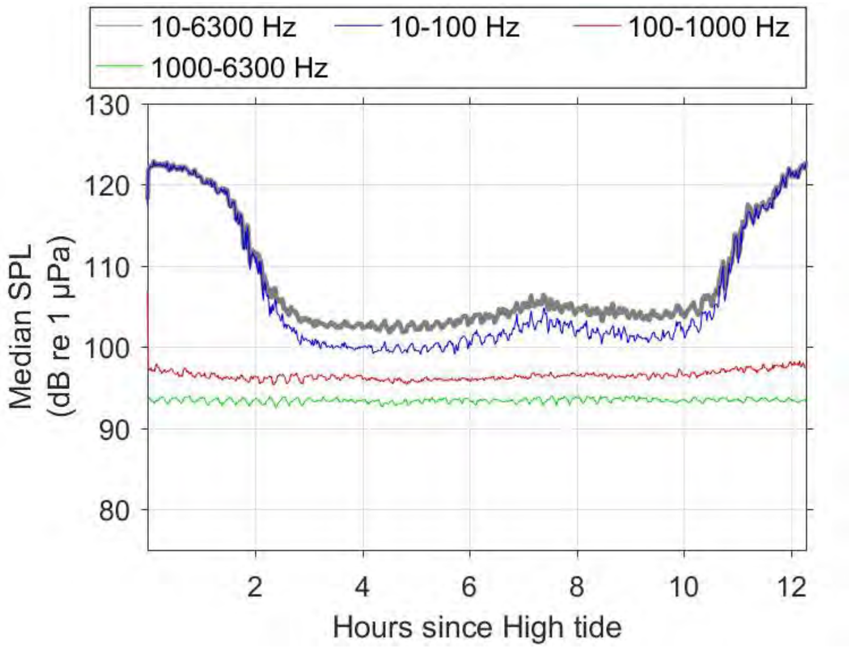

Figure 116. Station 7: Tidal median 1-min SPL in approximate-decade-bands.

4. Summary Discussion

4.1. Ambient and Anthropogenic

The total received sound levels in the Cook Strait region are influenced by sounds produced by wind, waves, geological seismic events, biological sources, and human activities. The soundscape of the Cook Strait region is strongly influenced by weather and anthropogenic sources. Fish and marine mammals were detected at all seven stations despite the often-elevated levels of noise.

Limited environmental data relevant to mooring design was available during mobilisation, and extensive fishing activity restricted possible deployment locations. To achieve the desired regional coverage, the deployment of moorings in high current areas (stns 2, 3, and 4) was required. Best efforts within reason were made to deploy moorings less likely to be influenced by pseudo-noise. For stns 2 and 3, the influences of pseudo-noise did not adversely influence the resulting data. Stn 3 performed surprisingly well, with only a small increase of flow noise on the flood tide. Stn 4 however was significantly influenced in a negative fashion, likely due to levels of flow and sediment movement beyond what was expected. These increased noise levels restricted the performance of automated marine mammal and seismic survey detection methods. It is likely that the seismic survey could be detected at this station if the detectors were optimised; however, currently this has not occurred. Data from the deep-water stns 5 and 6 were influenced the least by flow induced pseudo-noise, while data from stn 7 was influenced primarily in the frequency range 10–100 Hz. The moorings deployed vertically (stns 4–7) all used glass spheres in torpedo floats, positioned at 5 and 10 m above the AMAR. It is likely that the mooring design is responsible for the notches in the percentile plots for these stations at ~800 and 2000 Hz.

The contribution from shipping varies across the region, with bathymetry significantly effecting the received levels and the time period that individual vessels were detected for. Vessels at stn 1 were detected for a relatively short period of time due to the location the AMAR within the shallow (50 m) and restricted waters of Queen Charlotte Sound. In contrast, vessels at stns 5–7 were detected for hours, due to the location of the shipping lanes, the listening distance of these stations, and the way that sound propagates off the continental shelf.

The seismic survey in the South Taranaki had less influence on the overall soundscape recorded at stn 2 compared to the west coast Pegasus basin survey near stns 4–7. The structure of the recorded seismic impulses is significantly different between the surveys. The impulses from the South Taranaki survey contain strong frequency modes, while those from the Pegasus basis indicate strong multipath. Analysis of the received impulses in conjunction with logs from the seismic acquisition program would provide valuable information about the acoustic propagation and the geoacoustics in the Cook Strait region.

4.2. Marine Mammals

4.2.1. Odontocetes

Important findings include the persistent presence of Cuvier's beaked whales at stns 5, 6, and 7. Based on existing information on beaked whale click types and beaked whale sighting and stranding records in New Zealand, we suggest that the UnkBkd38 and UnkBkd55 beaked whale click types may respectively belong to Gray's (*Mesoplodon grayi*) (Trickey et al. 2014, Trickey et al. 2015) and strap-toothed (*M. layardii*) beaked whales. Gray's beaked whales have been sighted at sea off the east coast of the South Island (Dalebout et al. 2004) and are the most common species in the stranding records (Brabyn 1991). Strap-toothed beaked whales are the third most common species in the beaked whale stranding record, just after Cuvier's beaked whale (Brabyn 1991).

The acoustic occurrence of the other detected species is consistent with the local knowledge. Hector's dolphins were restricted to the coastal waters (stn 1). Sperm whales were most common at stn 5 located near Kaikoura Canyon, where the species' year-round occurrence is well described (Jacquet and Whitehead 1999). Because dusky dolphins (*Lagenorhynchus obscurus*), a common species in New Zealand waters, are not known to produce whistles (Vaughn-Hishorn et al. 2012), the dolphin whistles recorded in this study were produced by other species. A presumably significant portion of these signals could have been produced by common dolphins (*Delphinus delphis*), which are believed to be one of the most common cetacean species in New Zealand (Stockin et al. 2008). Bottlenose dolphin are likely the most common species at stn1 (Merriman et al. 2009).

4.2.2. Mysticetes

The seasonality of blue whale song detections is consistent with the winter peak and summer absence in song production by that species (Oleson et al. 2007, Stafford et al. 2007). The prevalence of the New Zealand song type at stn 2, located in the South Taranaki Gulf, also agrees with evidence suggesting that this area is used as a foraging ground, possibly on a year-round basis (Torres 2013). In contrast, Antarctic blue whale songs were recorded primarily east of Cook Strait. This species has been recorded previously south of New Zealand (Double et al. 2013). Some Antarctic blue whale detections had high signal-to-noise ratio, indicating that the recorded individual were near the recorder.

Despite extensive testing, the performance of the both types of automated detectors for blue whales was too low to consider their outputs. This was largely the results of vessel activity in the area, and the associated tonals triggering the detectors and leading to false alarms. The detectors worked well on files without higher levels of shipping noise, and future improvement and testing of the detectors is planned to increase their applicability.

Humpback whale detections were constrained over a 6–8-week window. The timing of the detections coincide with that of north-bound migrating whales (Dawbin 1956). The greater number of detections at stn 2 and 3 suggest that more whales migrate through Cook Strait than along the east coast of the North Island.

The Antarctic minke whale detections represent new information. The winter occurrence of the acoustic detections is consistent with baleen whale singing behaviour and suggests that some Antarctic minke whales migrate through, and possibly winter, in New Zealand waters. The low number of Southern right whale detections may be the result of a low numbers of individuals near the recording sites, most being farther offshore than the species’ preferred coastal habitat in the region, combined with high background noise levels at near-shore stations most likely to be frequented by right whales and limiting call detections.

Glossary

1/3-octave-band
Non-overlapping passbands that are one-third of an octave wide (where an octave is a doubling of frequency). Three adjacent 1/3-octave-bands comprise one octave. One-third-octave-bands become wider with increasing frequency. Also see octave.

ambient noise
All-encompassing sound at a given place, usually a composite of sound from many sources near and far (ANSI S1.1-1994 R2004), e.g., shipping vessels, seismic activity, precipitation, sea ice movement, wave action, and biological activity.

background noise
Total of all sources of interference in a system used for the production, detection, measurement, or recording of a signal, independent of the presence of the signal (ANSI S1.1-1994 R2004). Ambient noise detected, measured, or recorded with a signal is part of the background noise.

bandwidth
The range of frequencies over which a sound occurs. Broadband refers to a source that produces sound over a broad range of frequencies (e.g., seismic airguns, vessels) whereas narrowband sources produce sounds over a narrow frequency range (e.g., sonar) (ANSI/ASA S1.13-2005 R2010).

broadband sound level
The total sound pressure level measured over a specified frequency range. If the frequency range is unspecified, it refers to the entire measured frequency range.

cavitation
A rapid formation and collapse of vapour cavities (i.e., bubbles or voids) in water, most often caused by a rapid change in pressure. Fast-spinning vessel propellers typically cause cavitation, which creates a lot of noise.

continuous sound
A sound whose sound pressure level remains above ambient sound during the observation period (ANSI/ASA S1.13-2005 R2010). A sound that gradually varies in intensity with time, for example, sound from a marine vessel.

decibel (dB)
One-tenth of a bel. Unit of level when the base of the logarithm is the tenth root of ten, and the quantities concerned are proportional to power (ANSI S1.1-1994 R2004).

duty cycle
The time when sound is periodically recorded by an acoustic recording system.

fast Fourier transform (FFT)
A computationally efficiently algorithm for computing the discrete Fourier transform.

frequency
The rate of oscillation of a periodic function measured in cycles-per-unit-time. The reciprocal of the period. Unit: hertz (Hz). Symbol: *f*. 1 Hz is equal to 1 cycle per second.

hertz (Hz)
A unit of frequency defined as one cycle per second.

hydrophone
An underwater sound pressure transducer. A passive electronic device for recording or listening to underwater sound.

intermittent sound
A level of sound that abruptly drops to the background noise level several times during the observation period.

impulsive sound
Sound that is typically brief and intermittent with rapid (within a few seconds) rise time and decay back to ambient levels (NOAA 2013, ANSI S12.7-1986 R2006). For example, seismic airguns and impact pile driving.

median
The 50th percentile of a statistical distribution.

non-impulsive sound
Sound that is broadband, narrowband or tonal, brief or prolonged, continuous or intermittent, and typically does not have a high peak pressure with rapid rise time (typically only small fluctuations in decibel level) that impulsive signals have (ANSI/ASA S3.20-1995 R2008). For example, marine vessels, aircraft, machinery, construction, and vibratory pile driving (NIOSH 1998, NOAA 2015).

octave
The interval between a sound and another sound with double or half the frequency. For example, one octave above 200 Hz is 400 Hz, and one octave below 200 Hz is 100 Hz.

peak pressure level (PK)
The maximum instantaneous sound pressure level, in a stated frequency band, within a stated period. Also called zero-to-peak pressure level. Unit: decibel (dB).

peak-to-peak pressure level (PK-PK)
The difference between the maximum and minimum instantaneous pressure levels. Unit: decibel (dB).

percentile level, exceedance
The sound level exceeded *n*% of the time during a measurement.

power spectrum density
The acoustic signal power per unit frequency as measured at a single frequency. Unit: $\mu Pa^2/Hz$, or $\mu Pa^2 \cdot s$.

power spectral density level
The decibel level ($10\log_{10}$) of the power spectrum density, usually presented in 1 Hz bins. Unit: dB re 1 $\mu Pa^2/Hz$.

pressure, acoustic
The deviation from the ambient hydrostatic pressure caused by a sound wave. Also called overpressure. Unit: pascal (Pa). Symbol: p.

pressure, hydrostatic
The pressure at any given depth in a static liquid that is the result of the weight of the liquid acting on a unit area at that depth, plus any pressure acting on the surface of the liquid. Unit: pascal (Pa).

received level
The sound level measured at a receiver.

rms
root-mean-square.

sound
A time-varying pressure disturbance generated by mechanical vibration waves travelling through a fluid medium such as air or water.

sound exposure
Time integral of squared, instantaneous frequency-weighted sound pressure over a stated time interval or event. Unit: pascal-squared second ($Pa^2 \cdot s$) (ANSI S1.1-1994 R2004).

sound exposure level (SEL)
A cumulative measure related to the sound energy in one or more pulses. Unit: dB re 1 $\mu Pa^2 \cdot s$. SEL is expressed over the summation period (e.g., per-pulse SEL [for airguns], single-strike SEL [for pile drivers], 24-hour SEL).

sound pressure level (SPL)
The decibel ratio of the time-mean-square sound pressure, in a stated frequency band, to the square of the reference sound pressure (ANSI S1.1-1994 R2004).

For sound in water, the reference sound pressure is one micropascal (p_0 = 1 µPa) and the unit for SPL is dB re 1 µPa:

$$\mathrm{SPL} = 10\log_{10}\left(p^2 / p_0^2\right) = 20\log_{10}\left(p / p_0\right) \ .$$

Unless otherwise stated, SPL refers to the root-mean-square sound pressure level. See also 90% sound pressure level and fast-average sound pressure level. Non-rectangular time window functions may be applied during calculation of the rms value, in which case the SPL unit should identify the window type.

spectrogram
A visual representation of acoustic amplitude compared with time and frequency.

spectrum
An acoustic signal represented in terms of its power (or energy) distribution compared with frequency.

wavelength

Literature Cited

[NIOSH] National Institute for Occupational Safety and Health. 1998. *Criteria for a recommended standard: Occupational noise exposure*. Document Number 98-126. U.S. Department of Health and Human Services, NIOSH, Cincinnati, Ohio. 122 pp.

[NOAA] National Oceanic and Atmospheric Administration. 2013. *Draft guidance for assessing the effects of anthropogenic sound on marine mammals: Acoustic threshold levels for onset of permanent and temporary threshold shifts*, December 2013, 76 pp. Silver Spring, Maryland: NMFS Office of Protected Resources. http://www.nmfs.noaa.gov/pr/acoustics/draft_acoustic_guidance_2013.pdf.

[NOAA] National Oceanic and Atmospheric Administration. 2015. *Draft guidance for assessing the effects of anthropogenic sound on marine mammal hearing: Underwater acoustic threshold levels for onset of permanent and temporary threshold shifts*, July 2015, 180 pp. Silver Spring, Maryland: NMFS Office of Protected Resources. http://www.nmfs.noaa.gov/pr/acoustics/draft%20acoustic%20guidance%20July%202015.pdf.

[NRC] National Research Council. 2003. *Ocean Noise and Marine Mammals*. National Research Council (U.S.), Ocean Studies Board, Committee on Potential Impacts of Ambient Noise in the Ocean on Marine Mammals. The National Academies Press, Washington, DC. 192 pp. http://www.nap.edu/openbook.php?record_id=10564.

ANSI S12.7-1986. R2006. *American National Standard Methods for Measurements of Impulsive Noise*. American National Standards Institute, New York.

ANSI S1.1-1994. R2004. *American National Standard Acoustical Terminology*. American National Standards Institute, New York.

ANSI/ASA S1.13-2005. R2010. *American National Standard Measurement of Sound Pressure Levels in Air*. American National Standards Institute and Acoustical Society of America, New York.

ANSI/ASA S3.20-1995. R2008. *American National Standard Bioacoustical Terminology*. American National Standards Institute and Acoustical Society of America, New York.

Arveson, P.T. and D.J. Vendittis. 2000. Radiated noise characteristics of a modern cargo ship. *Journal of the Acoustical Society of America* 107(1): 118-129.

Au, W.W.L. and B. Wursig. 2004. Echolocation signals of dusky dolphins (*Lagenorhynchus obscurus*) in Kaikoura, New Zealand. *Journal of the Acoustical Society of America* 115(5): 2307-2313.

Baumgartner, M.F., S.M. Van Parijs, F.W. Wenzel, C.J. Tremblay, H.C. Esch, and A.M. Warde. 2008. Low frequency vocalizations attributed to sei whales (Balaenoptera borealis). *Journal of the Acoustical Society of America* 124(2): 1339-1349. <Go to ISI>://000258230500068.

Brabyn, M.W. 1991. *An analysis of the New Zealand whale stranding record*. Head Office, Department of Conservation.

Calderan, S., B. Miller, K. Collins, P. Ensor, M. Double, R. Leaper, and J. Barlow. 2014. Low-frequency vocalizations of sei whales (Balaenoptera borealis) in the Southern Ocean. *The Journal of the Acoustical Society of America* 136(6): EL418-EL423.

Dalebout, M.L., K.G. Russell, M.J. Little, and P. Ensor. 2004. Observations of live Gray's beaked whales (Mesoplodon grayi) in Mahurangi Harbour, North Island, New Zealand, with a summary of at-sea sightings. *Journal of the Royal Society of New Zealand* 34(4): 347-356.

Dawbin, W.H. 1956. *The migrations of humpback whales which pass the New Zealand coast*. *Transactions of the Royal Society of New Zealand*. Volume 84. J. Hughes, Printer, pp. 147-196.

Dawson, S.M. and C.W. Thorpe. 1990. A quantitative analysis of the sounds of Hector's dolphin. *Ethology* 86(2): 131-145.

Deane, G.B. 2000. Long time-base observations of surf noise. *Journal of the Acoustical Society of America* 107(2): 758-770.

Double, M., J. Barlow, B. Miller, P. Olson, V. Andrews-Goff, R. Leaper, P. Ensor, N. Kelly, M. Lindsay, et al. 2013. Cruise report of the 2013 Antarctic blue whale voyage of the Southern Ocean Research Partnership. *Report SC65a/SH/21 submitted to the Scientific Committee of the International Whaling Commission. Jeju Island, Republic of Korea*.

Eskesen, I.G., M. Wahlberg, M. Simon, and O.N. Larsen. 2011. Comparison of echolocation clicks from geographically sympatric killer whales and long-finned pilot whales. *Journal of the Acoustical Society of America* 130(1): 9-12.

Ford, J.K.B. 1989. Acoustic Behavior of Resident Killer Whales (Orcinus-Orca) Off Vancouver Island, British-Columbia. *Canadian Journal of Zoology* 67(3): 727-745. <Go to ISI>://A1989U167700029.

Jacquet, N. and H. Whitehead. 1999. Movements, distribution and feeding success of sperm whales in the Pacific Ocean, over scales of days and tens of kilometers. *Aquatic Mammals* 25(1): 1-13.

Madsen, P.T., M. Wahlberg, and B. Mohl. 2002. Male sperm whale (Physeter macrocephalus) acoustics in a high-latitude habitat: implications for echolocation and communication. *Behavioral Ecology and Sociobiology* 53(1): 31-41. <Go to ISI>://000179993400005.

Martin, B., K. Kowarski, X. Mouy, and H. Moors-Murphy. 2014. *Recording and identification of marine mammal vocalizations on the scotian shelf and slope*. *Oceans-St. John's, 2014*. IEEE, pp. 1-6.

McDonald, M.A., J.A. Hildebrand, S.M. Wiggins, D. Thiele, D. Glasgow, and S.E. Moore. 2005. Sei whale sounds recorded in the Antarctic. *Journal of the Acoustical Society of America* 118(6): 3941-3945.

McDonald, M.A. 2006. An acoustic survey of baleen whales off Great Barrier Island, New Zealand. *New Zealand Journal of Marine and Freshwater Research* 40(4): 519-529.

Merriman, M.G., T.M. Markowitz, A.D. Harlin-Cognato, and K.A. Stockin. 2009. Bottlenose dolphin (Tursiops truncatus) abundance, site fidelity, and group dynamics in the Marlborough Sounds, New Zealand. *Aquatic Mammals* 35(4): 511.

Miller, B.S., K. Collins, J. Barlow, S. Calderan, R. Leaper, M. McDonald, P. Ensor, P.A. Olson, C. Olavarria, et al. 2014. Blue whale vocalizations recorded around New Zealand: 1964–2013. *The Journal of the Acoustical Society of America* 135(3): 1616-1623.

Mohl, B., M. Wahlberg, P.T. Madsen, A. Heerfordt, and A. Lund. 2003. The monopulsed nature of sperm whale clicks. *Journal of the Acoustical Society of America* 114(2): 1143-1154. <Go to ISI>://000184637500052.

Mouy, X., M. Bahoura, and Y. Simard. 2009. Automatic recognition of fin and blue whale calls for real-time monitoring in the St. Lawrence. *Journal of the Acoustical Society of America* 126(6): 2918-2928. http://scitation.aip.org/content/asa/journal/jasa/126/6/10.1121/1.3257588.

Murray, S.O., E. Mercado, and H.L. Roitblat. 1998. Characterizing the graded structure of false killer whale (*Pseudorca crassidens*) vocalizations. *Journal of the Acoustical Society of America* 104(3): 1679-1688.

Nemiroff, L. and H. Whitehead. 2009. Structural characteristics of pulsed calls of long-finned pilot whales *Globicephala melas*. *Bioacoustics* 19: 67-92.

Oleson, E.M., S.M. Wiggins, and J.A. Hildebrand. 2007. Temporal separation of blue whale call types on a southern California feeding ground. *Animal Behaviour* 74: 881-894. <Go to ISI>://000250181100025.

Oswald, J.N., J. Barlow, and T.F. Norris. 2003. Acoustic identification of nine delphinid species in the eastern tropical Pacific Ocean. *Marine Mammal Science* 19(1): 20-37. <Go to ISI>://000180198700002.

Payne, R.S. and S. McVay. 1971. Songs of humpback whales. *Science* 173(3997): 585-597.

Rendell, L.E., J.N. Matthews, A. Gill, J.C.D. Gordon, and D.W. Macdonald. 1999. Quantitative analysis of tonal calls from five odontocete species, examining interspecific and intraspecific variation. *Journal of Zoology* 249: 403-410.

Risch, D., N.J. Gales, J. Gedamke, L. Kindermann, D.P. Nowacek, A.J. Read, U. Siebert, I.C. Van Opzeeland, S.M. Van Parijs, et al. 2014. Mysterious bio-duck sound attributed to the Antarctic minke whale (Balaenoptera bonaerensis). *Biology Letters* 10(4): 20140175.

Ross, D. 1976. *Mechanics of Underwater Noise*. Pergamon Press, New York. 375 pp.

Sirovic, A., J.A. Hildebrand, S.M. Wiggins, M.A. McDonald, S.E. Moore, and D. Thiele. 2004. Seasonality of blue and fin whale calls and the influence of sea lee in the Western Antarctic Peninsula. *Deep-Sea Research Part Ii-Topical Studies in Oceanography* 51(17-19): 2327-2344. <Go to ISI>://000226045100023.

Stafford, K.M., D.K. Mellinger, S.E. Moore, and C.G. Fox. 2007. Seasonal variability and detection range modeling of baleen whale calls in the Gulf of Alaska, 1999–2002. *Journal of Acoustical Society of America* 122(6): 3378-3390.

Steiner, W.W. 1981. Species-specific differences in pure tonal whistle vocalizations of five western North Atlantic dolphin species. *Behavioral Ecology and Sociobiology* 9: 241-246.

Stockin, K.A., G.J. Pierce, V. Binedell, N. Wiseman, and M.B. Orams. 2008. Factors affecting the occurrence and demographics of common dolphins (Delphinus sp.) in the Hauraki Gulf, New Zealand. *Aquatic Mammals* 34(2): 200.

Struzinski, W.A. and E.D. Lowe. 1984. A performance comparison of four noise background normalization schemes proposed for signal detection systems. *Journal of the Acoustical Society of America* 76(6): 1738-1742. http://scitation.aip.org/content/asa/journal/jasa/76/6/10.1121/1.391621.

Torres, L. 2013. Evidence for an unrecognised blue whale foraging ground in New Zealand. *New Zealand Journal of Marine and Freshwater Research* 47(2): 235-248.

Trickey, J.S., M.V.R. Reyes, S. Baumann-Pickering, M.L. Melcón, J.A. Hildebrand, and M.A. Iñíguez. 2014. Acoustic encounters of killer and beaked whales during the 2014 SORP cruise. *IWC Report SC/65b/SM12*.

Trickey, J.S., S. Baumann-Pickering, J.A. Hildebrand, M.V. Reyes Reyes, M. Melcón, and M. Iñíguez. 2015. Antarctic beaked whale echolocation signals near South Scotia Ridge. *Marine Mammal Science* 31(3): 1265-1274.

Vaughn-Hishorn, R.L., K.B. Hodge, B. Wursig, R.H. Sappenfield, M.O. Lammers, and K.M. Dudzinski. 2012. Characterizing dusky dolphin sounds from Argentina and New Zealand. *Journal of the Acoustical Society of America* 132(1): 498-506.

Wales, S.C. and R.M. Heitmeyer. 2002. An ensemble source spectra model for merchant ship-radiated noise. *Journal of the Acoustical Society of America* 111(3): 1211-1231. http://link.aip.org/link/?JAS/111/1211/1.

Webster, T.A., S.M. Dawson, W.J. Rayment, S.E. Parks, and S.M. Van Parijs. 2016. Quantitative analysis of the acoustic repertoire of southern right whales in New Zealand. *The Journal of the Acoustical Society of America* 140(1): 322-333.

Wenz, G.M. 1962. Acoustic ambient noise in the ocean: Spectra and sources. *Journal of the Acoustical Society of America* 34(12): 1936-1956.

Zimmer, W.M., M.P. Johnson, P.T. Madsen, and P.L. Tyack. 2005. Echolocation clicks of free-ranging Cuvier's beaked whales (Ziphius cavirostris). *The Journal of the Acoustical Society of America* 117(6): 3919-3927.

Appendix A. Acoustic Metrics

A.1. Sound Levels

Underwater sound pressure amplitude is measured in decibels (dB) relative to a fixed reference pressure of p_0 = 1 μPa. Because the perceived loudness of sound, especially impulsive noise such as from seismic airguns, pile driving, and sonar, is not generally proportional to the instantaneous acoustic pressure, several sound level metrics are commonly used to evaluate noise and its effects on marine life. We provide specific definitions of relevant metrics used in this report. Where possible we follow the ANSI and ISO standard definitions and symbols for sound metrics, but these standards are not always consistent.

The zero-to-peak sound pressure level, or peak sound pressure level (PK; dB re 1 µPa), is the maximum instantaneous sound pressure level in a stated frequency band attained by an acoustic pressure signal, *p* (*t*):

$$L_{p,pk} = 20\log_{10}\left[\frac{\max\left(\left|p(t)\right|\right)}{p_0}\right] . \qquad \text{(A-1)}$$

$L_{p,pk}$ is often included as a criterion for assessing whether a sound is potentially injurious; however, because it does not account for the duration of a noise event, it is generally a poor indicator of perceived loudness.

The peak-to-peak sound pressure level (dB re 1 µPa) is the difference between the maximum and minimum instantaneous sound pressure levels in a stated frequency band attained by an impulsive sound, *p*(*t*):

$$L_{p,pk-pk} = 10\log_{10}\left\{\frac{\left[\max\left(p(t)\right)-\min\left(p(t)\right)\right]^2}{p_0^2}\right\} . \qquad \text{(A-2)}$$

The root-mean-square (rms) sound pressure level (SPL; dB re 1 µPa) is the rms pressure level in a stated frequency band over a specified time window (*T*, s) containing the acoustic event of interest. It is important to note that SPL always refers to an rms pressure level and, therefore, not instantaneous pressure:

$$L_p = 10\log_{10}\left(\frac{1}{T}\int_T p^2(t)dt \Big/ p_0^2\right) . \qquad \text{(A-3)}$$

The SPL represents a nominal effective continuous sound over the duration of an acoustic event, such as the emission of one acoustic pulse, a marine mammal vocalisation, the passage of a vessel, or over a fixed duration. Because the window length, *T*, is the divisor, events with similar sound exposure level (SEL) but more spread out in time have a lower SPL.

The sound exposure level (SEL, dB re 1 µPa^2·s) is a measure related to the acoustic energy contained in one or more acoustic events (*N*). The SEL for a single event is computed from the time-integral of the squared pressure over the full event duration (*T*):

$$L_E = 10\log_{10}\left(\int_T p^2(t)dt \Big/ T_0 p_0^2\right) \qquad \text{(A-4)}$$

where T_0 is a reference time interval of 1 s. The SEL continues to increase with time when non-zero pressure signals are present. It therefore can be construed as a dose-type measurement so the integration time used must be carefully considered in terms of relevance for impact to the exposed recipients.

SEL can be calculated over periods with multiple acoustic events or over a fixed duration. For a fixed duration, the square pressure is integrated over the duration of interest. For multiple events, the SEL can be computed by summing (in linear units) the SEL of the *N* individual events:

$$L_{E,N} = 10\log_{10}\left(\sum_{i=1}^{N} 10^{\frac{L_{E,i}}{10}}\right) . \quad \text{(A-5)}$$

If applied, the frequency weighting of an acoustic event should be specified, as in the case of M-weighted SEL (e.g., $SEL_{LFC,24h}$). The use of fast, slow, or impulse exponential-time-averaging, or other time-related characteristics should else be specified.

Energy equivalent SPL (dB re 1 µPa) denotes the SPL of a stationary (constant amplitude) sound that generates the same SEL as the signal being examined, *p*(*t*), over the same period of time, *T*:

$$L_{eq} = 10\log_{10}\left(\frac{1}{T}\int_T p^2(t)dt \Big/ p_0^2\right) . \quad \text{(A-6)}$$

The equations for SPL and the energy-equivalent SPL are numerically identical; conceptually, the difference between the two metrics is that the former is typically computed over short periods (typically of one second or less) and tracks the fluctuations of a non-steady acoustic signal, whereas the latter reflects the average SPL of an acoustic signal over times typically of one minute to several hours.

A.2. 1/3-Octave-Band Analysis

The distribution of a sound's power with frequency is described by the sound's spectrum. The sound spectrum can be split into a series of adjacent frequency bands. Splitting a spectrum into 1 Hz wide bands, called passbands, yields the power spectral density of the sound. This splitting of the spectrum into passbands of a constant width of 1 Hz, however, does not represent how animals perceive sound.

Because animals perceive exponential increases in frequency rather than linear increases, analysing a sound spectrum with passbands that increase exponentially in size better approximates real-world scenarios. In underwater acoustics, a spectrum is commonly split into 1/3-octave-bands, which are one-third of an octave wide; each octave represents a doubling in sound frequency. A very similar measure is to logarithmically divide each frequency decade into 10 passbands, which are commonly misnamed the 1/3-octave-bands rather than deci-decades; we use this naming in the report. The centre frequency of the *i*th 1/3-octave-band, $f_c(i)$, is defined as:

$$f_c(i) = 10^{i/10} , \quad \text{(A-7)}$$

and the low (f_{lo}) and high (f_{hi}) frequency limits of the *i*th 1/3-octave-band are defined as:

$$f_{lo} = 10^{-1/20} f_c(i) \text{ and } f_{hi} = 10^{1/20} f_c(i) . \quad \text{(A-8)}$$

The 1/3-octave-bands become wider with increasing frequency, and on a logarithmic scale the bands appear equally spaced (Figure A-1). The acoustic modelling spans from band 10 ($f_c(10)$ = 10 Hz) to band 37 ($f_c(37)$ = 5.01 kHz).

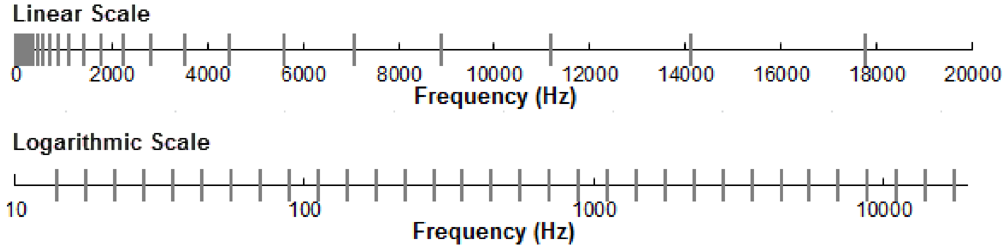

Figure A-1. One-third-octave-bands shown on a linear frequency scale and on a logarithmic scale.

The sound pressure level in the *i*th 1/3-octave-band $(L_b^{(i)})$ is computed from the power spectrum $S(f)$ between f_{lo} and f_{hi}:

$$L_b^{(i)} = 10 \log_{10} \left(\int_{f_{lo}}^{f_{hi}} S(f) df \right) . \tag{A-9}$$

Summing the sound pressure level of all the 1/3-octave-bands yields the broadband sound pressure level:

$$\text{Broadband SPL} = 10 \log_{10} \sum_i 10^{L_b^{(i)}/10} . \tag{A-10}$$

Figure A-2 shows an example of how the 1/3-octave-band sound pressure levels compare to the power spectrum of an ambient noise signal. Because the 1/3-octave-bands are wider with increasing frequency, the 1/3-octave-band SPL is higher than the power spectrum, especially at higher frequencies. Acoustic modelling of 1/3-octave-bands require less computation time than 1 Hz bands and still resolves the frequency-dependence of the sound source and the propagation environment.

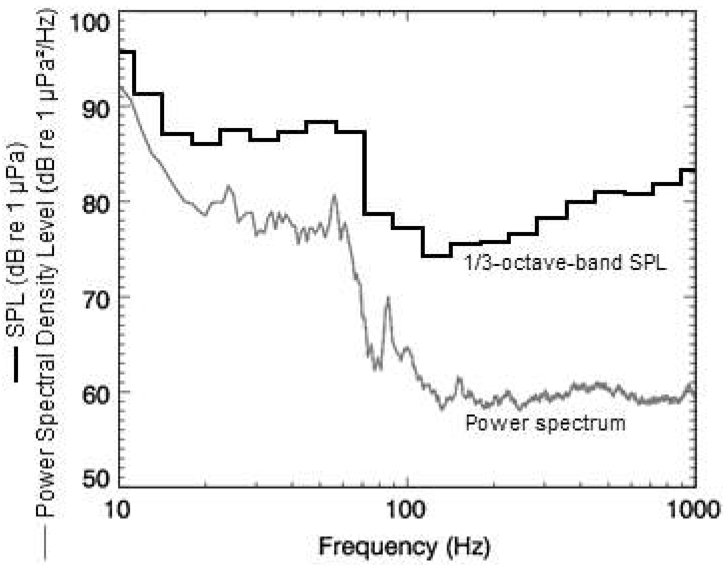

Figure A-2. A power spectrum and the corresponding 1/3-octave-band SPL of example ambient noise shown on a logarithmic frequency scale.

Table A-1. Third-octave-band frequencies (Hz).

Band	Lower frequency	Nominal centre frequency	Upper frequency
1	8.9	10	11.2
2	11.6	13	14.6
3	14.3	16	17.9
4	17.8	20	22.4
5	22.3	25	28.0
6	28.5	32	35.9
7	35.6	40	44.9
8	45.0	51	57.2
9	57.0	64	71.8
10	72.0	81	90.9
11	90.9	102	114.4
12	114.1	128	143.7
13	143.4	161	180.7
14	180.8	203	227.9
15	228.0	256	287.4
16	287.7	323	362.6
17	362.7	406	455.7
18	456.1	512	574.7
19	574.6	645	723.9
20	724.2	813	912.6
21	912.3	1024	1149
22	1,150	1,290	1,447
23	1,448	1,625	1,824
24	1,824	2,048	2,297
25	2,298	2,580	2,896
26	2,896	3,251	3,649
27	3,649	4,096	4,597
28	4,598	5,161	5,793
29	5,793	6,502	7,298
30	7,298	8,192	9,195
31	9,195	10,321	11,585
32	11,585	13,004	14,597

Table A-2. Decade-band frequencies (Hz).

Decade band	Lower frequency	Nominal centre frequency	Upper frequency
2	10	50	100
3	100	500	1,000
4	1,000	5,000	10,000

Appendix B. Acoustic Recorders

The AMAR sampled on a 15 min duty cycle: 630 s at 16 ksps, then 125 s at 250 ksps, and then 145 s of sleep. The 16 ksps recording channel had a 24-bit resolution with 6 dB of gain resulting in a spectral noise floor of 28 dB re 1 µPa^2/Hz and could resolve a maximum SPL of 165 dB re 1 µPa. The 250 ksps data were recorded at 16-bit resolution, with a spectral noise floor of 32 dB re 1 µPa^2/Hz and could resolve a maximum SPL of 171 dB re 1 µPa (no gain). The spectral noise floor represents the quietest sounds that can be recorded, and is directly comparable to the Wenz ocean noise spectra. Acoustic data were stored on internal solid-state flash memory.

B.1.1. Recorder Calibrations

A GRAS 42AC pistonphone calibrator (below), which is National Institute of Standards and Technology (NIST) traceable, was used to verify the sensitivity of the recording apparatus as a whole, i.e., the hydrophone, pre-amplifier, and AMARs. Calibration was undertaken in JASCO's warehouse prior to shipping to NIWA and then in NIWA's warehouse prior to deployment in the field and upon retrieval, as well as on the vessel. The pistonphone and its adapter were placed over the hydrophone and produced a known pressure signal on the hydrophone element (a 250 Hz sinusoid at 152.2 dB re 1 µPa) to verify the pressure response of the recording system. The system sensitivity was measured independently of the software that performed the data analysis, which allowed an independent check on the correct calibration of the analysis software. Both readings were verified for consistency before data were analysed.

Figure B-1. Split view of (left) a GRAS pistonphone calibrator, (middle) adaptors, and (right) a hydrophone.

Appendix C. Data Delivery

The data delivery includes:

Period: full, monthly, weekly, and daily

- Spectrograms and broadband and approximate-decade-band sound pressure levels:

Period: full, monthly, and weekly

- Spectral density level percentiles and statistical distribution of SPL in 1/3 Octave bands
- Daily sound exposure levels (SEL)
- Total and man-made associated SEL statistics, with daily total hours of vessel or seismic detection and daily vessel or seismic detections
- Rhythmic pattern analysis plots

Period: full and monthly

- Daily sound exposure levels (SEL)
- Total and man-made associated SEL statistics, with daily total hours of vessel or seismic detection and daily vessel or seismic detections

Per-file

- Sound level statistics .csv files
- Marine mammal, seismic, and shipping detections